

TWG

DOCUMENT 112-64

R

FOURTH TRANSDUCER WORKSHOP,

C

**TELEMETRY WORKING GROUP
INTER-RANGE INSTRUMENTATION GROUP
RANGE COMMANDERS COUNCIL**

C

**ARMY—NAVY—AIR FORCE
NATIONAL AND SERVICE RANGES**

DOCUMENT 112-64

FOURTH TRANSDUCER WORKSHOP

18-19 June 1964
Wright Patterson AFB, Ohio

Telemetry Working Group
Inter-Range Instrumentation Group
Range Commanders Council

Published by
Secretariat
Range Commanders Council
White Sands Missile Range, New Mexico 88002

CONTENTS

ATTENDANCE LIST

- SECTION I - Opening Remarks
 - SECTION II - Considerations in the Selection of a Transducer to Measure Both Static and Dynamic Linear Acceleration
 - SECTION III - Evaluation of a Transducer Information Center
 - SECTION IV - Some Aspects of Transducer Calibration Techniques
 - SECTION V - The Evaluation of Several Commercially Available Accelerometers
 - SECTION VI - Recent Developments in the Semiconductor Transducer Field
 - SECTION VII - Electronic Load Cell Applications in Rocket and Space Vehicle Testing and Design
 - SECTION VIII - A Hydraulic Step Function Pressure Generator for Transducer Evaluation
 - SECTION IX - Real Time Compensation of Thermal Sensors
 - SECTION X - Vibration Isolation of Flush Diaphragm Pressure Transducers Used on Rocket Motors
 - SECTION XI - Improvements in Plastic Film Pressure Transducers
 - SECTION XII - Transducers as Pre-Sampling Filters in Pulse Code Modulation Telemetry Systems
-

SECTION XIII

- Transducer Technology at the Air Force
Rocket Propulsion Laboratory, Edwards,
California

SECTION XIV

- Research on Transducers for Extreme
Environmental Temperatures

1964 TRANSDUCER WORKSHOP
ATTENDANCE

<u>NAME</u>	<u>AFFILIATION</u>	<u>LOCATION</u>
Aronson, P. M.	U.S. Naval Ord. Lab.	Silver Spring, Md.
Bagwell, D. W.	IBL Ballistic Res. Labs	Aberdeen Pr. Gr., Md.
Behymer, R. C.	SEMTC	W-PAFB, Ohio
Bialous, A. J.	General Electric	Schenectady, N. Y.
Bonfili, H. F., Lt.	AMRL (MRBAE)	W-PAFB, Ohio
Bronson, R. D.	General Dynamics	Ft. Worth, Texas
Bybee, R. N.	Thiokol Chemical Corp.	Brigham, Utah
Carter, F. V.	(APMO) AFAPL	W-PAFB, Ohio
Chapin, W. E.	Battelle Memorial Inst.	Columbus, Ohio
Chelner, H.	Rocketdyne	Canoga Park, Calif.
Cornthwaite, C.E.	NATC, Flt Test Division	Patuxent River, Md.
Cummings, F. E.	North American Aviation	Downey, Calif.
Dunbar, L. E.	Grumman Aircraft	Bethpage, N. Y.
Dykstra, J. D.	IBL Ballistic Res. Labs	Aberdeen Pr. Gr., Md.
Elliott, B.	BuWeps	Washington, D. C.
Finley, T.	NASA Langley	Hampton, Virginia
Fleming, L.	Bell & Howell Research	Pasadena, Calif.
Freyrik, H.	Lawrence Radiation Lab.	Livermore, Calif.
Gardenshire, L. W.	Radiation, Inc.	Melbourne, Florida
Golub, R.	Vertol Div., Boeing	Philadelphia, Pa.
Harman, H. S.	NASA-Marshall Sp. Flt. Ctr.	Huntsville, Ala.
Hille, H. K.	Aero Med Labs	W-PAFB, Ohio
Hiltner, J. S.	National Bur. of Stds	Washington, D. C.
Holley, F. J.	NASA - Goddard	Greenbelt, Md.
James, W. G.	AFFDL (FDCL)	W-PAFB, Ohio
Koyanagi, R. S.	National Bur. of Stds	Washington, D. C.
Kuhn, J.	Boeing-Wichita	Wichita, Kansas
Lake, J. B.	AFRPL (RPFDE)	Edwards AFB, Calif.
Lamothe, R. M.	Army Materials Res. Agency	Watertown, Mass.
Larder, R.	Lawrence Radiation Lab.	Livermore, Calif.
Laudermilk, T.R.	(APMO) AFAPL	W-PAFB, Ohio
Laudig, W. C.	ASPCD	W-PAFB, Ohio
Lederer, P. S.	National Bur. of Stds	Washington, D. C.
Long, J.	SEFIP	W-PAFB, Ohio
Lynch, J.	NATC, Flt Test Division	Patuxent River, Md.
Miller, J. A.	National Bur. of Stds	Washington, D. C.
Moore, R. M.	Geo. Washington University	Washington, D. C.
Moorman, L. A.	AFFDL (FDTE)	W-PAFB, Ohio
Nassauer, F.	Grumman Aircraft	Bethpage, N. Y.
Null, G. E.	Bur Naval Weapons	Pomona, Calif.
Pear, C.	Radiation, Inc.	Melbourne, Florida
Polishuk, P.	AFFDL (FDCL)	W-PAFB, Ohio
Rogero, S.	JPL	Box 458, Edwards, Calif.
Rybicki, G.	Avco, R&D Division	Wilmington, Mass.
Shumway, D. A.	AFFDL (FDCL)	W-PAFB, Ohio

NAMEAFFILIATIONLOCATION

Smith, F. D.	AFFDL (FDCL)	W-PAFB, Ohio
Snowball, H. M.	AFFDL (FDCL)	W-PAFB, Ohio
Thornburg, V. E.	Pratt & Whitney Aircraft	E.Hartford, Conn.
Viles, F.	Avco, R&D Division	Wilmington, Mass.
Vogt, S. H.	NASA-OART	Washington, D. C.
Wexler, A.	National Bur. of Stds	Washington, D. C.
Wright, W. A.	AFRPL(RPFDR)	Edwards AFB, Calif.
Yarlott, J. M.	Pratt & Whitney Aircraft	E.Hartford, Conn.

SECTION I

OPENING REMARKS

by

Jack Lynch
NATC
Patuxent River, Maryland

TRANSDUCER WORKSHOP
OPENING REMARKS
by
JACK LYNCH
Chairman, Transducer Committee
NATC, Patuxent River, Md.

Good Morning. Welcome to the Fourth Transducer Workshop. The members of the Transducer Committee of TWG extend their appreciation for the fine response to this meeting. Particularly we would like to acknowledge Mr. W. G. James, who has done such a fine job of coordinating the Workshop, and of course, the speakers who have put forth much time and effort in preparing the papers.

Most of you have been associated with the transducer field for a long time, far longer than myself, and need not be reminded of the constant advances in the state of the art and the need for new approaches to solve new problems. It is because of these changes that meetings such as this are necessary. The Transducer Workshop affords us the opportunity to get together, to listen to new solutions to new and old problems, and to exchange ideas. I would urge you to take advantage of this opportunity by actively entering the discussion.

For the new attendees, let me briefly summarize the objectives of the Transducer Committee of TWG. This committee informs the TWG of significant progress in the fields of telemetry transducers; maintains any necessary liaison between the TWG and NBS and their transducer program or any other related telemetry transducer efforts; coordinates TWG activities with other professional technical groups; collects and passes on information on techniques of measurement, evaluation, reliability, calibration, reporting, and manufacturing and recommends uniform practices for calibration, testing, and evaluation of telemetry transducers. I am current chairman of this Transducer Committee and the associate member of TWG from the Naval Air Test Center, Patuxent River. We at Patuxent are a large user of transducers and test instrumentation. In 1957 the Bureau of Aeronautics established at Patuxent the "Special Flight Test Instrumentation Pool." NATC was assigned the responsibility for determining the kind and amount of Special Flight Test Instruments required as incidental to the Bureau's development and procurement of piloted aircraft. Since that time the scope and capacity of the pool have increased until today the inventoried equipment is valued at \$25 millions.

Items other than transducers, such as oscillographs, galvanometers, and tape recorders are included in the Pool equipment. However, we currently have transducers on loan to over 100 contractors, government activities, and non-profit organizations. Most of the equipment on record at any time is located at contractor's plants or other test agencies.

The limited attendance at the Workshop allows us to conduct interesting and stimulating discussions. As we proceed with the papers, I would again remind you that a successful meeting depends not only on well written and well presented papers, but also on active participation from the audience.

SECTION II

CONSIDERATIONS IN THE SELECTION
OF A TRANSDUCER TO
MEASURE BOTH STATIC AND DYNAMIC LINEAR ACCELERATION

by

Robert D. Bronson
General Dynamics/Fort Worth
Fort Worth, Texas

INTRODUCTION

This paper pertains to transducers that respond to steady-state input acceleration. Therefore, discussion of the self-generating types, such as velocity pickups and piezoelectric accelerometers is omitted. The author does not care to argue the point that certain electronic circuits may be devised to permit nearly steady-state response from piezoelectric devices.

For dynamic measurements, the most important characteristic is amplitude-frequency response. In the wide temperature environments encountered in flight tests, temperature dependence may grossly affect accurate dynamic measurements.

In viscous damped instruments the transducer transfer function or sensitivity for dynamic inputs may be less than half of normal at minus 65 degrees Fahrenheit. Some transducers fitted with thermostatically controlled heater jackets have been used with mediocre success. The long term reliability of both the heater and thermostat in certain units is most questionable and each is subject to catastrophic failure. Perhaps a solid-state modular control circuit might supersede the simpler but unreliable bi-metallic thermostat. Heaters should also be improved. Evaluation tests must include life cycling tests while the assembly is subjected to low temperatures, temperature variations and vibration, shock and steady state accelerations.

It would be much better if true dynamic temperature compensation could be achieved without a heater jacket. If the operating temperatures are not too wide, the damping provided by gaseous, electronic, electromagnetic, or perhaps viscous means may give desirable results without a heater.

GENERAL PERFORMANCE CHARACTERISTICS

Important transducer characteristics are defined in Instrument Society of America Tentative Recommended Practice RP 37.1 entitled "Nomenclature and Specifications Terminology for Aero-Space Test Transducers with Electrical Output."

SPECIFICATIONS GUIDE

The Instrument Society of America Tentative Recommended Practice RP 37.5, entitled "Specifications Guide and Tests for Strain Gage Acceleration Transducers for Aero-Space Testing," is excellent reference material on the strain-gage devices. If enough of us use it for a procurement specification reference, perhaps the manufacturers who helped put the document together will come to recognize it for that purpose. With slight modifications this Recommended Practice makes a good guide for transduction principles other than the strain gage type. Incidentally, according to RP 37.5, a standard G is 980.665 cm/sec^2 . At General Dynamics/Fort Worth, when we use "earth's gravity" for plus or minus one-G calibration, we recognize that the local US Geodetic Survey figure of 979.458 cm/sec^2 furnishes only about plus or minus 0.999 G.

REQUIREMENTS

General

For any particular measurement task the instrumentation engineer must examine his requirements and decide what end result is needed. Just as a simple, moistened finger may serve to detect the direction of the wind, perhaps an accelerometer with a low natural frequency is desirable or satisfactory and perhaps an overall dynamic amplitude accuracy tolerance of plus or minus 50 per cent may be tolerable for a particular measurement.

General Dynamics/Fort Worth

In our Aerosystems Instrumentation Group at General Dynamics/Fort Worth we are usually interested in pushing the state-of-the-art for maximum frequency response and minimum error tolerances. Maybe we are prejudiced but we cannot understand how one manufacturer can recommend a virtually undamped device. Granted that it would be desirable to make measurements without phase shift, what will preclude ringing at the natural frequency? In a transducer which approaches conformance to a standard second-order system, it is preferred that the frequency response be predictable and repeatable through the rated ambient temperature range. The amplification, if any, near the natural frequency should not present an unreasonable peak.

PROCUREMENT

Specifications

The procurement of transducers should be based on performance specifications which are commonly understood by the manufacturer, the vendor, and the end user.

Acceptance Tests

The user's laboratory calibration and quality acceptance test procedures should be similar to the factory procedures and the user would be wise to request written test procedures from the vendor as part of the procurement activity.

DYNAMIC RESPONSE

Formula

In a second order system, dynamic amplitude response,

$$\frac{A_o}{A_i} = \frac{1}{\sqrt{\left[1 - \frac{(f_f)^2}{(f_n)^2}\right]^2 + \left[2h \frac{f_f}{f_n}\right]^2}}$$

where: f_f = forcing frequency

f_n = natural frequency (90-degree phase shift)

h = damping ratio.

Generally, if the damping ratio can be relied upon to stay between about 0.50 and 0.85 of critical, the devices known to approach second-order systems will produce dynamic data with sinusoidal inputs up to a frequency equal to one-third of the natural frequency with less than plus or minus 5 per cent error due to dynamic considerations.

Damping Ratios in Standard Commercial Units

The damping ratio in various commercially available accelerometers is as low as 0.06 and is sometimes greater than 8.0 at -65 degrees Fahrenheit.

Alternate Method of Specification

Amplitude-frequency response may also be specified for a particular frequency range and error tolerance consideration without reference to damping ratio or natural frequency. This alternate method is useful whether or not the transducer conforms to a standard second-order system curve.

Measurement

The method of laboratory measurement of natural frequency and damping ratio should be agreed upon by the vendor and user. Perhaps if sinusoidal inputs are expected in the actual measurement, these should be used in the laboratory calibration. If transient analysis is more important in end use, then these characteristics may be observed better in the decay curves which result from a step change in the input stimulus.

FIGURE OF MERIT FORMULAS

Mr. Lederer

Mr. P. S. Lederer (see Reference 1) suggests a figure of merit for accelerometers:

$$M = \left[\frac{(f_n)^2}{G} \right]$$

where f_n = natural frequency

G = full range span in G's.

In the simplest terms this means that for a given range, the higher the natural frequency, the better. And Lederer squares the natural frequency, so, doubling the natural frequency quadruples the figure of merit for a given range accelerometer. Lederer's report concerned only strain-gage transducers.

The Author

Since good instrumentation requires a high signal to noise ratio, a new figure of merit formula might be:

Figure of Merit:

$$M = \left[\frac{E_o}{G} \right] \left[\frac{(f_n)^2}{N} \right]$$

where E_o = full range open circuit output voltage (for a specific excitation voltage)

G = full range span in G's

f_n = natural frequency

N = maximum output noise voltage, peak to peak.

Note: E_o divided by G is the accelerometer sensitivity.

Nothing has been said yet about temperature dependence which includes thermal zero shift, thermal sensitivity shift, damping changes, and output resistance changes. Also, what about resolution, linearity, hysteresis, threshold, transverse sensitivity, and response to high level sound pressure?

TEMPERATURE EFFECTS

Damping Ratio Variation With Temperature

Concerning damping variations with temperature, Mr. Lederer wrote, "It appears, then, that temperature control is imperative for acceleration measurements at low ambient temperature with fluid damped accelerometers." This information was received too late as we had already purchased units from two vendors who still produce heaterless transducers advertised suitable for ambient temperatures of -65 to $+250$ degrees Fahrenheit. Of course, these transducers are pretty good at laboratory temperatures. But, this is a direct quotation from one vendor's catalog sheet:

"Damping of the accelerometer is achieved by viscous oil shearing. Very low viscosity oil is used, permitting exceptionally small viscosity changes in low and high temperature applications. This, in turn, minimizes damping change."

And another advertisement makes this grossly misleading statement:

"All X transducers, of any type, share one thing in common:

they are designed to produce accurate data unimpaired by the environments in which they operate."

Thermal Zero Shift

The typical maximum error tolerance for thermal zero shift is an average of ± 0.01 per cent of full scale per degree Fahrenheit over the rated ambient temperature range.

Thermal Sensitivity Shift

Thermal sensitivity shift maximum error tolerance is also typically ± 0.01 per cent per degree Fahrenheit. Since this is slope change, the error is percentage of actual measurand rather than full scale.

Output Resistance

In certain semiconductor bridge transducers, the output resistance varies drastically with temperature. If the user has an amplifier with very high input impedance this effect will be negligible. However, with a 10,000 Ohm load there would be an appreciable error due to this characteristic, which is usually not even mentioned in vendor specifications.

OTHER IMPORTANT CHARACTERISTICS

Threshold

Threshold is an interesting but often intangible characteristic. Occasionally we are asked, "Why don't you use so and so's accelerometer; it has threshold and resolution each 10^{-5} G?" Perhaps such a device is well suited to a closed loop system application, but for instrumentation purposes we feel that uniform amplitude-frequency response is our top priority specification item. Also, again, dependent on the desired end result, it is quite likely that in a measurement circuit, neither the accuracy need nor the necessary readout electronics equipment would be available to read 10^{-5} G. (Note: The ± 1 per cent nonlinearity error tolerance of one differential transformer device certainly does not help the user capture 10^{-5} G as an "accuracy.")

Nonlinearity and Hysteresis

Nonlinearity and hysteresis combined are usually less than \pm three-fourth per cent of full scale in open loop transducers.

Resolution

Resolution may be a problem with potentiometer-type accelerometers, wherein only a discrete number of different output levels exist. Thus, low amplitude sinusoidal measurements may show severe staircase distortion.

Transverse Sensitivity

Transverse sensitivity may be appreciable, especially in pendulous accelerometers. However, a tolerance for this error may be arranged if

it is properly recognized and accounted for as necessary for the desired end result.

Acoustic Noise Sensitivity

If the environment to be measured includes very high sound pressure levels, it would be appropriate to establish the acoustic noise sensitivity of the transducer.

NATURAL FREQUENCIES FOR PLUS OR MINUS 5 G ACCELEROMETERS ON THE MARKET

The natural frequencies span the following frequencies, grouped according to transduction principle:

Potentiometer:	11 to 45 cps
Bonded Strain Gage:	15 cps
Differential Transformer:	17 to 65 cps
Reluctance Bridge:	75 to 250 cps
Unbonded Strain Gage, Viscous damped:	300 to 375 cps
Servo-torquer:	50 to 300 cps (or higher)
Unbonded Strain Gage, Gas damped:	About 500 cps

COMMENTS ON COMMERCIAL UNITS BY TRANSDUCTION PRINCIPLE

Gas Damped

The gas damped strain gage accelerometer offers higher frequency response than previously available in fluid damped units. The manufacturer claims to have overcome the nonlinearity error which Mr. Lederer suggested would be encountered (see Reference 1). No heater is required and frequency response is excellent at ambient temperatures -65 to +270 degrees Fahrenheit. The Aerosystems Instrumentation Group at General Dynamics/Fort Worth intends to use this type device for flutter acceleration measurement in flight tests of the F-111 aircraft.

Differential Transformer

In our instrumentation group we have somehow avoided use of accelerometers which use either a differential transformer or two arm variable reluctance bridge transduction principle. Formerly, this type device was not available with a low nonlinearity tolerance. Now units can be

obtained with an advertised maximum nonlinearity tolerance of plus or minus one per cent.

Potentiometer

One manufacturer produces a potentiometer-type acceleration transducer which has a flexure to provide axial motion of the seismic mass, higher natural frequency than competitor's similar units, and damping ratio less sensitive to temperature changes due to a special damping orifice design. We are considering this transducer for the input to our airborne loop recorder. It is desirable to minimize complications of the electronic circuitry associated with this loop recorder and, since greater error tolerances are satisfactory, the potentiometer type is well suited to the application. Only in case of a flight "incident" will the last few minutes of flight data recorded on this loop recorder be analyzed.

Servo-Torquer

The most intriguing linear acceleration transducer on the market is a servo-torquer device which uses the same seismic mass and spring restraint for all ranges from plus or minus 0.5 to plus or minus 50 G. The transducer's integral electronics supply the transfer functions needed to provide a high natural frequency and uniform second-order system response characteristics. Damping variations are minor since damping is obtained electronically. This transducer provides 5 volt output and error tolerance as low as plus or minus 0.05 per cent of full scale for static input stimulus. It offers distinct precision measurement possibilities for aircraft "normal" acceleration. The high degree of accuracy attained in the transducer dictates improvement in the recording system electronics.

VERIFICATION OF PROCUREMENT PERFORMANCE SPECIFICATIONS

In conclusion, the customer would be wise to require 100 per cent factory test data on important specification requirements. Perhaps some characteristics can be logically considered for qualification or "type" tests and a transducer lot might be subject to, say, a 20 per cent random-sample complete testing to verify the integrity of the over-all performance specifications. If this approach is used, vendor specifications may be satisfactory. Eighteen or twenty pages of performance procurement specifications written by the customer will achieve very little unless tolerances are proved by tests.

REFERENCES

1. Lederer, P. S., General Characteristics of Linear Strain Gage Accelerometers Used in Telemetry, National Bureau of Standards Technical Note 150, June 1962.

SECTION III

EVALUATION OF A
TRANSDUCER INFORMATION CENTER

by

Messrs. James and Chapin
Wright-Patterson AFB, Ohio

EVALUATION OF A TRANSDUCER INFORMATION CENTER

As many of you know, Transducer users were surveyed in 1959 and 60 to determine their needs for information and services. This survey was conducted for the TWG Transducer Committee by Mr. Paul Polishuk of W-PAFB. As a result of this survey, the Transducer Handbook was prepared and periodically revised and up-dated, which went a long way toward meeting these needs; copies of the Handbook and its revisions were quickly and aggressively acquired by industry. It was recognized, however, that a more comprehensive, specialized service was needed by the transducer industry. Therefore, in August of 1962, the Air Force solicited bids for an evaluation of the feasibility and a pilot line operation of a Transducer Information Center; the Battelle Memorial Institute of Columbus, Ohio was the successful bidder for this effort. This paper represents essentially a progress report on this activity during the past twelve months.

It is important to note that this information center is not intended to be simply an "abstracting" or "indexing" service nor is it a report retrieval operation. It is intended to be a broad service, directed toward collecting technical information in the specific area of transducers and toward evaluation and filtering of this information into a form of condensed information useful to manufacturing, application, research, development, and planning activities. It is an organization staffed in part with scientists and engineers, and, to provide a basis for its primary service function, it conducts a selective data and information acquisition and processing program. It is, therefore, more of a question answering service than a document retrieval program; it is assumed that the latter function can be adequately satisfied by activities such as the Defense Documentation Center, NASA's "STAR" Activity, and/or direct inquiry to the original source of the information.

This kind of specialized service appears to be strongly needed for the field of Transducers (Sensors) for several reasons:

a. There are an extremely large number of transducer manufacturers (estimated at 6000 companies), each with a number of standard products; there is a general lack of standardization of terminology, nomenclature, specification sheet formats, and test techniques which further complicate the problem for individual applications engineers or engineering groups. This bulk and variety of information can best be handled by a specialist information center. It will also help to solve the standardization problem as a secondary purpose in a manner supplemental to the efforts of the NBS, and the Professional Societies.

b. Figure 1 shows the recent growth in the transducer literature as further evidence of the dynamic state of research, development, and applications activity in transducers, and the increasing importance of transducer requirements.

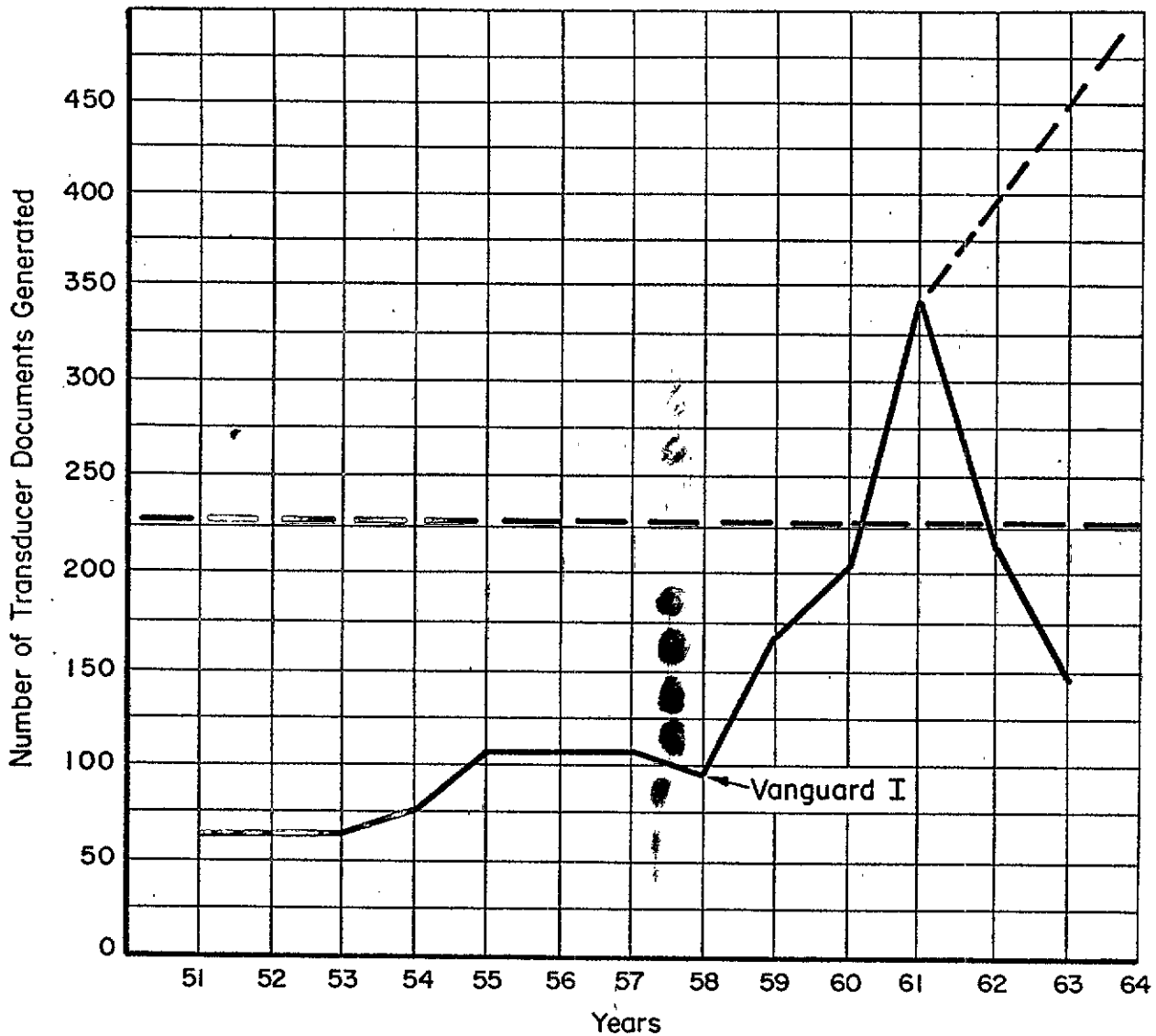


FIGURE 1. ANNUAL LITERATURE GENERATION ON TRANSDUCERS

Note: The apparent decrease in the number of new articles and reports generated in 1962 and 1963 is due to the lag in secondary publication (abstract and announcement bulletins). The extrapolation line for the generation of documents includes trade literature.

c. Further evidence of the need for a transducer information center is the natural evolution of localized activities of this general type and the response of industry to these activities. A Transducer Handbook was published (WADC TR 61-67) which gave a general discussion of transducer techniques and listed descriptive information on some of the current transducers available from industry. Demand for these handbooks was instantaneous, extensive, and lasting; approximately 800 copies have been distributed directly (not counting copies distributed by DDC) and requests are still averaging about 2 per day. In September, 1963, the ISA published a Transducer Compendium which lists an even greater number of transducers and their characteristics. The significant point here is that the very fact that these activities have evolved and the strong response to these limited activities is positive evidence of the strength of the need for a centralized, integrated T. I. C. of adequate scope to satisfy the demands for quick and specific support of transducer research, development, and applications efforts.

d. Government groups responsible for transducer technology are widely scattered and although specialized by application have a significant amount of commonality in measurement parameters and techniques. Results of pertinent testing, applications studies, development and research efforts are often not separated into separate reports but are instead distributed or buried in one or more volumes of a report on a vehicle, system, or subsystem; furthermore, wide distribution of these reports often lags the initial draft of the report by 8 to 12 months and sometimes lags the completion of the transducer portion of the work even more. The existence and effective operation of a T. I. C. would help solve both the problem of coordination and of timely and relatively complete cognizance of pertinent transducer work in progress; finally, an acceptable degree of inter- and intra-service coordination cannot be maintained without the operation of a T. I. C.

e. Transducer user groups have a very wide range of interests and needs which can best be satisfied by a central, integrated, T. I. C. operation. Transducers are used to support several types of activity with many common needs for transducer information: Basic and Exploratory Research, System or Product Development, Performance Demonstration (qualification or certification), Control and Monitoring of Operational Systems, and Product Improvement. The dominant needs are of two general classes: (1) Identification of available transducers, or nearest possible match, to meet requirements (particularly for unusual environments and/or parameters), and (2) establishing confidence in selected transducers in terms of other test results and/or applications experience. Both of these needs can be efficiently met by a T. I. C. with due consideration to AF Regulation 80-24. As a bonus for meeting these needs, quantitative information is assimilated for use by government organizations to support planning and programming concerning the state of the art capabilities and, of more usefulness, actual needs and requirements of the nation which either cannot be met, or can be met only marginally.

f. Finally, T. I. C. operations should also benefit the product improvement activities of transducer manufacturers by bringing test results and applications experience forcefully to their attention, thereby encouraging, focussing, and shortening the product improvement cycle, as well as providing a means for the manufacturers to indicate changes made to correct operational problems.

A careful review of the above needs for a Transducer Information Center will lead to a rather detailed understanding of the potential users of such a service and of the types and scope of the services they need, which, in turn, should provide the general framework for organizing and operating a T. I. C.

a. The most obvious asset of such an information center is a continuously updated file on available transducers and their characteristics, both as claimed by the manufacturers and as confirmed by laboratory or applications experience. The typical customers interested in this kind of capability include transducer users, (e.g., missile and airframe prime contractors, their major sub-contractors, testing agencies, and researchers) and Government Agencies concerned with the management and direction of the development of advanced systems; in addition, this information would be of vital significance to researchers active in other areas, such as, medicine, bionics, or the general physical sciences who have need for transducers to aid their research, but have neither the time nor the inclination for developing special transducers for their purposes. Typical of the questions expected from this group are: "What transducers are available for measuring some parameter (such as, blood flow rate) in some given range to a given accuracy and in the presence of specified environments?" and "What test experience is available on the performance of the Sensitall Company's Model 101 pressure transducer for sensing fuel pressure on operational missiles?" Successful servicing of this need would result in improved quality of instrumentation being used, reduced duplication in testing and evaluation efforts, improved identification of critical problem areas with the resulting focussing of attention and test and evaluation, and improved confidence in the reliability, accuracy and validity of the instrumentation used for solving applications problems.

b. Closely related to servicing the above need area, is the potential of the T. I. C. for improving manufacturer's product improvement activities and encouraging and helping to form standardization in test procedures, data sheets, reports, testing methods, specification sheets, etc. To avoid the possibility of favoritism or misleading test results, transducer manufacturers should be allowed and encouraged to review and comment upon any test results accessed into the T. I. C. concerning performance or applications experience with their transducers; problems and areas needing improvement in their transducers will thereby be brought directly and forcefully to their attention and changes made in the transducer design or manufacture to overcome experience deficiencies and made quickly known to potential users. Thus the product improvement

cycle is shortened, encouraged, and focussed with the resulting benefits to both the manufacturer and users. Standardization in the test methods, data sheets, reports, etc., will be a natural long range development which will result from any large scale attempts to exchange needs, requirements, test experience, applications experience, and the related transducer characteristics; this is confirmed in that the most immediate and apparent pressure resulting from the publication of the Transducer Handbook, the ISA Transducer Compendium, and the efforts of the ISA and TWG Working Groups, is indeed toward the standardization of nomenclature, terminology, and specification and data sheet formats.

c. Another service of the T. I. C. of value to R & D activities in transducers is to provide a functional interface with other information agencies. For example, materials characteristics needed for preliminary transducer design is not normally available in the materials information centers in a form or from the viewpoint suitable for interpretation and use by the transducer researchers; in addition, transducer researchers are often not fully aware of the information available from other centers and/or find it difficult to phrase their requirements in a form suitable for answering by these other services. Similar problems and questions exist on the interface with radiation effects, infra-red characteristics, ground test equipment, etc., areas of information center operation. As a short range benefit, the T. I. C. could smooth this interface in both directions, in and out of the related information centers, making the information required quickly accessible to the transducer researcher; as a longer range benefit, the typical needs and characteristics required by the transducer industry might be made known to the related information agencies who in turn could alter their information structure as required to make the direct interface with transducer users more practical.

d. Finally, as a nearly free benefit of satisfying the above needs, the information is available for improved R & D planning, both by industry and government activities and for improved coordination within and between government agencies responsible for transducer research and development. For example, periodic review of the numbers and types of requests for transducers whose requirements in terms of accuracy, environmental resistance, reliability, etc., could not be met by currently available or advanced development transducers would provide quantitative indication of specific transducer areas requiring additional R & D activities. Precontract investigations of alternate approaches to problem solutions, state of the art, and related R & D programs could be conducted by the government agencies involved, thus reducing the contract time period required, and the amount of uninformed unproductive duplication in contracted efforts sponsored by various government activities.

e. There are at least two vital and essential characteristics of any T. I. C. operation required for successfully accomplishing the above services: First, quick accurate access to information both from transducer manufacturers and transducer users is required in order to maintain a truly current information level and avoiding the 12 - 24 month

publication lag presently being experienced through normal publications channels; and secondly, the organization responsible for the T. I. C. operation should have and maintain the image of being both technically capable, and of having no "axe to grind" either present or future, as either a potential manufacturer or a user of transducers. I believe that without these two characteristics, any attempt at T. I. C. operation would result in only superficial coverage and would be a total waste of time and effort.

During the Battelle study, approximately 200 transducer users were surveyed to obtain a more quantitative indication of their needs. The physical parameters, the environments, and T. I. C. services are listed in Table 1 in order of their relative importance as expressed during this survey.

<u>PARAMETERS</u>	<u>ENVIRONMENTS</u>	<u>T. I. C. SERVICES</u>
Pressure	High Temperature	State of Art Reports
Temperature	Room Temperature	Inquiry Response
Acceleration	Nuclear Radiation	Data Sheets (On Request)
Vibration	Cryogenic Temp.	Visit Provisions
Strain	Vacuum	Accession Lists
Shock	Corrosive Vapors	Bibliographies (On Request)
Force		Special Reports
Air Flow		Data Sheets (Routine Basis)
Load		Contract Compilations
Radiation		

TABLE 1: Definition of Industry Needs

After thus defining the needs of a T. I. C., several data retrieval systems were evaluated, including computerized techniques, with respect to the total costs involved both in inputting and outputting of the system, and with respect to the scope and flexibility inherent in these data retrieval systems. A manual system of data retrieval has been selected for initial implementation which is suitable for eventual conversion to a computerized method when the scope and use rate of the information center grows to the point where the computerized system is justified. Details of this system are described in the Technical Report FDL-TDR-64-34.

A small scale pilot operation of a transducer information center has been conducted with very limited funds during the past 8 months. Approximately 600 carefully selected documents were read into the system and coded with respect to research reports, performance data, proprietary and classified restrictions, manufacturers specification, trade literature, survey reports, state of the art reports, bibliographies, internal papers, trip reports, etc. Extensive travel and personal contacts were accomplished with key personnel among transducer manufacturers, users,

and government agencies to encourage inclusion of truly current information, and for check-back contacts to obtain feedback on the actual success or difficulties in the T. I. C. operation. All companies visited were very cooperative and strongly encouraged the continuation and expansion of the T. I. C. operation. The hard products produced by the T. I. C. include the following:

a. Four quarterly accession lists were published which indicated the reports in abstract form which had been read into the T. I. C. system. These accession lists were published in one hundred copies which were soon exhausted by industry requests.

b. Two data summary lists were published indicating data on file concerning specific performance characteristics of specific transducers.

c. A number of manufacturers' specification sheets were photographically reduced to a 5 x 7 card size to demonstrate the economic feasibility of this technique, the readability without special aids of the 5 x 7 reduced size, and the ease of filing and retrieval of this reduced card size. Typical of hard products which could be produced by full scale T. I. C., but which were not generated under the pilot run operation, include special report extracts, special summary reports and monographs on selected measurement problems, and state of the art and/or survey reports.

The "soft" product of the T. I. C. was quick, positive response to inquiries. Inquiries were received both by telephone and by letter and were averaging approximately 12 a month, even though publicity on the operation of the T. I. C. was intentionally and specifically restrained.

The costs for full scale operation of a transducer information center have been analyzed and separated into the fixed and variable components. The total costs depend, of course, upon the number and scope of special reports required, the use rate, and the quantity of hard products produced. An initial funding level of approximately \$200,000.00 per year would allow accession of current literature, accession of previously published transducer literature at a reasonable rate, and a utilization rate which appear reasonable. This funding rate also appears reasonably consistent with the funding rate of other information centers known to be in operation in other technical specialty areas.

In conclusion, the needs and benefits of a comprehensive transducer information center have been definitized, and operational feasibility has been at least partially demonstrated by a limited pilot-line operation of such a center at Battelle Memorial Institute. Some minor problems of implementation still require additional evaluation such as, the feasibility of truly assuring protection of sensitive material--including both proprietary and security restrictions--the establishment of smooth links with sources and users of the information both transducer manufacturers and users, and finally the solution of the problem of

handling test results on specific commercial products in terms of possible conflict with Air Force Regulation 80-20, industry restrictions, and the associated legal problems. These aspects of T. I. C. operations will be evaluated in the subsequent pilot operation of the T. I. C.

SECTION IV

SOME ASPECTS OF TRANSDUCER
CALIBRATION TECHNIQUES

by

Paul S. Lederer
National Bureau of Standards
Washington, D. C.

Dynamic Characteristics of Pressure Transducers

The need for the precise measurement of rapidly varying pressures has been increasing rapidly. The fidelity with which the output of a pressure transducer represents the pressure input at a particular instant depends on the dynamic characteristics of the transducer.

Accordingly many efforts are under way to determine the dynamic characteristics of such pressure transducers. If a pressure transducer is a linear system, the dynamic characteristics are given by the "transfer function" of the device, usually expressed by two curves: one showing the ratio of output amplitude to input amplitude as a function of frequency; the other one showing phase shift (or time delay) between output and input as a function of frequency.

For pressure transducers, these two curves cannot be obtained directly in most cases, since sinusoidal pressure generators of sufficiently wide amplitude and frequency ranges are not available. It is theoretically possible to obtain the transfer function of a device such as a pressure transducer from its response to a transient input whose mathematical description is known¹. The best one for the purpose appears to be the step-function of gas pressure generated by the shock tube, provided the rise time is fast enough to shock excite all resonances of the transducer under test.

Pressure transducers are relatively complicated systems as shown by the shock tube responses of some typical ones in Figure 1. It is apparent that a number of resonances are present in each response. In theory, the transfer function of such a complicated system can also be obtained from its stepfunction response. Several techniques have been described^{2 3 4}, some of which employ digital computer techniques to calculate the transfer function from transducer output amplitudes at proper sampling intervals. These amplitudes are usually read off a photograph of the transducers stepfunction response. Even with sophisticated computer techniques, the determination of the transfer function takes a relatively long time. Furthermore this operation is not fully justified unless the transducers output during the actual measurement is also sampled similarly so that the input time function (the actual pressure amplitude) can be computed from the output and the previously computed transfer function. This second computation takes even longer. Very little information is available on the effect of errors (amplitude, sampling interval, etc.) on the calculated results, particularly on the fidelity of the final values of the computed input pressures.

In view of this, we have suggested a different and simpler approach. Most of these transducers have a number of lightly damped resonances. Since a resonance has a 180° phase shift associated with it, transients with frequency components on either side of a resonance will be distorted. Accordingly, we feel that a transducer should be relied upon to reproduce

faithfully only those transients whose frequency content is below the lowest resonance of the transducer. We believe the frequency response and phase response for a lightly damped system below the lowest resonance will be very similar to those of a single degree of freedom system, provided the transient pressure to be measured does not shock excite the other resonances. We feel that the lowest frequency of resonance constitutes a reasonable limit for the proper use of such a transducer.

An experimental technique was developed at the National Bureau of Standards for detecting the lowest resonance of a pressure transducer from its shocktube response⁵. This technique consists essentially of subjecting the transducer to a pressure stepfunction by means of a shock tube and feeding the resultant transducer output to an oscilloscope (for a photographic record) and simultaneously to a special magnetic transient recorder. This recorder records and preserves the transducers transient output, which is played back repetitively 60 times per second into an automatically scanning electronic spectrum analyzer. A photograph of the screen of the analyzer, with an exposure time of about one minute, produces a picture showing the frequency components present in the transient.

The major components used: 1) the shock tube, 2) the magnetic transient recorder, 3) the spectrum analyzer, are shown in figures 2 and 3. A detailed description as well as the results of system tests are given in reference 5. The system is capable of detecting the presence of resonances in the range of 1 kc to 100 kc. System tests indicate that in the presence of a major resonance with a frequency between 10 kc and 100 kc, a second resonance with a frequency of up to 80% of that of the major resonance can be readily detected if its amplitude is at least 5% of the major resonance. As the separation of the frequencies increases, low frequencies with amplitudes of less than 3% of the major are detectable. For a major resonance near 5 kc, a second resonance of up to 3.5 kc is detectable if its amplitude is at least 9% of the major.

One source of error exists in the recorder circuits which themselves may be set into oscillation by the transient signals. Their resonances occur at about 1.3 kc and 4.2 kc and are readily identifiable in all photographs of transducer analyses.

Results of the analysis of several commercial pressure transducers are shown in the following pictures. Fig. 4 shows the shock-tube response and spectrum analysis of an unbonded strain gage pressure transducer, range 50 psig, with a flat diaphragm. Manufacturers' literature indicates a natural frequency ranging from 4 kc to 15 kc for transducer ranges from 10 psi to 150 psi. Based on this, the computed natural frequency for a 50 psi range would be about 9 kc. The literature further states "flat frequency response to 10% of natural frequency," in this case up to about 900 cps. From the response to a pressure step of 52.2 psi two resonances can be seen readily. One appears to be near 20 kc, and the other one, of much smaller amplitude, near 40 kc. Spectrum analysis confirms these values by showing

two high-frequency resonances close together, 36 kc and 41 kc. The photo also shows the low-frequency spectrum with the major resonance at 16.6 kc, and the two inherent electrical system resonances (1.3 kc and 4.2 kc). Then at 6.8 kc it shows, fairly pronounced, what appears to be the lowest resonance of the transducer (a value close to the computed "natural frequency" of 9 kc).

Fig. 5 shows responses and analyses of a 50 psi-range, flat diaphragm pressure transducer employing a different unbonded strain gage system. As is apparent from the shock-tube responses, there is very little damping present. The ringing continues for more than 8 msec. The main ringing frequency appears to be 8 kc with a super-imposed small amplitude near 48 kc. Spectrum analysis confirms these values as a double peak near 8.2 kc and single peak at 55.6 kc. Examination of the low-frequency end of the spectrum does not reveal any significant low-frequency resonances other than the two electrical resonances previously referred to. Presumably, the lowest significant resonance is given by the lower value (8.0 kc) of the double-peaked major resonance. The manufacturer's value of approximate natural frequency for this type of pressure transducer, 50-psi range, is given as 9 kc.

Fig. 6 presents shock-tube response and spectrum analysis of a pressure measuring system consisting of a quartz crystal pressure transducer and a one-stage electrometer amplifier. This transducer is capable of sensing pressures up to 3,000 psi and is described as having a "natural frequency" of 48 kc. In Fig. 6, the response to a step of 47 psi, shows a small amount of ringing at about 50 kc confirmed by resonances at about 42 kc and 46 kc. The low-frequency spectrum, in addition to the electrical system resonances, shows a low resonance at 7.1 kc, followed by another smaller one at about 8 kc.

The results obtained with a miniature quartz crystal pressure transducer and charge amplifier are shown in Fig. 7. This transducer, designed to sense pressures up to 5,000 psi, is described as having a "natural frequency" of 150 kc. The picture of the system response to a 48.4 psi step, shows the dominant ringing frequency to be about 130 kc. This is beyond the range of the recorder-analyzer system and was therefore not confirmed. A rather strong resonance exists at 43.5 kc. The low-frequency spectrum, includes the two familiar electrical resonances, and what appears to be a small resonance at 6.9 kc, and a small triple peak centered at about 10.4 kc. The 6.9 kc resonance is believed to be a true transducer resonance, as shown by its absence in the picture in the lower right corner of Fig. 7 which shows the response of recorder-analyzer system to an electrical square wave.

Fig. 8 shows test results on an unbonded strain gage pressure transducer, range 1,000 psi, with built-in damping. The response to a 493 psi step is shown. Note the relatively small amplitude of ringing. The analysis indicates the major resonance to be about 56 kc. Also shown is the

low-frequency end of the spectrum, which is explored in greater detail. The latter shows, in addition to the usual two electrical resonances, a small resonance at about 46 kc and a larger one at 6.6 kc. For this type of transducer, manufacturers' literature lists "approximate natural frequency" as 23.5 kc.

Finally, Fig. 9 shows results obtained from tests on a capacitive pressure transducer, range 50 psi, to a pressure step of 46 psi. A phenomenon similar to creep is apparent. In the same figure the response of this transducer to a step pressure of 42.5 psi is shown with a faster time base. The frequency of ringing in this picture is about 45 kc, confirmed by the spectrum analysis. The low-frequency end of the spectrum shows, in addition to the usual inherent electrical resonances, a pronounced resonance at 8 kc. Manufacturers' literature claims a "natural frequency" of 112 kc for this transducer.

Fig. 10, the shock tube response of a "damped" strain-gage pressure transducer shows the presence of creep again.

The existence of creep and hysteresis in many pressure transducers intended for static or quasistatic measurements, has been recognized for some time, as shown by the common practice of exercising a pressure gage over its range just prior to calibration or use for precise measurements. Presence of creep or hysteresis for such devices can be detected by static calibration techniques.

The last two pictures present evidence, however, that these non-linearities exist for such short relaxation times that they can not be uncovered statically. Ray Smith of our group has been investigating these non-linearities with the aid of a liquid medium step function calibrator, based on a design by Dr. D. P. Johnson of NBS and which is shown in Fig. 11.

The requirements of a dynamic pressure generator for uncovering such a phenomenon as short term creep, is that it generates a monotonic pressure change (one without overshoot) with a fast enough rise time to permit study of the creep character, but not so fast as to shock excite the transducer into oscillation.

A detailed account of the construction and operation of the device, as well as some of the results obtained with it are given in reference 6.

An example of the characteristics one may encounter is shown in the following pictures. Fig. 12 shows the results of static calibration of an unbonded strain-gage pressure transducer which has been in storage for about five years. Fig. 13 shows its response to the stepfunction of pressure of Fig. 14. Fig. 15 finally shows the response of the transducer to the same pressure step after several dozen operations, from zero to 2000 psi and a few operations zero to 3000 psi. Subsequent static calibrations of this transducer disclosed no measurable hysteresis.

The liquid stepfunction calibrator was useful in determining how much the creep had been reduced by exercise. In other cases it is the only device to uncover this creep as shown below.

Fig. 16 shows the response of an unbonded strainage pressure transducer to a pressure step of about 300 psi generated in the liquid medium calibrator, after the transducer had been allowed to rest over night. Fig. 17 shows the response of the same transducer after it had been exercised over the pressure range, 0 to 300 psi, 120 times since the response of Fig. 16. Static calibrations, before and after these two responses, showed no measurable hysteresis.

Two techniques have been described for the determination of some of the dynamic characteristics of pressure transducers which affect the transducers ability to correctly reproduce transient pressures.

Paul S. Lederer
Research Engineer
Mechanical Instruments Section
National Bureau of Standards

References

1. "Experimental and Mathematical Techniques for Detecting the Dynamic Response of Pressure Gages" C. H. Hylkema and R. B. Bowersox Memorandum 20-68 JPL Oct. 6, 1953.
2. "Digital-Computer Calculation of Transducer Frequency Response from its Response to a Stepfunction" R. B. Bowersox and J. Carlson Progress Report 20-331 JPL July 26, 1957.
3. "Dynamic Testing of Pressure Transducers - A Progress Report", J. Inskip, Tech. Report 32-268, JPL Dec. 6, 1961.
4. "Evaluation and Modification of Existing Prototype Dynamic Calibration System for Pressure Measuring Transducers" Houston Engineering Res. Corp. Edwards AFB Report RTO-TDR-63-9, March 1963.
5. "An Experimental Technique for the Determination of the Fidelity of the Dynamic Responses of Pressure Transducers" P. S. Lederer and R. O. Smith NBS Report 7862, May 1963.
6. "A Liquid Medium Stepfunction Pressure Calibrator" R. O. Smith ASME Paper 64-WA-263, November 1963.

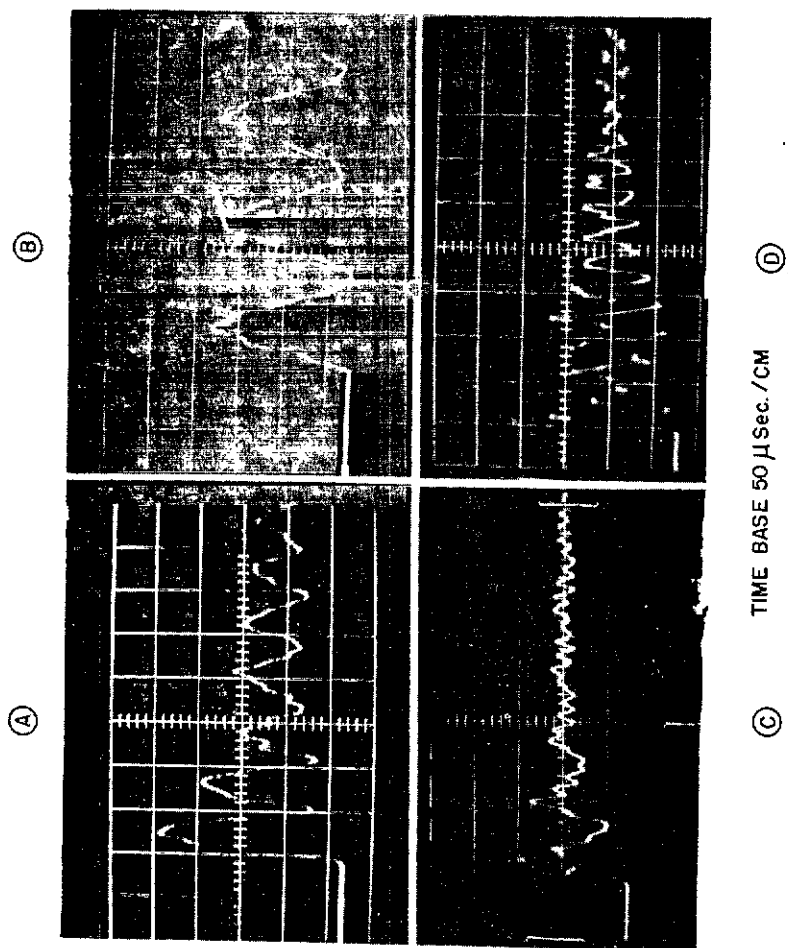


Fig. 1 RESPONSES OF FOUR "FLUSH DIAPHRAGM" PRESSURE TRANSDUCERS TO STEP FUNCTION PRESSURES OF ABOUT 50 PSI GENERATED IN A SHOCK TUBE

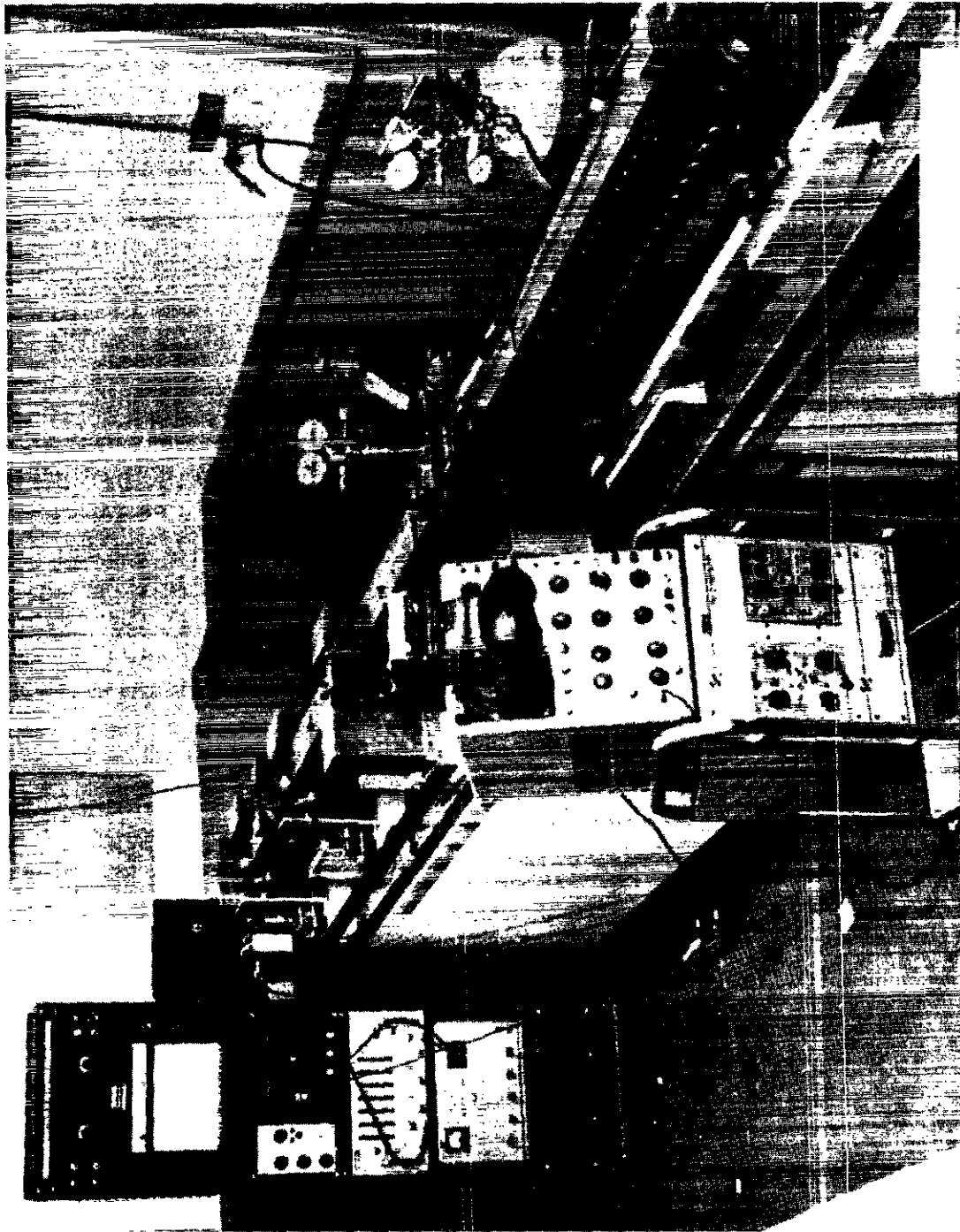


Fig.2 SHOCK TUBE

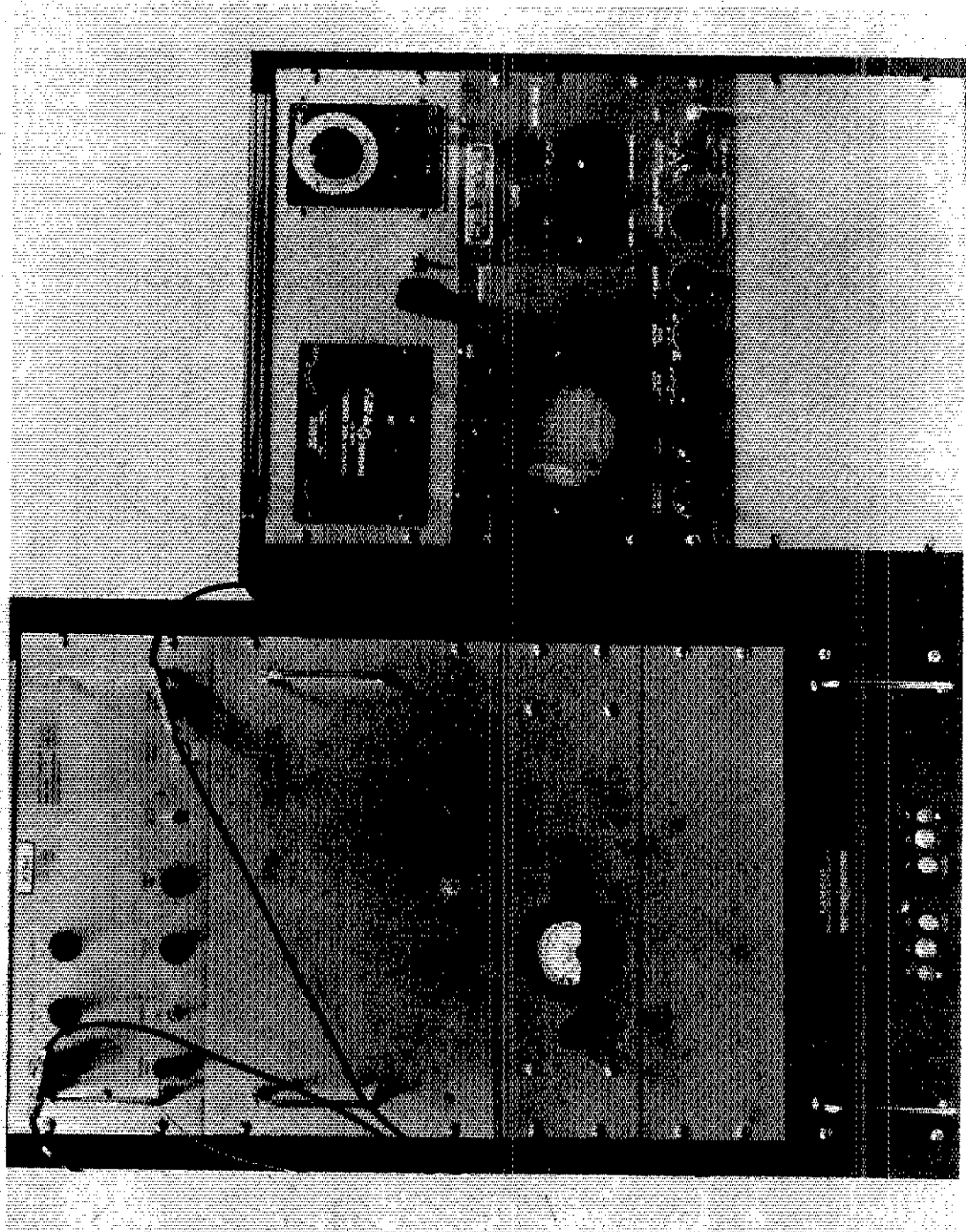
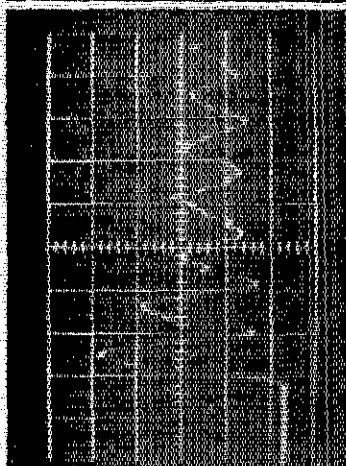


Fig. 3 MAGNETIC TRANSIENT RECORDER AND WAVE ANALYZER

RESPONSE OF TRANSDUCER
TO 52.2 PSI PRESSURE STEP

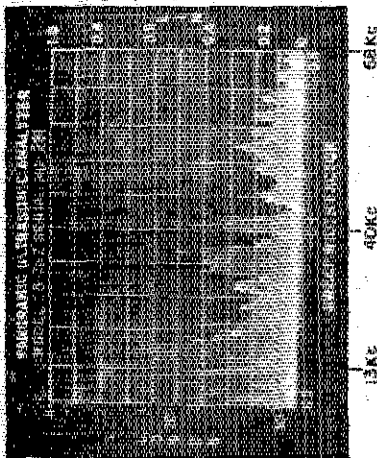
(A)



TIME BASE 50 μSec./CM

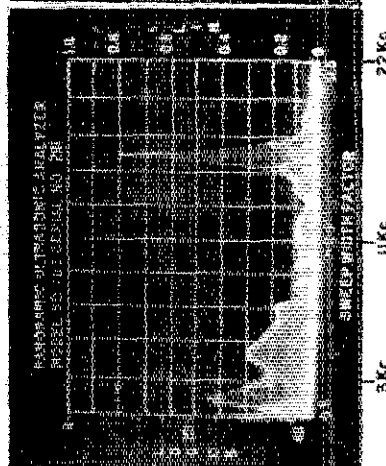
FREQUENCY ANALYSIS OF
SHOCK TUBE RESPONSE
OVER FREQUENCY RANGE
FROM ABOUT 5 KC TO 68 KC

(B)



(C)

FREQUENCY ANALYSIS OF
SHOCK TUBE RESPONSE
OVER FREQUENCY RANGE
FROM ABOUT 1.5 KC TO 22 KC



(D)

FREQUENCY ANALYSIS OF
SHOCK TUBE RESPONSE
OVER FREQUENCY RANGE
FROM ABOUT 14.8 KC TO 19 KC

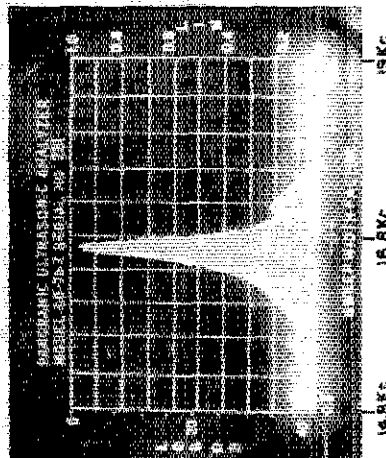
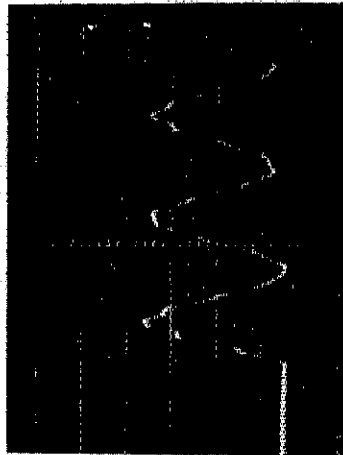


Fig. 4 SHOCK TUBE RESPONSE OF UNBONDED STRAINGAGE PRESSURE TRANSDUCER AND FREQUENCY ANALYSIS

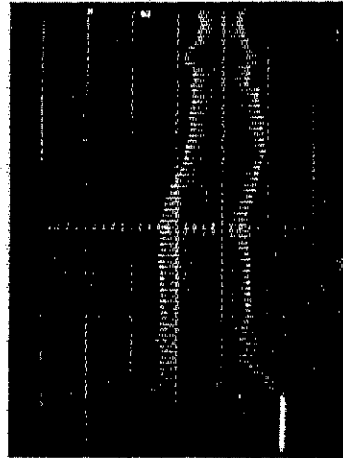
RESPONSE OF TRANSDUCER
TO 51.1 PSI PRESSURE STEP

(A)



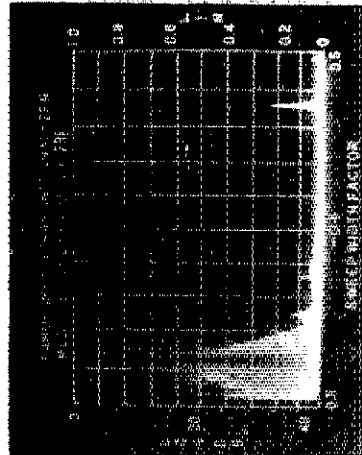
RESPONSE OF TRANSDUCER
TO 45.9 PSI PRESSURE STEP

(B)



(C)

FREQUENCY ANALYSIS OF
SHOCK TUBE RESPONSE
OVER FREQUENCY RANGE
FROM ABOUT 4 Kc TO 64 Kc



(D)

FREQUENCY ANALYSIS OF
SHOCK TUBE RESPONSE
OVER FREQUENCY RANGE
FROM ABOUT 1 Kc TO 13.5 Kc

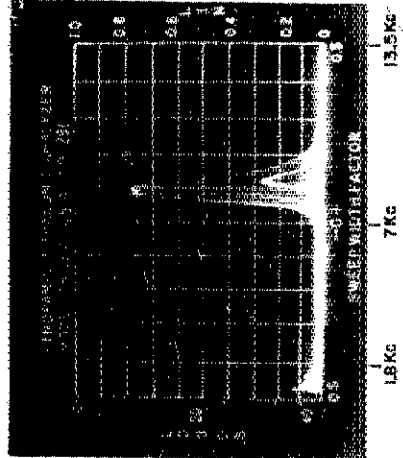
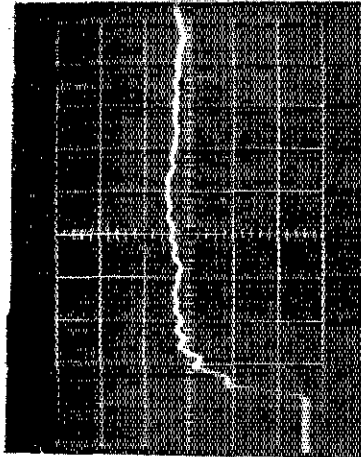


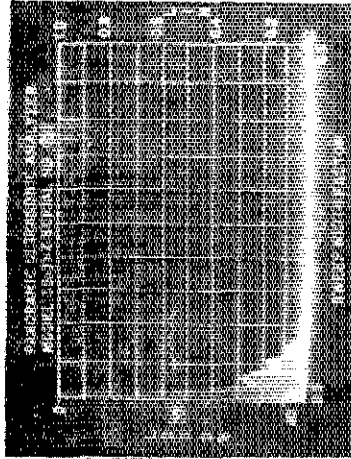
Fig. 5 SHOCK TUBE RESPONSE OF UNBONDED STRAINGAGE PRESSURE TRANSDUCER AND FREQUENCY ANALYSIS

RESPONSE OF TRANSDUCER
TO 47 PSI PRESSURE STEP
TIME BASE 50 μSec./CM

(A)



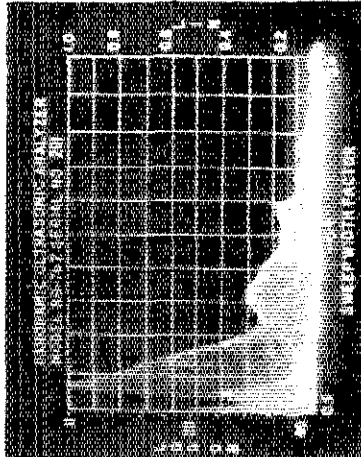
(B)



FREQUENCY ANALYSIS OF
SHOCK TUBE RESPONSE
OVER FREQUENCY RANGE
FROM ABOUT 3.6 Kc TO 59 Kc

(C)

FREQUENCY ANALYSIS OF
SHOCK TUBE RESPONSE
OVER FREQUENCY RANGE
FROM ABOUT 1 Kc TO 11.8 Kc



(D)

FREQUENCY ANALYSIS OF
SHOCK TUBE RESPONSE
OVER SAME FREQUENCY
RANGE AS IN (B) BUT WITH
DISPLAY AMPLITUDE 10 TIMES
THAT AS IN (B)

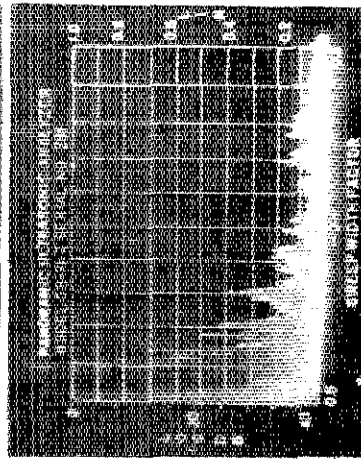
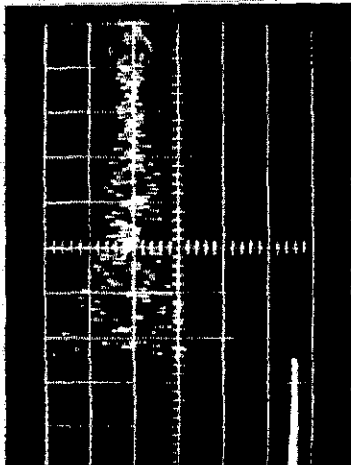


Fig. 6 SHOCK TUBE RESPONSE OF PIEZO-ELECTRIC PRESSURE TRANSDUCER WITH ELECTRO-METER AMPLIFIER AND FREQUENCY ANALYSIS

RESPONSE OF PRESSURE
TRANSDUCER AND CHARGE
AMPLIFIER TO 48.4 PSI
PRESSURE STEP

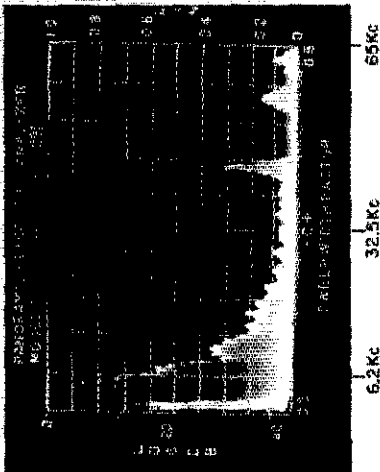
(A)



TIME BASE 100 μsec./CM

FREQUENCY ANALYSIS OF
SHOCK TUBE RESPONSE
OVER FREQUENCY RANGE
1 Kc TO 65 Kc

(B)



(C)

FREQUENCY ANALYSIS OF
SHOCK TUBE RESPONSE
OVER FREQUENCY RANGE
FROM ABOUT 400CPS TO 12.8Kc



(D)

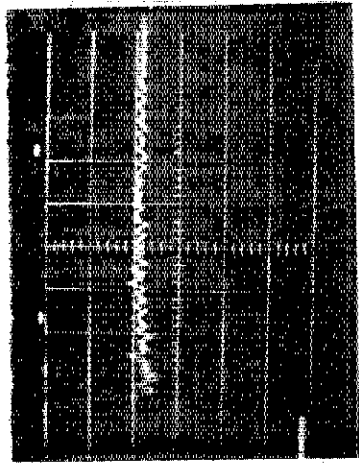
FREQUENCY ANALYSIS OF
ELECTRICAL STEP FUNCTION
RESPONSE OF RECORDING
SYSTEM OVER FREQUENCY
RANGE FROM ABOUT 500CPS
TO 14.2 Kc



6.8 Kc
13.00 CPS
14.2 Kc
RESONANCE AT 1300 CPS
RESONANCE AT 4200CPS

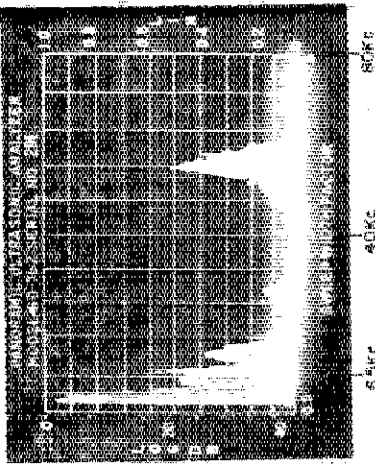
Fig 7 SHOCK TUBE RESPONSE OF MINIATURE PIEZO-ELECTRIC PRESSURE TRANSDUCER
WITH CHARGE AMPLIFIER AND FREQUENCY ANALYSIS

(A)



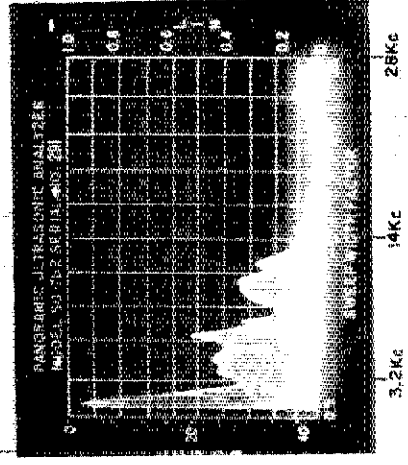
RESPONSE OF TRANSDUCER TO PRESSURE STEP OF 493PS

(B)



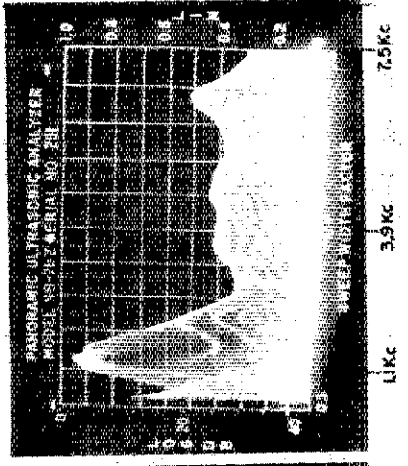
FREQUENCY ANALYSIS OF SHOCK TUBE RESPONSE OVER FREQUENCY RANGE FROM ABOUT 3.3 Kc TO 80 Kc

(C)



FREQUENCY ANALYSIS OF SHOCK TUBE RESPONSE OVER FREQUENCY RANGE FROM ABOUT 1.6 Kc TO 28 Kc

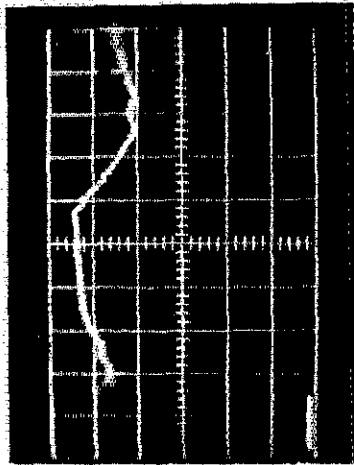
(D)



FREQUENCY ANALYSIS OF SHOCK TUBE RESPONSE OVER FREQUENCY RANGE FROM ABOUT 1 Kc TO 7.5 Kc

Fig 8 SHOCK TUBE RESPONSE OF DAMPED UNBONDED STRAINGAGE PRESSURE TRANSDUCER AND FREQUENCY ANALYSIS

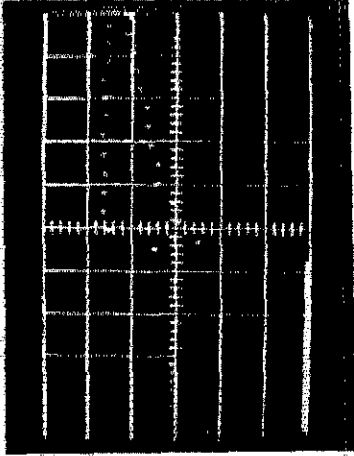
RESPONSE OF PRESSURE
TRANSDUCER SYSTEM TO 464 PSI
PRESSURE STEP
Note Creep



(A)

TIME BASE 1 millisecond / CM

RESPONSE OF SYSTEM
TO 42.5 PSI STEP

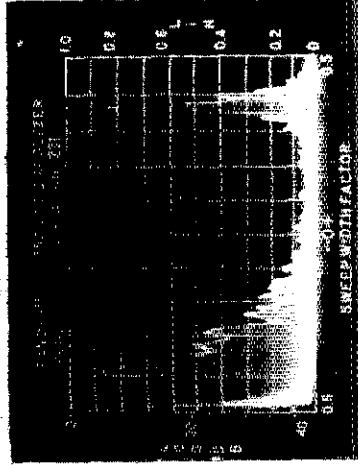


(B)

TIME BASE 50 μsec / CM

FREQUENCY ANALYSIS OF
SHOCK TUBE RESPONSE OVER
FREQUENCY RANGE FROM
ABOUT 3 KC TO 54 KC

(C)



FREQUENCY ANALYSIS OF
SHOCK TUBE RESPONSE
OVER FREQUENCY RANGE
FROM ABOUT 1 KC TO 12 KC

(D)

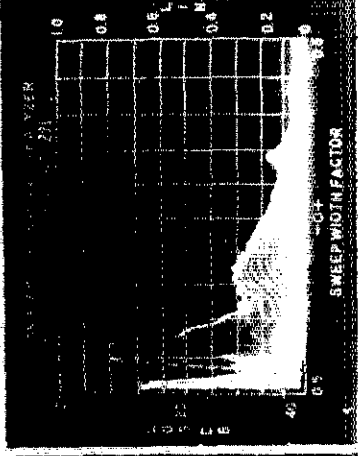


Fig. 9 SHOCK TUBE RESPONSES OF CAPACITIVE PRESSURE
TRANSDUCER AND FREQUENCY ANALYSIS

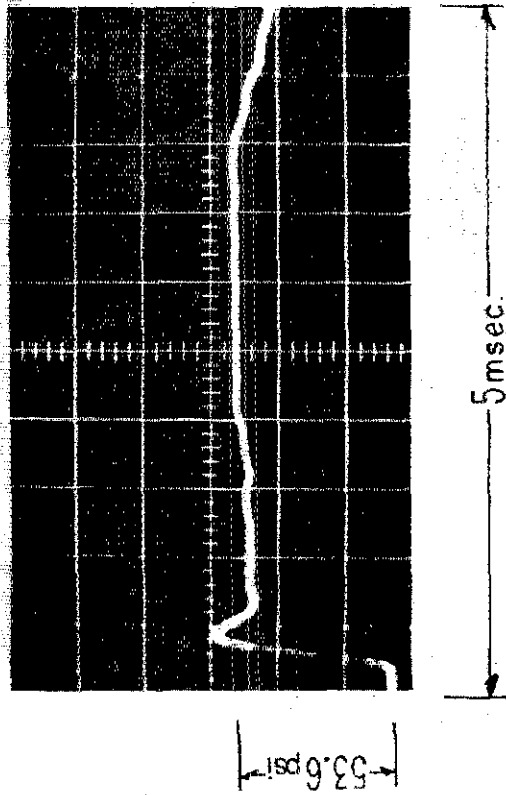


Fig.10 SHOCK-TUBE RESPONSE OF AN OIL DAMPED
TRANSDUCER

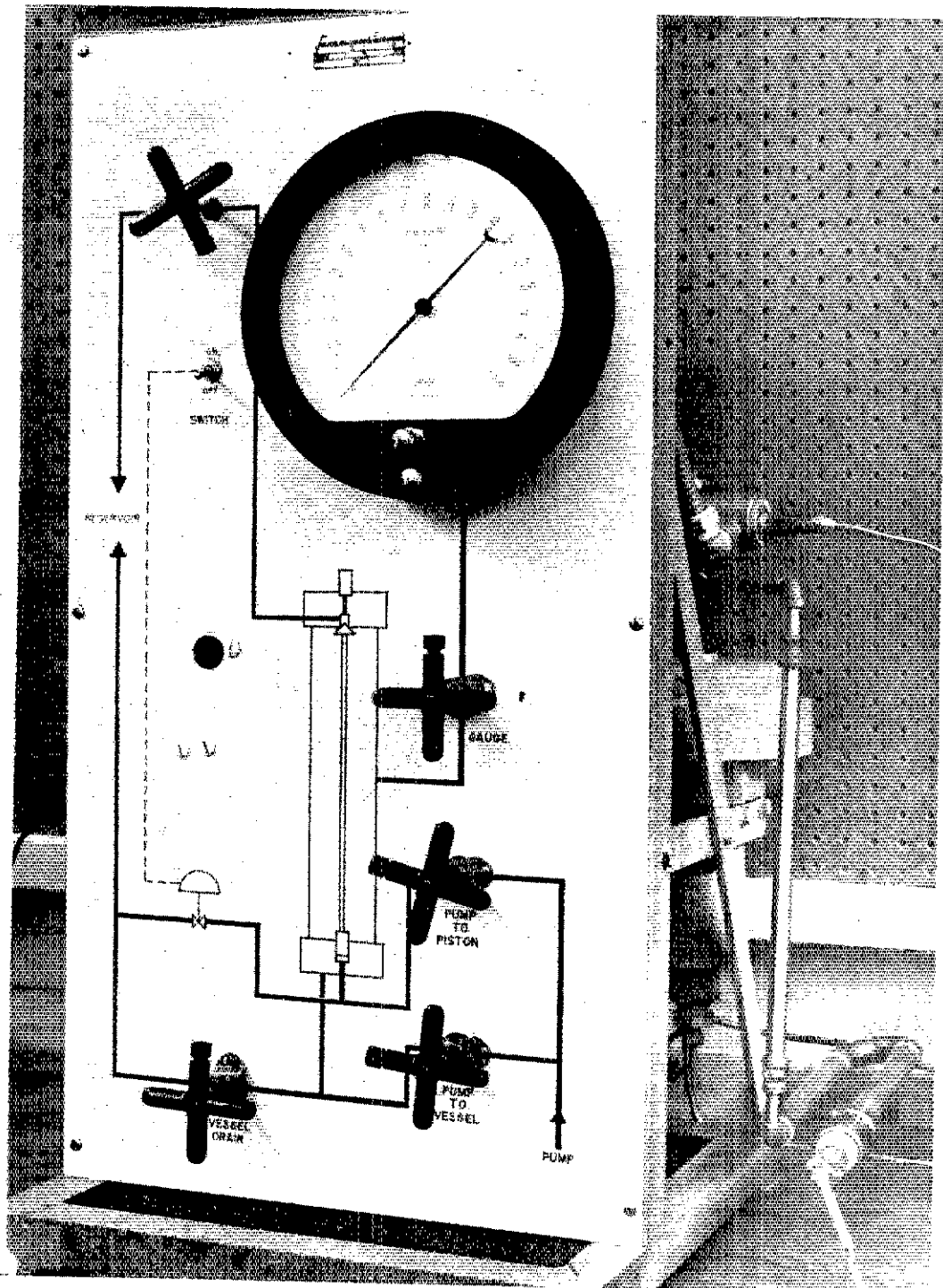


Fig. II LIQUID MEDIUM STEP-FUNCTION
PRESSURE CALIBRATOR

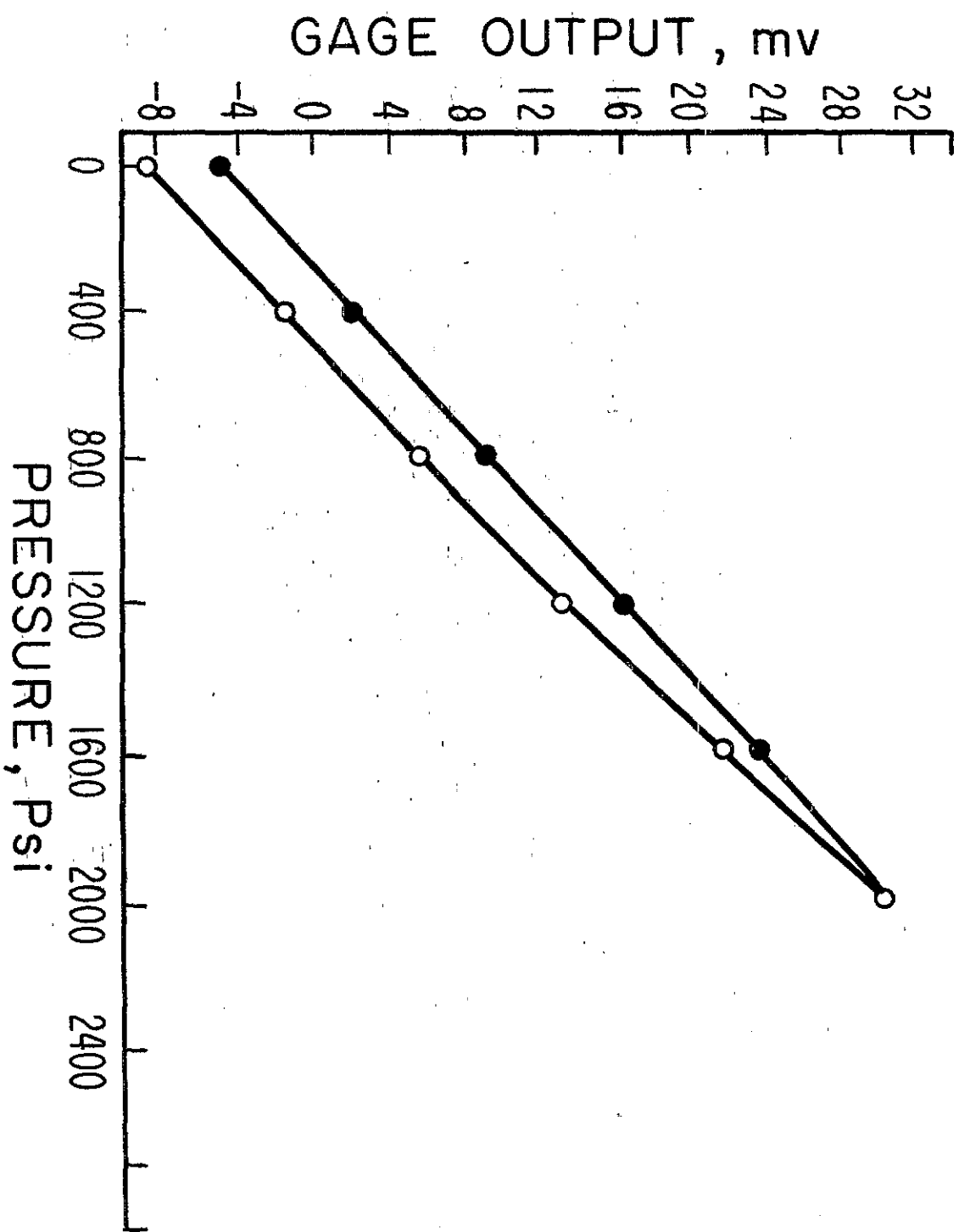


Fig.12 STATIC CALIBRATION OF A TRANSDUCER

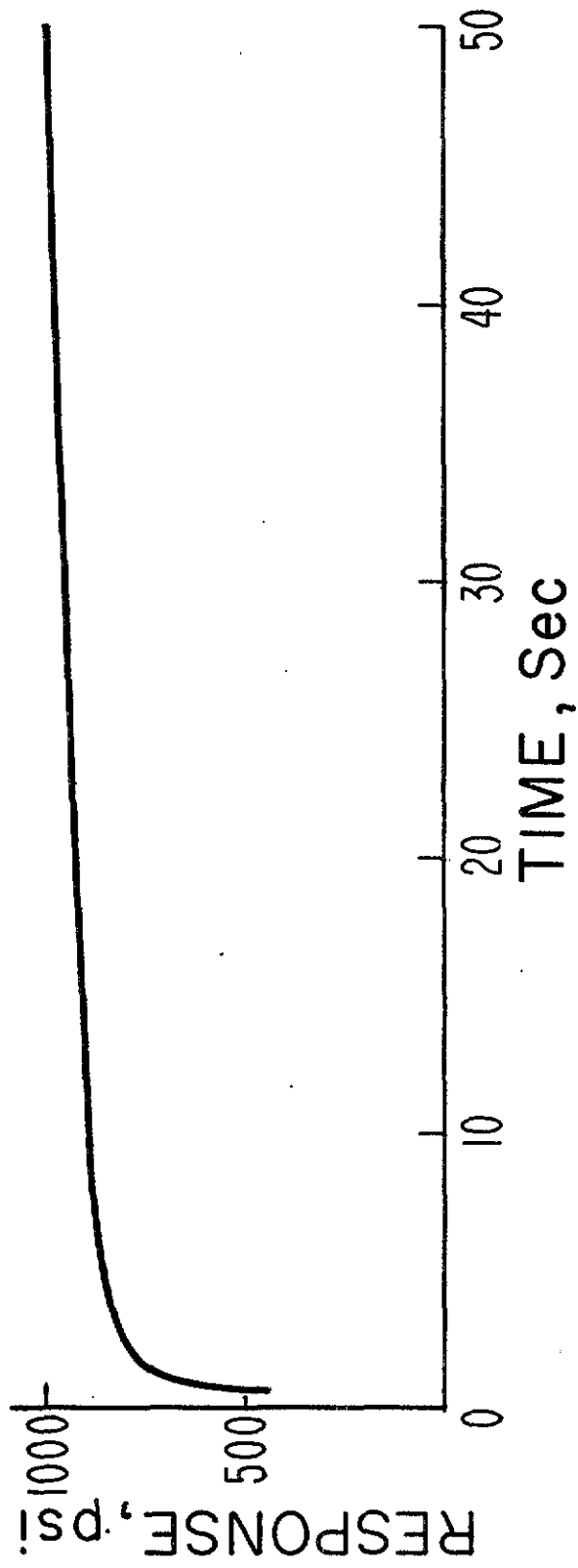
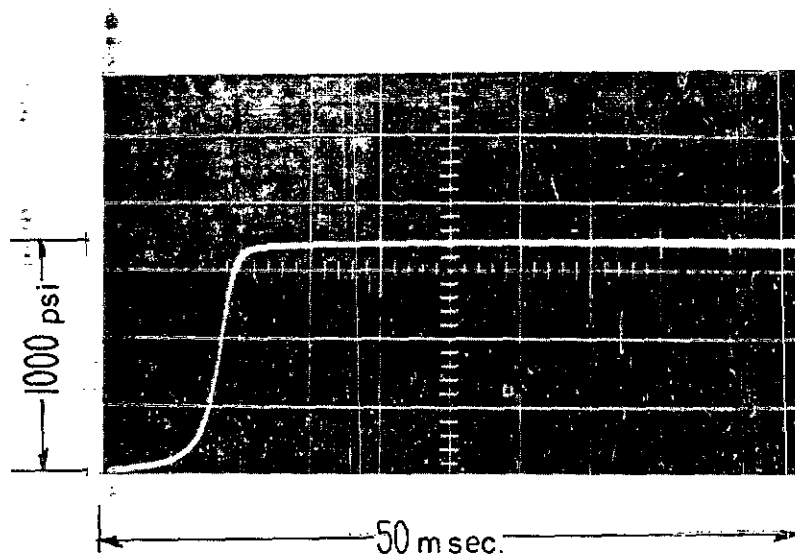


Fig.13 RESPONSE TO A STEP-FUNCTION
OF THE TRANSDUCER OF SLIDE 12



RESPONSE OF A BONDED STRAIN GAGE TRANSDUCER
 CONSIDERED A FAITHFUL ANALOG OF THE STEP-
 APPLIED TO THE GAGE OF SLIDE 12

Fig. 14

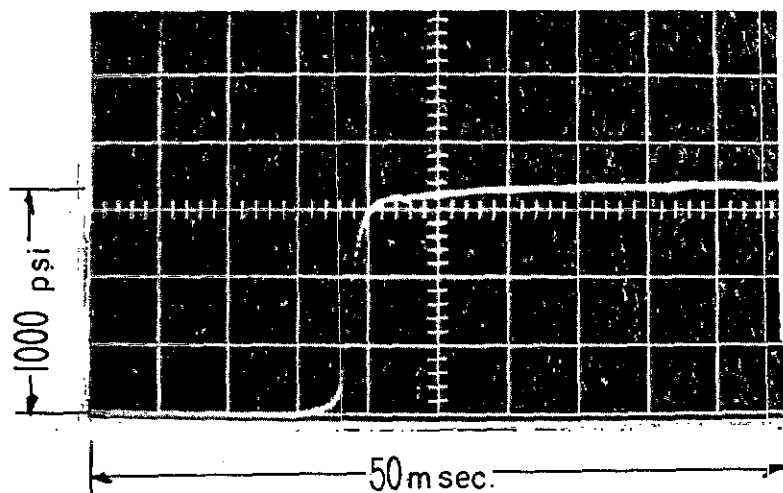


Fig. 15 RESPONSE TO A STEP-FUNCTION OF THE TRANS-
 DUCER OF SLIDE 12 AFTER EXERCISE

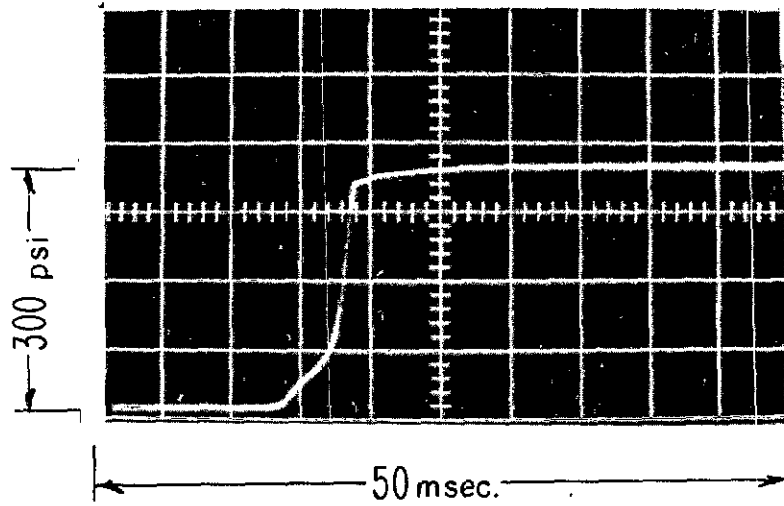
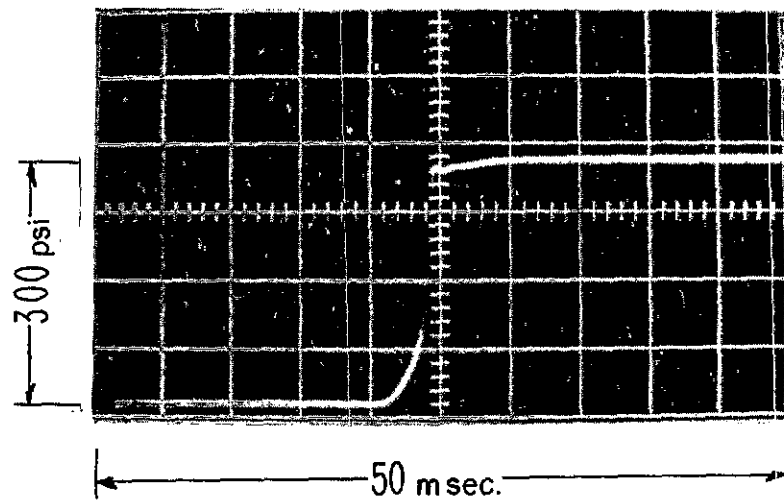


FIG. 16 STEP FUNCTION RESPONSE BEFORE EXERCISE



G. 17 STEP FUNCTION RESPONSE AFTER EXERCISE

SECTION V .

THE EVALUATION OF SEVERAL COMMERCIALY
AVAILABLE ACCELEROMETERS

by

Tom D. Finley
NASA Langley Research Center
Langley AFB, Virginia

THE EVALUATION OF SEVERAL COMMERCIALY AVAILABLE ACCELEROMETERS

By Tom D. Finley*
NASA Langley Research Center

Ten years of experience in calibrating accelerometers at Langley Research Center has revealed that often these instruments will not meet claims as advertised and that many factors affecting performance are not included in manufacturers' specifications. This has led to the accelerometer evaluation program presently underway at Langley. The purpose of the program is to aid in the effort to obtain more accurate and more reliable data from commercially available accelerometers.

This paper discloses some of the problems encountered during accelerometer calibrations and discusses some of the techniques, in particular the continuous plot, which can be used to reveal instrument errors.

The first and major portion of this paper deals with one accelerometer of the servo type, Brand A; the second part is a collection of findings on accelerometers of different types. (The names of the manufacturers are withheld to avoid prejudice and allow the reader to look objectively at the problems discussed.)

I. Brand A

Brand A servo accelerometer was the first brand to be tested in our present accelerometer evaluation program. Evaluation of this accelerometer is still incomplete. It was chosen for our first evaluation because its design features as advertised indicated conformance to Langley Research Center telemetry and general application requirements; and because this brand of accelerometer was in frequent use in ground facilities and in space payloads. Figure 1 is a sketch of a cutaway view of Brand A and figure 2 is an operational block diagram. These figures will be helpful in a discussion of the instrument's operation. The flexure-supported seismic mass, which houses two capacitor plates, moves with respect to the stationary capacitor plates when subjected to acceleration. This motion unbalances a capacitance bridge (made up of the sensing capacitors and two fixed capacitors which are not shown) and the bridge output current flows in the force coil of the seismic mass. This force coil current in the magnetic field provides the restraining force which servo controls the position of the mass. This current also flows through a range resistor which can be selected to vary the range of the accelerometer.

1. The nonlinearity and hysteresis were determined using three methods. Each method had limitations but it was felt that all would help to better determine these characteristics.

(a) The results of the first method are shown in figure 3. The instrument was ranged for $\pm 0.5g$ full scale and positioned on a dividing

*Aerospace Technologist.

head. The output was read directly on a differential voltmeter. The upper graph is a direct plot of the accelerometer's output versus the input acceleration obtained by tilting in the field of gravity. The second graph represents the deviation of the output from a best straight line. With this method it was determined that the nonlinearity was approximately 0.04 percent full scale and the hysteresis was 0.01 percent full scale.

(b) The second method employed self-test or current insertion (fig. 4). The plot shows the error between the output voltage of the accelerometer (ranged at $\pm 3g$) and the voltage across a resistor in the current insertion circuit. (The force simulating acceleration was obtained by passing a current through a compensating coil wound on the same core as the forcer coil.) This method indicated approximately 0.01-percent full-scale nonlinearity and 0.01-percent full-scale hysteresis.

(c) The third method used was the error plot technique in which two similar accelerometers (ranged at $\pm 50g$) were accelerated simultaneously on a centrifuge and the difference in the outputs of the two instruments was plotted continuously on an X-Y plotter. The plot in figure 5 shows the results obtained using this method and indicates that the difference in linearity of the two instruments was 0.015 percent full scale and the hysteresis difference between the two accelerometers was 0.005 percent full scale. Thus all three methods indicate hysteresis of 0.01 percent or less and nonlinearity of 0.04 percent or less.

2. The effects of temperature on the scale factor of the accelerometer were investigated by performing $\pm 1g$ calibrations on the instrument at $-28^{\circ}F$, $94^{\circ}F$, and $180^{\circ}F$. The scale factor change for the $208^{\circ}F$ change was only 0.001 percent/ $^{\circ}F$ (manufacturer claimed 0.02 percent/ $^{\circ}F$). The zero shift of four Brand A accelerometers is plotted in figure 6. It should be noted that one of these instruments ranged for $\pm 50g$ shifted 0.1 percent full scale which would be 10 percent full scale when ranged for $\pm \frac{1}{2}g$.

3. The dynamic characteristics of the accelerometer are a function of the load resistor (fig. 7). The curves show that as the load resistor increases (i.e., the range decreases) the natural frequency decreases and the damping ratio increases. (The data shown are based on ± 5 -volt full-scale output.) Figure 8 shows the resulting change in response of the instrument when ranged for $\pm 0.5g$ and when ranged for $\pm 50g$. In the latter case the response is flat within ± 5 percent to 400 cps while in the former the flat response extends to only 10 cps. It should be noted that if less output is permissible (a smaller load resistor) the wider flat-frequency response can be maintained.

4. Damping stability - Tests were also performed on the accelerometer to determine the change in frequency response with temperature and vacuum. Figure 9 shows the accelerometer's frequency response under atmospheric pressure at $78^{\circ}F$, atmospheric pressure at $175^{\circ}F$, and 0.02 psia at $78^{\circ}F$. There was no change in response. This dynamic stability constitutes a notable advantage over many other types of instruments.

5. Damping technique - One unit was available for testing on which the hermetic seal had accidentally been broken. The portion of damping force due to the air in the instrument was determined from the frequency response at pressures of 1 atmosphere and 1 mm Hg. (The manufacturer claimed that the instrument was electrically damped.) The results are shown in figure 10. Ranged $\pm 50g$, the accelerometer changed from 0.8 critical to almost zero damping with the removal of the air. Ranged at $\pm 1g$ the accelerometer changed from 1.5 to 0.25 critical damping which indicated that, although there is a small amount of damping due to other factors, most of the damping developed was from the encased gas (or air).

6. The input voltage was one factor which affected the accelerometer's frequency response. The manufacturer rates the instrument at an input voltage of 28 volts d-c ± 10 percent. Figure 11 shows the frequency response and natural frequency changes when one unit was calibrated at 26 volts, 28 volts, and 30 volts. Note that the response varied as much as 20 percent near the natural frequency. From tests on several other samples it was found that the magnitude of the change was greater on underdamped units.

7. The amplitude of the imposed dynamic acceleration also affects the frequency response of the accelerometer (fig. 12). The response of a $\pm 50g$ instrument varied as much as 20 percent near the natural frequency when calibrated at $1g$ and at $50g$. Determination at $1g$ and at $10g$ differed by less than 2 percent. The amplitude effects on dynamic response were accompanied by progressively greater distortion above about $20g$. The peak value of the output waveform was only approximately 1.25 times the rms value when subjected to $50g$ sinusoidal vibration.

8. The problem of mounting resonances was investigated by plotting the instrument's response from 10 cps to 10 kc. On several Brand A accelerometers the response remained below 10 percent above 500 cps. On another unit the output increased to 5.6 times the input at 5700 cps (fig. 13).

9. The electrostatic attraction between the capacitor plates of the accelerometer can present a problem. When the instrument was ranged to $\pm \frac{1}{2}g$ the servo loop gain was so low that when the power was applied to the accelerometer, the seismic mass would remain against one of the fixed capacitor plates. Under these conditions the output voltage would go to 13 volts and the instrument would remain inoperative until the mass was shaken loose or power was removed and applied while the instrument was in another position. The manufacturer suggests the use of zener diodes to remedy this problem.

10. Tests performed employing current insertion in the compensation coil provided an accurate measure of the variation in output current per g with a large change of range resistor, 500 to 50,000 ohms ($\pm 50g$ and $\pm 0.5g$, respectively). The difference between the output current and a fraction of the insertion current was plotted against the value of the inserted current (similar to fig. 3). The inserted current simulated acceleration. Of the two units tested, the output current per g of one accelerometer increased 1 percent and the other decreased the same amount. Thus, for greater accuracy, range resistor changes on the accelerometer should be followed by calibrations or the accelerometer

should be calibrated originally with several range resistors to permit future range changes in the field.

11. The accelerometer's sensitivity to acoustic noise was in question because of the configuration of the seismic mass and the gas coupling. Acoustic noise from 20 to 2000 cps at levels of 120 to 140 dB was imposed on an accelerometer ranged $\pm 5g$ and ranged $\pm 50g$. The effect was small and the data fell within the experimental error of the tests.

12. The scale factor change with input voltage variation was determined on several different ranges. With a ± 10 -percent change in the input voltage (tolerance given by the manufacturer) sensitivity of an accelerometer ranged at $\pm 0.5g$ changed approximately 1 percent. The higher ranges were less affected.

13. Some preliminary life tests have been conducted on Brand A accelerometers. The units were subjected to a two-axis vibration of 8g to 10g peak and frequencies from 10 cps to 2000 cps. One unit suffered a failure after 70 hours. Another unit was placed in the environment and failed after 14 hours. In the final test in this series a sample of this accelerometer from a lot recently delivered to Langley was subjected to this environment for 1000 hours with no effect on performance.

II. The following is a collection of findings on accelerometers of different types:

Brand B Servo Accelerometer

The instrument was lightweight, 1.7 ounces, and relatively inexpensive. The sample tested was a $\pm 1g$ unit with a full-scale output of ± 7.5 volts. The unit was placed in a $\pm 10g$ vibration field for 1000 hours, suffered no failures, and later repeated its original calibration. The frequency response was flat within ± 15 percent to 170 cps. In terms of static response the linearity was 0.03 percent and the hysteresis 0.16 percent. One very serious effect occurred when the negative input voltage was reduced (the manufacturer recommends a ± 15 -volt d-c input power ± 15 percent). When the negative voltage was reduced 15 percent the $-g$ sensitivity decreased approximately 10 percent (fig. 14).

Brand C Servo Accelerometer

This $\pm 3g$ unit had a 0- to 5-volt d-c output and a 28-volt d-c input. The unit was found to have flat frequency response ± 2 percent to 120 cps and ± 10 percent to 400 cps. The static calibration repeated within 0.1 percent after approximately 1000 hours in a 10g vibration field. There was a region near 300 cps where the output displayed noticeable distortion.

Brand D Servo Accelerometer

Brand D air-damped servo accelerometers, although much lighter and less temperature sensitive than the oil-damped units, had unusual dynamic characteristics. The frequency response dropped off and then rose in the region of the natural frequency. A very serious defect in the instrument was its fragile bearing structure. After the units were subjected to dynamic calibrations near

their natural frequency, the output waveforms were distorted (fig. 15). The manufacturer said that the bearings had been fractured and stated "We wish to stress to you . . . that we do not recommend high gain electrically damped units to be used for relatively high g vibration studies." It should be noted, however, that the failure occurred during a calibration within the amplitude and frequency range of the instrument as specified in the manufacturer's literature.

Brand E Strain-Gage Accelerometer

These liquid-damped unbonded strain-gage accelerometers are in wide use at Langley because of their size, weight, simplicity, and cost. Most of these units perform satisfactorily but many have displayed difficulties because of trash and gas bubbles in the damping fluid. Reproduced in figure 16 is an X-ray photograph of two transducers which plainly shows the presence of gas bubbles. Figure 17 shows continuous plots of a Brand E accelerometer output versus acceleration imposed on a centrifuge. The malfunction was repeatable and was caused by trash or debris in the damping fluid. It should be noted that these malfunctions would be very difficult to discover without the use of a continuous plot. Figure 18 represents a direct plot of the output of a Brand E accelerometer versus acceleration. These excursions were not repeatable and it is presumed that they are caused by a bubble in the fluid. Figure 19 shows a continuous plot of the frequency response of another Brand E accelerometer. As the plot was proceeding, the shaker was inverted, righted, and inverted again. The gas bubble thus passed over the seismic mass giving a changing response.

Conclusions

1. Accelerometer acceptance tests should include tests for the following characteristics:

(a) Distortion:

(1) Static - Discontinuities can result from trash and air bubbles in the damping fluid.

(2) Dynamic - Damaged bearings, air bubbles, and nonlinear damping can cause poor wave shapes or unstable frequency response.

(b) Damping Stability - The instrument should be calibrated under vacuum to determine if the seal is sufficient to maintain damping (either air or liquid).

(c) Resonances - The instrument's response should be continuously plotted to 10 kc or higher to disclose any mounting or spurious resonance.

(d) Scale factor vs. input voltage.

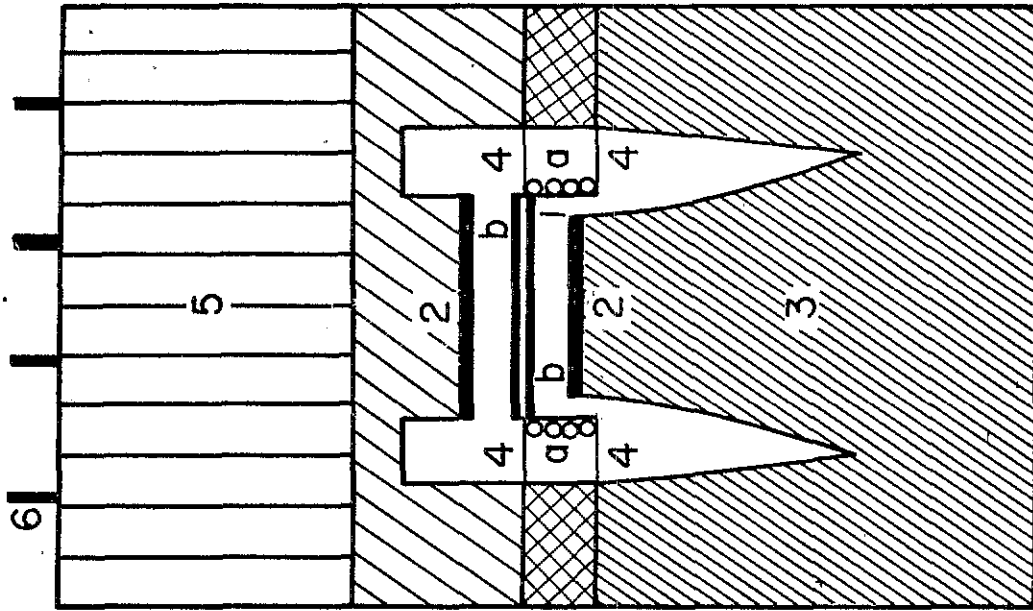
(e) Damping vs. input voltage.

(f) Damping vs. amplitude.

2. The following techniques can be used effectively to detect faults in accelerometers:

(a) X-rays of liquid-damped instruments.

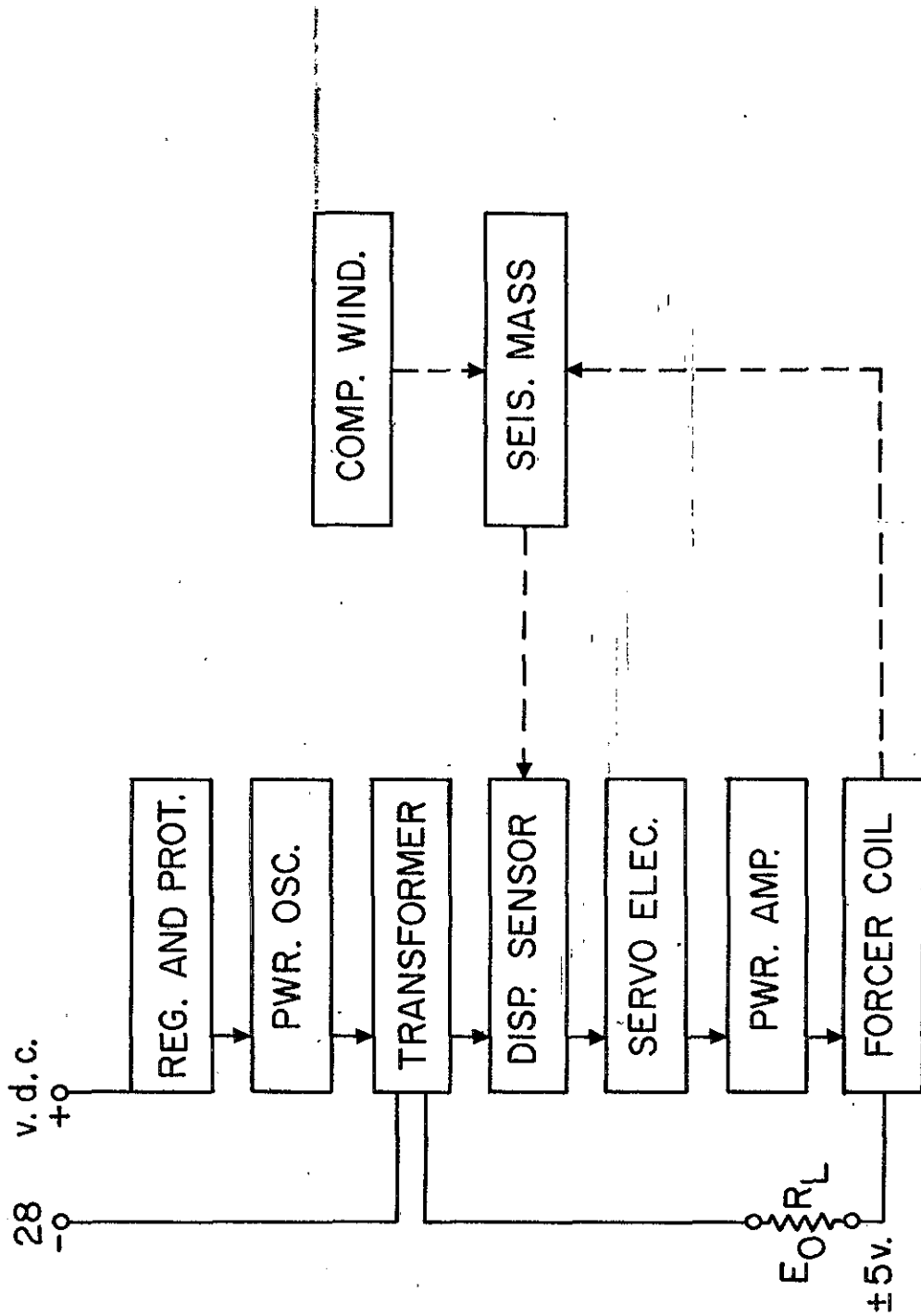
(b) Continuous X-Y plotting (Dynamic and Static) - Many of the problems discussed in this paper would have been virtually impossible to detect without the use of this technique.



1. SEISMIC MASS
 - a. FORCER COIL AND COMP. COIL
 - b. MOVING PLATES
2. FIXED PLATES
3. MAGNET
4. FLEXURES
5. ELECTRONICS
6. EXTERNAL CONNECTIONS

NASA

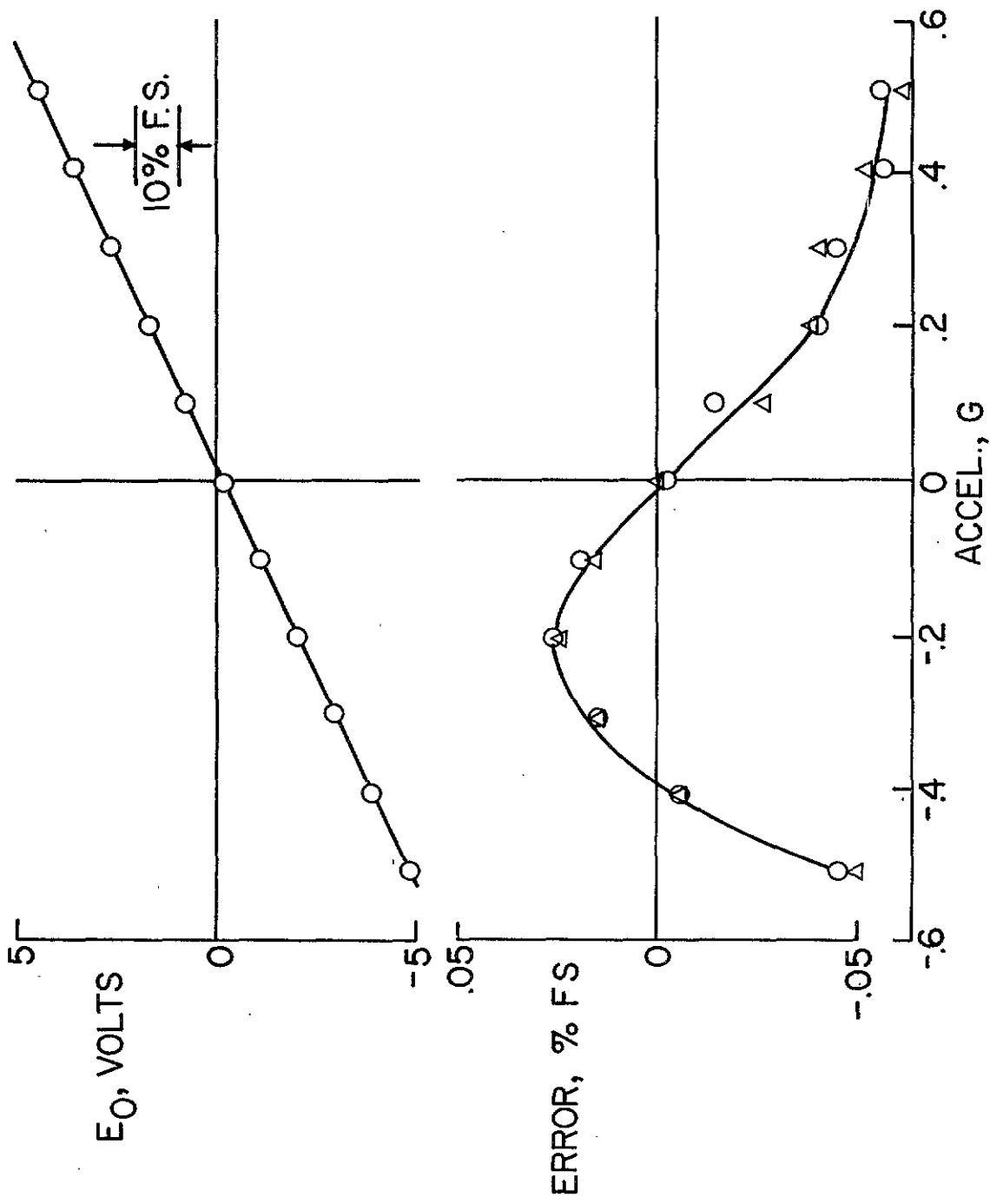
Figure 1.- Brand A - Cutaway view.



8-A

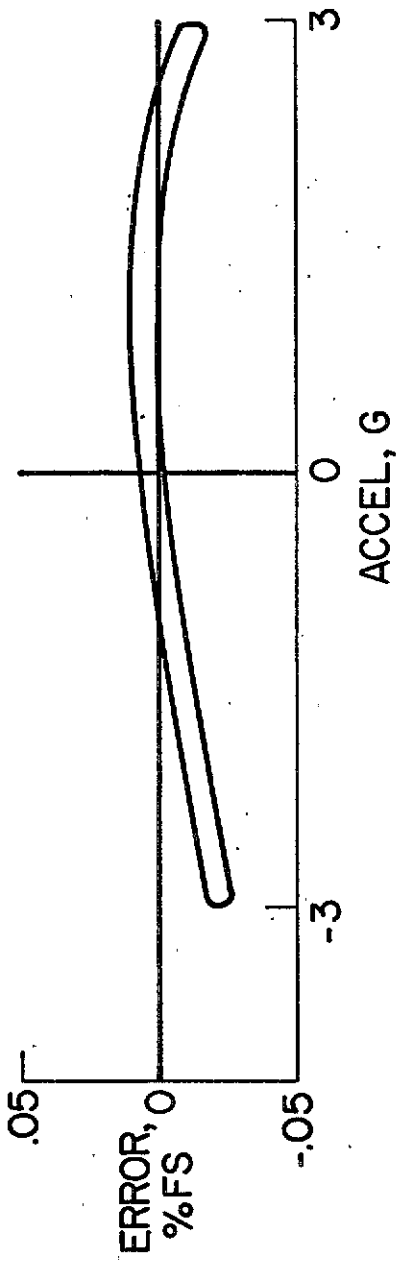
NASA

Figure 2.- Brand A - Operational block diagram.

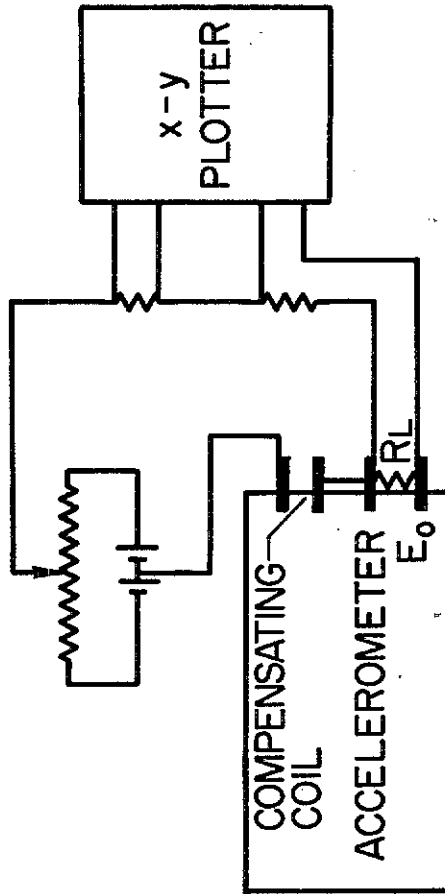


NASA

Figure 3.- Brand A - Nonlinearity and hysteresis, direct calibration.

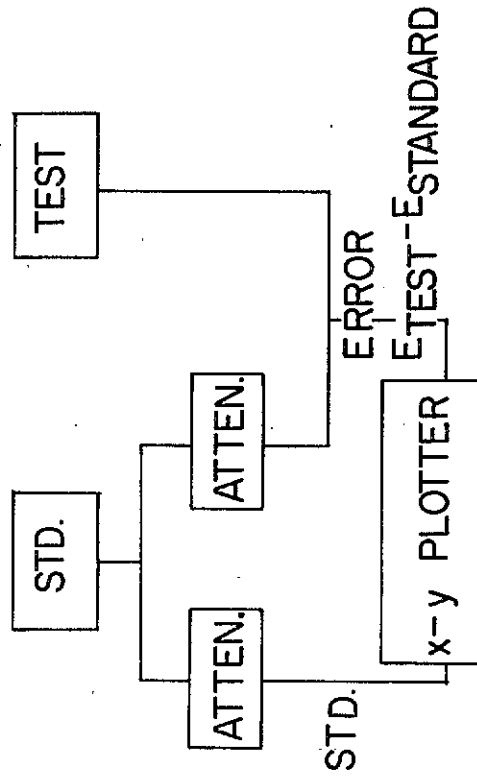
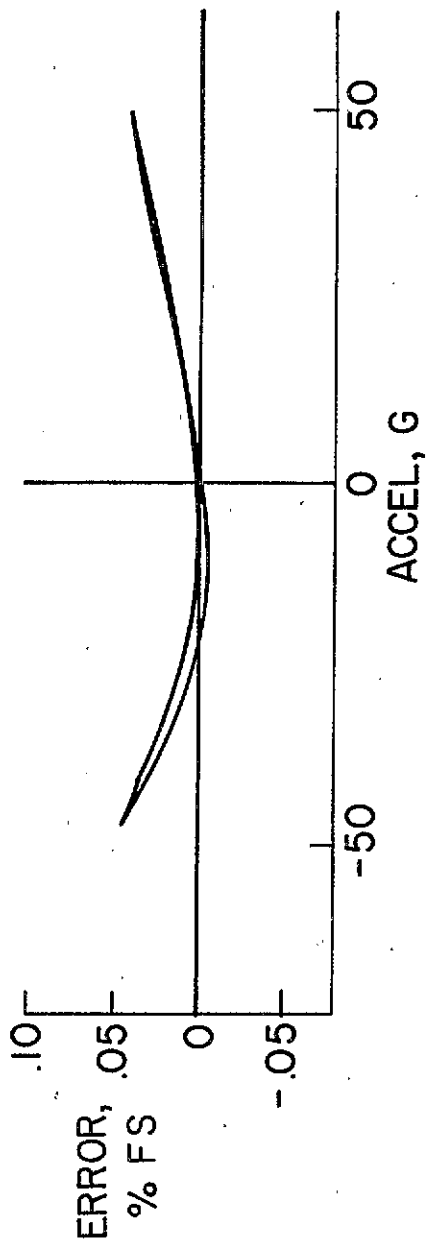


V-10



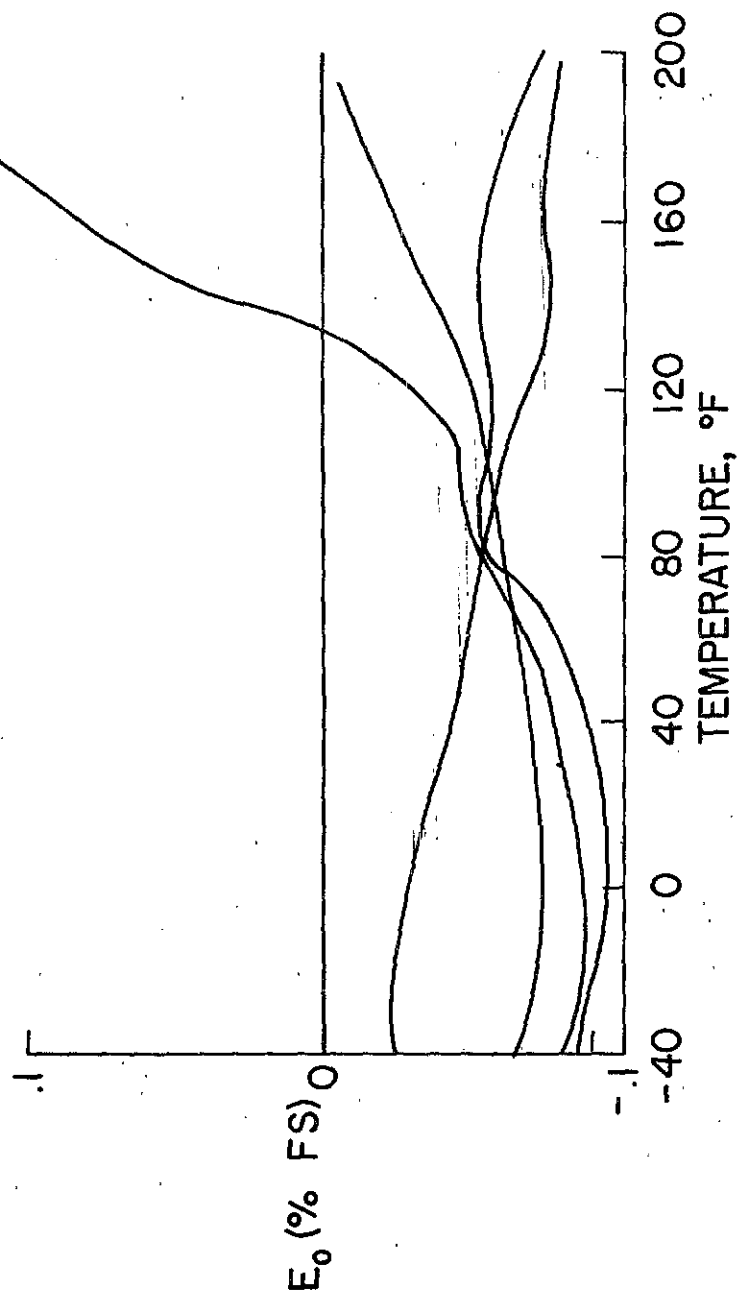
NASA

Figure 4.- Brand A - Nonlinearity and hysteresis, self test.



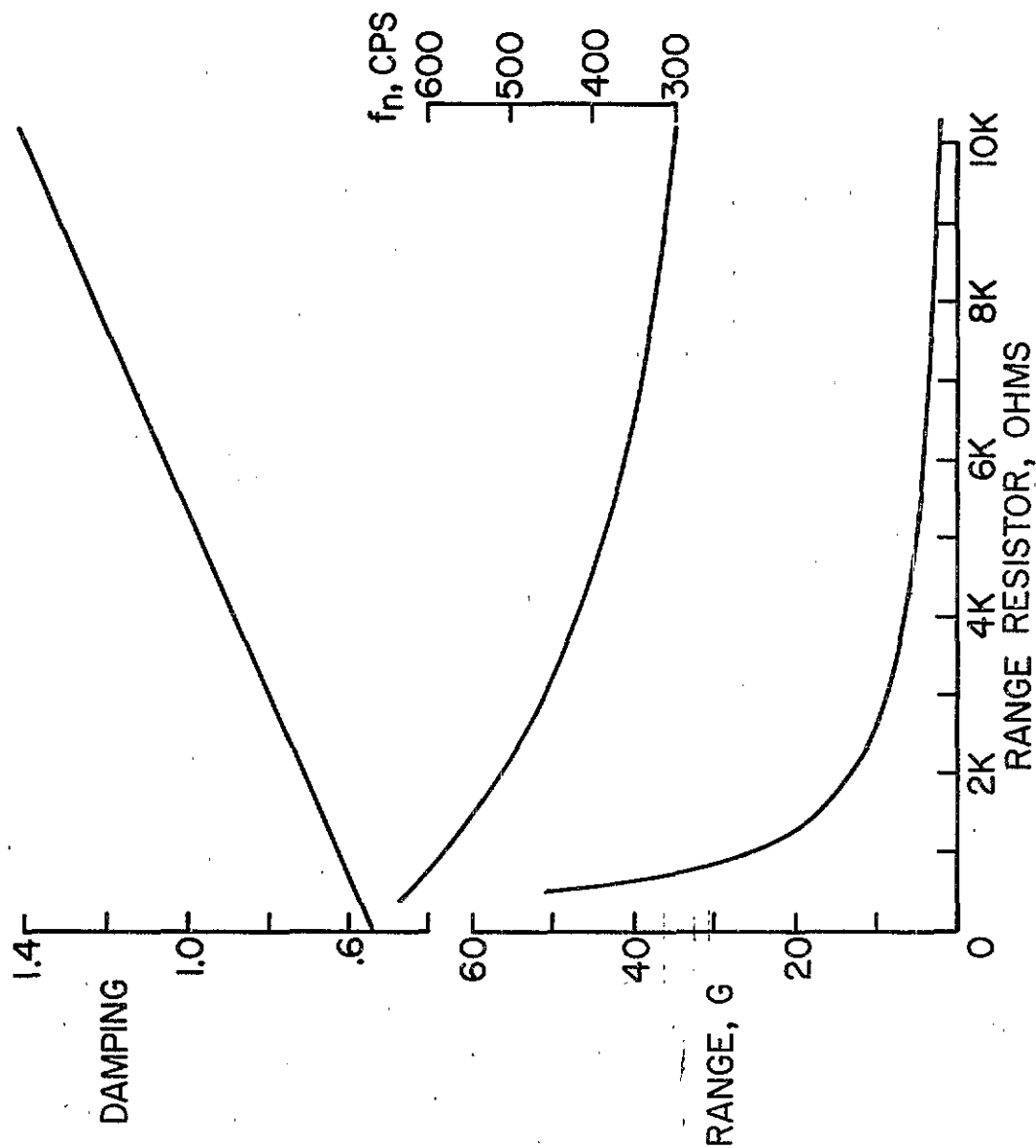
NASA

Figure 5.- Brand A - Nonlinearity and hysteresis, error plot.



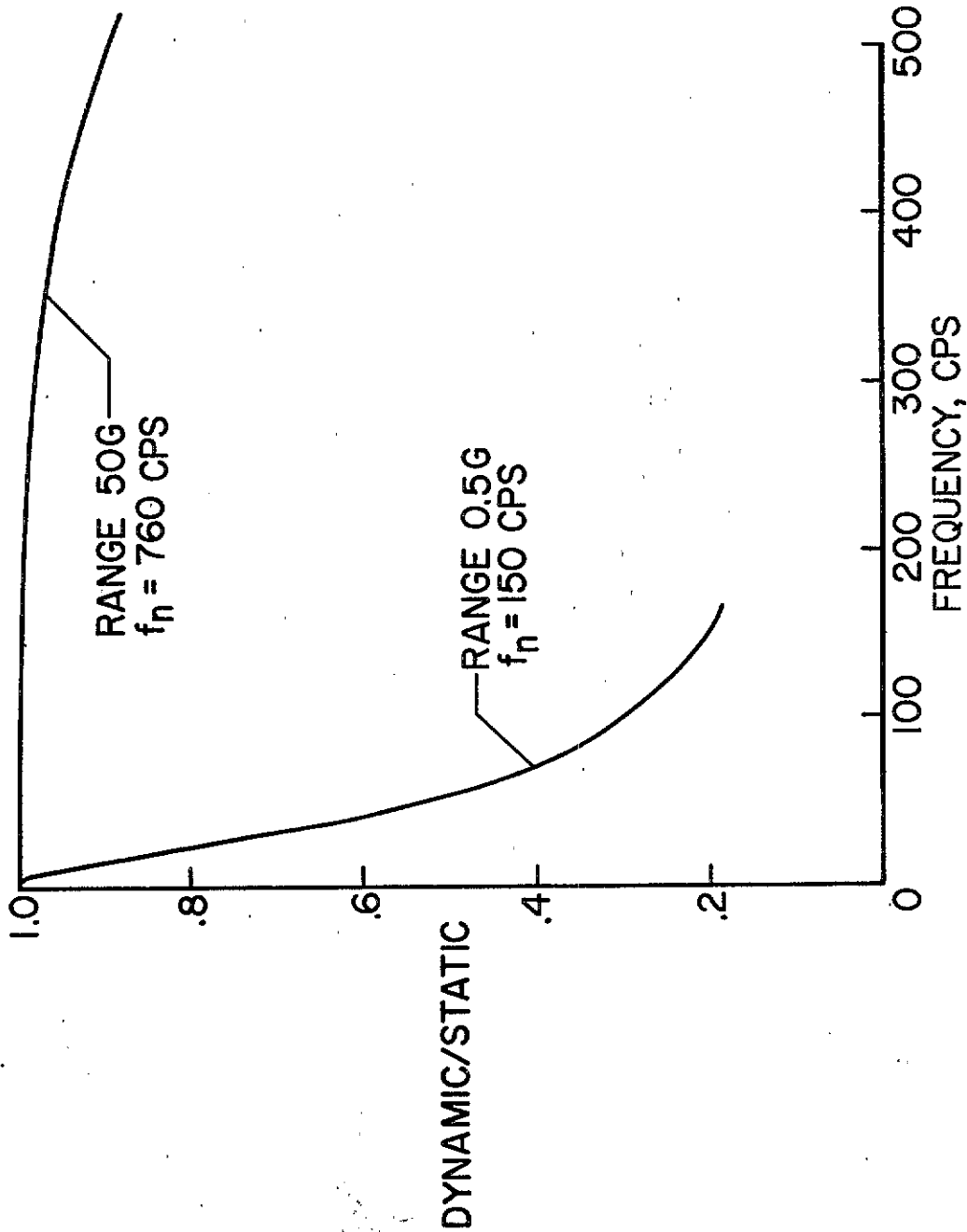
NASA

Figure 6.- Brand A - Temperature zero shift.



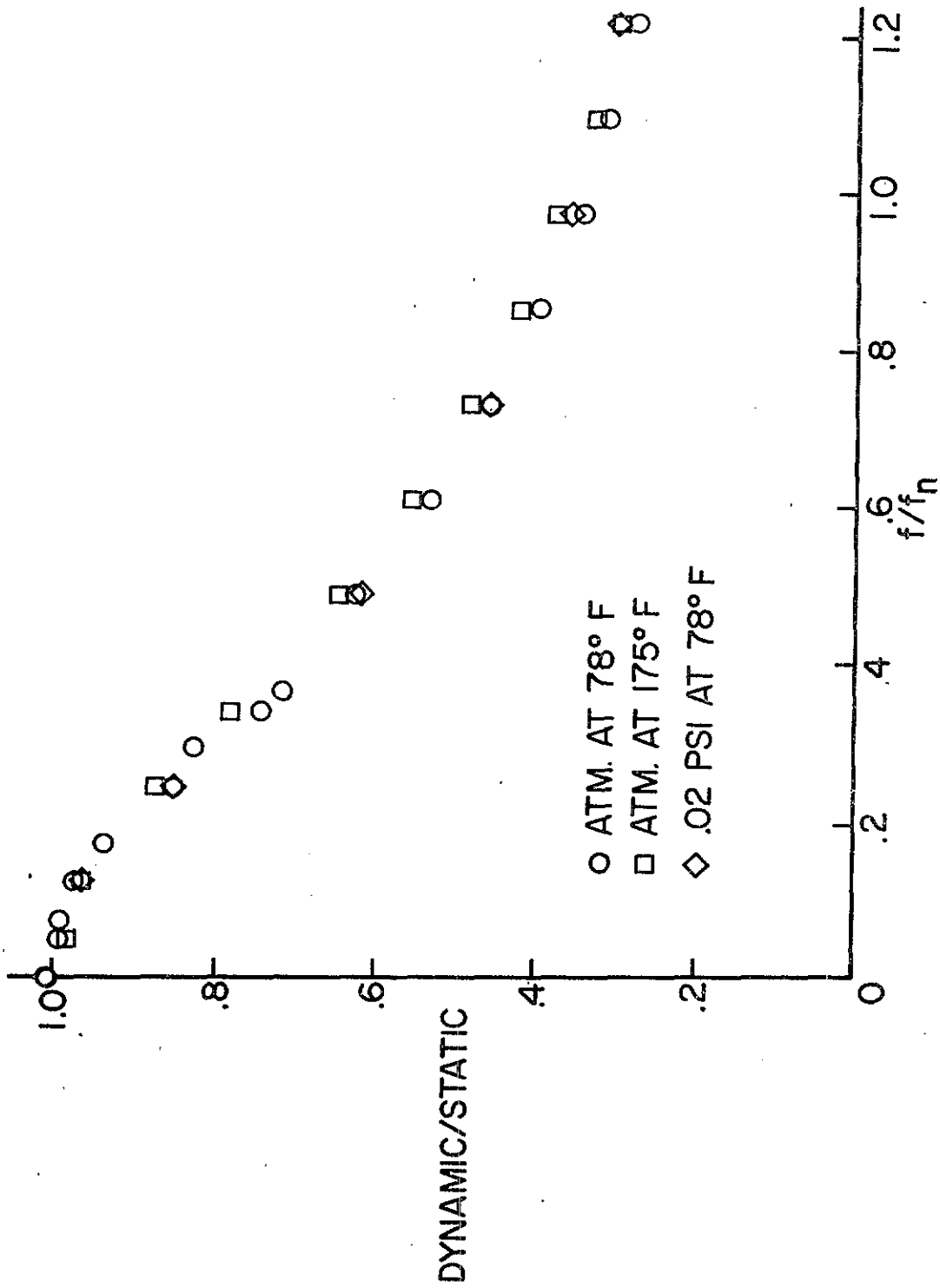
NASA

Figure 7.- Brand A - Dynamic characteristics.



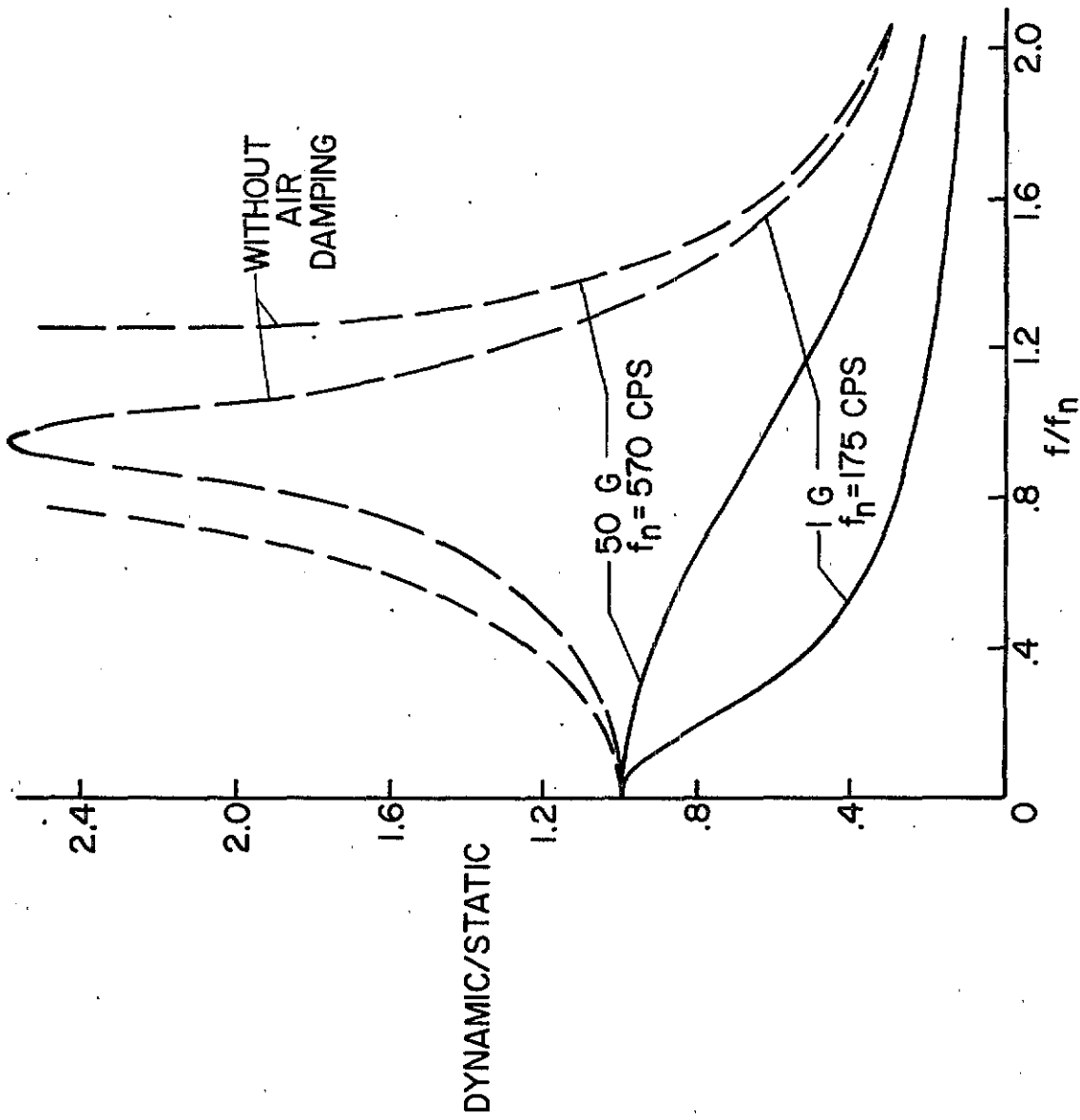
NASA

Figure 8.- Brand A - Frequency response at different ranges.



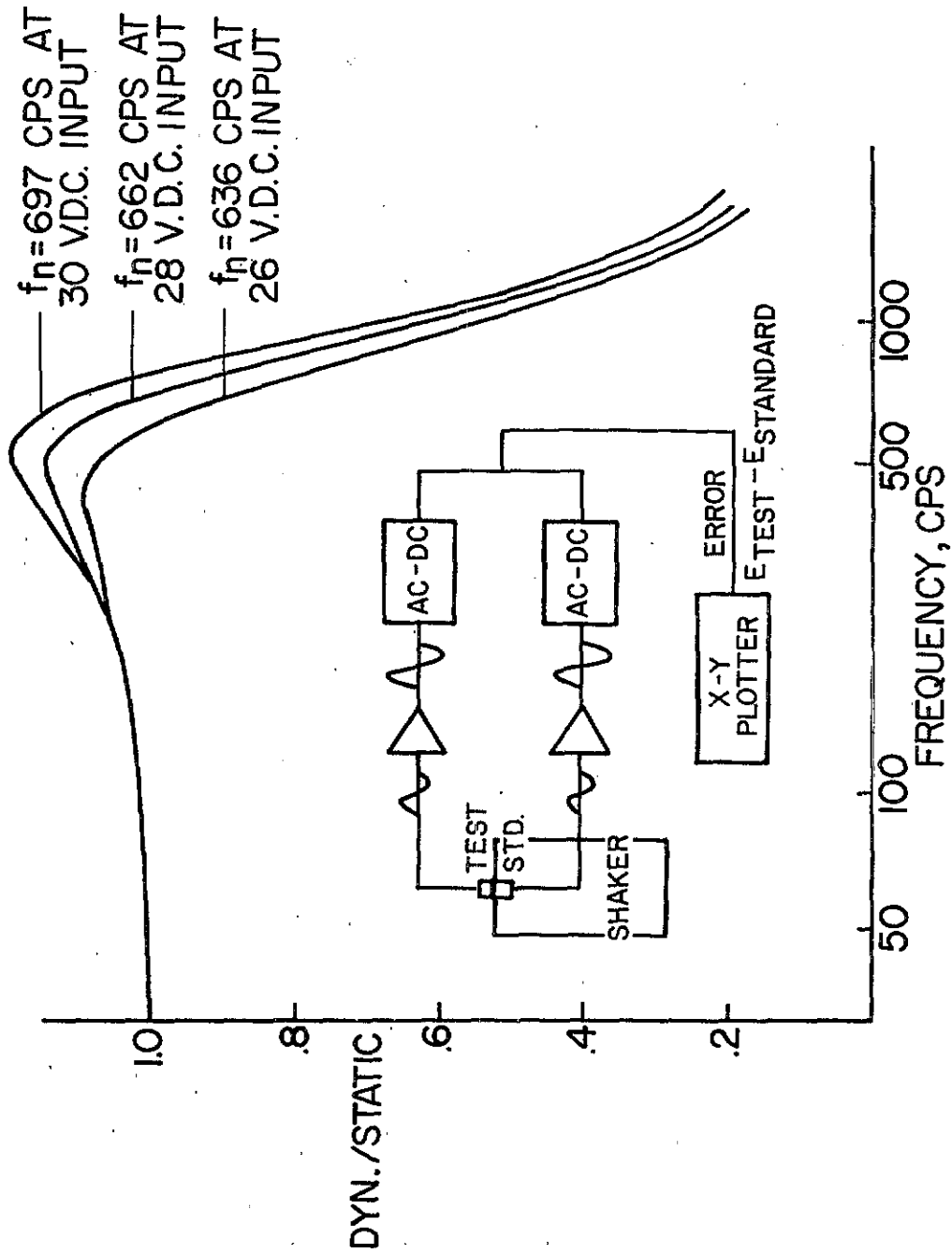
NASA

Figure 9.- Brand A - Damping stability.



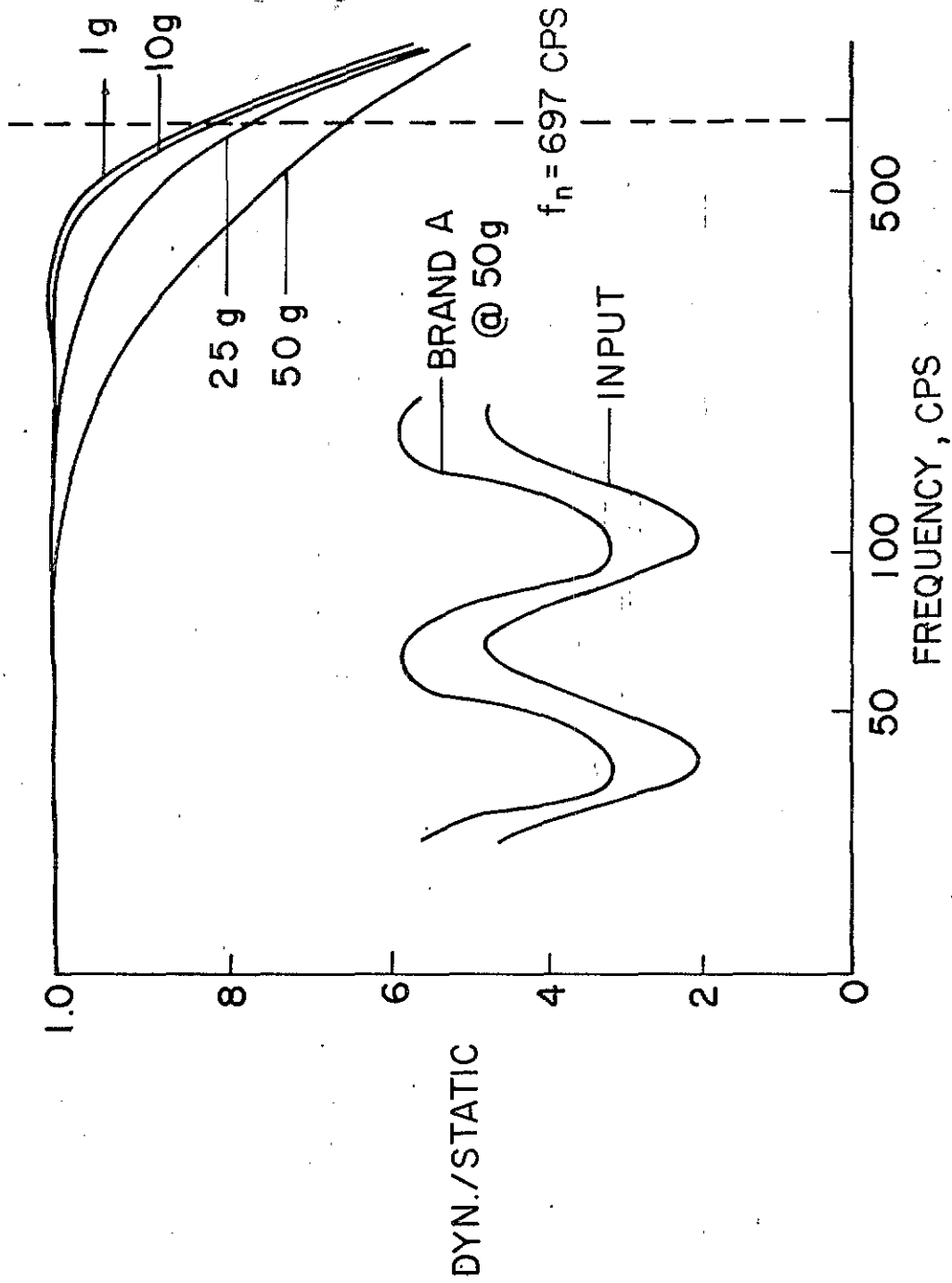
NASA

Figure 10.- Brand A - Damping technique.



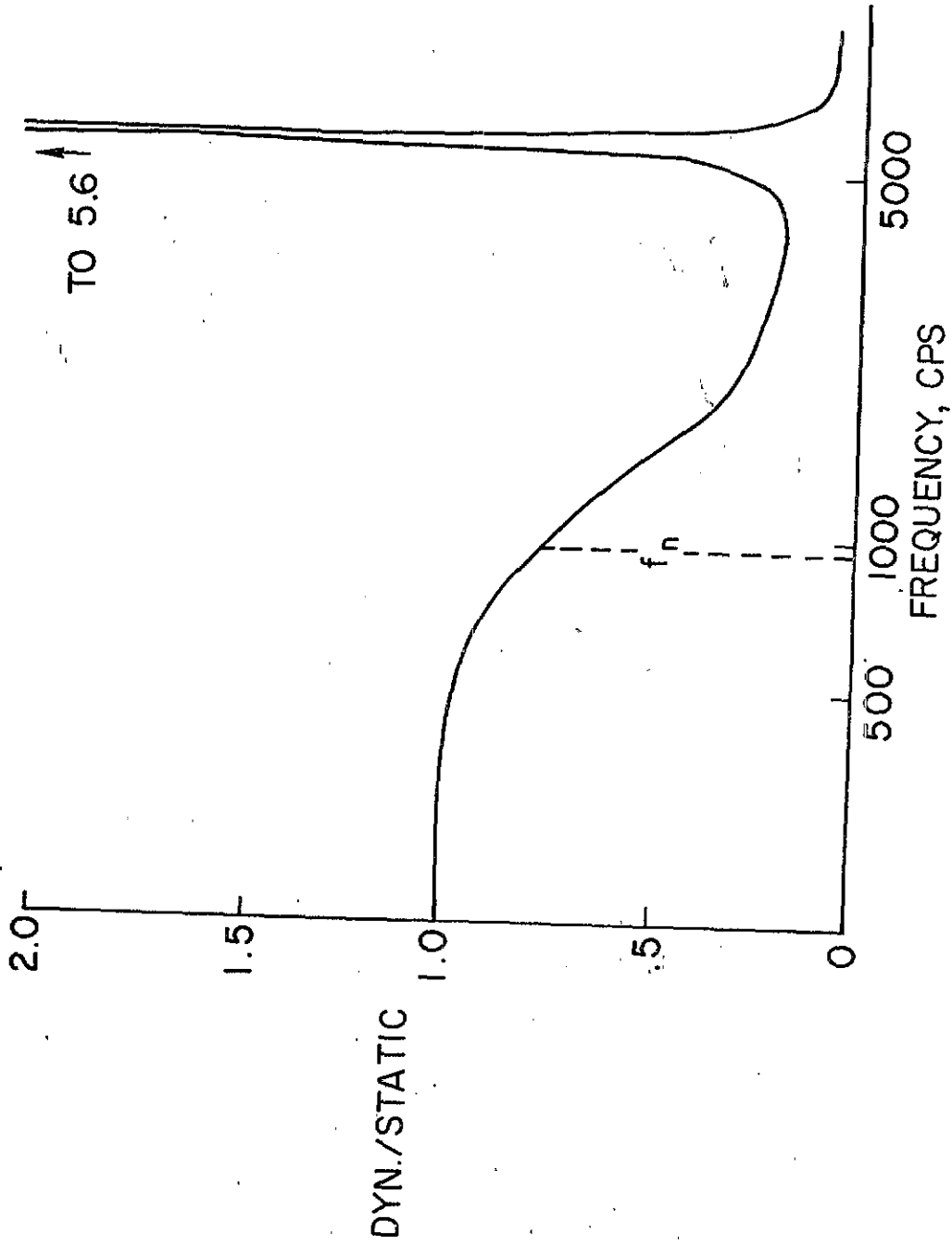
NASA

Figure 11.- Brand A - Damping versus input voltage.



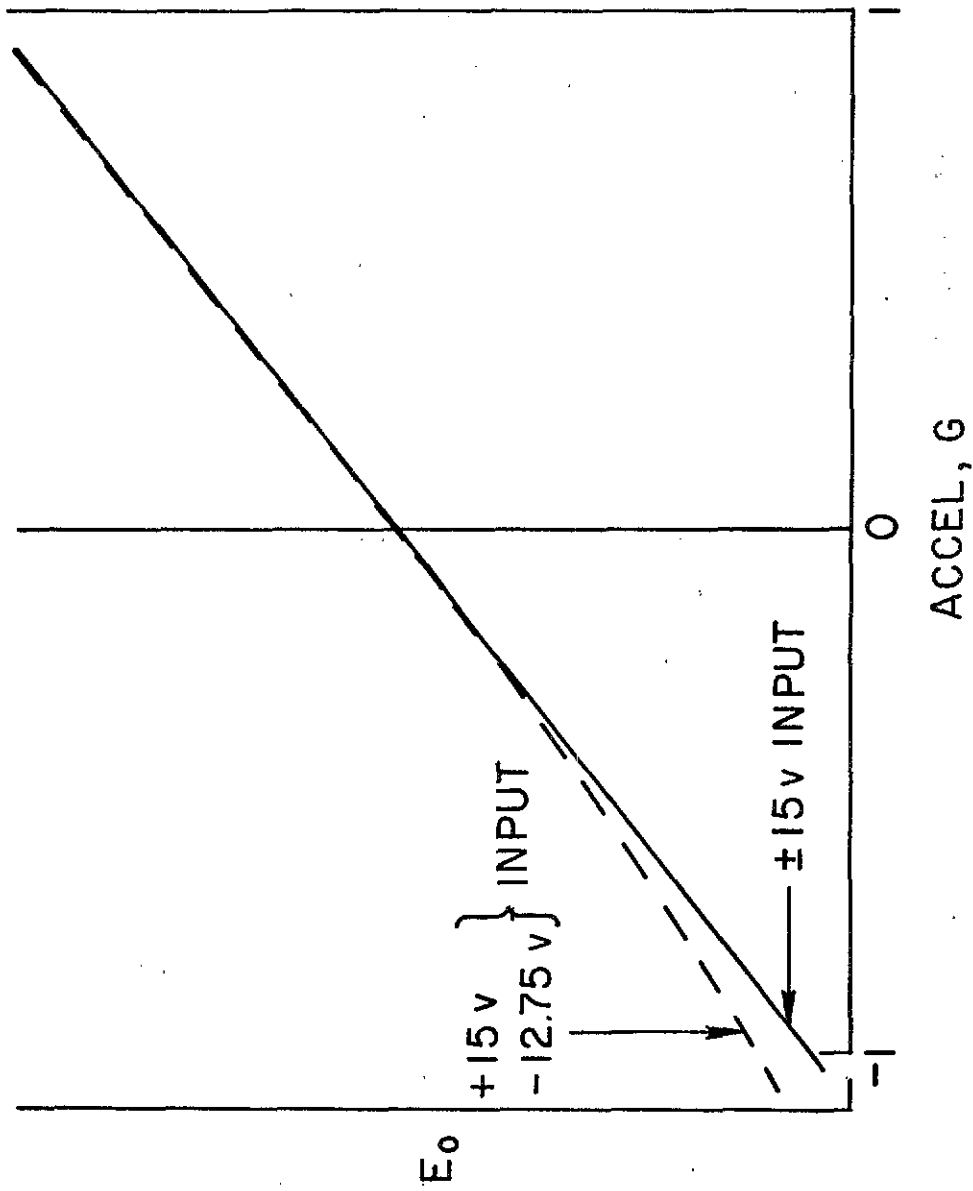
NASA

Figure 12.- Brand A - Damping versus amplitude.



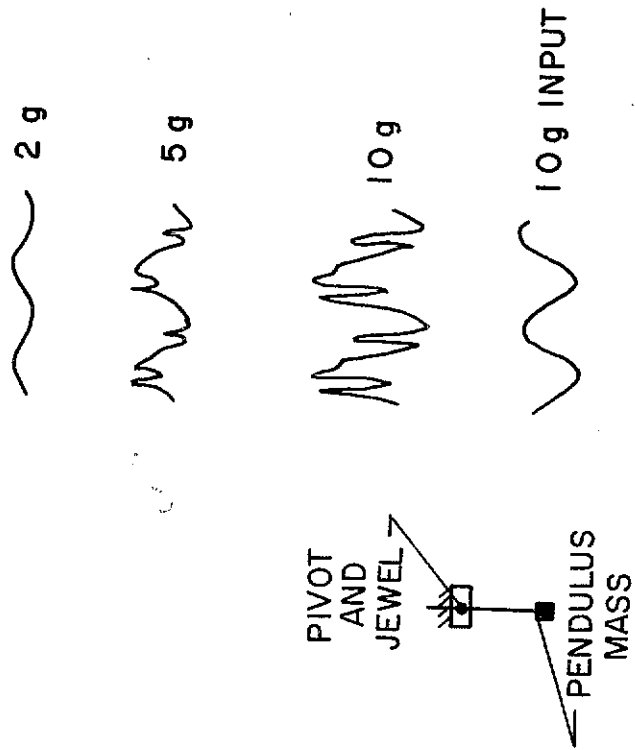
NASA

Figure 13.- Brand A - Mounting resonance.



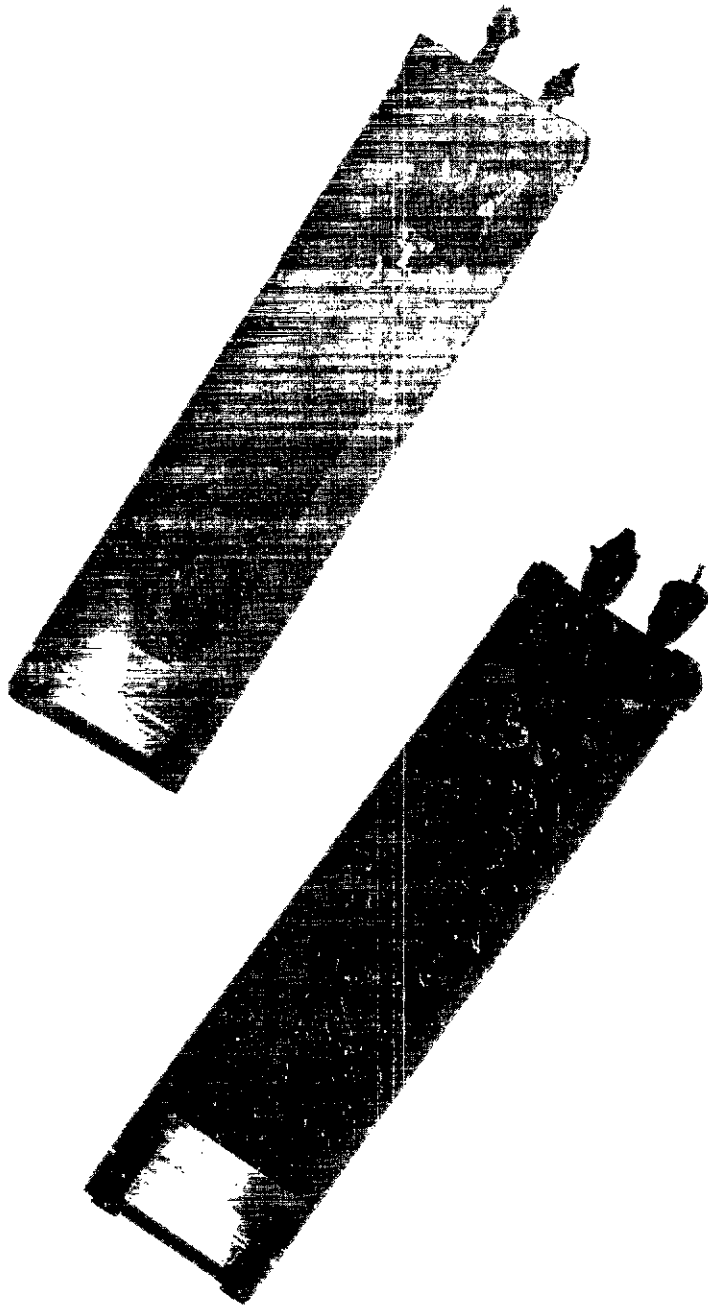
NASA

Figure 14. - Brand B - Sensitivity change with input voltage variations.



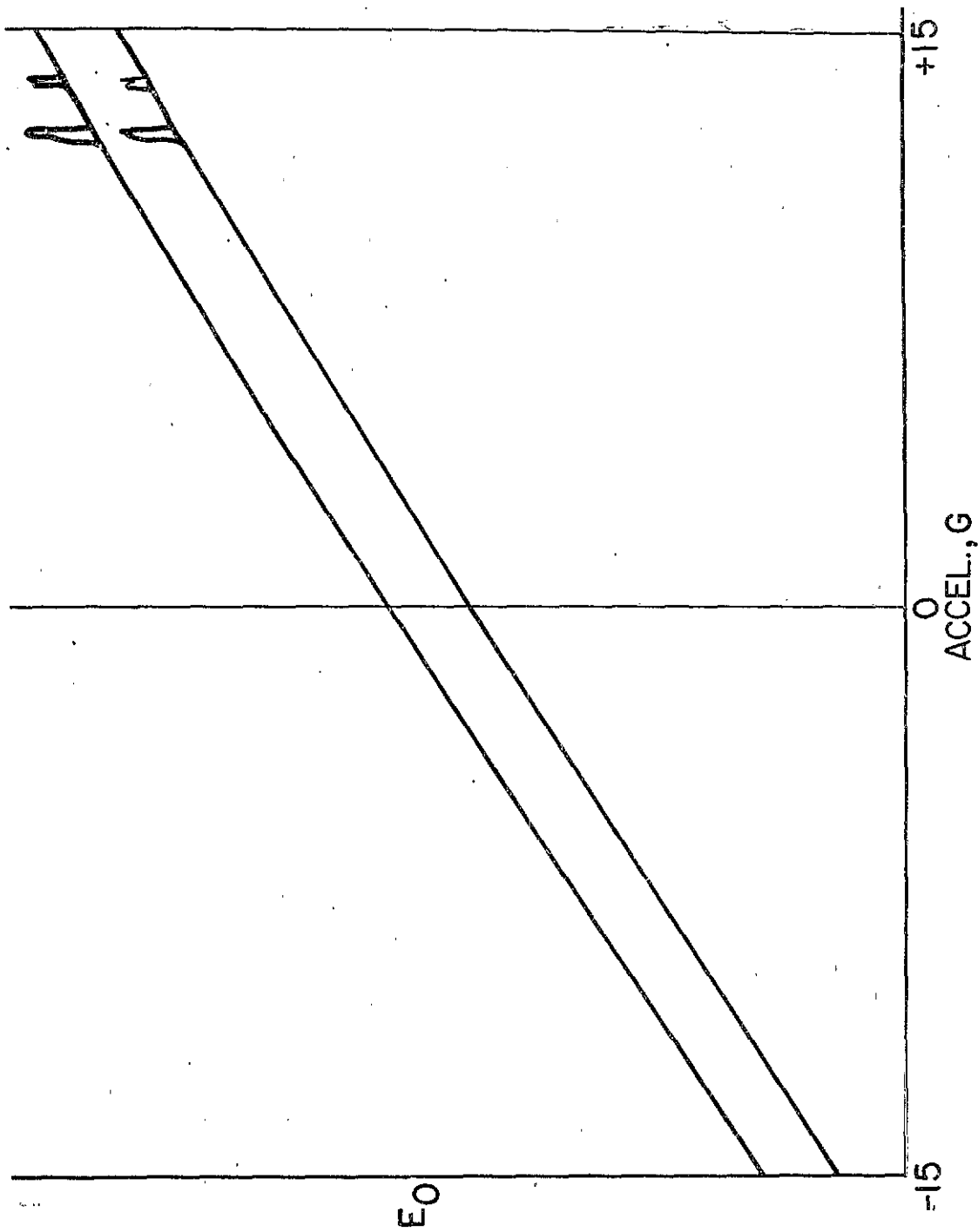
NASA

Figure 15.- Brand D- Dynamic distortion.



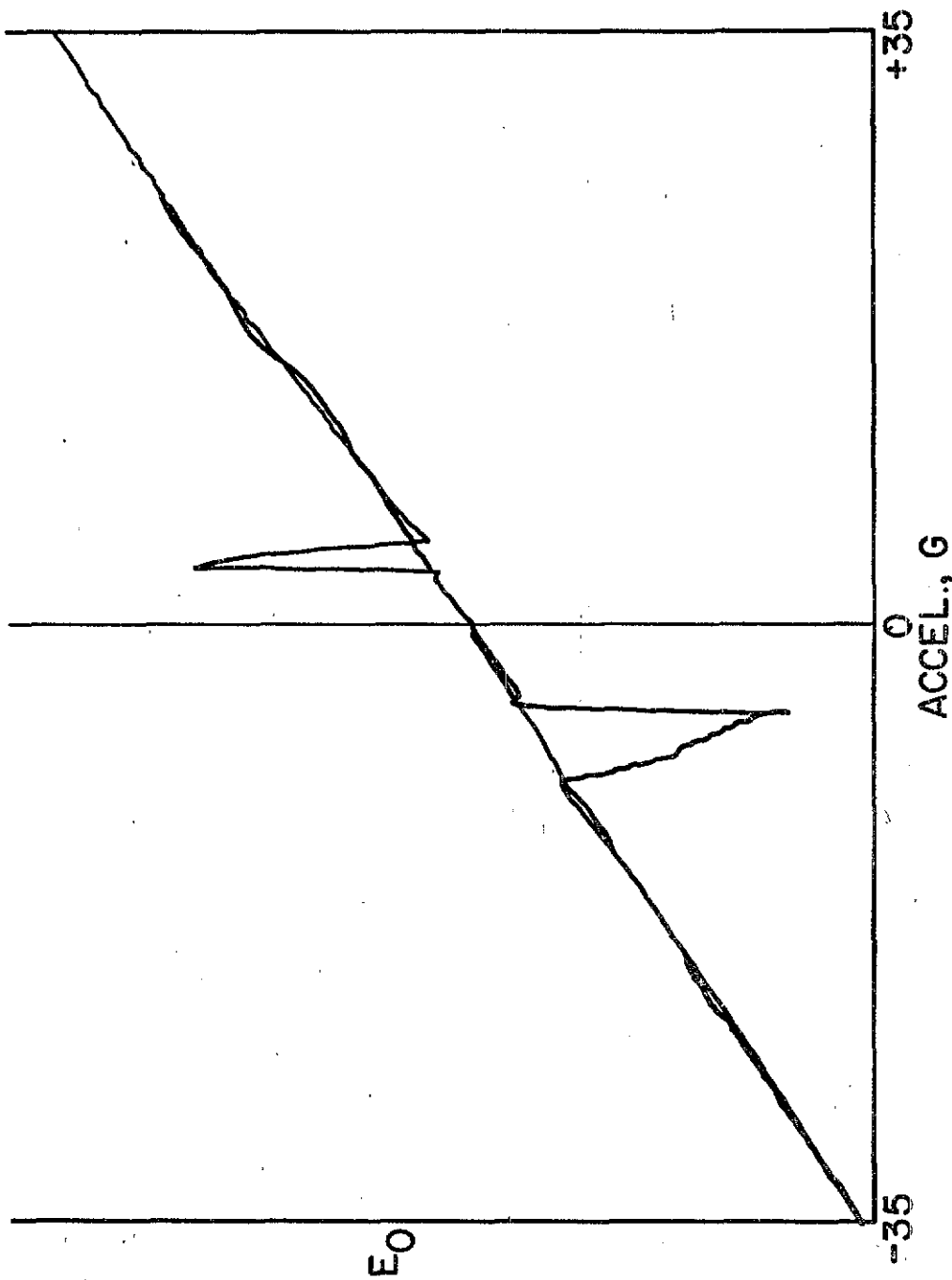
NASA

Figure 16.- Brand E - X-ray showing gas bubbles.



NASA

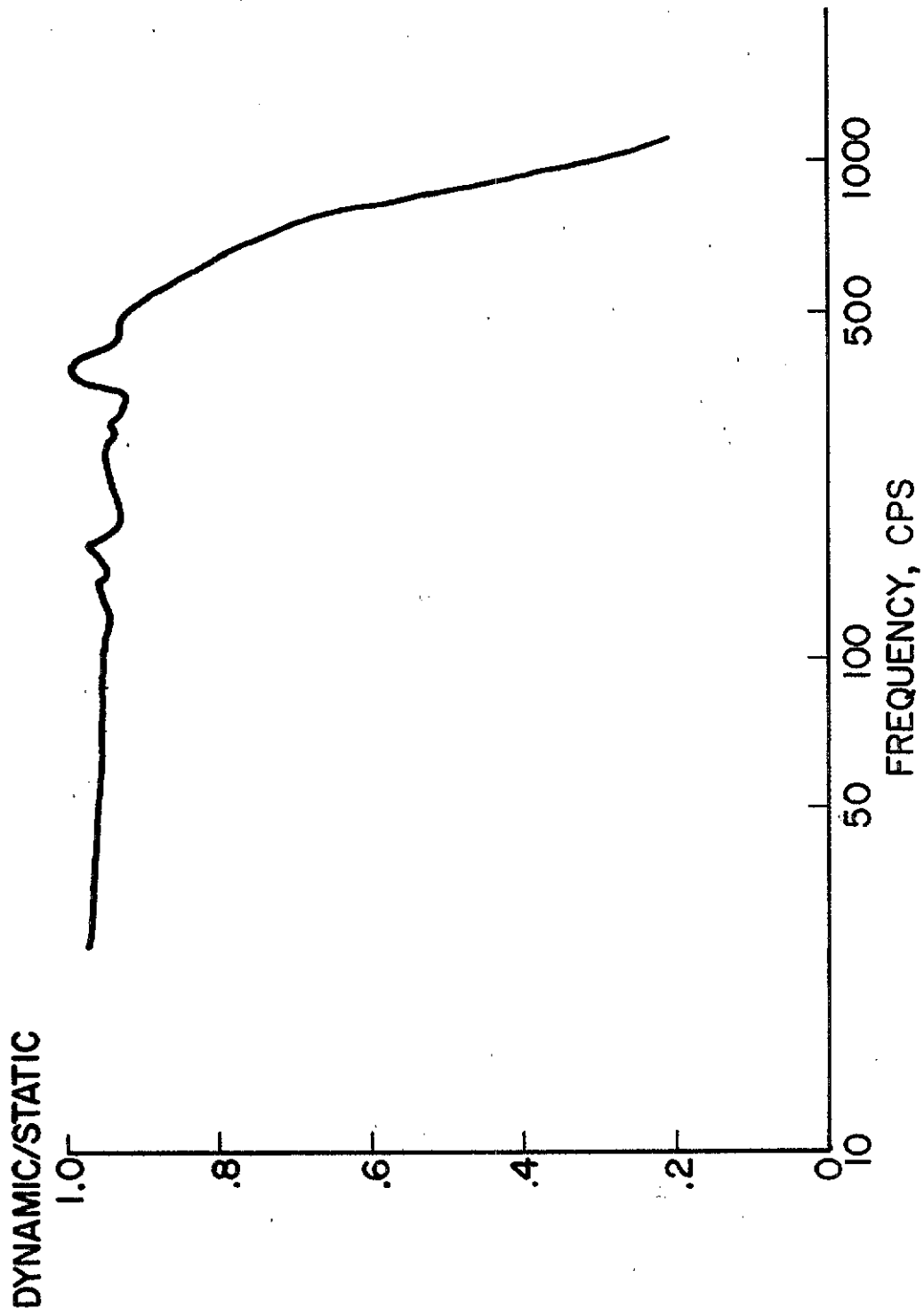
Figure 17.- Brand E - Continuous direct plot, static.



NASA

Figure 18. - Brand E - Continuous direct plot, static.

V-24



NASA

Figure 19.- Brand E - Continuous plot, dynamic.

SECTION VI

RECENT DEVELOPMENTS IN THE
SEMICONDUCTOR TRANSDUCER FIELD

by

H. Chelner
North American Aviation, Inc.
Canoga Park, California

RECENT DEVELOPMENTS IN THE
SEMICONDUCTOR TRANSDUCER FIELD

by

H. CHELNER
North American Aviation, Inc.
Canoga Park, California

ABSTRACT: A number of pressure, force, and fluid velocity semiconductor strain gage transducers have been developed over the past four years by the Rocketdyne Research Instrumentation Group. These transducers are specifically designed for investigations into rocket engine problem areas. Many of the transducers are miniature. They have been installed inside of the rocket engine obtaining measurements at positions that were heretofore inaccessible. Others are exceptionally durable and are used to obtain measurements in severe environments. All of the transducers were designed for a specific application but are not limited by their design and are capable, with minor modifications, of presenting solutions to a number of instrumentation problem areas.

There are two characteristics of semiconductor gages which permit designs leading to greatly improved performance. The first is the high gage factor which is approximately 100 to 200 as compared to the 2 to 4 obtained from conventional wire gages. Secondly, the semiconductor nature

of the gage permits usage of technology which allows miniaturization. The end product is a very high frequency, low mass, acceleration insensitive, product.

The one big disadvantage of semiconductor gages is their temperature sensitivity. Temperature stabilization has been under study for many years with the resulting development of a number of compensation techniques.

The following transducers are some of those developed specifically to answer research project needs. Their design objective, design, and characteristics will be discussed as well as some of their applications. The PE-60 HDN is a medium frequency ($f_n=20\text{KC}$) temperature compensated probe pressure transducer especially useful for chamber pressure measurements. Its long $1/8$ " diameter probe is pressure sealed against the measuring media with two O-rings, the probe tip being erodable, contourable, and replaceable. This transducer has proved to be very rugged and durable having a history of survival through severe explosions and liquid oxygen fires.

A miniaturized version of the probe transducer is the PE-621 HDN. This transducer has a natural frequency of approximately 50 KC and is small enough to be mounted in the injector ring of a rocket engine. A number of transducers located across an injector are used to determine the type and characteristic frequencies of instability in a rocket engine.

For very high frequencies, the PE-40 HDN diaphragm type miniature semiconductor pressure transducer is used. The transducer is 1/4" in diameter, weighs less than 3 grams, has a natural frequency in excess of 100 KC, and is relatively insensitive to acceleration in all planes. It is thin enough to mount inside and normal to the surface of impellar blades, a number of transducer monitored continuously being capable of describing the dynamic pressure loading on the blade. These transducers have also been successfully mounted in the fuel ring groove of a rocket injector. When used in conjunction with the PE-621 HDN transducers, they define the coupling between the feed system and the combustion zone thereby qualifying the relative stability of an injector design.

The SLC-10ADNB is a low compliance semiconductor load cell especially useful in defining the pulse mode of space engines. Present models being used at Rocketdyne have a spring constant of approximately 1.4×10^6 lbs/in and are designed to operate at the 25 pound force range with 15 millivolts output. A very new innovation in force measuring techniques is the SLC-20 ACC. By design, all force applied to this transducer is supported directly on the surface of four transverse piezo resistive gages. The result is a minimizing of the compliant section thereby producing increased frequency response and or output voltage.

For high frequency fluid velocity measurement, the SFVS-20AFW has proven exceptionally useful. This transducer utilizes four longitudinal piezo resistive gages in a fully active bridge configuration diffused into a small cantilevered silicon wafer. The transducer has a natural frequency of 20,000 cycles in air. It has been used to measure high frequency fluid velocity oscillatory phenomena in single pulse and continuous pulse feed systems. These tests were designed to characterize the resulting natural frequencies and wave modulations with a computer program in order to obtain modeling factors for bends, constriction, etc., in typical rocket engine feed systems.

Additional designs and new concepts are presently being formulated or are on the drawing boards. In the application and usage of the semiconductor strain gages for transducer development, the surface has been barely scratched. For instance, it is within the present technology to produce a pressure transducer having 200 mv output, 350 ohms impedance, capable of calibration by electrical simulation, and having a natural frequency of over a megacycle.

SECTION VII

ELECTRONIC LOAD CELL APPLICATIONS
IN ROCKET AND SPACE VEHICLE TESTING AND DESIGN

by

H. S. Harmon
Instrument Development Branch
Test Laboratory
MSFC

ELECTRONIC LOAD CELL APPLICATIONS

IN ROCKET AND SPACE VEHICLE TESTING AND DESIGN

Load cells, along with pressure and temperature measuring devices, are the work horse transducers of space vehicle testing and design. A large majority of all measurements are made with these devices. Today, we will concentrate on the electronic load cell application in Rocket and Space Vehicle Testing and Design.

Structural Testing:

Handled primarily by the P&VE Lab, Experimental Structures Section, load cells are used in series with hydraulic cylinders and electro-mechanical shakers to determine the amount of static and dynamic load applied to practically every shape, and/or configuration used in a Rocket and Space Vehicle. These tests are made as required on air frames and components of the vehicle. A typical example of this type test was performed on the Saturn out board LOX and fuel suction lines to determine lateral and angular translation.

The fuel suction line was mounted on the test fixture. The top flange, normally attached to the flowmeter, was connected to a translation mechanism which translated that end plus or minus one inch in the three required directions, (1) horizontally parallel, (2) horizontally perpendicular, and (3) vertically perpendicular to an axial line through the turbopump flange. The flowmeter flange face was always moved parallel to its original position. The LOX suction line was similarly mounted and translated. The sign of the translation directions were taken as plus when the turbopump flange was moved away from the flowmeter flange.

The translation directions are shown relative to the turbopump flange but would be identical to the actual procedure of translating the flowmeter end in the same direction but with opposite sign.

The turbopump flange was attached by use of load cells and flex joints to a rigid support. Six load cells were used to measure loads and moments during the translation in the three (3) previously mentioned attached flex joints transmitted loads along the axis of each individual load cell with a minimum (less than 2%) error due to loads in a transverse direction.

All test stands structures and fixtures are tested by simulating loads with hydraulic cylinders and load cells and measuring the effects of loading with strain gages.

Ground support and launch equipment is similarly tested.

Weighing:

Load Cells are daily increasing their role in high accuracy precision weighing and in many applications, replacing the bulky mechanical lever type systems.

Specially tailored electronic load cell systems are approaching accuracies of .02 percent reading. These applications include dry weight determination of Space Vehicles.

Propellant Weight:

The amount of propellant is weighed with various load cell configurations and used for topping and level control. Load cells are used at lift off to determine the mass of the vehicle as it leaves the launch pad.

The volume of the propellant tanks on Space Vehicles are determined by weighing the tanks filled with water and converted to volume.

Level sensors and level controllers are checked by the same method.

Load cells are used to determine the center of gravity and mass moment of inertia of all Space Vehicles.

Thrust and Torque:

Thrust is a measurement of engine performance, therefore, each vehicle on the Test Stands is provided with a set of load cells for thrust measurement. Accuracies of .5% of reading are easily attained.

Component Testing:

The Components Test Section of Test Laboratory use load cells for measuring performance of models, gas turbine torque, steam generators, gear boxes, pumps, motors, and etc.

Thrust Measurement on Saturn V. (Force Transducer for Project Saturn):

Saturn I, with 1,500,000 pounds thrust, and its successor, Saturn V, with 7,500,000 pounds thrust, require many force measurements during design, fabrication, and testing stages of development. For the most part, commercial available strain gage load cells are used for these measurements, but as the thrust and total vehicle weight increases, commercial or industrial off-the-shelf load cells are not available, especially in the size or dimensions required. Saturn V, for instance, requires four 3.5 million pounds cells with a 10" x 10" x 4" high outside dimension. These load cells measure hold down force and weight. These transducers were, however, furnished by the industry. A prototype was built by MSFC as a backup.

This load cell was built by the Instrument Design Branch of Test Laboratory.

Several approaches were considered, among them, the "swiss cheese" design, which is nothing more than a piece of steel with holes drilled symmetrically throughout the load bearing area. The holes are gaged with strain gages and arranged in a parallel series fashion, in order to integrate the output, making the cell less sensitive to load distribution. Another approach considered was the concentric ring design. This design uses a number of rings, one inside the other, each ring having a number of strain gages in series and parallel. A multi-column approach was considered, which utilizes a number of one inch rectangular columns.

A design using ten rectangular columns arranged in a parallel fashion and bolted to a base and bridge plate was selected. It was felt that this design offered several advantages as a study model. Number one, it was easy to build, machine, and gage. If the gage should fail, it could be disassembled and easily repaired. Also, each column could be studied and tested separately to its capacity. The cell was designed with a safety factor of at least two.

The columns were made of 4340 steel and properly heat treated for desired strength.

Each column was magniflaxed, gaged, and tested separately to 200,000 pounds in a load cell calibrator. Each gage was read separately to check the effects of off-center loading and load distribution. The cell was then assembled and sent to Denver, Colorado, Bureau of Reclamation, for calibration in a 5 million pounds testing machine.

SECTION VIII

A HYDRAULIC STEP FUNCTION PRESSURE GENERATOR
FOR TRANSDUCER EVALUATION

by

J. D. Dykstra
U. S. Army
Ballistic Research Laboratories
Aberdeen Proving Ground, Maryland

A HYDRAULIC STEP FUNCTION PRESSURE GENERATOR FOR
TRANSDUCER EVALUATION

INTRODUCTION

The problem of determining the dynamic response of pressure transducers has been recognized for many years. Many techniques have been used with some success¹ but no combination of them has been sufficient to answer all questions. Particularly there has been a gap between very fast test loading, as with a shock tube, with poor amplitude accuracy and limited duration, "static" calibration with very high accuracy, but requiring loading times of at least tens of seconds. The device discussed here is one possible compromise, combining relatively fast-loading and indefinite duration with reasonably good amplitude accuracy.

This Step Function Pressure Generator is based on a fast opening valve developed by Johnson and Cross of the National Bureau of Standards in the course of a program on dynamic pressure calibration supported by the U. S. Army Ballistic Research Laboratories. A 50,000 psi prototype was built in 1958 and gave some very promising results but it was cantankerous and difficult to operate. When BRL support was terminated the equipment was put on the shelf. Subsequently, the Interior Ballistics Laboratory of BRL had built, under the supervision of J. L. Cross of NBS, a 5000 psi version. This is the equipment which will be the principal subject of this paper. At about the same time R. O. Smith of NBS had another 5000 psi version built by American Instrument Company.

Johnson and Cross published none of their data although a description of the device was given by Dan Johnson at the Sixth Meeting of the JANAF Solid Propellant Rocket Static Test Panel in August 1958. One of their records has been published with brief description by Schweppe, et al¹, and was included by R. O. Smith in a paper on his experience with his 5000 psi version presented at the Winter Meeting of the ASME, November 1963². Some of our early experience was presented in a paper at the 11th Meeting of the JANAF Solid Propellant Rocket Static Test Panel in September 1962³.

¹ J. L. Schweppe et al, "Methods for the Dynamic Calibration of Pressure Transducers," NBS Monograph 67 1963

² R. O. Smith, "A Liquid-Medium Step-Function Pressure Calibrator," ASME Paper Number 63-WA-263

³ J. D. Dykstra, "Evaluation of Pressure Transducer Response With a Pressure Step Generator," in the Eleventh Meeting Bulletin of the JANAF Solid Propellant Rocket Static Test Panel, SPSTP/11, September 1962 (Meeting Bulletin is classified CONFIDENTIAL)

DESCRIPTION

A simplified drawing of the basic device is shown in figure 1. The Fast Opening Valve (FOV) is completely contained in a cylindrical pressure vessel with provision for closely coupling the test transducer to one end, and for bleeding the mounting cavity. The entire system is filled with oil.

If the bleed valve and bypass are open, the FOV will be held closed by pressure in the reservoir. A step is initiated by closing the bleed and bypass valves and opening the dump valve. Reservoir pressure forces the piston into the cylinder, at a rate controlled by a constriction in the dump line. As the piston moves, it stretches the thin valve stem until the pull on the head about balances the pressure holding it closed. When the valve begins to open the pressure in the port rises quite rapidly due to the small volume, thus reducing the restraining force on the head and allowing the stretched stem to fully open the valve very quickly. The thin stem provides both efficient energy storage and decoupling of the valve head from the mass of the piston so that the head can move much faster than if the piston also had to be accelerated.

The essential features are (1) a valve mechanism combining a large amount of stored energy with low inertia to allow fast opening, and (2) a design allowing very close, simple coupling between the pressure reservoir and the test transducer. The latter characteristic is a result of inclosing the valve mechanism in the pressure vessel and use of an integral low volume bleed valve. While these features are not unique to this device, they are essential for good performance.

The FOV is closed by applying a slight overpressure in the cylinder which forces the valve head into the port, after which the bleed valve can be opened, dropping the pressure in the port, and the bypass valve opened to release the overpressure. The stem guide is a close-fitting sleeve around the stem, fastened only to the piston. It provides alignment and prevents buckling of the stem during valve closure and provides some control of head motion during opening.

The BRL device was designed to generate steps in the range of 1000 to 5000 psi with rise times of less than one millisecond, and to be semi-automatic in operation. The unit as delivered is largely self-contained, requiring only 110 V AC and 100 psi air for control functions in addition to the test transducer and associated equipment. It is contained in a 6-1/2 foot relay rack (Fig. 2). Pressure is generated by a hand (or foot) pump under the table and controlled by manual pump and return valves and a precision bourdon gage on the panel.

Operate and reset cycles are initiated by push buttons and controlled by a stepping relay programmer. Figure 3 shows the back of the rack. Electrical control is at the top. The Fast Opening Valve is contained in the vertical cylinder near the center of the rack with the test transducer mounted in the top. Other components are auxiliaries required for the automatic cycling. All of the pressure plumbing is in 1/16 OD stainless tubing.

PERFORMANCE

In practice the BRL device has been found to operate well in the region from 500 to 3000 psi with the valve stems currently available. The upper limit for a given stem has been set by the strength of the head-stem and stem-piston connections and it is not known how far this could be extended by redesign. The lower limit for a particular stem should theoretically be the lowest pressure at which sufficient elongation of the stem would occur before stem tension overcame pressure on the head. In practice the limit has been found to be considerably higher due to a tendency for the valve to leak slightly as stem tension increases. Figure 4 is a record of an extreme case of this. The source of the trouble appears to be misalignment of the head, stem, and port and the condition will vary somewhat from test to test as well as from one assembly to the next. At low pressures several factors combine to magnify the effect. There is less force on the head at low pressure so seating is not as good, piston motion is slower so the leak lasts longer, and a given pressure rise will be a larger fraction of a low pressure. The record of Figure 5 is more representative of the performance in the useable operating range.

The piston motion during valve opening causes an increase in next reservoir volume and therefore a drop in pressure. Since the motion is slow, pressure equilibrium in the reservoir is maintained and the test transducer will not see the pressure ramp which occurs before valve opening. In practice, however, some piston travel occurs after valve opening and that portion of the pressure ramp also appears on the test record. Figure 5 shows both reservoir pressure and test transducer for a fairly severe case. The magnitude of the effect depends on relative piston displacement to reservoir volume, on oil compression and therefore pressure, and on amount of piston travel after valve opening. Only the latter is adjustable and in our unit only with some difficulty. However, ramp is typically held to less than 5% of step and lasts anywhere from 10 to 100 ms.

Two other effects may be mentioned. One is a slight tendency for port pressure to rise during bleed valve closure before firing. This is a function of port volume and bleed valve design and our worst case has been about 5 psi. It is generally not detectable. Another is a slight drop in port pressure just before FOV opening. This is presumably caused by a slight movement of the head as stem tension increases, without breaking the seal, due to relief of deformation in the head-port contact area. This drop cannot exceed 15 psi plus any increase on bleed closure, and for our unit 10 psi is the most observed, generally much less. The effect also tends to cancel any slight leak.

The leading edge of the step generally consists of a smooth inflection from the base line into a fast rising portion lasting 200 to 300 μ s, followed by varying amounts of oscillation (Fig. 6). In the BRL device two distinct types of oscillators have been observed. One has a frequency in the range of 1500-2500 cps and amplitude of up to about 20% of step level, peak to peak. This frequency is detectable only with near minimum port volumes and close coupled high frequency transducers. It appears to be directly related to the rise time and so considerable effort has been expended on identification of its source. It now appears that this is related to mechanical oscillation of the head-stem system. The frequency is very close to the mechanical resonance of the head and stem measured in air, and replacement of the original head and stem with a lighter assembly raised the frequency of the pressure oscillation and shortened the rise time.

Both the most direct evidence, and the most puzzling, is shown in figure 7. Here for each head weight are displayed simultaneously both pressure oscillation (upper trace) and head displacement (lower trace) as sensed by a piezo electric pressure transducer and capacitance type proximity transducer, both located in the valve port. The correspondence of both frequency and damping is apparently exact. The record in figure 8 was made after insertion of a teflon snubber between the valve head and the end of the stem guide. The different head motion is reflected in the pressure record but some additional disturbances are also seen which were apparently masked by the head-induced oscillation before. These records raise a question however as to the nature of the coupling between head motion and pressure oscillation. A first inclination is to consider the valve head as a piston moving in and out of the port. However, the indicated

phase of the displacement and pressure variation is incorrect to support this view. It appears that as the valve head rebounds, re-entering the port, the pressure in the port decreases. Neither the transit time of a pressure wave from the valve head to the pressure transducer nor any electrical or mechanical phase shift in the pressure or displacement measuring systems appears to offer an explanation. Acoustic resonance of the oil column in the reservoir was considered and this frequency was calculated to be of the right order of magnitude, but a test in which the reservoir length was effectively halved with an aluminum filler showed no change in the pressure oscillation or head motion. Thus the question of a coupling mechanism remains unanswered even though a cause and effect relationship has been reasonably well established.

The second type of oscillation observed on the pressure step appears at considerably higher frequencies, typically 5 to 20 Kc, and appears to be related to the size and shape of the port and transducer mounting cavity. Its amplitude may be over 50% of the step, peak to peak, with variable damping and often several mixed frequencies. In most records at other than minimum volume it hides the low frequency component except for control of rise time. Figure 6 is fairly typical of this type of signal. Although little study has been made of it, it appears that excitation of these high frequencies by an apparently slow rising pressure wave implies generation of a shock wave in the port. The general motion of the valve head is well below sonic velocity in the oil, but other factors of geometry etc. may combine to allow formation of a shock. It is believed in any case that these higher frequencies can be eliminated from the signal seen by the test transducer by increased damping in the port, either by port constriction or use of a higher viscosity oil than the very light fluid now used, or both, without serious degradation of the rise time.

DISCUSSION

Brief study of the dynamics of the system will convince one that prediction of the pressure waveform for a given set of parameters is extremely difficult if not impossible. The interactions between mechanical and fluid systems are quite complex and the fluid system itself is not well described by a simply linear model but has aspects of both viscous bulk flow and elastic wave propagation. However, some limiting conditions and general effects may be noted.

If the valve opens rapidly enough, conditions approaching those in a shock tube hold and equilibrium time is largely a function of the pressure transmitting characteristics of the liquid (velocity of sound) and the size and shape of the port. It has been found in shock tube studies that under these conditions in most fluids, pressure and viscosity have little effect on rise time. Considerable oscillation is possible with damping dependent largely on port geometry and fluid elasticity. A different behavior will occur if the valve is opened very slowly. In the limiting case the orifice is so small that pressure equilization within the port is rapid compared to the rate of change of pressure. Then the rise time become independent of port shape but is controlled by port volume, fluid viscosity, and pressure. In the limiting case, approach to final pressure is asymptotic.

Practically, it may be assumed that the pressure step generator operates somewhere between these extremes, with some characteristics, e.g. the valve head induced oscillation, not related to either model. In fact for the BRL device it appears that actual rise time is largely determined by the head-port interaction in the case of the free head, and by other factors if head motion is restrained as in the case of Figure 8. Over the limited range from 500 to 3000 psi no effect of pressure on rise time can be detected. Neither can any effect of port volume or shape over a fairly wide range, although changes in the nature of the oscillation are obvious. This is perhaps plausible since in all cases the acoustic resonance of the port has been well above the head-stem frequency that appears to determine the rise time. All the evidence suggest that in these tests the flow limited condition has not been approached.

It is interesting to compare these results with some obtained with the other versions of the device. The design was conceived in a study of high pressure calibration techniques, and the prototype operated most successfully in the range from 5 K to 50 Kpsi. Both subsequent versions were designed for up to 5 K psi. The BRL device has been used mostly in the 500 to 3 K psi region. Smith at NBS has reported only work in the region below 1 Kpsi². A comparison of some of the important physical characteristics of the devices is found in the sketches of figure 9*. Internal dimensions are to approximately equal scale from one design

* Sketches and numerical data in the following are the responsibility of the author. Prints of the equipment, records, and other information were made available by J. L. Cross, Pressure & Vacuum Section, NBS & P. S. Ledere, Mechanical Instruments Section, NBS, and their help is gratefully acknowledged.

to the other, though many details are omitted for clarity. Some of the salient factors are tabulated in Table I. Note that the pressure range given is that for which some data is available. Where several stem diameters are available, it is not expected that each will work over the entire operating range. It is believed that Smith has done most of his work with the .062 in. and heavier stems and most of the BRL work has been with the .078 in. stem. The stem diameter is of interest because with port area, pressure, and stem length it determines the elongation of the stem at valve opening and therefore the distance thru which the valve moves quickly. Force on the head at the upper operating pressure is quite different from one unit to the next, and if the stems do not vary accordingly, the elongation and consequent rapid valve opening can also be quite different.

The maximum opening for the prototype was somewhat less than in the BRL device. Figure 10 shows some typical records obtained by NBS with the prototype, using light oil. The effect of pressure on rise time appears to be small. Frequency of major oscillation changes in the pressure range from just over 6 Kc to about 8 Kc at the higher pressure. This frequency is well above the calculated stem resonance and appears likely to be oscillation in the long connecting passage. The direction and magnitude of the frequency shift tend to support this view because of the increase in sound velocity with increasing density due to compression. The rise time of about 150 μ s is not consistent with this frequency but would correlate with a period of about 500 μ s or frequency of 2 Kc.

The effect of an extreme change in fluid viscosity is shown in Figure 11. These records were obtained by NBS with the prototype filled with SAE 50 oil. At the lowest pressure (and smallest rapid valve opening) the rise time is materially increased. At the higher pressures rise time is still somewhat greater than with the light oil, but is not strongly dependent on pressure. The oscillation however is essentially eliminated. It may be noted that the effect of viscosity can be quite complex if there are areas of flow restriction other than the valve, e.g. the small connecting passage of both NBS designs, and particularly at high pressure where viscosity increases quite rapidly.

Smith's reported work² is in some contrast to this. His effort is directed toward use of the device to measure transducer creep rather than dynamic sensitivity, though the two are admittedly related. For this he feels that any overshoot in the pressure step is undesirable, including effect of piston generated ramp.

Therefore, much of his effort has been directed toward slowing the rise time and damping the ringing in order to generate a monotonic step. He states that he has found that he could achieve this for any one pressure by empirical adjustment of port and mounting cavity shape and volume, and oil viscosity. Figure 12 reproduced from Smith's report shows a typical variation of waveform with pressure. Although the conditions are not stated in the report, this is believed typical of results obtained with the .075 in. stem, SAE-20 or 30 oil, and some cavity extension. The rise times here range for a few hundred μ s to 2 ms. His monotonic steps seem typically to have had rise times in the range from 2 to 10 ms.

Records taken with light oil and minimum cavities at around 1 Kpsi seem to look much like those made with the prototype, with rise times of about 200 μ s. The frequency of oscillations however seems to range from 1.5 to 3.5 Kc. Smith is also bothered by pressure rise on bleed valve closure and a small pressure variation just before the step. Both conditions are exaggerated by the low pressures used, but in many cases seem worse even at 1 Kpsi than in our experience. The bleed valve problem may be due to use of a rather large screw-operated valve stem and a long constricted bleed passage running past the stem. Manual operation of the bleed valve probably tends to encourage both faster stem motion and greater volume displacement than is provided by the air operated valves in the prototype and BRL equipment. The shape of the pre-step transient suggests the presence of an elastic wave in the stem prior to valve opening. This is reinforced by the observation that failure to equalize the cylinder and reservoir pressure prior to dumping the cylinder, so that the stem is initially under compression rather than relaxed, seems to increase the amplitude of the transient. Both the prototype and the BRL equipment use constricted dump lines to limit the rate of cylinder pressure change in order to avoid excessively rapid piston motion. In the prototype it was found necessary to use some 9 ft. of 1/16" bore high pressure tubing between the cylinder and a fast dump valve to eliminate hash on the baseline and rising edge of the step. In Smith's device piston rate is probably determined primarily by the opening rate of a relatively slow air operated valve, though tubing resistance and the setting of a manual valve also in the line may have some effect. Piston travel time prior to opening is not available for either NBS's device. In our unit it is typically 40 to 80 ms.

It is the opinion of this author that Smith's device, as reported used, is operating on the borderline between stretched and solid stem behavior. Many of the reported characteristics are consistent with this view but the most direct are the effect of pressure on rise time, the 2-10 ms rise times of his monotonic steps against the 200-300 μ s produced in the prototype with even heavier oil, and the extremely small calculated elongations for stem and pressure combinations known to have been used. Smith's work certainly is valuable and the approach is legitimate within his frame of reference. I do not feel, however, that his data can be taken as characteristic of the stretched stem valve system.

It is interesting that there is little evidence to show that the head-stem resonant frequency has any direct effect on the rise time of either NBS device, although our experience would suggest it should. The calculated frequencies are only approximations but the range is considerably greater than the observed differences in unmodified rise time. However, there is also no evidence to prove it has no effect and while it would appear that at most head frequency is only one of several factors in rise time, the question must be left open.

TRANSDUCER TESTS

Most of the BRL work with the pressure step generator has been directed toward understanding the characteristics and limitations of the equipment and little specific testing of transducers has been done. However, in the course of the work about 10 different transducers have been used for varying amounts of testing. These have included several bonded and one unbonded strain type, one capacitance type, and several varieties of piezo transducers. They have been examined with varying precision according to the immediate test objective and several apparent anomalies have been found. Figure 13 shows one of these cases. The transducer is a hydrostatically loaded tourmaline crystal in a BRL designed housing, used for measuring gun chamber pressures. These transducers are typically filled with beeswax or silicone grease, but this particular unit was experimentally potted in a soft plastic. Not only has the normally present oscillation been almost eliminated but pressure rise appears to continue for several milliseconds. Figure 6 was a test of a similar transducer filled with silicone grease for comparison. Although the step pressure was not high enough for a definitive test of a high pressure transducer, it appears that significant loss of high frequency information might have been expected with the plastic filled unit.

Figure 14 is from a test of another piezo transducer, a commercially available unit having a diaphragm loaded quartz element. The upper trace is reservoir pressure, the lower the test transducer. Both channels had their zero level suppressed; the sensitivity was about 50 psi/cm. The test pressure was about 1 Kpsi. The initial response of the test transducer as seen in faster sweep records appears normal. This longer record reveals a rise of about 10 psi over the first second after the step. This effect has not been noted in other samples of the same type.

Smith² has also reported finding creep effects with durations of from several ms to several seconds in various transducers, and feels that some of these effects would not be detectable by shock tube or static testing.

CONCLUSIONS

The limited test data presented seem to indicate that the response of a pressure transducer to a transient may deviate from that predicted from both static calibration and shock testing and that a step generating device with a rise time of a fraction of a millisecond and indefinite duration can be useful in studying such response. A pressure step generator based on the stretched-stem valve of Johnson and Cross appears to have some promise for this application. It is not obviously superior in all respects to some other approaches however. Smith's work would seem to indicate that a roughly similar device with an essentially non-stretching stem can be useful and is probably less prone to generation of oscillation even if somewhat slower. Many of the side effects in either approach can be reduced by careful design. A smaller valve port would reduce the stem load and allow use of a smaller piston with consequently less volume displacement for a given opening. Pressure reduction due to piston motion can also be reduced by increased reservoir volume, preferably obtained by increasing vessel diameter rather than length to reduce any effect of the reservoir resonance. At low pressures a different type of bleed valve might be useful, e.g. a ball valve or stopcock.

If the stretched-stem design is retained, use of a shorter stem and/or lighter head offers some possibility for decreasing rise times. More effective control of head motion to prevent excessive bounce may help to reduce oscillation.

More basic than the type of valve actuation is the choice of pressure medium. It may be that for pressures below about 1 Kpsi a gas would have significant advantages. Several problems in the low pressure step generators can be traced to the very low compressibility of oils in this range. Small volume changes would be much less troublesome using a gas and might allow use of smaller total volumes. If the more difficult leak problem can be overcome, helium offers sound velocity and therefore cavity resonance frequencies not greatly lower than oil, and if cavity sizes can be reduced may provide appreciably faster steps. Aaronson⁴ of the Naval Ordnance Laboratories has reported a gas medium step generating device based on an impact operated valve. His valve head is a flat plate with an "O" ring seal located inside the pressure vessel, with the valve stem extending out through the opposite end of the vessel to the impact assembly. With this simple device he generates steps with a rise time of around 100 μ s and moderate oscillation at pressures from near zero to 1000 psi. It appears at least possible that development of this idea might provide a unit with better performance at low pressures than a new generation of liquid medium stretched-stem valve devices.

There seems little doubt that at pressures above perhaps 1000 to 2000 psi a liquid medium is indicated for safety and convenience and the stretched-stem valve designs discussed here offer at least a starting point for further development. It is believed that the work reported offers considerable hope that a practical device for evaluation of the dynamic response of pressure transducers in the 1 ms and up time scale can be achieved and that at least a few ideas about how it might be done have been generated.

⁴ F. M. Aaronson and R. H. Waser, "Pressure-Pulse Generator for the Calibration of Pressure Gages," U. S. Naval Ordnance Laboratory Report No. NOLTR 63-104, November 1963

TABLE I

CHARACTERISTIC	NBS (PROTOTYPE)	
Pressure Range (1)	5K-50K	500-5K
Reservoir I. D. (1)	1.25	1.34
Reservoir inside length	20.5	17.8
Net Reservoir Volume	19.5	23.5
Port diameter (2)	.22	.39
Port area (2)	.034	.119
Force on valve head (3)	1700	357
Stem diameter (4)	.22	.062
Stem area	.034	.003
Stem stress (3) (4)	50	119
Stem length	17	17
Stem elongation (3) (4)	.029	.070
Piston area	.075	.147
Piston area/valve port area	2.2	1.2
Piston displacement (min) (3) (4)	.0019	.0090
Volume change	.01	.038
Equiv Pressure Change (5) %	.05	8.2
Head weight	-----	.0034
Approx head-stem resonance	KCPS 2.8	KCPS 2.5
Transducer cavity (7) length	1	.188
Transducer cavity (8) volume	in ³ .016	in ³ .013

1. Operating range for which data is available
2. At valve seat
3. At maximum operating pressure (note 1)
4. Where several diameters are listed not all will necessarily cover the full operating range, but calculations given ignore this fact.
5. Assuming linear oil compressibility of .4%/KPSI
6. Aluminum, all others steel
7. With minimum transducer volume
8. With valve seated

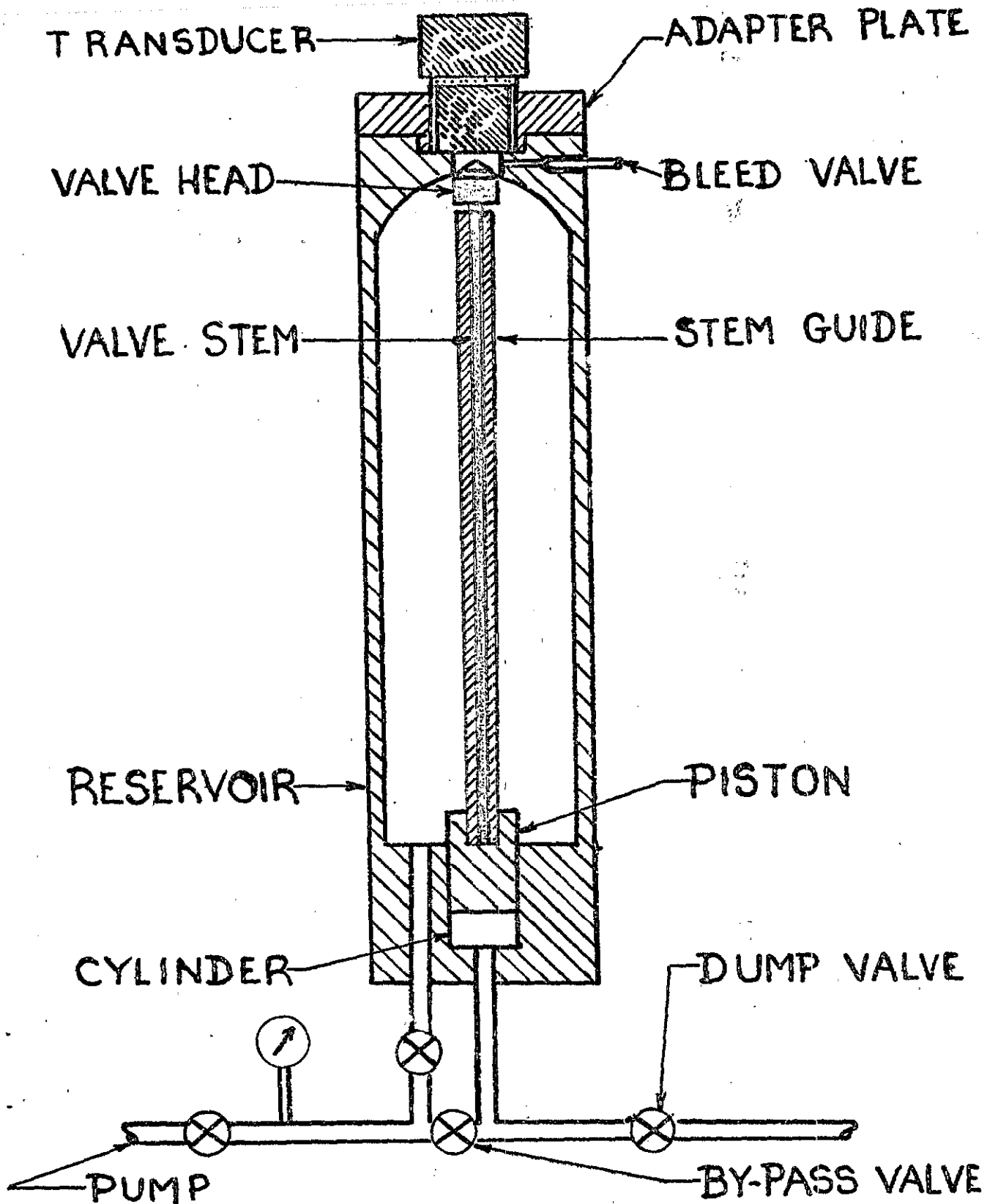


FIG.1. SIMPLIFIED SECTION OF FAST-OPENING VALVE

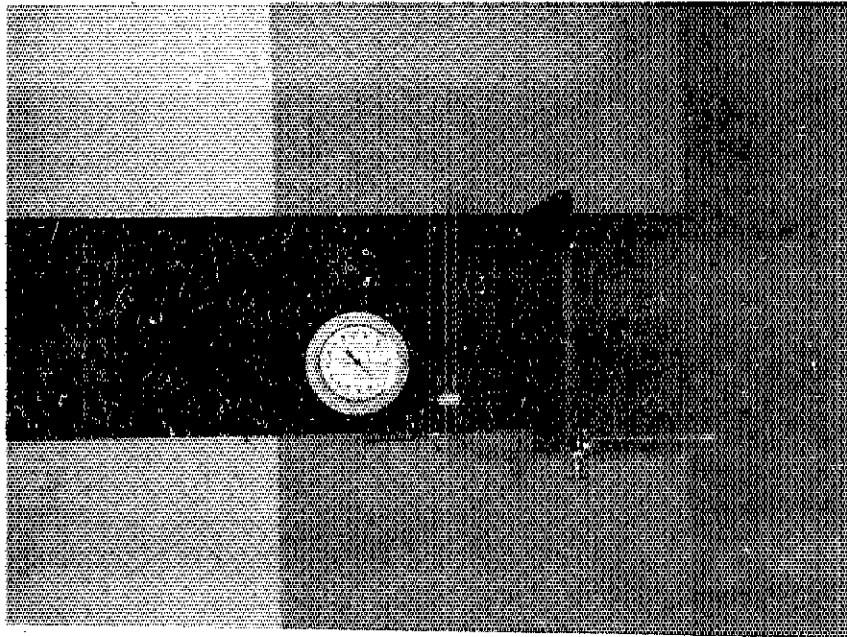


Fig. 2 BRL pressure step generator
front view

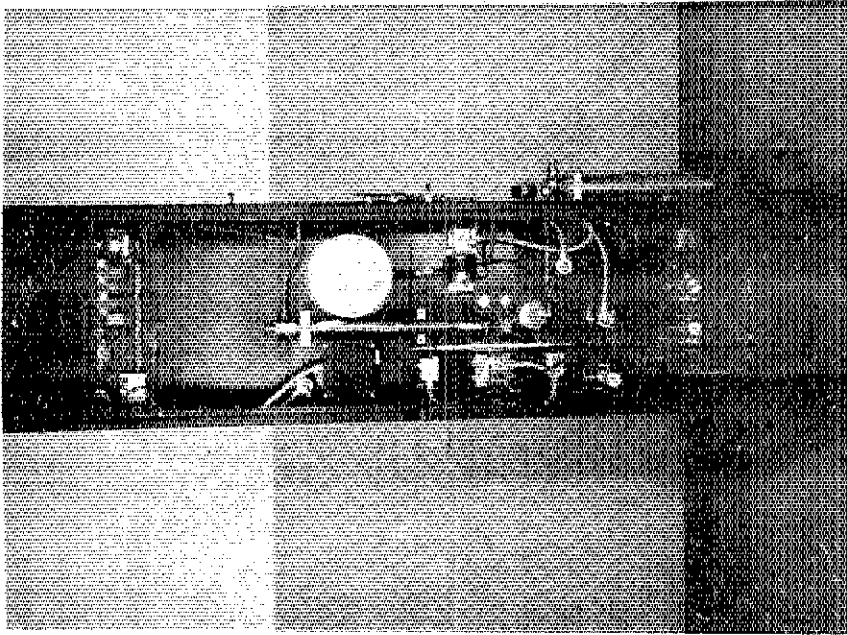


Fig. 3 BRL pressure step generator
rear view

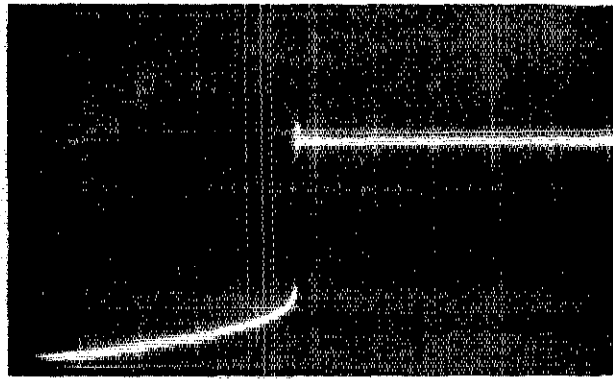


Fig. 4 Effect of valve leakage before step
 Step pressure 2.5 Kpsi Sweep 50 ms/cm

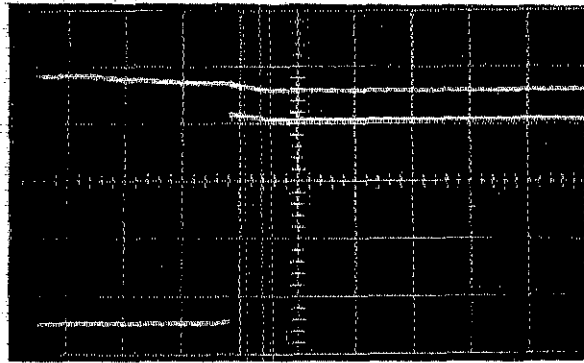


Fig. 5 Effect of piston motion on pressure
 upper trace - reservoir pressure
 lower trace - test transducer
 Step pressure 960 psi Sweep 50 ms/cm

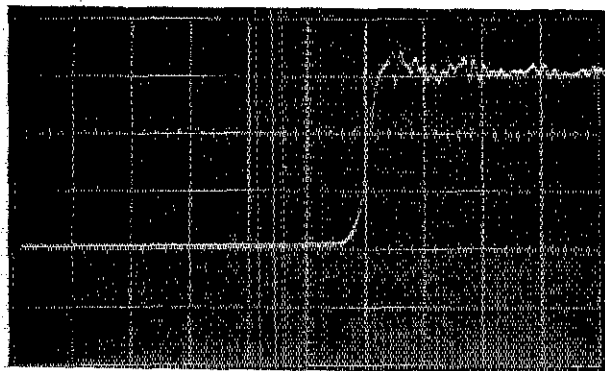
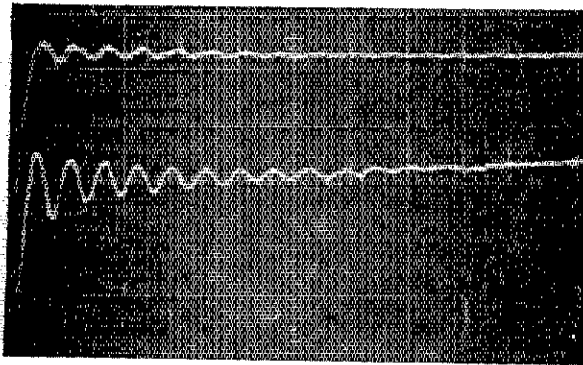
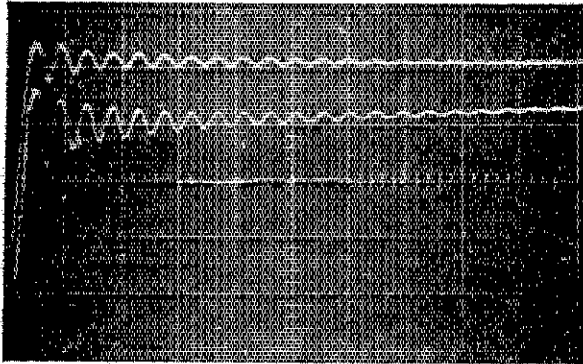


Fig. 6 Typical "good" step detail
 Step pressure 3 Kpsi Sweep 500 μ s/cm



a. Heavy head



b. Light head

Fig. 7 Valve head motion and pressure oscillation

upper trace - pressure step
 lower trace - valve head displacement
 Step pressure 1 Kpsi Sweep 1 ms/cm

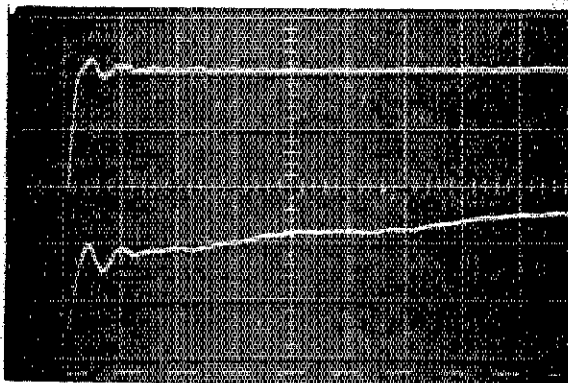
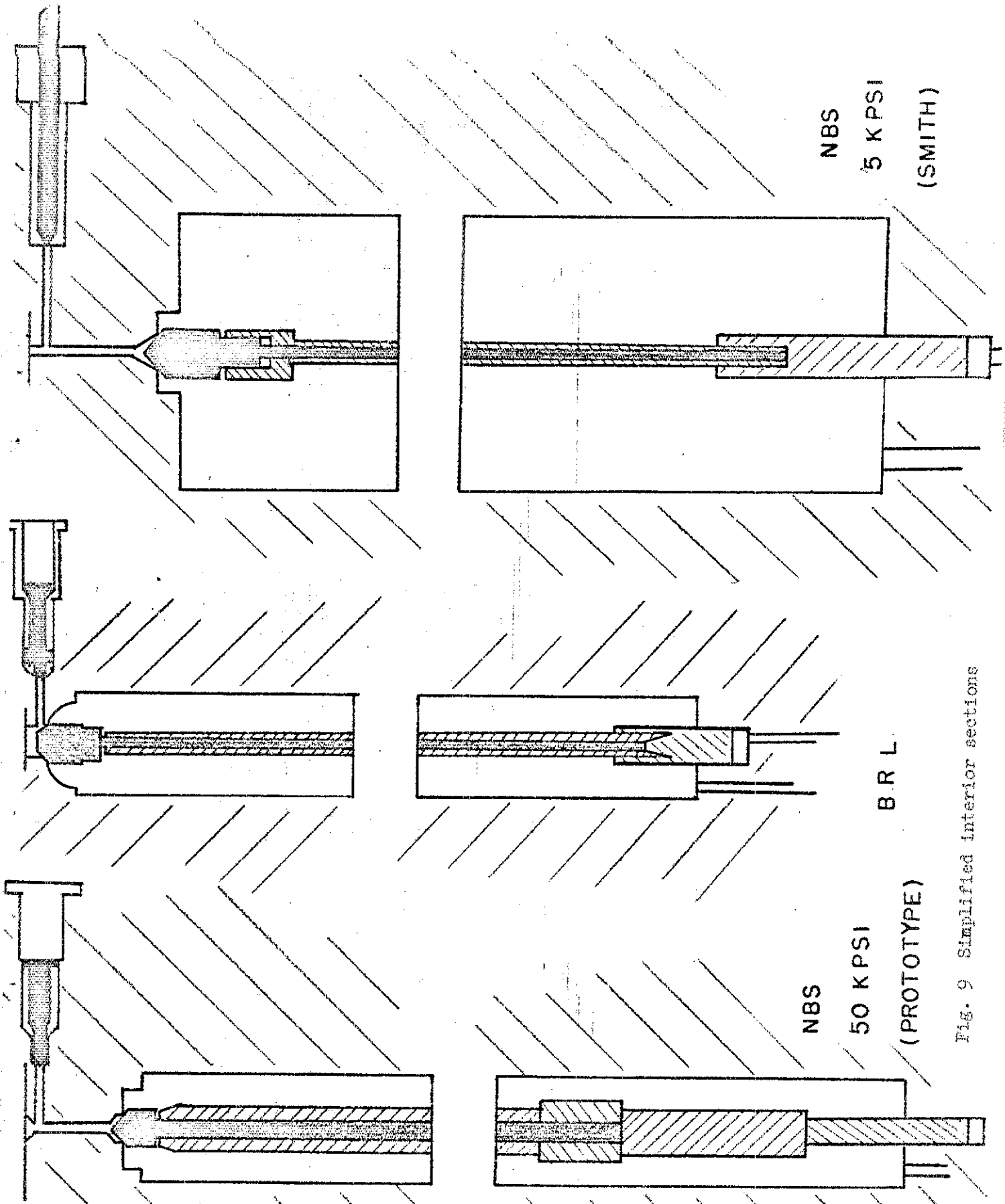


Fig. 8 Valve head motion and pressure oscillation with valve head restrained by Teflon Block

upper trace - pressure step
 lower trace - valve head displacement
 Step pressure 1 Kpsi Sweep 1 ms/cm

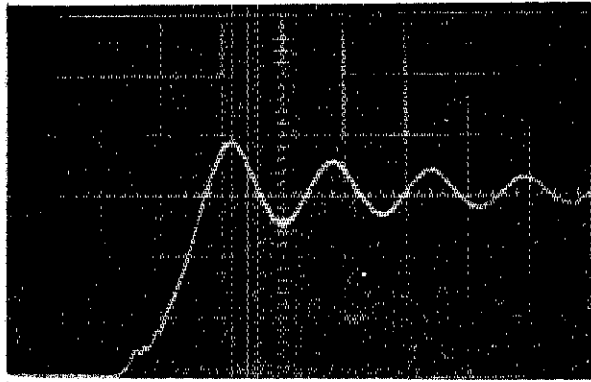


NBS
5 KPSI
(SMITH)

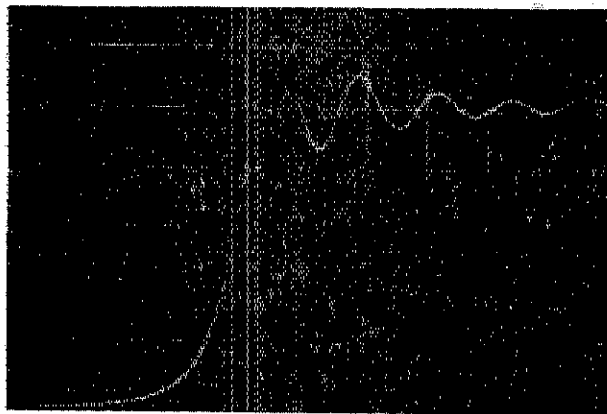
B R L

NBS
50 KPSI
(PROTOTYPE)

Fig. 9 Simplified interior sections

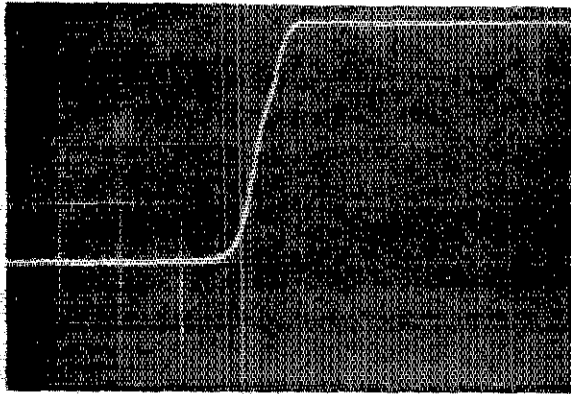


a. 13.6 Kpsi

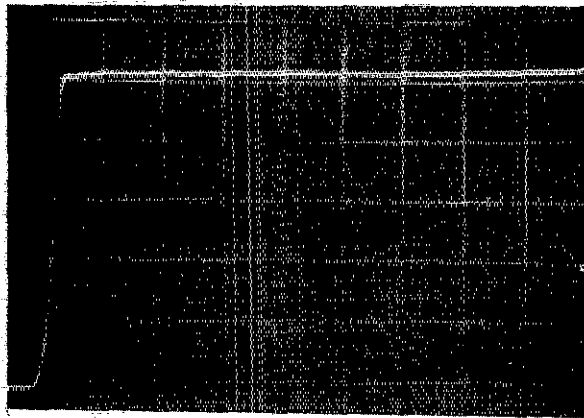


b. 47.7 Kpsi

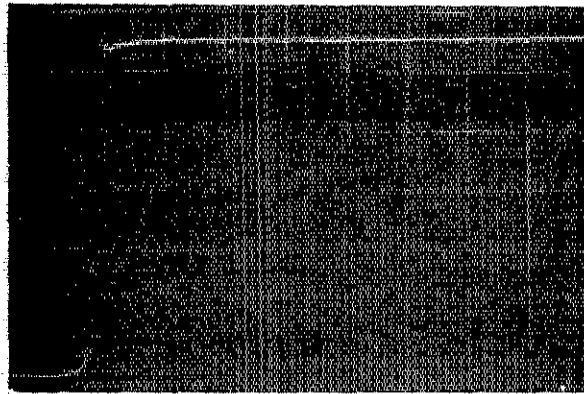
Fig. 10 NBS records made with the prototype device
Low viscosity oil Sweep 100 μ s/cm



a. 3.8 Kpsi



b. 10 Kpsi



c. 27.6 Kpsi

Fig. 11 NBS records made with the prototype device
High viscosity oil Sweep 1 ms/cm

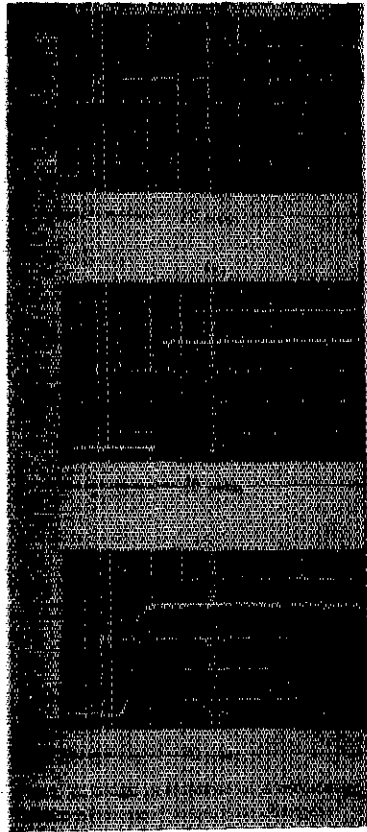


Fig. 12 Records from Smith's report on the NBS low pressure step generator showing effect of pressure on risetime

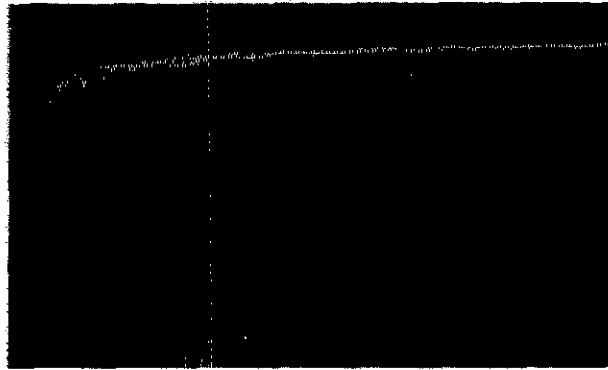


Fig. 13 Response of a tourmaline transducer with
short term creep effect
Step pressure 2 Kpsi Sweep 500 μ s/cm

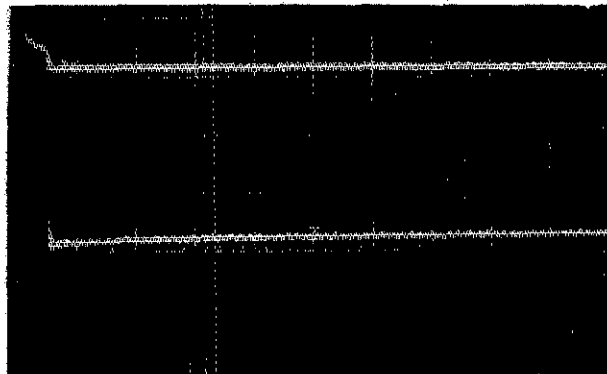


Fig. 14 Response of a quartz transducer with long-
term creep effect
upper trace - reservoir pressure
lower trace - test transducer
Step pressure 1 Kpsi Sweep 100 ms/cm
Scope sensitivity 50 psi/cm

SECTION IX

REAL TIME COMPENSATION OF THERMAL SENSORS

by

George B. Rybicki
Research and Advanced Development Division
AVCO Corporation
Wilmington, Massachusetts

RESEARCH AND ADVANCED DEVELOPMENT DIVISION
AVCO CORPORATION
Wilmington, Massachusetts (01887)

REAL TIME COMPENSATION OF THERMAL SENSORS

by

George B. Rybicki

(This work was supported by Contracts AF33(657)7989 and AF33(657)11630)

Presented at the Sensor Workshop

Flight Dynamics Laboratory
Wright-Patterson Air Force Base, Ohio

18-19 June 1964

ABSTRACT

Generalized equations for two surface non-homogeneous temperature sensors with buried thermocouple junctions are developed using Green's theorem and eigenvalue solutions. It is shown that the response function of a system containing linear conductivity and heat capacity characteristics can be expressed as a series of exponential terms with correlated coefficients and decay rates. The convergence of the series is rapid and constants can be applied to find a few lumped parameter compensation analogue networks, which effect real time compensation and surface condition computation.

Response testing of sensors and experimental compensation illustrates application of the theory. System noise and dead time are considered.

I. INTRODUCTION

When a thermal sensor is used to track a temperature or heat flux, serious errors may be caused by intrinsic time lags, which prevent the sensor from following rapidly varying inputs. Previous methods of compensation for this effect^{1,2} have required computation of the response function of the sensor from knowledge of its geometry and material properties, which is then used in a digital correction program. However, the material properties and geometry are often not known very exactly, and the digital methods are not well suited to real time compensation applications.

In this paper a method is presented which effects the desired compensation using simple analogue techniques and is applicable to a rather general class of thermal sensors. The foundation of the method is a theorem which shows that the response functions for this general class of sensors is always a sum of decaying exponentials, the parameters of which may be found from auxiliary experiments. These parameters may then be used to determine the constants of the analogue compensation network.

The application which prompted this work was a temperature attitude sensing system³ where it was possible to extend the usable frequency domain by a decade using the present method. In any situation where time lags are present there is a possibility for application of this method for response improvement.

II. DISCUSSION OF THE METHOD

A. A Typical Thermal Sensor

The basic thermal measurement device that will be considered here is the thermocouple junction, which measures the temperature at a single point, the junction. However, the complete thermal sensor is always more complex,

as the junction is surrounded by the thermocouple materials, which in turn are usually imbedded in other materials. The thermal phenomenon to be measured usually occurs at the surface of the complete sensor, removed spatially from the location of the junction, and this introduces a time lag into the measurement.

Figure 1 diagrams somewhat schematically the features of a typical thermal sensor. It consists of several materials, A, B, C which occupy a region of space R bounded by a surface σ . This bounding surface may be further subdivided into two surfaces, σ_1 and σ_2 called the front surface and back surface, respectively. The thermal phenomenon to be measured occurs at the front surface σ_1 , only. The point marked ξ on the diagram is the location of the thermocouple junction.

B. The Heat Equation

The materials composing the sensor will be considered to have constant thermal properties, so that density, ρ , specific heat, C_p , and thermal conductivity, K, will all be independent of temperature. They may, however, vary arbitrarily with position; in particular, the functions

$\rho(\vec{r})$, $C_p(\vec{r})$, and $K(\vec{r})$ will be defined over the entire region R of the sensor, so that interfaces between materials may correspond to surfaces of discontinuity of these functions. With this understood, the heat equation governing the temperature $T'(\vec{r}, t)$ of the sensor is

$$\left\{ \rho C_p \frac{\partial}{\partial t} - \nabla \cdot (K \nabla) \right\} T'(\vec{r}, t) = 0 \quad (1)$$

Some typical boundary conditions which may be employed are: 1) specification of the flux on σ_1 , with an adiabatic flux condition on σ_2 ; 2) specification of the incident flux on σ_1 , with a Newton's cooling law over σ_1 and σ_2 . These boundary conditions fall under the general form of

$$k(\vec{r}) \vec{n}(\vec{r}) \cdot \nabla T' + D(\vec{r}) T' = \begin{cases} N(\vec{r}) + F(t) & , \text{ on } \sigma_1 \\ N(\vec{r}) & , \text{ on } \sigma_2 \end{cases} \quad (2)$$

where the forcing function $F(t)$ is assumed to be constant over the entire surface σ_1 . This is a necessary assumption, for a forcing function which may vary with both position and time is equivalent to many forcing functions, and more than one thermocouple would be required to perform any compensation computations.

Before solving these equations it is convenient to solve the system

$$\nabla \cdot (k \nabla) f(\vec{r}) = 0 \quad (3)$$

$$k \vec{n} \cdot \nabla f + Df = N(\vec{r}) \quad \text{on } \sigma \quad (4)$$

for the time independent function $f(\vec{r})$, which is the solution to (1) and (2) in the absence of any forcing function. Subtracting this function from $T'(\vec{r}, t)$ gives a new function $T(\vec{r}, t)$ which is the temperature disturbance caused by the presence of $F(t)$. This function satisfies

$$\left\{ \rho c_p \frac{\partial}{\partial t} - \nabla \cdot (k \nabla) \right\} T(\vec{r}, t) = 0 \quad (5)$$

$$k \vec{n} \cdot \nabla T + DT = \begin{cases} F(t) & \text{on } \sigma_1 \\ 0 & \text{on } \sigma_2 \end{cases} \quad (6)$$

It is convenient to deal with the function $T(\vec{r}, t)$ rather than $T'(\vec{r}, t)$ and this will be done for the remainder of this paper. Ignoring the time independent solution $f(\vec{r})$ only amounts to a re-zeroing of the thermocouple readings.

Finally, let $u(\vec{r})$ be defined by

$$u(\vec{r}) = \rho(\vec{r}) c_p(\vec{r}) T(\vec{r}, 0) \quad (7)$$

This is a convenient measure of the initial temperature distribution.

The system of equations (5), (6), and (7) may be solved by the method of Green's functions and eigenfunction expansion, and this is done in Appendix I. The transfer function $\bar{K}_\xi(s)$ describing the response of the thermocouple temperature $T_\xi(t)$ to the forcing function $F(t)$ is defined by

$$\bar{T}_\xi(s) = \bar{K}_\xi(s) \bar{F}(s) \quad (22)$$

where the bars denote Laplace Transforms of the unbarred quantities.

In Appendix I it is shown that $\bar{K}_\xi(s)$ has the form

$$\bar{K}_\xi(s) = \sum_n \frac{A_n \lambda_n}{s + \lambda_n} \quad (33)$$

Denoting the time response of $T_\xi(t)$ to a unit step input of $F(t)$ by $H_\xi(t)$ it is also shown that

$$H_\xi(\infty) - H_\xi(t) = \sum_n A_n e^{-\lambda_n t} \quad (41)$$

In these equations the quantities λ_n are positive and are eigenvalues of a certain differential operator associated with the heat conduction equation. The quantities A_n may be positive or negative.

The results (33) and (41) are particularly useful because they give a priori information about the response functions of the sensor. It is not evident just how much information is contained in these relationships, but experience has indicated that for a typical sensor, only a few of the parameters A_n and λ_n need be determined in order to effect an adequate compensation. This seems to be due to the fact that in most reasonable

sensor geometries the successive values of the λ_n are quite separate, in fact at large η they are approximately proportional to n^2 .

Step input response data is sufficient to determine the parameters A_n and λ_n using equation (41). For this purpose plotting the unaccomplished response on semi-log paper is quite useful. Once these parameters have been obtained, equation (33) gives the transfer function for the response of the thermocouples to the forcing function $F(t)$.

C. Compensation Methods

The basic idea of the compensator is to find a network with a transfer function which is the inverse of the transfer function describing the response of the thermocouple reading to the forcing function, that is $K_c(s)$. There are many ways of accomplishing this, but perhaps the simplest is the Transfer Function Method of Simulation⁷ which may require as little as one operational amplifier, for which the already necessary thermocouple boosting amplifier may be used. In addition to the small amplifier requirement this method seems ideally suited to deal with functions like $A_m \lambda_m / (S + \lambda_m)$ occurring in (33), which need only resistor-capacitor networks for simulation.

Diagram 2a shows a compensating network with a transfer function $K_c(S)$ which is the inverse of (33), and this would provide the general solution of the compensation problem if the values of A_n were all positive (or all negative). The network of figure 2b gives a minus sign in front of the A_2 term and may thus be useful.

D. "Dead Time" and Noise

It is well known for special cases, and is proved in general in Appendix II, that the temperature rise in the interior of a solid due to a

step input at the surface is extremely slow in the vicinity of $t=0$. This singular behavior introduces an effective time delay in the response in the presence of noise since the compensation cannot be carried to the point where the compensator must work on signal levels smaller than the noise level. Even decreasing the noise by a large factor will have negligible effect on decreasing this "dead time", because the response function approaches zero so rapidly at $t=0$.

A rough value of the "dead time" may be defined as the time it takes for a step input of "average" value to produce a signal at the thermocouple above the noise level.

III. COMPENSATION OF A SENSOR

An application of the method will now be described. The sensor was a nickel disk with an attached thermocouple which was mounted so as to be almost thermally isolated from the supporting structure. It was designed to operate at high temperatures (about 2000°F) which were obtained by placing the sensor in a lamp radiation facility. The incident heat flux balanced the radiation loss of the disk at equilibrium. The incident flux could be controlled quickly by changing the position of the sensor relative to the lamps. A multichannel recorder tracked the incident flux, thermocouple output, as well as other data.

Note that for small flux changes (in this case less than 10 percent) it is sufficiently accurate to linearize the exact equations to get them in the form considered in Part I.

The step response of the sensor was found to be that given in Figure 3. Tangent lines were fitted to the initial and final portions of this curve, and this data was used to fit a two-term equation of the form (41). This yielded

$$\begin{aligned}
 A_1 &= 0.914 \\
 \lambda_1 &= 0.276 \text{ sec}^{-1} \\
 A_2 &= 0.086 \\
 \lambda_2 &= 0.218 \text{ sec}^{-1}
 \end{aligned}$$

At first only the time constant λ_1 was compensated for. It was expected that the long time constant λ_2 would persist, as it did, but in addition, another short time constant $\lambda_3 \approx 4 \text{ sec}^{-1}$ was discovered which is not obvious on Figure 3. A circuit compensating for both λ_1 and λ_3 shown in Figure 4a was tested and yielded excellent high-frequency response, but poor low-frequency response due to the uncompensated λ_2 constant. Response curves are given in Figures 5 and 6. Figure 5 shows the step response which shows a sharp rise in the compensated output, but also a slow drift due to the λ_2 constant. Figure 6 shows the response to an arbitrary signal fed in manually in a somewhat random fashion. The compensated output follows the input amazingly well, even when the uncompensated signal shows scarcely any variation at all.

Figures 7 and 8 show the amplitude and phase response to sinusoidal inputs. It may be seen that the amplitude has been very nearly compensated, while the phase is almost linear with frequency, indicating a time delay of about 0.05 seconds, which is the "dead time" for this arrangement.

An additional circuit shown in Figure 4b was used to compensate for the long constant λ_2 . The resulting step input response is shown in Figure 9 and it may be seen that the drift has been eliminated. An arbitrary response curve using this circuit is shown in Figure 10, and it may be seen that the high-frequency response is still excellent.

IV. CONCLUSIONS

The methods presented here should be of use in many situations where thermal time lags occur, and improvements in response comparable with the example presented here may be expected.

APPENDIX I

To solve equation (5) subject to (6) and (7) we use the method of Green's function⁴. We solve for a function $G(\vec{r}t; \vec{r}'t')$ satisfying

$$\left\{ c_p \rho \frac{\partial}{\partial t} - \nabla \cdot (K \nabla) \right\} G(\vec{r}t; \vec{r}'t') = \delta(\vec{r} - \vec{r}') \delta(t - t') \quad (8)$$

and subject to

$$K \vec{n} \cdot \nabla G + D G = 0, \text{ on } \sigma_1 \text{ and } \sigma_2 \quad (9)$$

and,

$$G(\vec{r}t; \vec{r}'t') = 0, \text{ when } t < t' \quad (10)$$

It may be shown⁵ that G also satisfies

$$\left\{ -c_p \rho \frac{\partial}{\partial t} - \nabla \cdot (K \nabla) \right\} G(\vec{r}'t'; \vec{r}t) = \delta(\vec{r} - \vec{r}') \delta(t - t') \quad (11)$$

with

$$K \vec{n} \cdot \nabla G(\vec{r}'t'; \vec{r}t) + D G(\vec{r}'t'; \vec{r}t) = 0 \text{ on } \sigma_1 \text{ and } \sigma_2 \quad (12)$$

$$\overline{G}(\vec{r}'t'; \vec{r}t) = 0, \quad t' < t \quad (13)$$

Multiplying (5) by $G(\vec{r}'t'; \vec{r}t)$ and (11) by $T(\vec{r}t)$, subtracting the two, integrating over R and over t from 0 to t'^+ , and using the divergence theorem we have

$$T(\vec{r}t') = \int_R (dv) G(\vec{r}'t'; \vec{r}0) u(\vec{r}) + \int_0^{t'} dt \int_{\sigma} d\sigma \vec{n} \cdot (G\nabla T - T\nabla G) K \quad (14)$$

The surface integral may be written

$$\int_{\sigma} d\sigma \{ G(K\vec{n} \cdot \nabla T + DT) - T(K\vec{n} \cdot \nabla G + DG) \} \quad (15)$$

and using the boundary conditions (6) and (12) we see that (15) may be written

$$\int_{\sigma_1} d\sigma G(\vec{r}'t'; \vec{r}t) F(t) \quad (16)$$

Now it is clear from (11), (12) and (13) that G depends only on the difference $(t-t')$, not on t and t' separately. Thus we write

$$G(\vec{r}t; \vec{r}'t') = G(\vec{r}\vec{r}'; t-t') \quad (17)$$

Using this fact along with (16), we now write (14), letting $\vec{r} = \vec{\xi}$ and interchange t and t' , as

$$T_{\vec{\xi}}(t) = \int_R (dv) G(\vec{\xi}\vec{r}; t) u(\vec{r}) + \int_0^t dt' K_{\vec{\xi}}(t-t') F(t') \quad (18)$$

where

$$T_{\xi}(t) = T(\vec{\xi}t) \quad (19)$$

and

$$K_{\xi}(t) = \int_{\sigma_1} d\sigma G(\vec{\xi}\vec{r}; t) \quad (20)$$

Equation (18) is a basic result, for it gives the temperature variation of the thermocouple T explicitly as a function of the initial sensor temperature distribution and the time behavior of the forcing function $F(t)$ on the exterior surface. To avoid the necessity of carrying along the term involving the initial temperature distribution, let us choose the zero of time such that $U(r) = 0$. In terms of re-entry conditions, this means that we start measuring time before the sensors become heated significantly. Thus, we write

$$T_{\xi}(t) = \int_0^t dt' K_{\xi}(t-t') F(t') \quad (21)$$

Let us take the Laplace transform of (21) using the convolution theorem for Laplace transforms. This yields

$$\bar{T}_{\xi}(s) = \bar{K}_{\xi}(s) \bar{F}(s) \quad (22)$$

$$\bar{K}_{\xi}(s) = \int_{\sigma_1} d\sigma \bar{G}(\vec{\xi}\vec{r}; s) \quad (23)$$

$$\left\{ c_{pp} s - \nabla \cdot (k \nabla) \right\} \bar{G}(\vec{r} \vec{r}'; s) = \delta(\vec{r} - \vec{r}')$$

We may solve (24) in terms of an expansion in eigenfunctions $\psi_n(\vec{r})$ of the eigenvalue equation

$$\frac{1}{c_{pp}} \nabla \cdot (k \nabla \psi_n) = -\lambda_n \psi_n \quad (25)$$

with

$$k \vec{n} \cdot \nabla \psi_n + D \psi_n = 0, \quad \text{on } \sigma_1 \text{ and } \sigma_2 \quad (26)$$

These eigenfunctions are orthonormal and complete⁶. That is,

$$\int_R (dv) \psi_m(\vec{r}) \psi_n(\vec{r}) = \delta_{mn} \quad (27)$$

and

$$\sum_n \psi_n(\vec{r}) \psi_n(\vec{r}') = \delta(\vec{r} - \vec{r}') \quad (28)$$

Let \bar{G} be expanded in terms of these eigenfunctions

$$\bar{G}(\vec{r} \vec{r}'; s) = \sum_{mn} B_{mn}(s) \psi_m(\vec{r}) \psi_n(\vec{r}') \quad (29)$$

into (24)

Substituting (28) and (29) and using (25) we have

$$\sum_{mn} \psi_m(\vec{r}) \psi_n(\vec{r}') [(s + \lambda_m) B_{mn}(s) - (c_p \rho)^{-1} \delta_{mn}] = 0 \quad (30)$$

which yields

$$B_{mn}(s) = \frac{(c_p \rho)^{-1} \delta_{mn}}{s + \lambda_n} \quad (31)$$

Substituting this into (29) gives

$$\bar{G}(\vec{r}, \vec{r}'; s) = \sum_n \frac{(c_p \rho)^{-1} \psi_n(\vec{r}) \psi_n(\vec{r}')}{s + \lambda_n} \quad (32)$$

and with (23) we have finally

$$\bar{K}_{\vec{\xi}}(s) = \sum_n \frac{\lambda_n A_n(\vec{\xi})}{s + \lambda_n} \quad (33)$$

where

$$A_n(\vec{\xi}) = \frac{1}{\lambda_n} \psi_n(\vec{\xi}) \int_{\sigma_1} d\sigma (c_p \rho)^{-1} \psi_n(\vec{r}) \quad (34)$$

Note that the eigenvalues are all positive. This may be proved as follows:

Multiply (28) by $c_p \rho \psi_n(\vec{r})$:

$$\psi_n \nabla \cdot (K \nabla \psi_n) = -\lambda_n c_p \rho \psi_n^2 \quad (35)$$

Integrating (3) over volume R, using the divergence theorem and the boundary condition (26) we obtain

$$\lambda_n = \frac{\int_R (dv) K (\nabla \psi_n)^2 + \int_{\sigma} d\sigma D \psi_n^2}{C_p \rho \int_R (dv) \psi_n^2} \quad (36)$$

from which it is easily seen that

$$\lambda_n \geq 0 \quad (37)$$

This is equivalent to the statement that the solutions to the heat equation are stable, which requires the poles of the transfer function (33) to be in the left half plane.

The values of $A_n(\vec{\xi})$, however, may be positive or negative, depending upon whether the sign of the eigenfunction $\psi_n(\vec{\xi})$ and the sign of the integral in (34) are the same or not.

The transfer function is related to the Laplace transform of the unit step input response $\bar{H}_{\vec{\xi}}(s)$ by

$$s \bar{H}_{\vec{\xi}}(s) = \bar{K}_{\vec{\xi}}(s) = \sum_n \frac{\lambda_n A_n(\vec{\xi})}{s + \lambda_n} \quad (38)$$

so that

$$\bar{H}_{\vec{\xi}}(s) = \frac{1}{s} \sum_n A_n(\vec{\xi}) - \sum_n \frac{A_n(\vec{\xi})}{s + \lambda_n} \quad (39)$$

The quantity $\sum_n A_n$ has an important interpretation. Using a well known theorem on Laplace transforms and (38) we have

$$H_{\xi}(\infty) = \lim_{t \rightarrow \infty} H_{\xi}(t) = \lim_{s \rightarrow 0} s \bar{H}_{\xi}(s) = \sum_n A_n(\vec{\xi}) \quad (40)$$

Thus, $\sum_n A_n(\vec{\xi})$ is the final value reached at the thermocouple after a long time when the exterior surface is subjected to a unit step input. We now invert $\bar{H}_{\xi}(s)$ back into the time domain, using (3) and (40). This gives

$$H_{\xi}(\infty) - H_{\xi}(t) = \sum_n A_n e^{-\lambda_n t} \quad (41)$$

APPENDIX II

It will now be proved that the initial response of an interior temperature to a step input rises slower than any power of t , or, equivalently, the derivatives of the response are all zero at $t=0$. Denote the p -th derivative of $H_{\xi}(t)$ at $t=0$ by $H_{\xi}^{(p)}(0)$, $p \geq 1$. Then from equations (25), (34), and (41) it follows that

$$H_{\xi}^{(p)}(0) = \int_{\sigma_1} d\sigma (c_p \rho)^{-1} [-(c_p \rho)^{-1} \nabla \cdot (k \nabla)]^{p-1} \sum_n \psi_n(\vec{r}) \psi_n(\vec{\xi}) \quad (42)$$

and using (28)

$$H_{\xi}^{(p)}(0) = \int_{\sigma_1} d\sigma (c_p \rho)^{-1} [-(c_p \rho)^{-1} \nabla \cdot (k \nabla)]^{p-1} \delta(\vec{r} - \vec{\xi}) \quad (43)$$

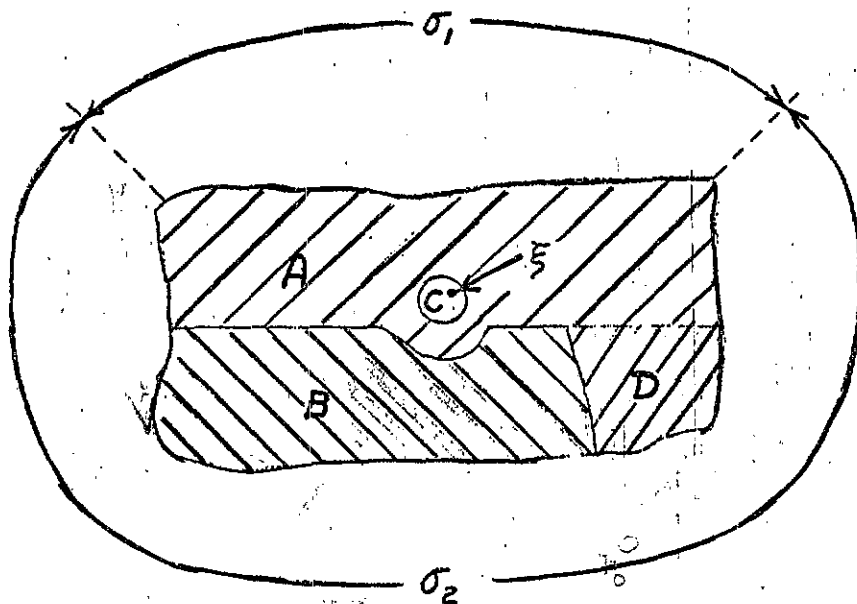
The integrand of this is a sum of terms each containing a factor of a multiple gradient of a δ -function $\delta(\vec{r} - \vec{\xi})$. For ξ not on the surface, this integral must clearly vanish. Thus

$$H_{\xi}^{(p)}(0) = 0, \quad p \geq 1, \quad \xi \text{ not on } \sigma_1 \quad (44)$$

and our assertion is proved.

REFERENCES

1. Beck, James, V., Correction of Transient Thermocouple Temperature Measurements in Heat-Conducting Solids; Part I, Procedures of Thermocouple Temperature Correction in Solids Possessing Constant Thermal Properties; Part II, The Calculation of Transient Heat Fluxes Using the Inverse Convolution; and Part III, Certain Correction Kernels for Temperature Measurements in Low Conductivity Materials, Avco RAD-TR-7-60-38 (Parts I, II, and III) 8 February 1961, 30 March 1961, and 21 July 1961.
2. Beck, James, V., Calculation of Surface Heat Flux from an Internal Temperature History, Trans. ASME, Journal of Heat Transfer, vol. 84, Series C, 1962.
3. Viles, F. M., Rybicki, G. B., et al. Research on Temperature Attitude Sensing for Re-Entry Vehicles, Phase II - Final Report, (U) ASD-TR-61-539, Vol. II.
4. Morse, Philip, M. and Feshbach, Herman, Methods of Theoretical Physics. Part I, Chapter 7, McGraw-Hill, 1953.
5. Op. Cit. P. 858 The proof given assumes ρ , C_p , and K constant, but the modification for our case are slight.
6. Op. Cit. Chapter 6, p. 676-790.
7. Chestnut, H., and Mager, R. W. Servomechanism and Regulating Systems Design, Vol. I, Wiley and Sons (New York 1959), p. 553 ff

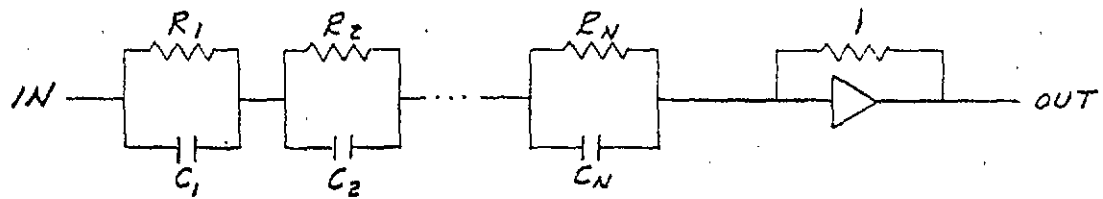


$$H_{\xi}(\infty) - H_{\xi}(t) = \sum_n A_n e^{-\lambda_n t}$$

$$\bar{K}_{\xi}(s) = \sum_n \frac{\lambda_n A_n}{s + \lambda_n}$$

$$\bar{K}_{\xi}(s) \bar{K}_c(s) = 1$$

FIGURE 1 - TYPICAL THERMAL SENSOR

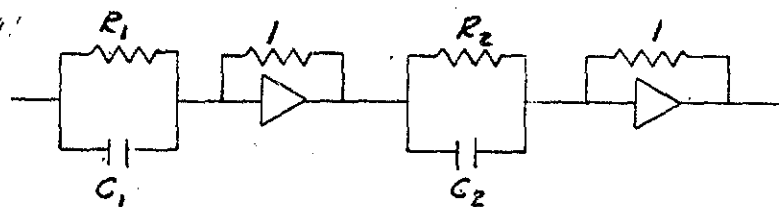


$$\bar{K}_c(s) = - \left[\sum_{n=1}^N \frac{A_n \lambda_n}{s + \lambda_n} \right]^{-1} \quad A_n \geq 0$$

$$R_n = A_n$$

$$C_n = \frac{1}{\lambda_n A_n}$$

FIGURE 2a - COMPENSATOR FOR A_n POSITIVE



$$\bar{K}_c(s) = \left[\frac{A_1 \lambda_1}{s + \lambda_1} - \frac{A_2 \lambda_2}{s + \lambda_2} \right]^{-1} \quad A_1 \lambda_1 = A_2 \lambda_2$$

FIGURE 2b - COMPENSATOR WITH A_1 AND A_2 OF OPPOSITE SIGN

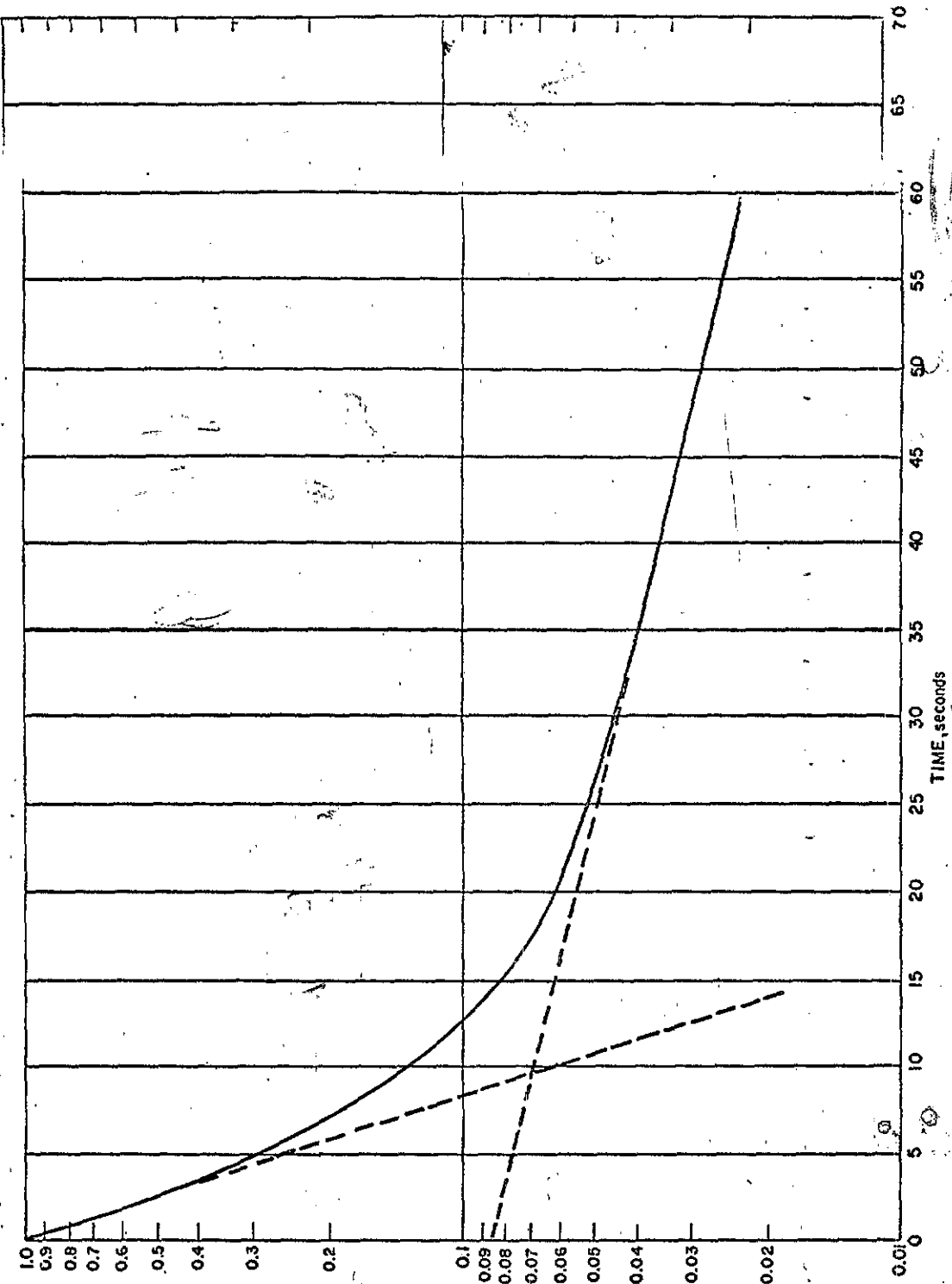


Figure 3 LOG NORMALIZED UNACCOMPLISHED RESPONSE

$$\frac{0.1}{1 - 0.1} = \frac{0.09}{1 - 0.09}$$

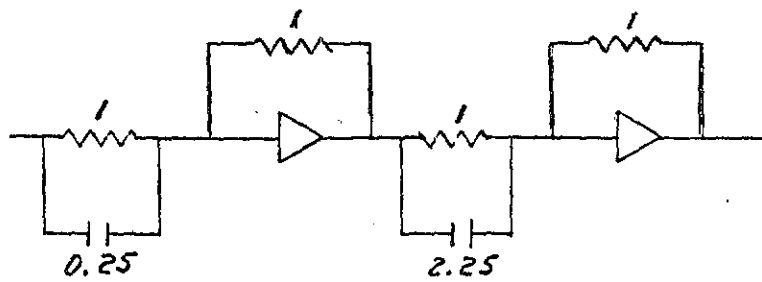


FIGURE 4a - COMPENSATION NETWORK FOR λ_1 AND λ_3

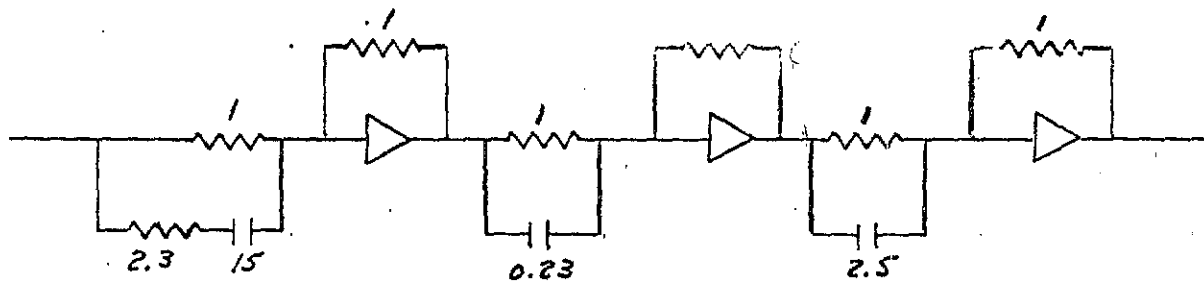


FIGURE 4b - COMPENSATION NETWORK FOR λ_1 , λ_2 , AND λ_3

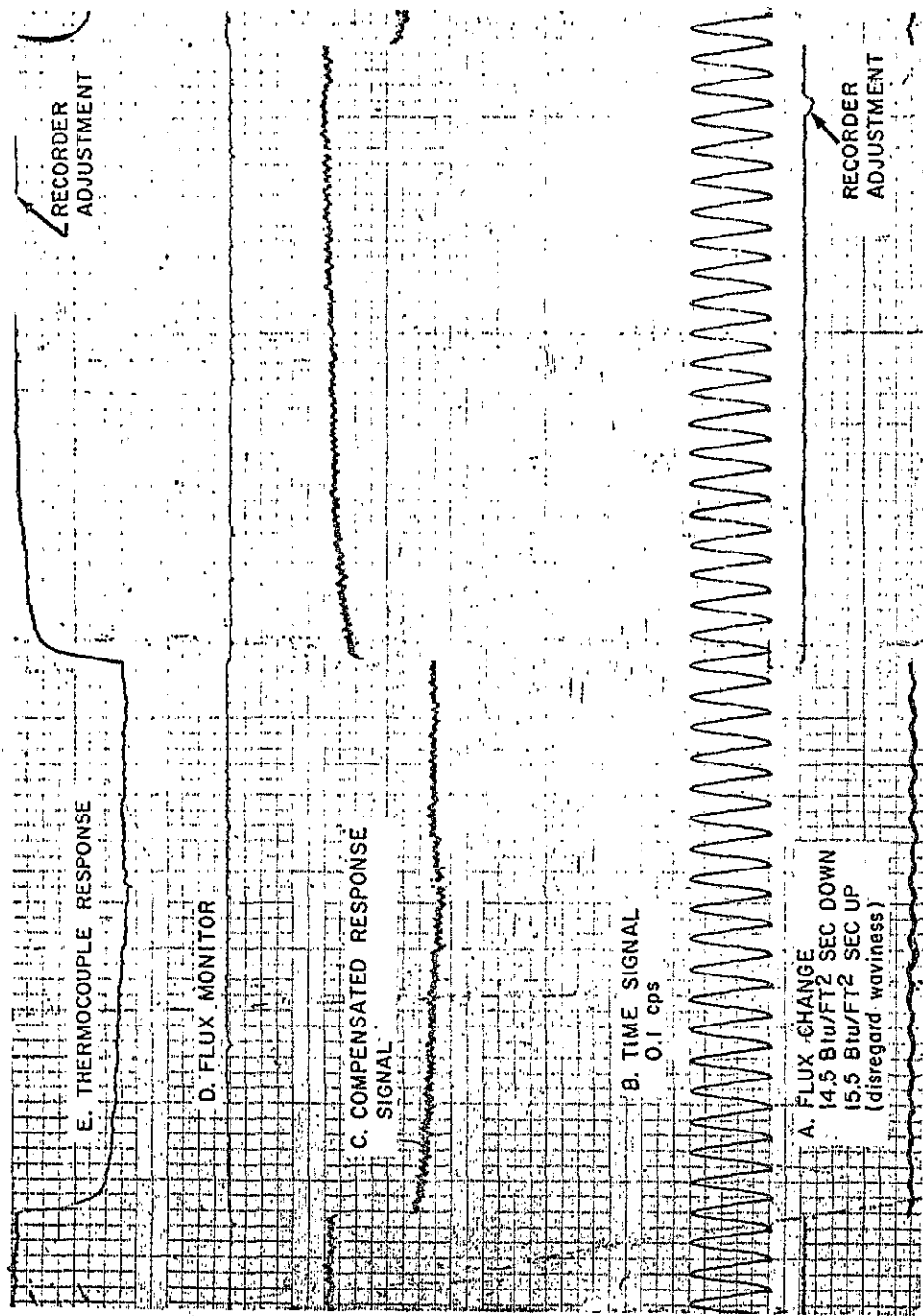


Figure 5 RESPONSE TO STEP FLUX CHANGE

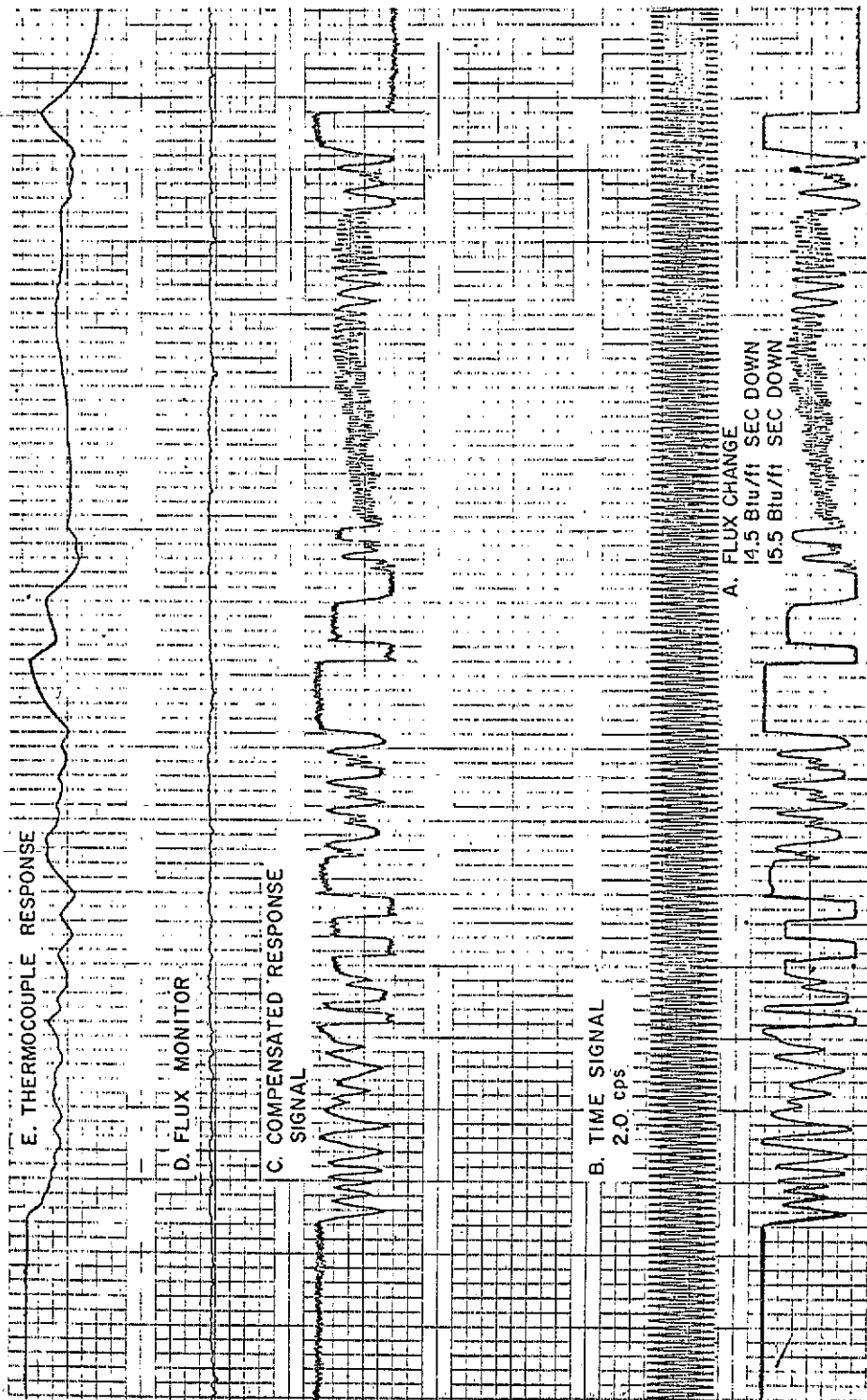


Figure 6 RESPONSE TO ARBITRARY VARIATIONS

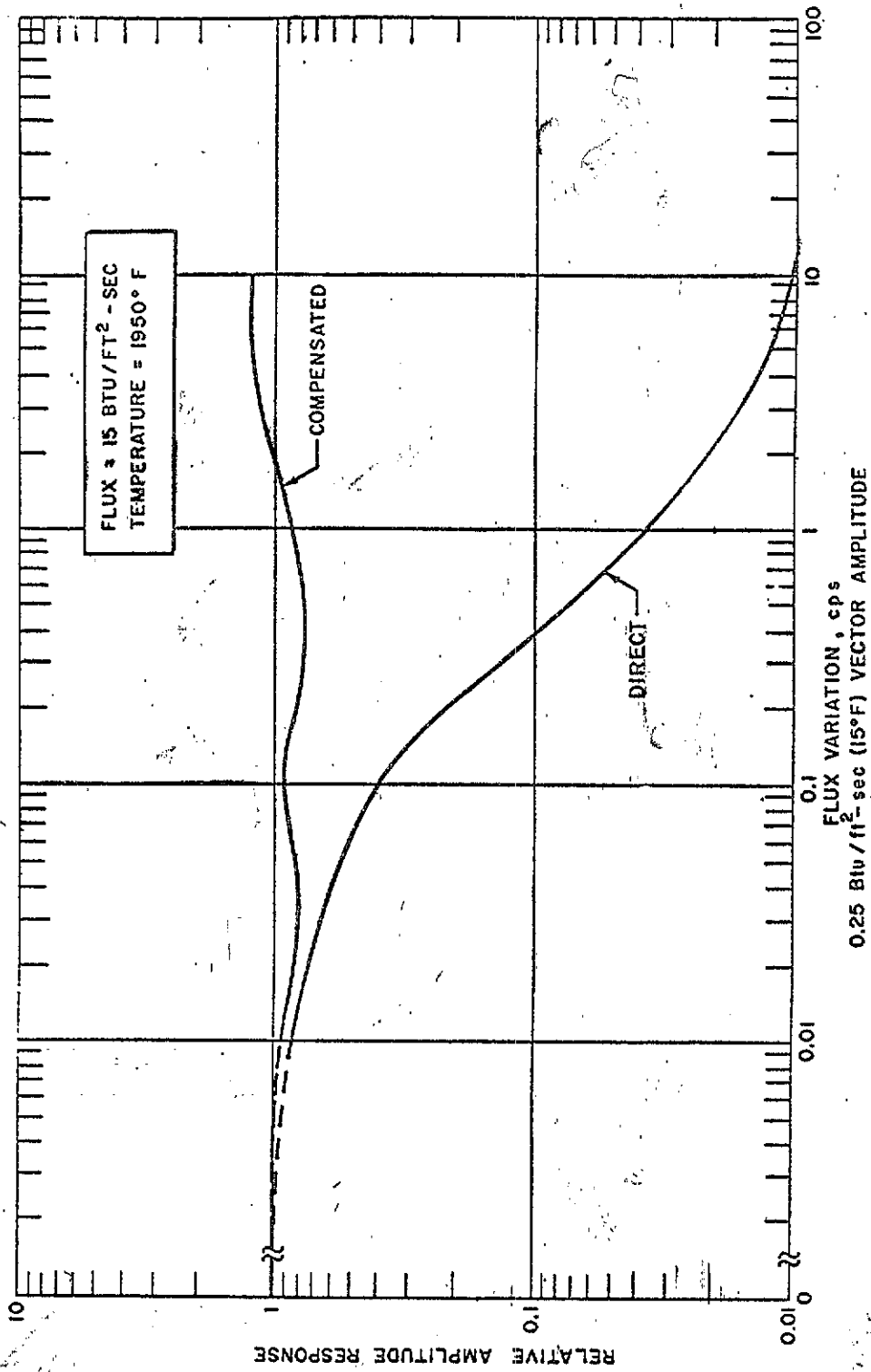


FIGURE 7 - RELATIVE AMPLITUDE RESPONSE FOR SINUSOIDAL FLUX VARIATION - DIRECT AND COMPENSATED

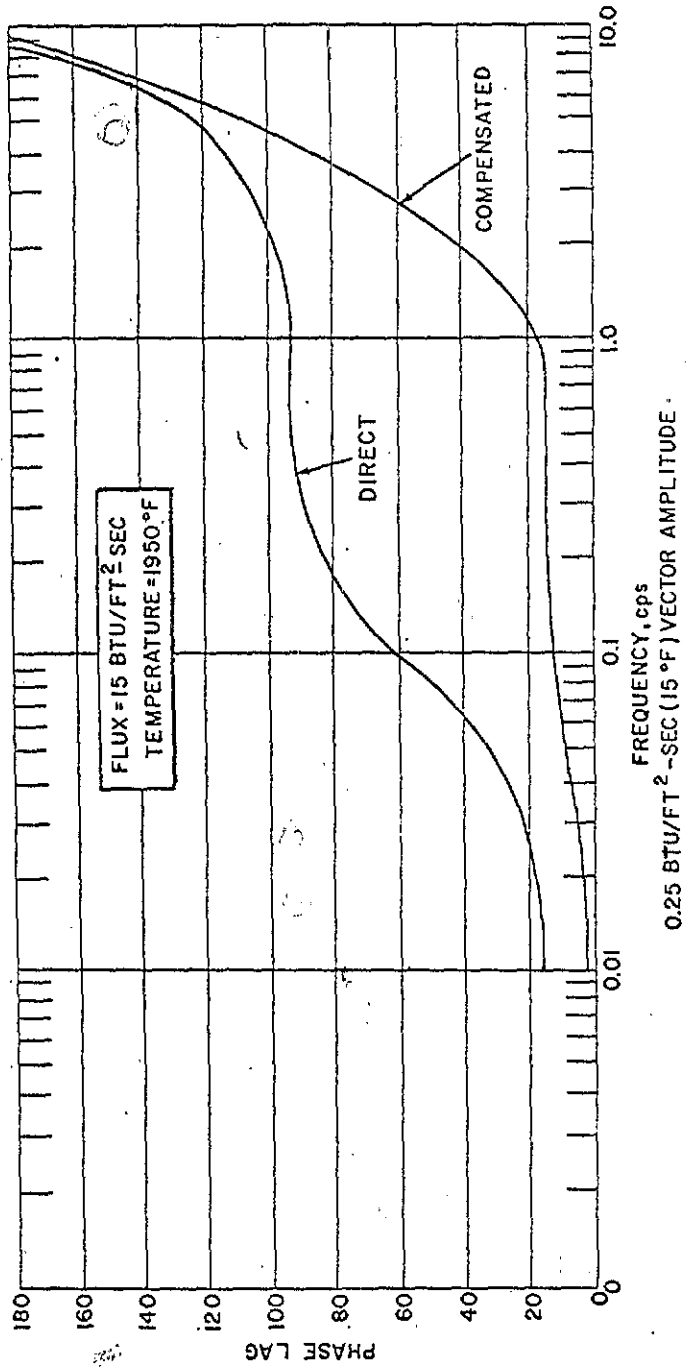


FIGURE 8 - RESPONSE PHASE LAG FOR SINUSOIDAL FLUX VARIATION-DIRECT AND COMPENSATED

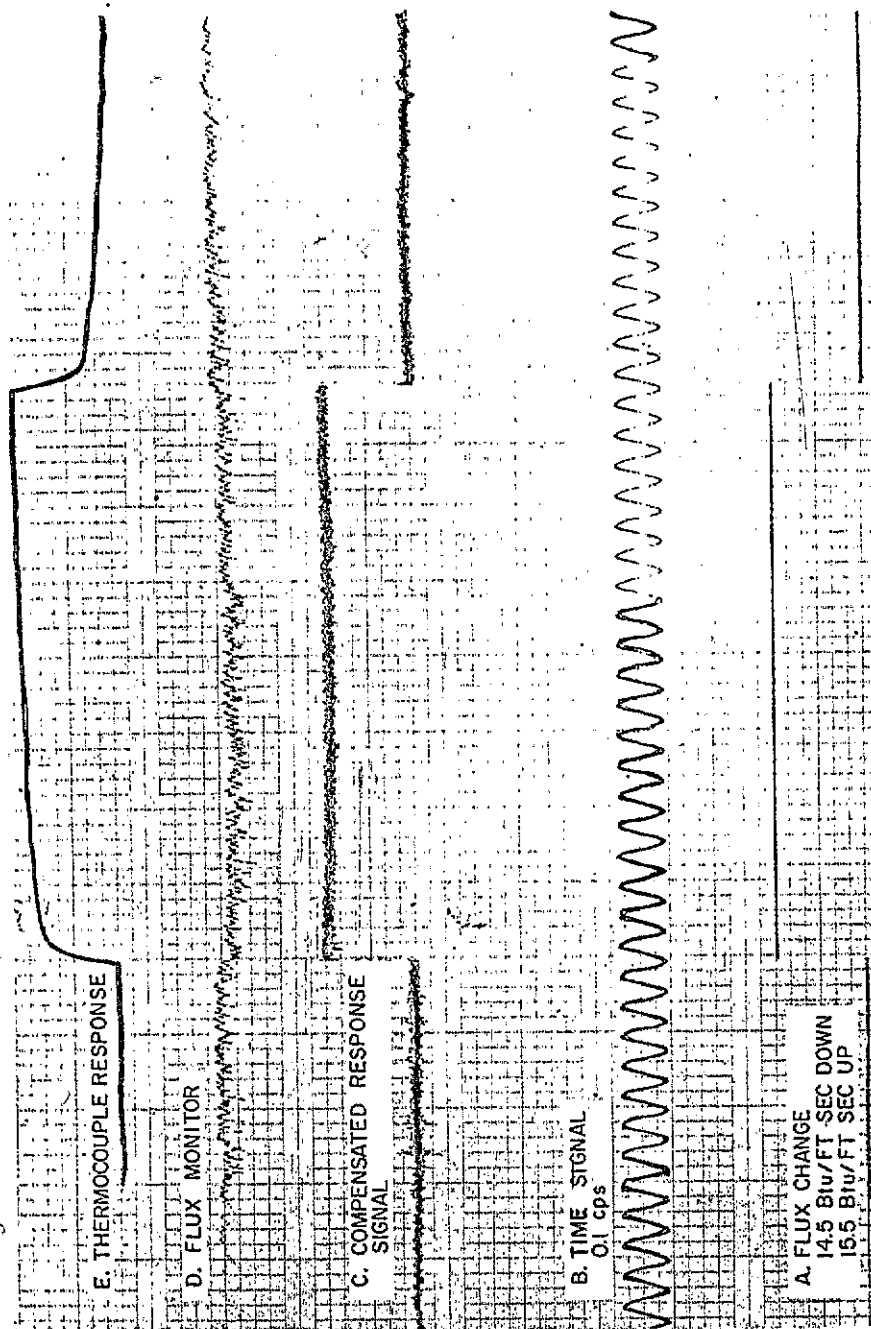


Figure 9 RESPONSE TO STEP INPUT WITH LONG TIME COMPENSATION

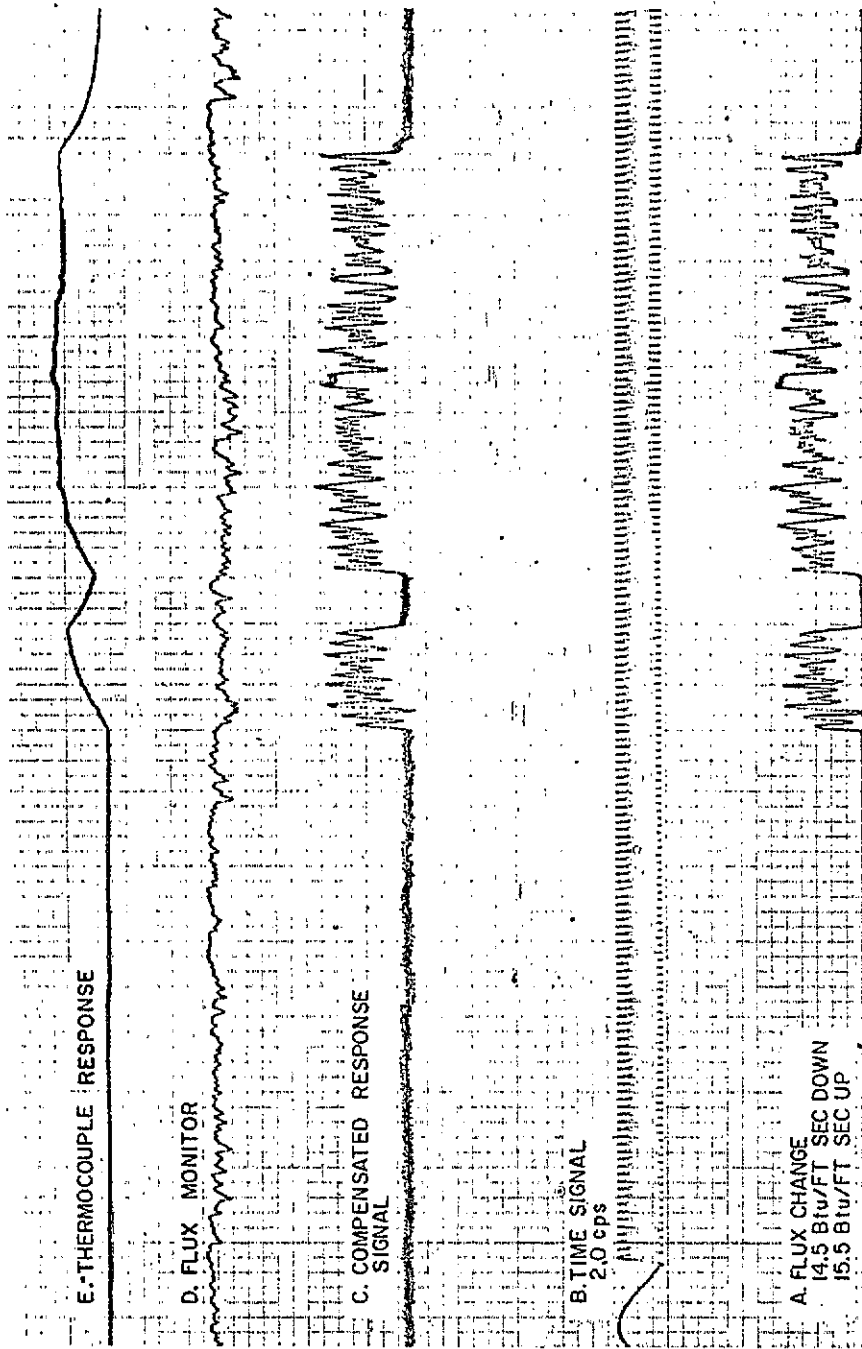


Figure 10 RESPONSE TO ARBITRARY FLUX VARIATIONS WITH LONG TIME COMPENSATION

SECTION X

VIBRATION ISOLATION OF
FLUSH DIAPHRAGM PRESSURE TRANSDUCERS
USED ON ROCKET MOTORS

by

Steve Rogero
Jet Propulsion Laboratory
Pasadena, California

VIBRATION ISOLATION
of
FLUSH DIAPHRAGM PRESSURE TRANSDUCERS
used on
ROCKET MOTORS

Steve Rogero

JET PROPULSION LABORATORY
Pasadena, California.

VIBRATION ISOLATION OF FLUSH DIAPHRAGM PRESSURE TRANSDUCERS USED ON ROCKET MOTORS¹

Steve Rogero

Introduction

Pressure measurements made in the presence of high acceleration forces, e.g., rocket motor chamber pressure measurements made during unstable combustion, can be seriously degraded by a transducer's sensitivity to acceleration. Attempts to separate that portion of the signal produced by real pressure from that portion which is produced by vibration are seldom satisfactory. The most direct solution to the problem is to keep the transducer isolated from vibration by using a shockmount of some type. This discussion will include general and specific information on the design and evaluation of shockmounts for flush diaphragm pressure transducers which have been developed for use on programs at JPL.

A portion of the Rocket Motor Injector Research Program conducted by the JPL Propulsion Research Section used a pentaboraine-hydrazine propellant combination resulting in a series of extremely "rough" runs (Ref. 1). Chamber pressure data recorded during this series of runs seemed highly suspect, and several of the very rugged Model 352 Photocons were damaged by excessive vibration. On subsequent runs Model 352's mounted in blind taps (rigidly attached to chamber wall, but not exposed to pressure) yielded outputs up to 50% of transducer full scale due to vibration alone. Tests of 352's on the "high g generator" (Ref. 2) at levels up to 1000 peak gs confirmed the manufacturer's stated transducer acceleration sensitivity at from .001% to .002% of full scale/peak g. Concurrent with the transducer acceleration sensitivity tests the development of a shockmount for use with flush diaphragm transducers was begun.

Photocon Shockmount. The first attempt at isolating the transducer resulted in a mount similar in principle to that shown in Slide 1, but with a different clamping and padding arrangement. The isolation characteristics were relatively poor, and there was little vibration attenuation below 8 kcps. Even so, pressure data taken using this mount were far superior to that taken with the transducer rigidly mounted. Refinements in the original design produced the arrangement shown in Slide 1, and vibration tests were conducted to determine the best material, thickness, etc. for use as padding in the shockmount. These tests were conducted on a Ling vibration table using a dummy transducer of the same mass and shape as a Model 352 Photocon or, in some cases, the transducer itself with water-filled connecting lines and cables. Instrumentation consisted of accelerometers mounted on the table and on the transducer, or dummy. Inputs to the mount were held constant at 10 peak gs over the range from 50 cps to 10 kcps. The isolating characteristics of the mount as determined from these tests are shown in Slide 2. These characteristics were

¹From Technical Report No. 32-624 entitled "Measurement of the High-Frequency Pressure Phenomena Associated with Rocket Motors" by Steve Rogero, Jet Propulsion Laboratory, Pasadena, California, May 1964.

checked at maximum shaker output (up to 50 peak gs) and found to be the same as for lower levels.

The fixture to which the shockmount was attached during vibration tests allowed pressurization of the mount to 500 psi for the purpose of simulating the chamber pressure seen during actual runs. (The area of the mount exposed to chamber pressure is approximately 1.5 in²; thus for every 100 psi of chamber pressure there was a 150 lb. "preload" on the pads.) As expected, an increase in chamber pressure produced an increase in the stiffness of the rubber pads and a corresponding increase in the resonant frequency (f_r) of the mount. With the 3/8 inch neoprene pad the f_r increased on the order of 150 to 200 cps for each 100 psi increase in chamber pressure, i.e., from 250 cps at zero psig to 950 cps at 400 psi.

Since the shockmount is a simple spring-mass system and its resonant frequency proportional to the square root of the spring constant

$$f_r = \frac{1}{2\pi} \sqrt{\frac{K}{M}}$$

it was thought that by using softer rubber, the spring constant, and hence the resonant frequency could be lowered. Silicone rubber pads 1/8 inch thick in Shore-hardnesses of 20, 30, and 40 were obtained and the characteristics compared with that of neoprene (approximately 55 Shore-hardness). The results were somewhat disappointing in that no lowering of resonance occurred. The reason becomes apparent upon inspection of the curves in Slide 3. For although the silicone is quite soft by comparison with the neoprene when both are in the relaxed state, there is little difference in spring constants when both are subjected to the compressive forces present at 300 psi chamber pressure. Since the neoprene is generally more durable, exhibits better damping, and is easier to obtain, it was used in all subsequent tests. In all cases the use of two or three laminations exhibited better characteristics (especially with regard to damping) than did a single thickness. The use of more than three laminations, however, showed no appreciable improvement and was considerably more difficult to assemble, with the transducer, into the mount.

In evaluating the characteristics of the shockmount during actual run conditions, accelerometers were mounted directly on the motor chamber adjacent to the transducer mounts and cemented to the transducer or isolated portion of the transducer. Data recorded during unstable runs indicated peak g levels on the chamber of from 2000 to 6000 gs with attenuation by the shockmount of from 2:1 to 10:1. The accuracy of the vibration data (generally in the 10 kcps to 20 kcps range) may have been severely compromised by the frequency response capabilities of the tape recording system (d.c. to 10 kcps). Some examples of pressure data recorded using Photocon transducers in hard and soft mounts are shown in Slide 4.

*Resonant frequency as used here refers to the frequency at which amplification is at a maximum.

Pressure Compensated Shockmount. It was apparent from information gained in evaluating the original transducer shockmount that a serious limitation in lowering the resonant frequency of the mount was the preload placed on the springs (or pads) by chamber pressure. Much consideration was given the possibility of somehow compensating for the effect of chamber pressure, with the end result shown in Slide 5 (a rather complex design in terms of seals and assembly, but straightforward in principle). Through a series of passages in the lower portion of the mount, chamber pressure is allowed to act on the area A_2 which is $\pi(r_2^2 - r_1^2)$. Then, if the area A_1 , directly exposed to chamber pressure, equals the area A_2 , vented to chamber pressure, the upward force normally exerted on the mount will be cancelled. (For A_2 to equal A_1 , r_2 must equal $\sqrt{2r_1}$). With the preload thus eliminated, the spring constant of the upper pads (silicone O-rings) may be very low and, as was learned from tests, the pads are required only to reposition the transducer in the event it should be displaced by instantaneous differences in pressure on A_1 and A_2 . A prototype shockmount was constructed and tested in the same manner as the original Photocon mount. The effects of neoprene and silicone pads and seals were evaluated as well as the changes in resonant frequency with the addition of mass to the suspended portion -- with the following general conclusions:

1. (Slide 6) The pressure-compensated mount accomplished vibration isolation characteristics comparable to that of the existing Photocon mount with only 1/20 of the mass. Similar compensation on the Photocon mount should result in a resonant frequency below 100 cps.

2. Spring constant characteristics (at 300 psig simulated chamber pressure) are dependent on the type of seals used rather than the padding material. In fact, at chamber pressure, removal of the positioning seals does not affect the resonant frequency. It appears that as the seals are compressed they grip the sides of the adaptor and in the presence of vibration tend to distort rather than slide.

3. (Slide 7) Without pressure compensation, the shockmount resonance would be greatly increased and the isolating capabilities reduced. This can be seen where the compensating holes were plugged and all rubber except the lower seal and upper pad were removed. This condition is worse than if the transducer were rigidly mounted to the shaker of chamber wall.

As a supplement to the information obtained on the vibration table, several tests were conducted to evaluate the shockmount on the side and end of the shocktube. Slide 8a shows the response of a Kistler Model 603 rigidly mounted to the side of the shocktube. Slide 8b shows the output of the same transducer in the same location with the diaphragm blanked. The output here is due to vibration alone. Slide 8c is the output of the same Kistler mounted in the pressure compensated shockmount. Slide 8d is the output of a shockmounted Kistler with blanked diaphragm. Slides 8e and 8f are the outputs of blanked transducers which were respectively rigidly mounted and shockmounted on the end of the shocktube.

A transducer installed on a rocket motor, or shocktube, may see accelerations from one or both of two sources, i.e., transmission through the supporting structure, in the case of rigid mounts, or an imbalance of force produced by a pressure differential across the suspended portion of a shockmounted adaptor. The latter situation is especially noticeable in the case of a low mass system (such as the Kistler) exposed to high amplitude pressure spikes or steps. Proof of the acceleration source can be seen in Slide 8g, where the shockmounted portion as well as the transducer itself was blanked off in an end mounted configuration. (For this test as well as the others illustrated in Slide 8 the downstream section of the tube was pressurized to 150 psi prior to passage of the shock wave.) The shockmount was exposed to wall vibrations only, and, as Slide 8g indicates, decoupling between the end plate and the transducer was such that the output due to vibration was negligible. Acceleration due to forces on the transducer itself can be reduced by increasing the mass of the suspended portion. The use of Mallory 1000 (a tungsten-copper alloy) in the adaptor would increase the mass three times and result in 1/3 the acceleration output for a given force. A side effect would be a reduction of the shockmount resonant frequency by $\frac{1}{\sqrt{3}}$.

The pressure compensated shockmount appears quite usable. This basic design, with a few minor changes to facilitate its operational use, will be incorporated into the instrumentation system on forthcoming instability tests.

Conclusion

Outputs due to vibration can comprise a significant portion of the pressure data taken on rocket motor runs. The separation of vibration induced signals from real pressure data is difficult, if not impossible, and should only be attempted by comparing the output of a "live" transducer with the output of a similar blanked transducer mounted nearby. Transducers can and should be shockmounted whenever possible, however, shockmounts must be carefully evaluated to prevent a possible worsening of the vibration environment.

Slides:

1. Photocon shockmount used on RMIR program.
2. Isolating characteristics of various Photocon shockmount configurations.
3. Compressibility of materials used in Photocon shockmount.
4. Acceleration effects in the output of a Photocon transducer.
5. Pressure compensated transducer shockmount.

6. Isolating characteristics of pressure compensated transducer shockmount.
7. Isolating characteristics of shockmount with and without chamber pressure compensation.
8. Shocktube evaluation of pressure compensated shockmount.

References:

1. Nerheim, N. M., "On the Experimental Performance of the Pentaboraine-Hydrazine Propellant Combination," An Experimental Correlation of the Nonreactive Properties of Injection Schemes and Combustion Effects in a Liquid-Propellant Rocket Engine (In Eight Parts). Part VIII, Technical Report No. 32-255, Jet Propulsion Laboratory, Pasadena, California, April 1962. CONFIDENTIAL
2. Walenta, I. E. and Connor, B. V., "A Sinusoidal Vibrator for Generating High Accelerations at High Frequencies," Technical Report No. 32-13, Jet Propulsion Laboratory, Pasadena, California, January 1960.

SECTION XI

IMPROVEMENTS IN PLASTIC FILM
PRESSURE TRANSDUCERS

by

Messrs. J. M. Yarlott and A. B. Dager
Pratt & Whitney Aircraft
East Hartford, Connecticut

ACKNOWLEDGEMENT:

The authors wish to acknowledge the many engineers and technicians who contributed to the developments described herein.

Abstract

This paper describes a miniature pressure transducer suitable for measuring fluctuating pressures on the surfaces of axial flow compressor blades and vanes. The 1/8" diameter transducer is of the capacitive type fabricated from two layers of metalized plastic film. Fluctuating pressures cause displacement of the outer film. This motion is resisted by the spring action of air trapped in microscopic cavities in the mating surfaces. The combination of low diaphragm mass and high spring rate of the tiny air cavities results in a very high natural frequency. Transducers with fundamental natural frequencies greater than 100KC have been tested on the rotating blades of a 28" diameter single stage compressor at speeds up to 10,000 rpm. The transducer fabrication and installation techniques are described in detail and experiences gained in calibration and use are related.

Contents

	<u>Page</u>
Abstract	iii
I Introduction	1
II Requirements	1
A. Frequency Requirement	
B. Sensitivity Requirement	
C. Size Requirement	
1. Thickness	
2. Diaphragm Area	
D. Weight Requirement	
III The Transducer	3
A. General Considerations	
B. Construction and Fabrication Details	
C. Attachment to a Surface	
IV Installation and Signal Transfer Techniques	4
A. Leadwires	
B. Sliprings	
C. Electronics	
V Dynamic Characteristics	4
A. Introduction	
B. Calibration Techniques	
1. Shock Tube	
2. Electromagnetic Calibrator	
3. Spark Calibrator	
C. Sensitivity	
1. Manufacturing Variations	
2. Stability	
D. Noise	
E. Acceleration Sensitivity	
F. Aerodynamic Effects	
1. Test Apparatus	
2. Some Interesting Results	
VI Applications	7
VII Conclusion	7
References	

Illustrations

1. Compressor Blade Wakes Detected by a Hot-wire Anemometer
2. Pulse-shaped Wake Waveform
3. Schematic Drawing of a High-frequency Pressure Transducer
4. Film-type Pressure Transducer
5. Jig for Installing Film Type Pressure Transducer Diaphragms
6. Film Pressure Transducers Mounted on a JT8D Second Stage Compressor Blade
7. Film-type Pressure Transducers on Rotor Blades of JT8 Rig After Running More Than 30 Hours At Rotor Speeds Up to 10,000 RPM
8. Slipring Assembly
9. Block Diagram of Capacitive Film Pressure Transducer System
10. Shock Tube for Calibration of Film Pressure Transducers
11. Film Pressure Transducer Response to Shock Tube Step Pressure Pulse of 4.6 psi
12. Transfer Function of a Film Pressure Transducer System
13. Electromagnetic Calibrator For Film Pressure Transducers
14. Output of Film Pressure Transducer Using Electromagnetic Calibrator
15. Capacitor-discharge Spark Calibrator For Film Pressure Transducers
16. Film Pressure Transducer Response to Capacitor Discharge Spark
17. Free Jet and Spoked Wheel Apparatus
18. Frequency Response of a Film Pressure Gage Mounted on a 3/8 Inch Diameter Rod
19. Variations of Frequency Response of The Cylinder Mounted Transducer With Angular Location Relative to The Leading Edge
20. Frequency Response of a Film Pressure Gage Mounted Mid-chord on The Suction Side, One-inch From The Tip of A JT8 First Stage Compressor Blade
21. Sample Frequency Spectra From a Film-type Pressure Transducer In A JT8 Single Stage Compressor Test Rig

"Improvements in Plastic Film Pressure Transducers"

I Introduction:

One phase of efforts to reduce axial flow turbojet compressor noise included research into noise generating mechanisms using single stage compressor rigs. Early in the program it was learned that a major component of the noise was due to the cutting of stator wakes by the rotor, and vice-versa. Since experimental data was needed of the transient aerodynamics on the surface of airfoils, a program was begun to develop a film-type pressure transducer which could be placed on the blades and vanes of axial flow compressors.

The Instrumentation Group at Pratt & Whitney Aircraft had gained considerable experience in strain gage systems (references 1 and 2). In order to take advantage of this experience it was decided that: (a) the transducers should be applied to airfoil surfaces in a manner similar to bonded strain gages, and (b) signals should be transferred from rotating parts using existing slipping assemblies. The program with these objectives has been successful. Multiple transducers on blades and vanes have operated satisfactorily for the duration of a 30 hour compressor test. It is the object of this paper to describe the fabrication and installation of the transducers and to relate some of the experiences gained in their calibration and use.

II Requirements:

A. Frequency Requirement

A film-type pressure transducer installed on rotating blades or stationary vanes must respond to a succession of wakes from the upstream cascade of airfoils. An example of measurements of wakes from rotor blades made with a hot-wire anemometer in a compressor rig is shown in Figure 1. The frequency response of the hot-wire anemometer system was adequate for measuring the wake widths, but not the heights. Both of these would be needed to determine the frequency content of the signal. In order to determine the highest frequencies present in sharp compressor blade wakes, the waveform was represented ideally as a pulse as shown in Figure 2. The number of significant harmonics contained in the pulse were determined analytically. "Significant" harmonics were arbitrarily defined as those having levels within 20db of the fundamental. This resulted in the relationship

$$n = \frac{4.5}{d}$$

where n = The highest significant harmonic number
d = Pulse duty cycle

Returning to Figure 1, d for the sharp wakes was measured and found to be about .08. Thus n, the highest significant harmonic, would be 55. The highest wake

Numerals in parenthesis refer to references cited on page 11

passing frequency anticipated was 5000 cps. Significant harmonics would extend to 55 x 5000 cps, or 275KC.

B. Sensitivity Requirement

The amplitude of the pressure fluctuation to be measured was estimated from compressor noise data, at from 0.1 to 10.0 psi peak-to-peak. The minimum acceptable transducer output for adequate resolution on the proposed readout equipment was about 10 millivolts. Thus the minimum transducer output would be 10 millivolts for a pressure signal of 0.1 psi peak-to-peak, or 100 mv/psi.

C. Size Requirement

1. Thickness

Because its intended use was to measure pressure fluctuations on the surface of airfoils, the dimensions of the pressure transducer were to be minimal. A study of the effects of finite transducer size was made by Burpo (3). For locally faired transducers located along the chord from 10 to 100% of the chordal distance from the leading edge and for upstream Mach number less than 0.4 it was shown that a protuberance height less than .5% of chord would have less than 1% effect on the pressure profile as determined from overall performance measurements. For a typical compressor chord length of 2.5" the transducer height would be restricted to .0125" using this criterion. The effect of local disturbances could be reduced by use of a sleeve extending from the leading edge to the trailing edge over a portion of the airfoil span with the transducer diaphragm flush with the sleeve outer surface. This would result in a smooth axial surface but would present an obstruction to spanwise flow in the boundary layer.

2. Diaphragm Area

The diaphragm diameter would have to be small to avoid ultrasonic directivity effects, and to reduce the effects of averaging. At ultrasonic frequencies pressure perturbation wavelengths would approach the diameter of even the smallest transducer. When this occurs the transducer response depends upon the direction of incidence of the pressure wave. For example, in the transverse direction one can imagine that for a sinusoidal wavelength exactly equal to a sub-multiple of the diaphragm diameter, the average diaphragm displacement would be zero. As the frequency is increased, the net output for non-sub-multiples would come from smaller and smaller portions of the diaphragm which would in effect reduce the sensitivity. For the normal direction of incidence, however, there would be a pressure doubling due to reflection of the incident wave which is independent of frequency. The limit of smallness of the diaphragm diameter would be that imposed by sensitivity and handling requirements.

D. Weight Requirement

The steady acceleration that would be experienced by a transducer mounted on a blade of a 28" diameter rotor was calculated to be about 40,000 G at the

highest rig speeds, (10,000 rpm). The transducer would have to be strong enough and light enough to remain undistorted while subjected to such acceleration. Also the adhesive used between the transducer and the airfoil would be required to have a great enough shear strength to keep the transducer in place. These requirements were met in the capacitive film type transducer described herein.

III The Transducer:

A. General Considerations

In order for a capacitive pressure transducer to have a uniform response with frequency, the motion of the diaphragm would have to be stiffness controlled with the natural frequency considerably above the upper end of the desired passband. This was achieved by using a method developed by Wright (4). High stiffness resulted from the use of microscopic air cavities typified by the diagram in Figure 3, which was reproduced from reference 4. Each tiny cavity contains a volume of air having great stiffness due to its small size. The capacitance between the upper surface of the Mylar and the bottom of the cavities is a function of the separation between them. A fluctuating pressure on the diaphragm causes small motions of the diaphragm thereby fluctuating the capacitance. A method developed by Schultz (5), which used a deliberate air cavity was tried, but an upper natural frequency limit of 20KC discouraged its adaptation to our needs. Piezoelectric transducers were also investigated but were found less desirable than the capacitive transducer because of their greater acceleration sensitivity.

B. Construction and Fabrication Details

A sketch of a film-type pressure transducer is shown in Figure 4. It comprises several layers of metal and plastic film bonded together with adhesives. The base layer is 2 mil Mylar which serves as both a base material and an insulator. The center electrode is aluminum foil molded over a base made of Armstrong cement. The center conductor is connected to the electrode with silver conducting paint, and bonded to the base layer with Eastman 910 cement. The conductor is covered with a bonded 1 mil layer of Mylar. The diaphragm material, 1/4 mil Mylar, is installed after stretching it in a jig shown in Figure 5. The jig has a rubber tipped plunger used to press the stretched diaphragm into place. Eastman 910 cement is used as diaphragm adhesive because of its quick-setting properties. The thickness of the sensitive portion of the transducer is less than .010", and its diameter is 1/8".

C. Attachment to a Surface

Eastman 910 cement was also used to attach the transducers to airfoils, examples shown in Figures 6 and 7. Since the transducers were pliable, they could be attached to curved surfaces having a little as 1/4" radius.

IV Installation and Signal Transfer Techniques:

A. Leadwires

Leadwires were installed in much the same way as the transducer. A small ribbon or wire conductor, about .003" diameter, was found necessary to reduce shunt capacity. The conductor was sandwiched between layers of Mylar. The sandwich was bonded to the surface with Eastman 910 cement. Electrostatic shielding was provided by a layer of silver conducting paint contacting the bare metal surface of the airfoil at the edges of the assembly. The flat leadwork was spliced to small diameter coaxial cable at the first possible point where there would be no obstruction to airflow.

B. Sliprings

When the transducers were installed on rotating parts, the small diameter coaxial cables were routed to a slipring through a hollow shaft. A photograph of a slipring assembly is shown in Figure 8. A standard PWA slipring was arranged to use coaxial cable externally as well as internally. The only signal conductors which were unshielded were the brushes and rings themselves.

C. Electronics

The output of a slipring channel was connected to the cathode follower of an Altec DC biased capacitive microphone system. This system is schematically illustrated in Figure 9. In stationary installations, the cathode followers would be put as close to the transducers as possible. The low frequency cut-off using this system was calculated to be less than one cps.

V Dynamic Characteristics:

A. Introduction

Since this transducer was developed for a specific application, determination of its dynamic characteristics was limited to the specific requirements. The transducer was treated as part of a measurement system, and calibrations were performed which included: the transducer, leadwires, electronic circuit, and readout device. The various calibration techniques used are described below including an attempt to determine the effect of aerodynamic performance of the supporting surface upon the dynamic characteristics. This was consistent with the philosophy that the transducer included the pressure gage itself, its physical support, and its coupling to the pressure source.

B. Calibration Techniques

1. Shock Tube

Primary calibration of the pressure transducer was accomplished with the shock tube shown in Figure 10. The shock tube used .0004" Saran as the

diaphragm material. Provisions were made to evacuate or pressurize the tube on either side of the diaphragm. In normal use, the short end was pressurized to about 1.3 atmospheres. The diaphragm was ruptured with a plunger causing a low intensity shock wave to propagate down the tube to the end-mounted transducer. The transducer was consequently subjected to a pulse of 5 millisecond duration having a rise time of less than one microsecond. A plot of the response of a transducer to the leading edge of the shock pulse is shown in Figure 11. From this data, the transducer "rise-time" and sensitivity were determined directly. A method of getting from the time domain to the frequency domain described in reference (6) was used to obtain the frequency response plot shown in Figure 12. This shows a flat response within $\pm 3\text{db}$ to 340KC .

2. Electromagnetic Calibrator

In-place sensitivity checks were made using a modified warning device comprising an electromagnetically actuated hammer striking a flat plate at the rate of 120 cps. The noise thus generated was transmitted to the transducer by means of a high pressure flexible hose. The end of the air hose was tightly held against the transducer as shown in Figure 13. An "O" ring seal was used to protect the transducer and assure repeatability by preventing leakage of sound. A typical calibration is shown in Figure 14. The initial pulse of this waveform was produced when the hammer struck the steel plate. This caused the plate to "ring" until struck again. This apparatus provided a means of checking sensitivity with an accuracy of $\pm 5\%$, but no rise time measurements were possible due to the low operating frequency range.

3. Spark Calibrator

A modified aircraft spark plug was used to produce a spark which could be used to check the transducer rise time. Use of the device is illustrated in Figure 15. A typical transducer output is shown in Figure 16. The reader is referred to reference 7 for further details on this method.

C. Sensitivity

1. Manufacturing Variations

It was found that the sensitivity could be affected by manufacturing variations. An unusually irregular electrode surface resulted in increased sensitivity, while seepage of adhesive between the diaphragm and electrode caused reduced sensitivity. A sensitivity of 100 mv/psi was generally achieved.

2. Stability

A shelf-life investigation of the stability of sensitivity is currently underway. Preliminary results indicate a drift toward greater sensitivity occurs during the first week. The effect of aging beyond one week appears to be small. The effects of ambient pressure and temperature changes have not yet been adequately checked.

D. Noise1. Electrical Noise

Electrical noise was not a problem in stationary installations of the transducer. Noise in a rotating installation consisted almost entirely of once-per-revolution pulses produced by the slipring. Recent minor modifications to the slipring arrangement have lowered this noise to 5 millivolts peak-to-peak.

E. Acceleration Sensitivity

An investigation was made to determine the possible side effects from the mounting of the transducers on vibrating parts wherein the transducer would behave like an accelerometer. The acceleration sensitivity was computed as follows:

The equivalent inertia force per unit area of the diaphragm is the product of its mass and acceleration divided by its area, or:

$$P = \sigma G g$$

Where: σ = mass per unit area
 G = acceleration in G's
 g = acceleration due to gravity
 P = equivalent inertia pressure

This result is the same by Rule et al (7) in the evaluation of acceleration response of capacitive pressure transducers. It was found that the calculated and measured acceleration sensitivities were in good agreement. This was true for frequencies well below the natural frequency.

The mass per unit area of the 1/4 mil aluminized Mylar diaphragm material was about 0.392×10^{-6} slug / sq. in. Solving for P/G:

$$\text{Acceleration sensitivity} = \frac{P}{G} = 12.65 \times 10^{-6} \text{ psi per g.}$$

It would take a vibration amplitude of 4 mils at 5000 cps to give an acceleration output corresponding to the pressure threshold level of 0.1 psi.

F. Aerodynamic Effects1. Test Apparatus

It was desired to find the effect of aerodynamic performance of the supporting surface upon the dynamic characteristics of the transducer. Some preliminary work was done using the apparatus shown in Figure 17. A free jet and a spoked wheel were arranged to provide a flow interrupted by sharp wakes. The wake passing frequency was controlled by wheel speed, and the jet velocity was varied up to Mach 0.2. The surface to be tested

was held in the free jet just downstream of the spoked wheel. Tests were conducted on both an airfoil-mounted and a cylinder-mounted transducer. Observations were limited to the amplitude of the fundamental of wake passing frequency. Controlled variables were: jet velocity, wake passing frequency, angular position of the transducer relative to the leading edge of the cylinder (θ), and angle of incidence of the airfoil chord (α_{CH}).

2. Some Interesting Results

Results for the transducer mounted on the cylinder at $\theta = 110^\circ$, given in Figure 18, indicated that the output was a function of frequency. The actual frequency was in the transducer flat frequency response region, yet there was a peak in the response occurring at a value of $fd/V = .2$, which corresponds to the Strouhal number for vortex shedding from a cylinder (9). The frequency response for angles other than $\theta = 110^\circ$, shown in Figure 19, shows a strong θ dependence. Results for the airfoil given in Figure 20 indicate the presence of a similar peak, corresponding to $fb/V = .44$, the vortex shedding reduced frequency for the airfoil (10). Additional peaks (not shown) were noted at blade vibrating resonant frequencies. The transducer was placed on the convex surface midway between leading and trailing edge.

While these tests were not considered conclusive, they indicated that transducers with lower natural frequencies, and resultant higher sensitivities might be useful when installed on a convex surface of airfoils, since the frequency response of the surface appeared to be a function of the vortex shedding frequency. The vortex shedding frequency would be quite low compared to the frequency imposed by sharp wakes.

VI Applications

Currently, film-type pressure transducers are being used on compressor blades and vanes at Pratt & Whitney Aircraft. Pressure fluctuation data is being gathered relevant to compressor blade stall, vibration excitation, and noise generation. Some sample results of the spectra obtained in a single stage rig are shown in Figure 21.

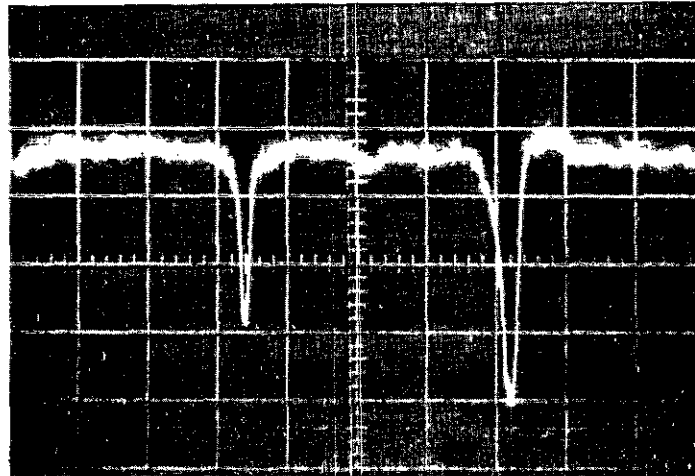
VII Conclusion

A high frequency-response film-type pressure transducer has been developed which is suitable for mounting on aerodynamic surfaces with negligible aerodynamic interference. Although the effects of environmental changes such as pressure and temperature have not been fully evaluated, it has been possible to obtain data which has proven useful in compressor development and noise reduction programs.

References

- (1) R. E. Gorton, and R. W. Pratt "Strain Measurements on Rotating Parts", SAE Quarterly Transactions, (October 1949)
- (2) E. A. Potter "Slipring Techniques for Aircraft Gas Turbine Engine Development", Strain Gage Readings Vol 6 No 2 (June - July 1963), pp 11-32
- (3) F. Burpo "Development of a Subminiature Surface Mounted Pressure Transducer", (Bell Helicopter Company, Report No. 299-199-200, January 1963)
- (4) Wayne M. Wright "High Frequency Electrostatic Transducers for Use in Gases", Harvard University Technical Memorandum #47, (April 1962)
- (5) T. J. Schultz "Air-Stiffness Controlled Condenser Microphone", Journal of the Acoustical Society of America, Vol 28 No 3, (May 1956)
- (6) D. J. Simmons "Finding Transfer Functions From Pulse Responses", Electronic Design, (March 16, 1964)
- (7) Leo Beranek "Acoustic Measurements", (New York: John Wiley & Sons, 1949) pp. 429
- (8) E. Rule, et al "Vibration Sensitivity of Condenser Microphones", Journal of Acoustical Society, Vol 32 No 7, (July 1960)
- (9) Anatol Roshko "Experiments on the Flow Past a Circular Cylinder at Very High Reynolds Number", Journal of Fluid Mechanics, Vol 10 Part 3 (May 1961)
- (10) Y. C. Fung "The Theory of Aeroelasticity", (New York: John Wiley & Sons, 1955) pp. 318

COMPRESSOR BLADE WAKES DETECTED BY
HOT-WIRE ANEMOMETER



0.1 V/CM.



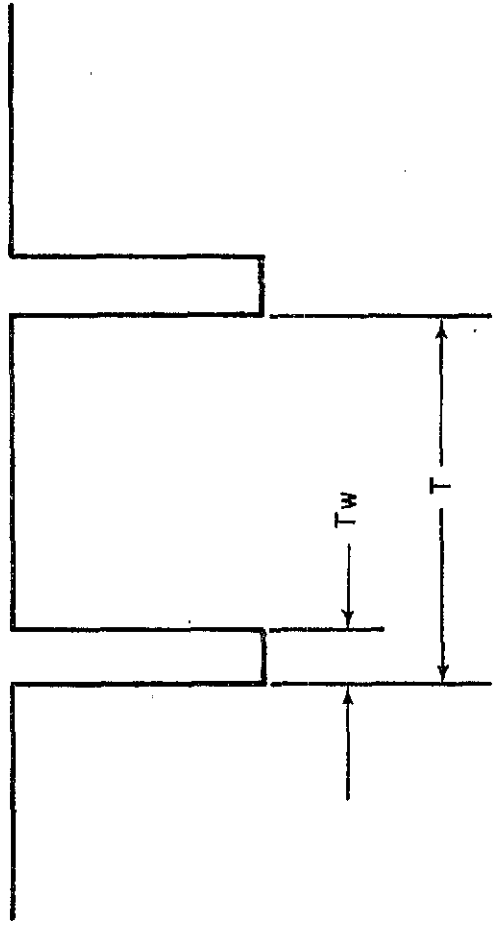
TIME: 100 μ SEC./CM.

ROTOR SPEED: 4300 RPM
NUMBER OF BLADES
IN ROTOR=32

XP-38951

FIGURE 1

PULSE SHAPED WAKE WAVEFORM



$$d = \frac{T_W}{T}$$

- T_W = WAKE WIDTH
- T = WAKE SPACING
- d = DUTY CYCLE

FIGURE 2

SCHEMATIC DRAWING OF A HIGH-FREQUENCY PRESSURE TRANSDUCER

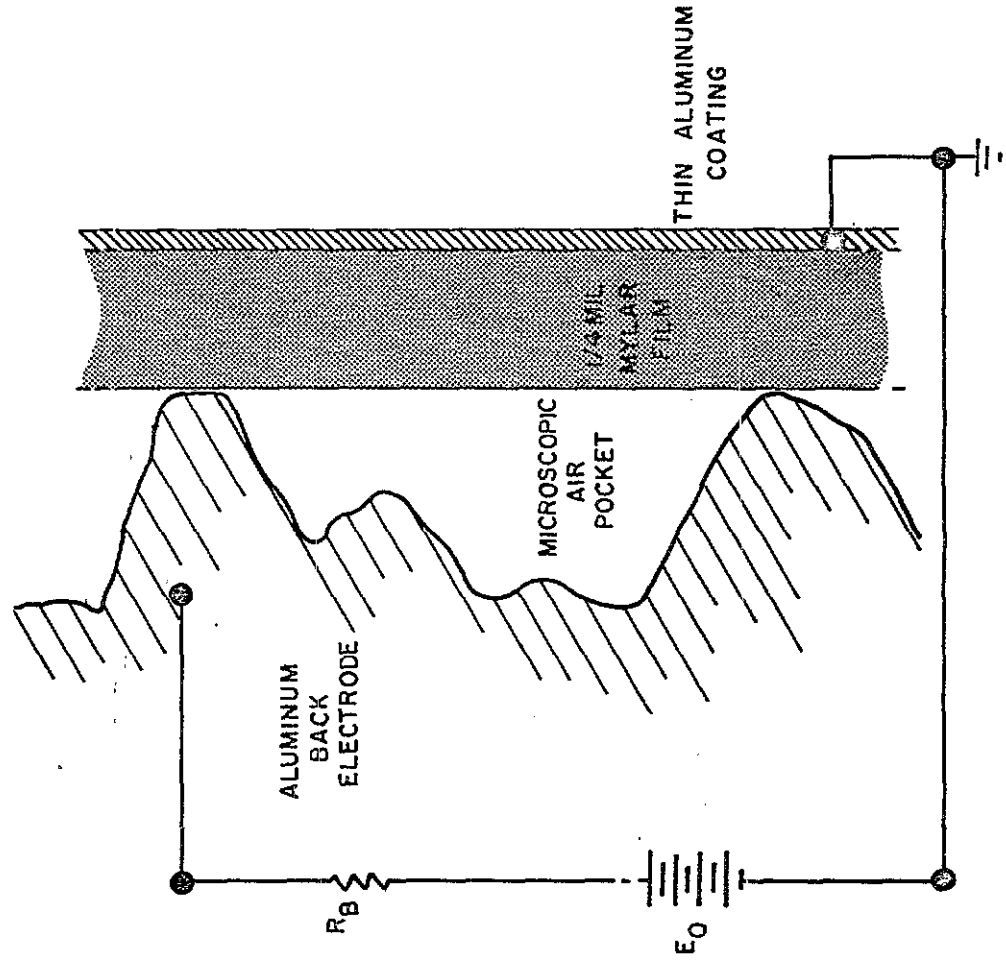
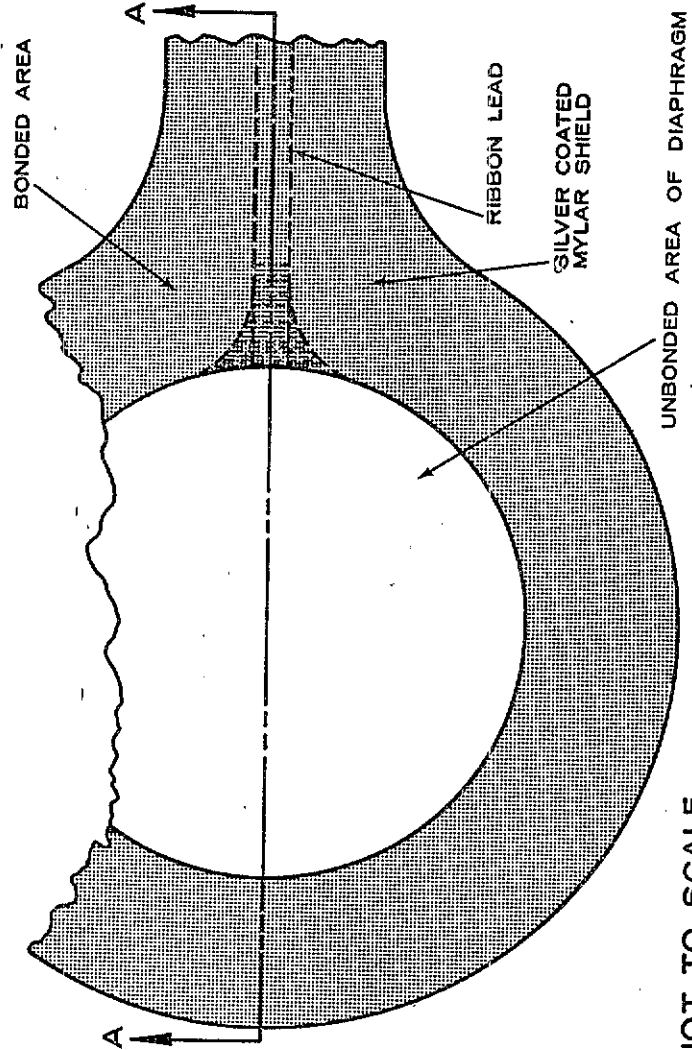
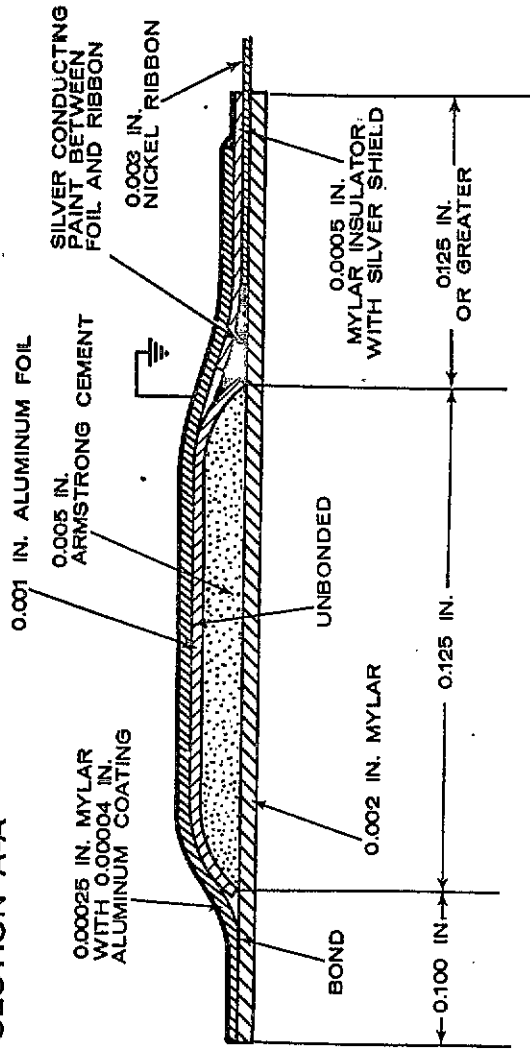


FIGURE 3

FILM TYPE PRESSURE TRANSDUCER

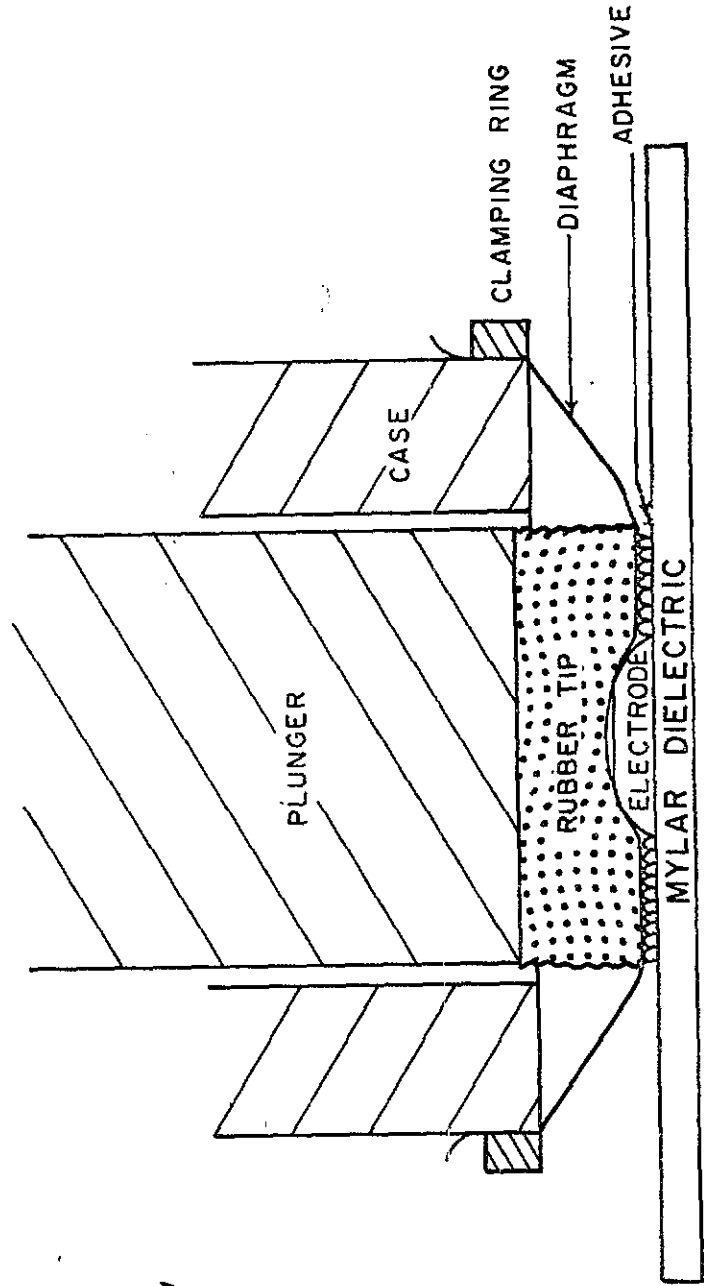
SECTION A-A



NOT TO SCALE

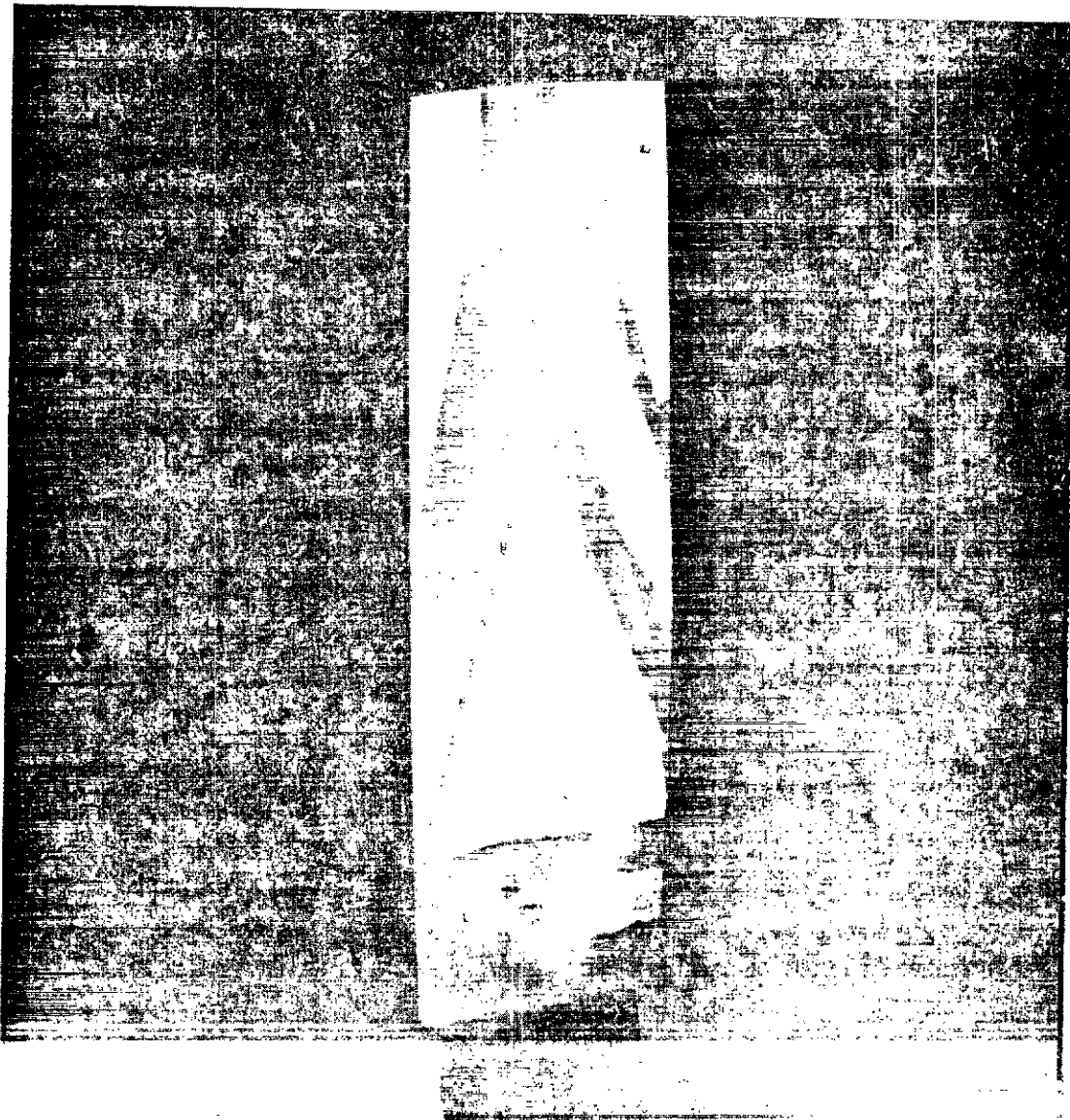
FIGURE 4

JIG FOR INSTALLING FILM-TYPE PRESSURE
TRANSDUCER DIAPHRAGMS



XI-13

FIGURE 5

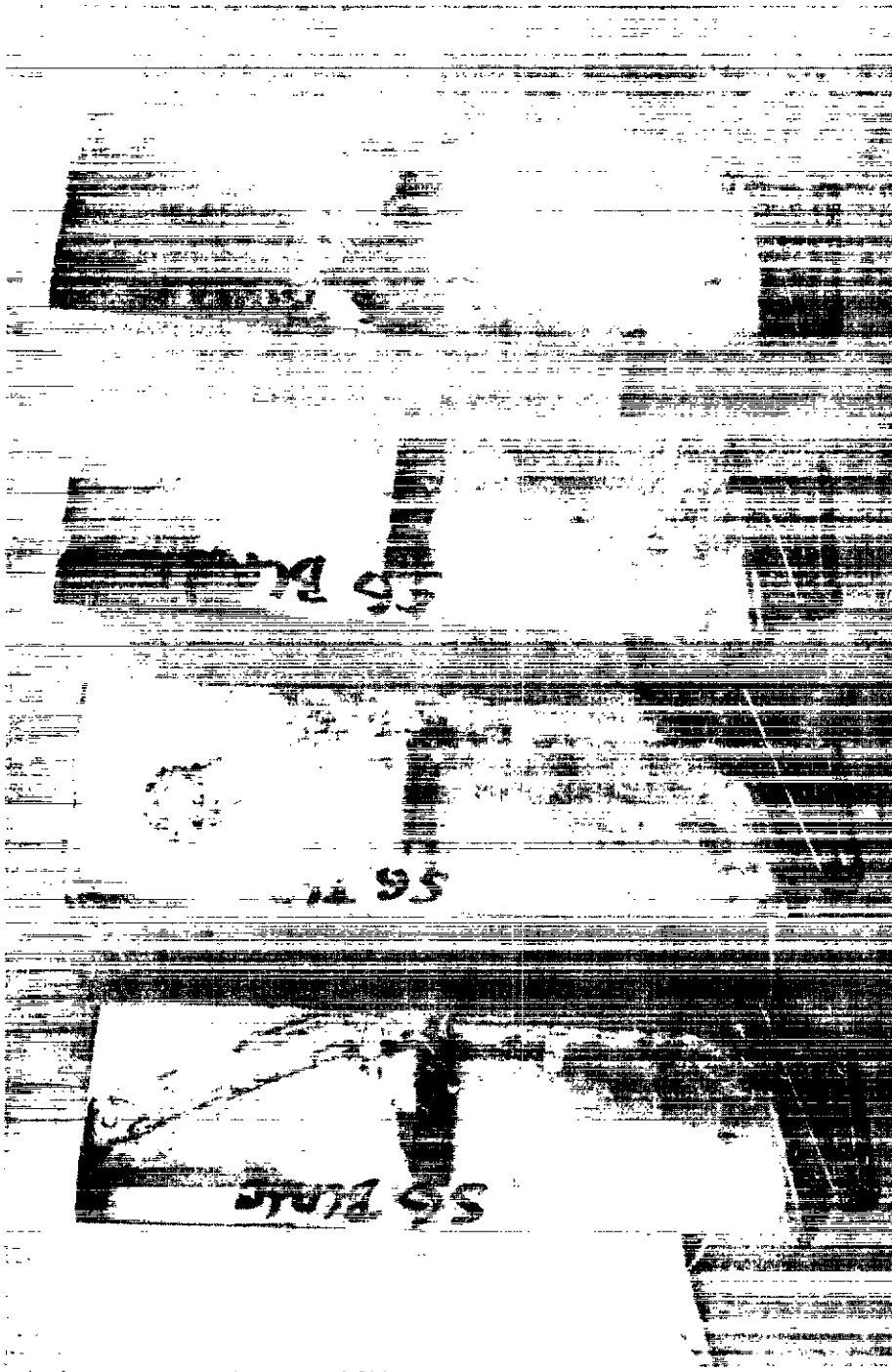


FILM PRESSURE TRANSDUCERS MOUNTED ON JT8D SECOND STAGE
COMPRESSOR BLADE.

5/14/64

XP-38724

FIGURE 6



FILM TYPE PRESSURE TRANSDUCERS ON ROTOR BLADES OF JT8 RIG AFTER
RUNNING MORE THAN 30 HOURS AT ROTOR SPEEDS UP TO 10000 RPM.

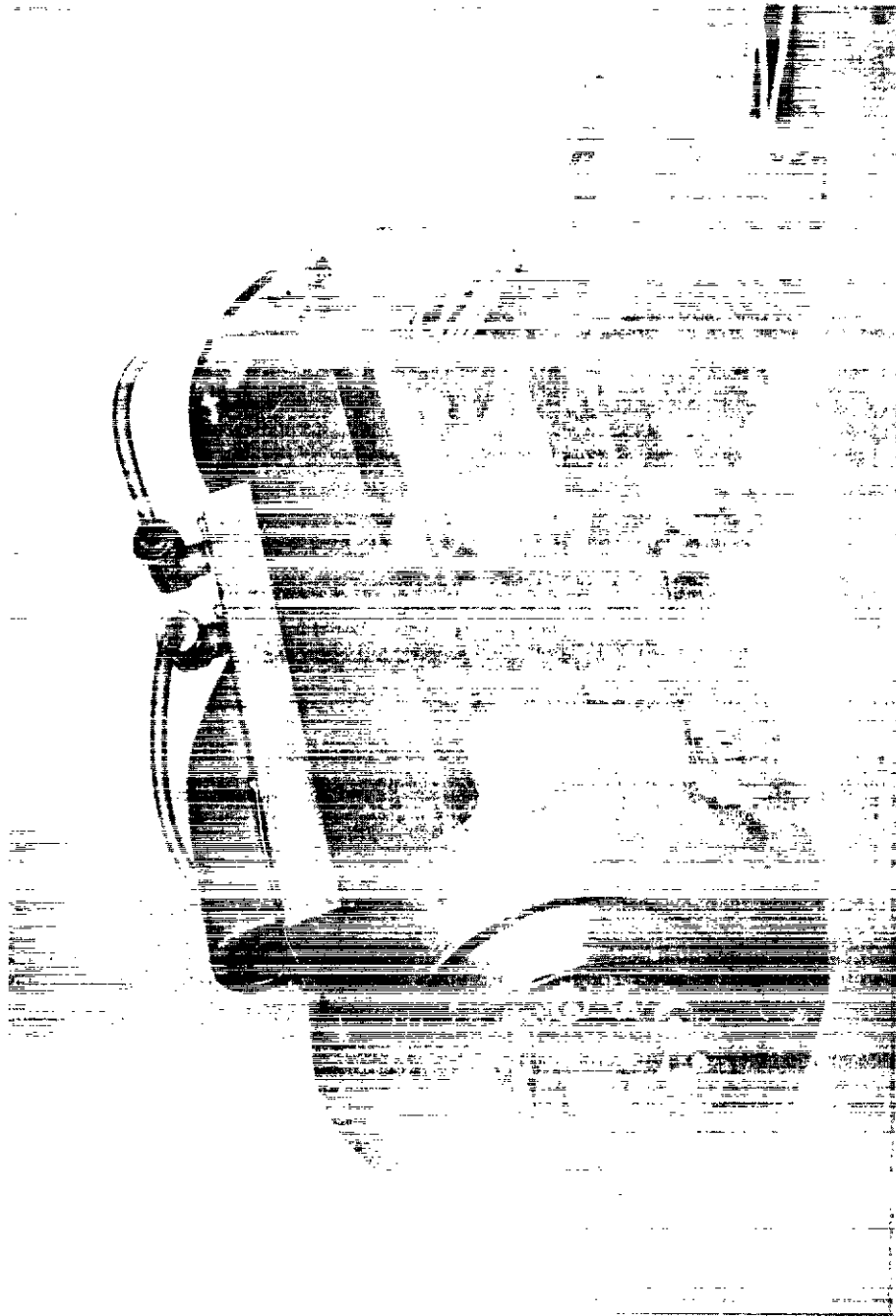
XP-36329

3/4/64



FIGURE 7

XP-36329



SLIP RING ASSEMBLY.



3/13/64

XP-36659

FIGURE 8

BLOCK DIAGRAM OF CAPACITIVE FILM PRESSURE TRANSDUCER SYSTEM

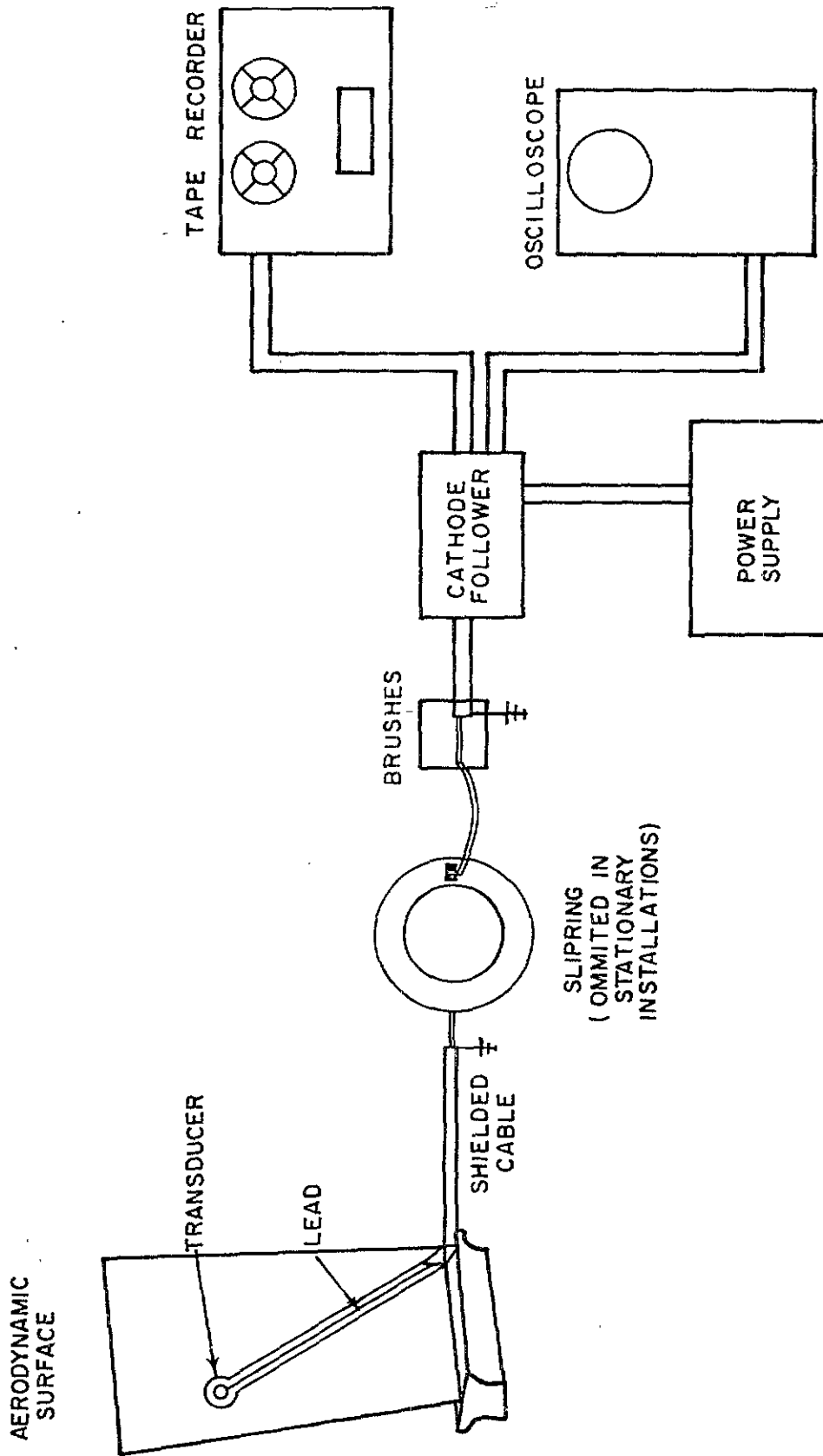
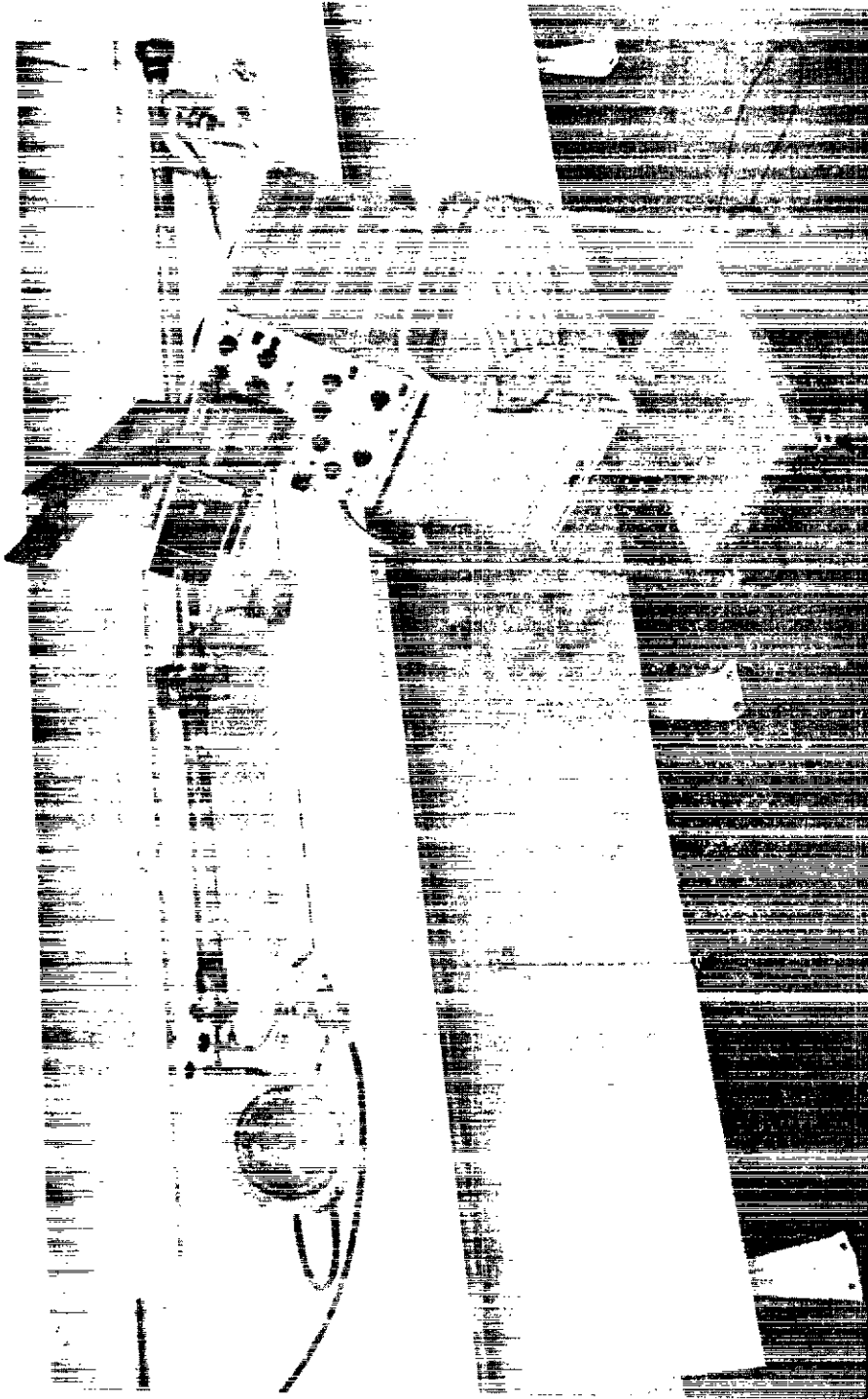


FIGURE 9

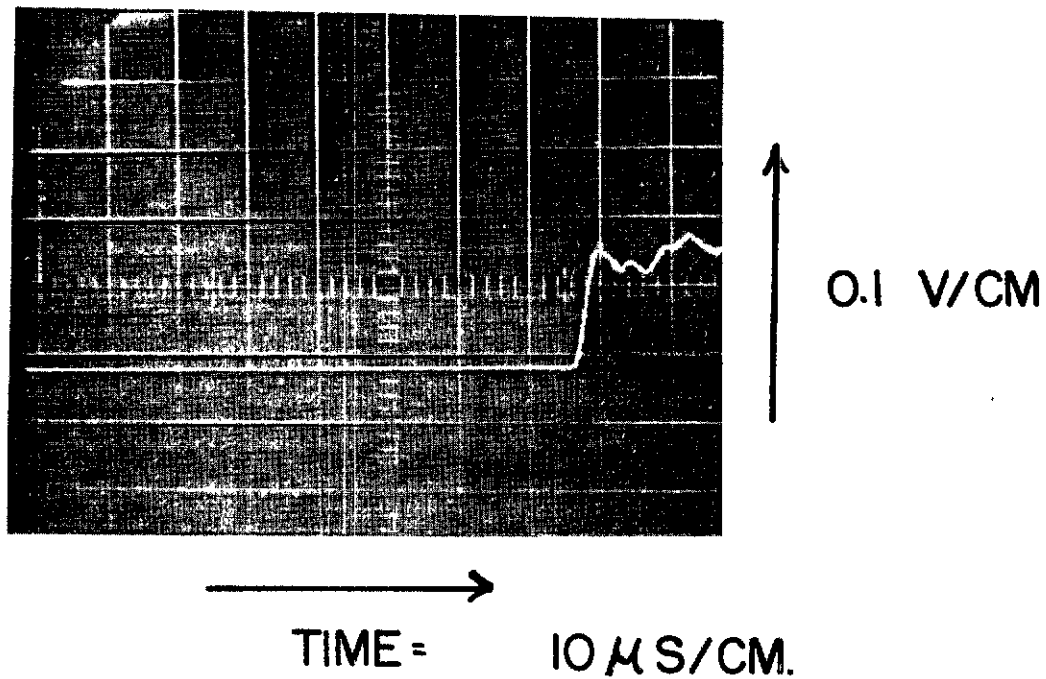


SHOCK TUBE FOR CALIBRATION OF FILM PRESSURE TRANSDUCERS.

X-17225

FIGURE 10

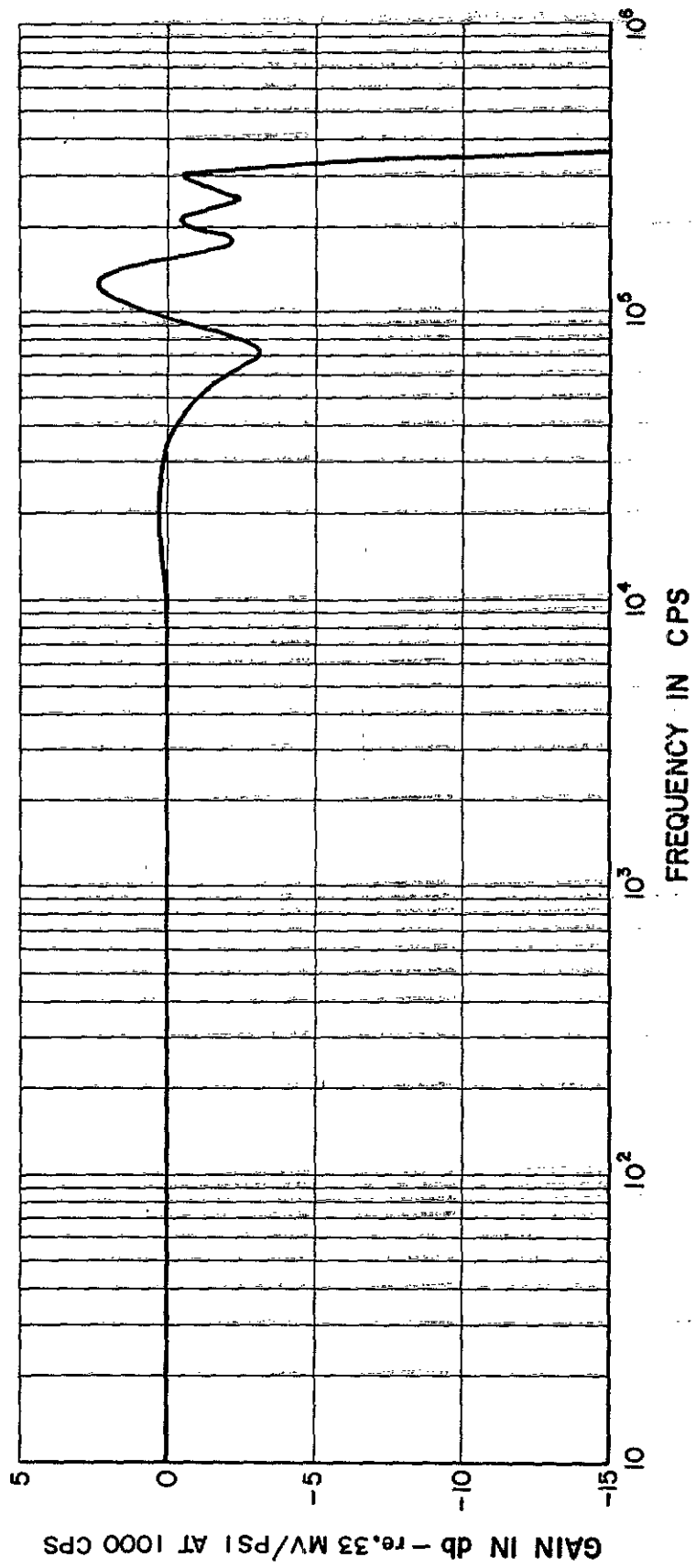
FILM PRESSURE TRANSDUCER RESPONSE
TO SHOCK TUBE STEP PRESSURE PULSE OF 4.6 PSI



XP-38952

FIGURE II

TRANSFER FUNCTION OF A FILM PRESSURE TRANSDUCER SYSTEM



02-IX

FIGURE 12



ELECTROMAGNETIC CALIBRATOR FOR FILM PRESSURE TRANSDUCERS.

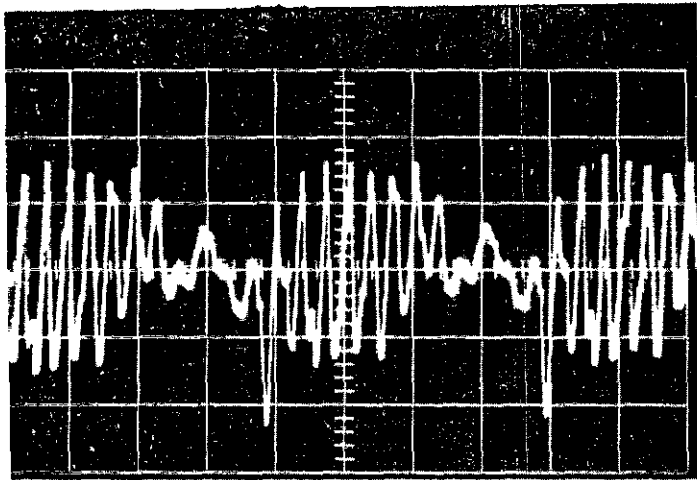
5/14/64



XP-38723

FIGURE 13

OUTPUT OF FILM PRESSURE TRANSDUCER
USING ELECTROMAGNETIC CALIBRATOR



5 MV/CM

→
TIME = 2 MS/CM

INTENSITY OF HIGHEST
AMPLITUDE IS
.523 ± .026 PSI
PEAK - TO - PEAK

XP-38954

FIGURE 14



XP-38/22



CAPACITOR - DISCHARGE SPARK CALIBRATOR FOR FILM PRESS RE
TRANSDUCERS.

5/14/64

FIGURE 15

FILM PRESSURE TRANSDUCER RESPONSE
TO CAPACITOR DISCHARGE SPARK

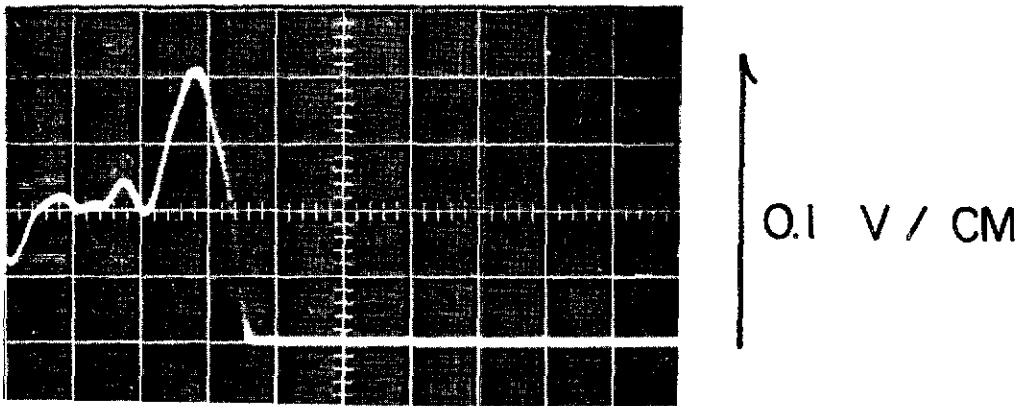
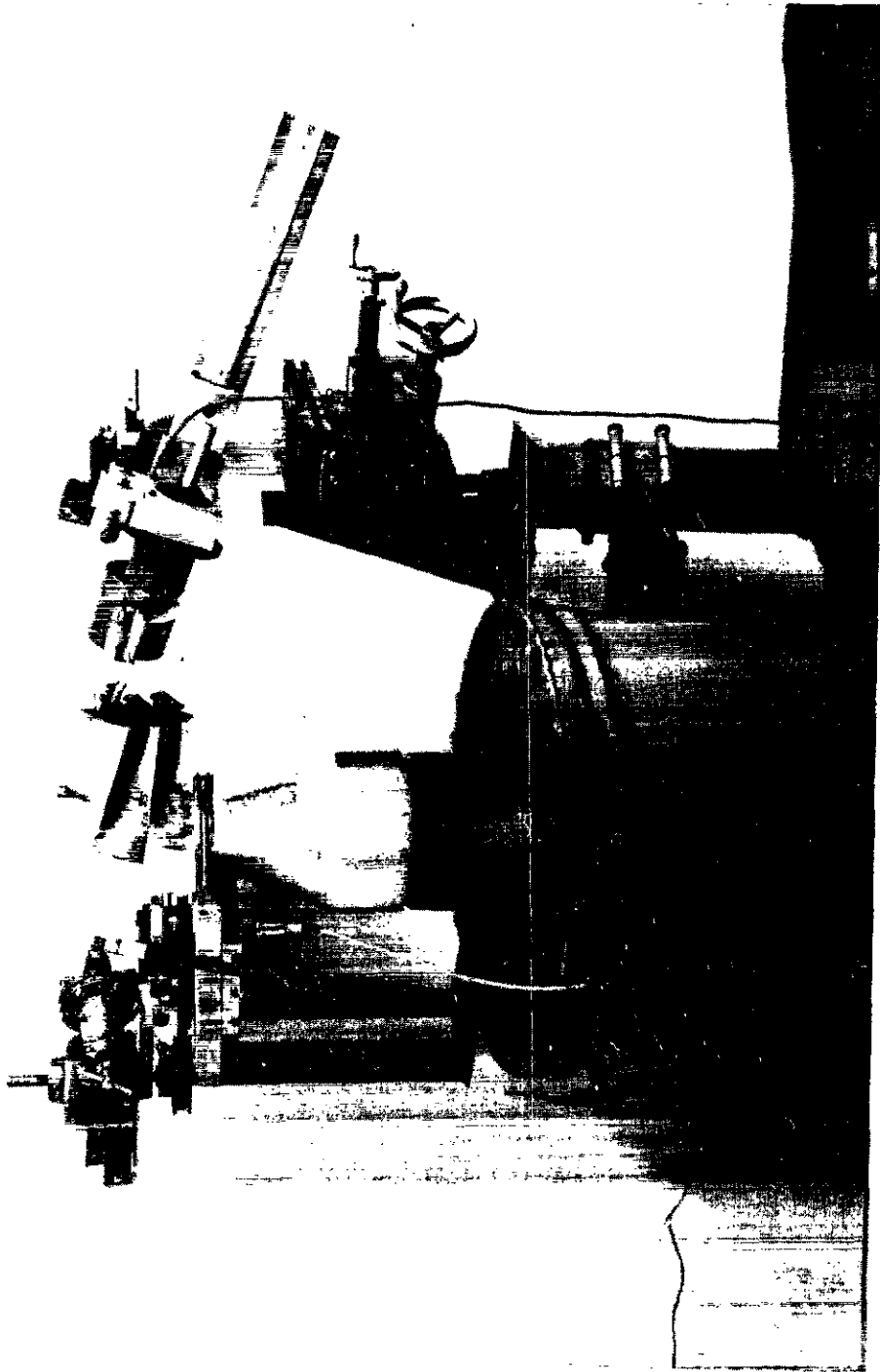


FIGURE 16

XP-38953



FREE JET AND SPOKED WHEEL APPARATUS.

5/20/64

FIGURE 17



XP-38942

FREQUENCY RESPONSE OF A FILM PRESSURE GAGE MOUNTED ON A 3/8 INCH DIA ROD

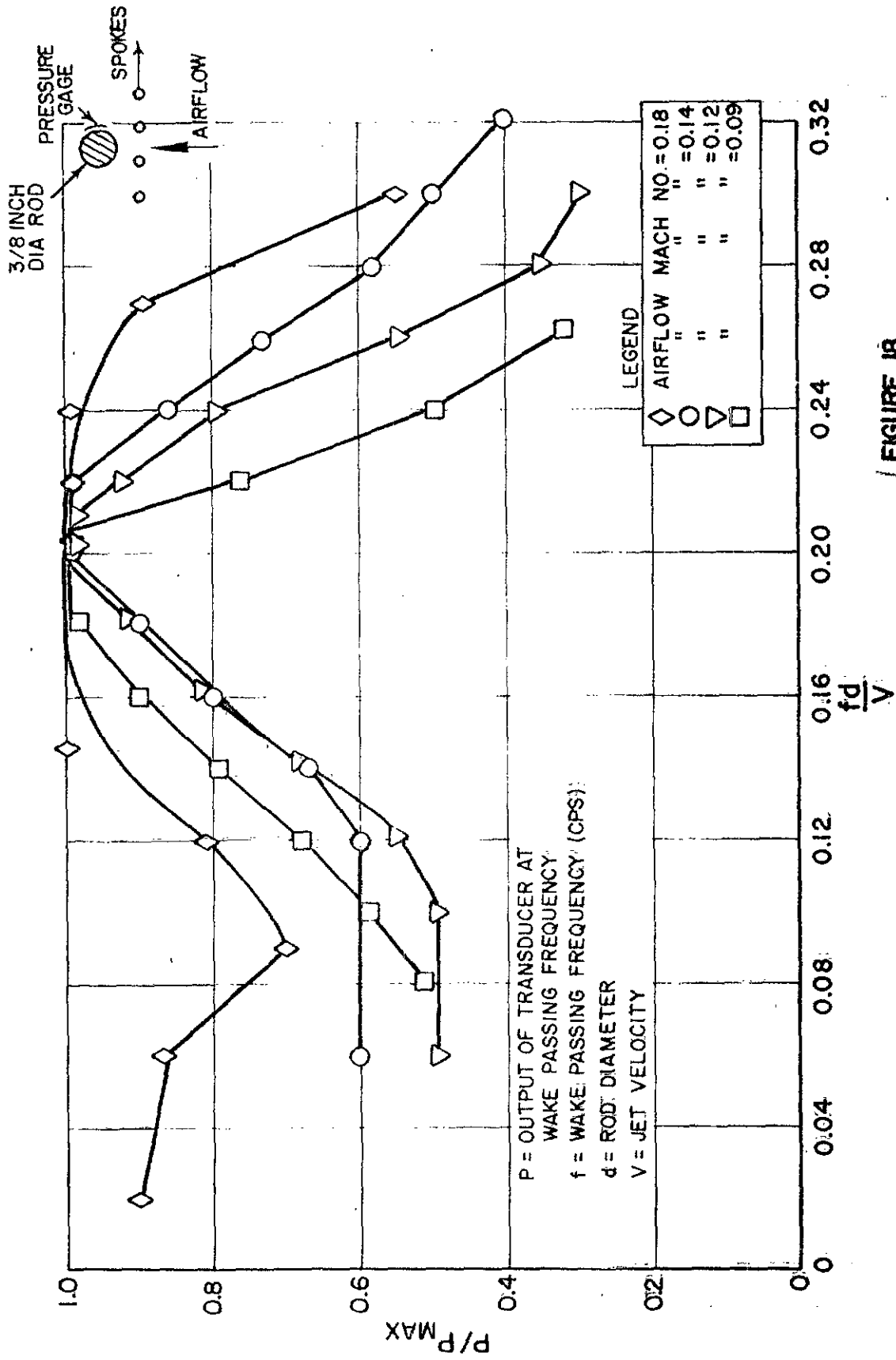
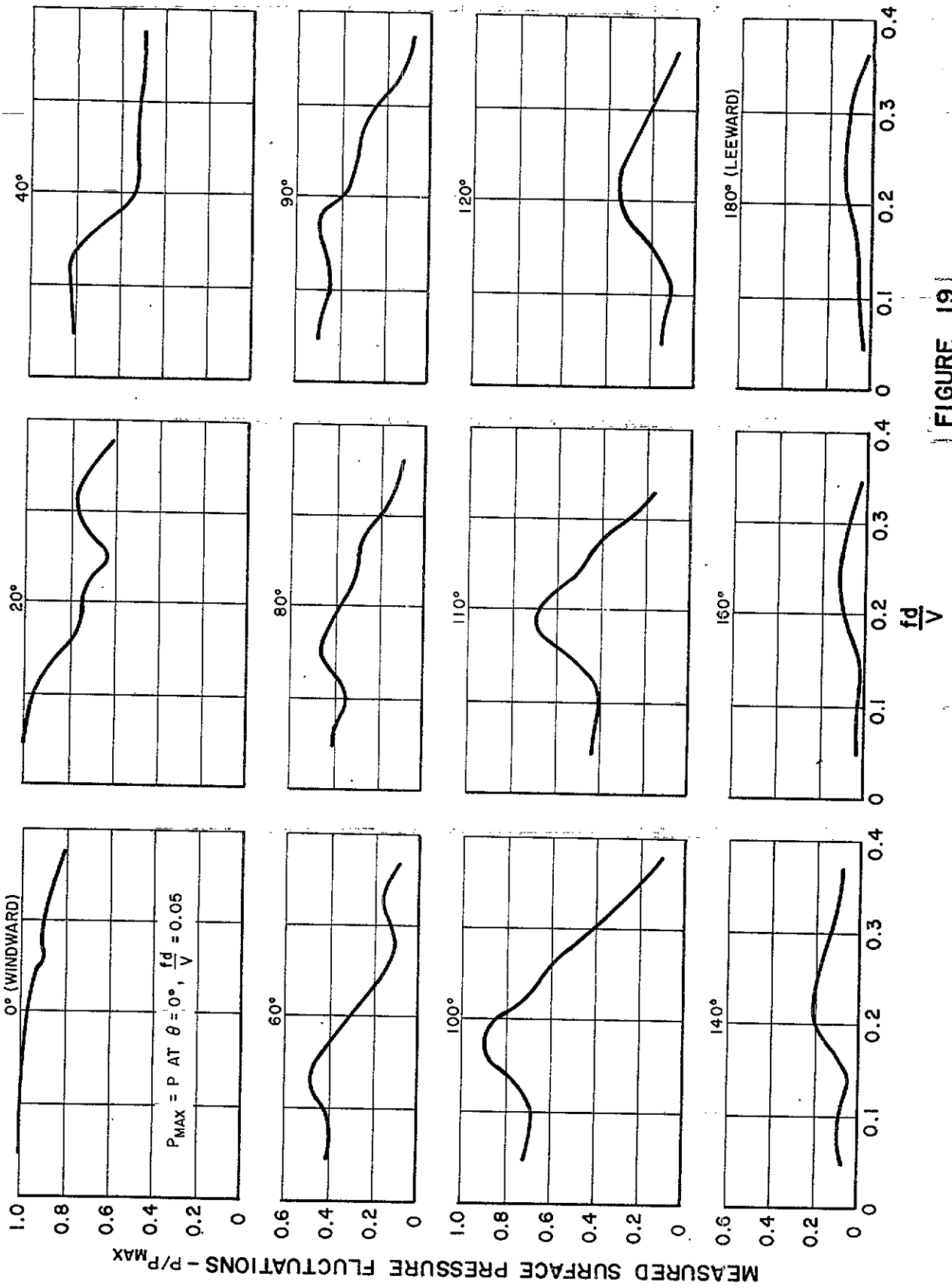


FIGURE 18

CYLINDER AERODYNAMIC RESPONSE vs ANGULAR LOCATION
 RELATIVE TO LEADING EDGE AT MACH 0.12 AIRFLOW



[FIGURE 19]

FREQUENCY RESPONSE OF A FILM PRESSURE GAGE
 MOUNTED MID-CHORD ON THE SUCTION SIDE,
 ONE INCH FROM THE TIP OF A JT8 FIRST STAGE COMPRESSOR BLADE

$\alpha_{CH} = 3^\circ$ AIRFLOW MACH NO. = 0.3

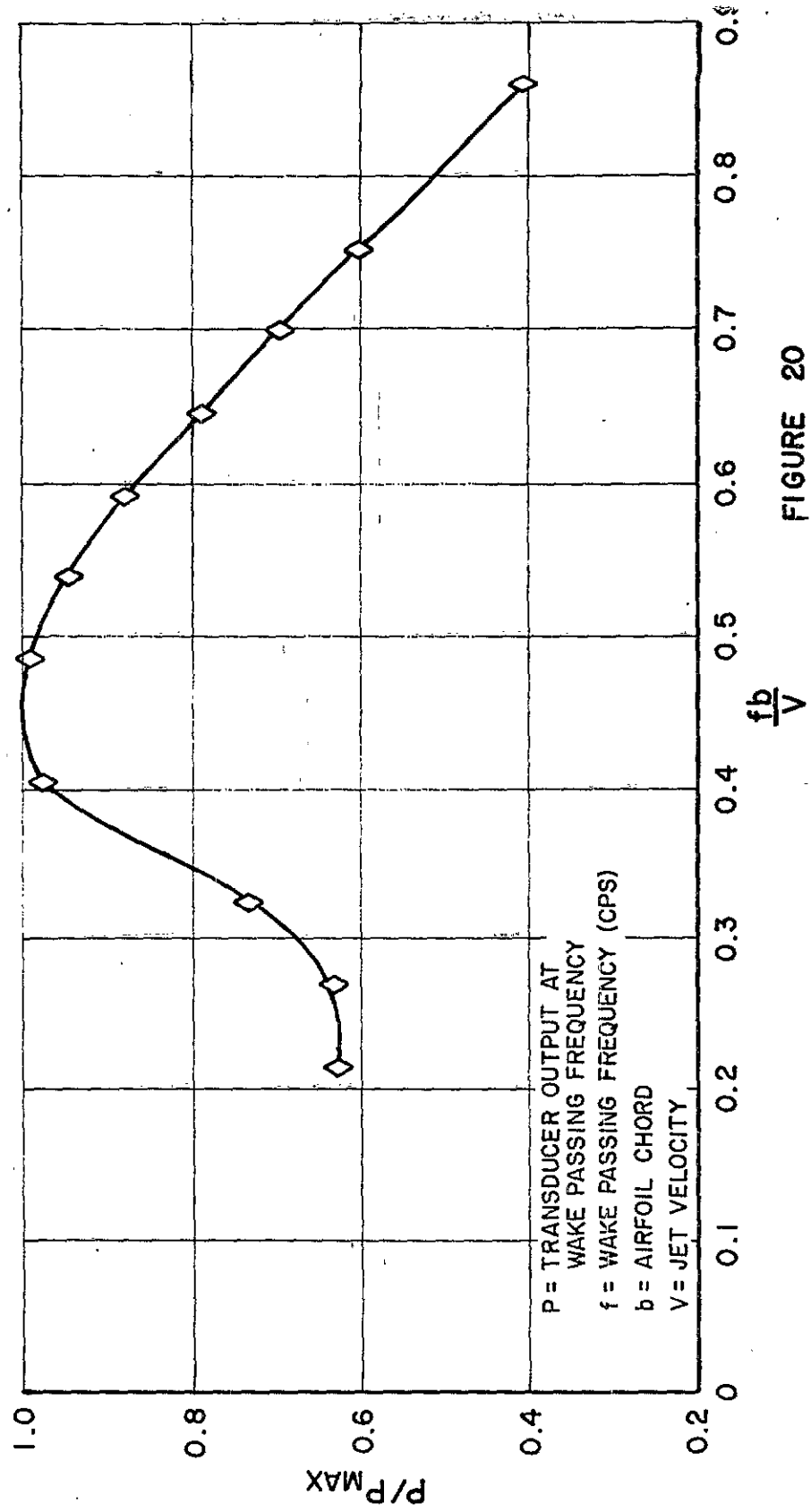


FIGURE 20

SAMPLE FREQUENCY SPECTRA FROM A FILM TYPE PRESSURE TRANSDUCER INSTALLED IN A JT8 SINGLE STAGE COMPRESSOR TEST RIG

TRANSDUCER LOCATION: JT8 FIRST ROTOR BLADE,
CONVEX SIDE, 90% SPAN,
50% CHORD

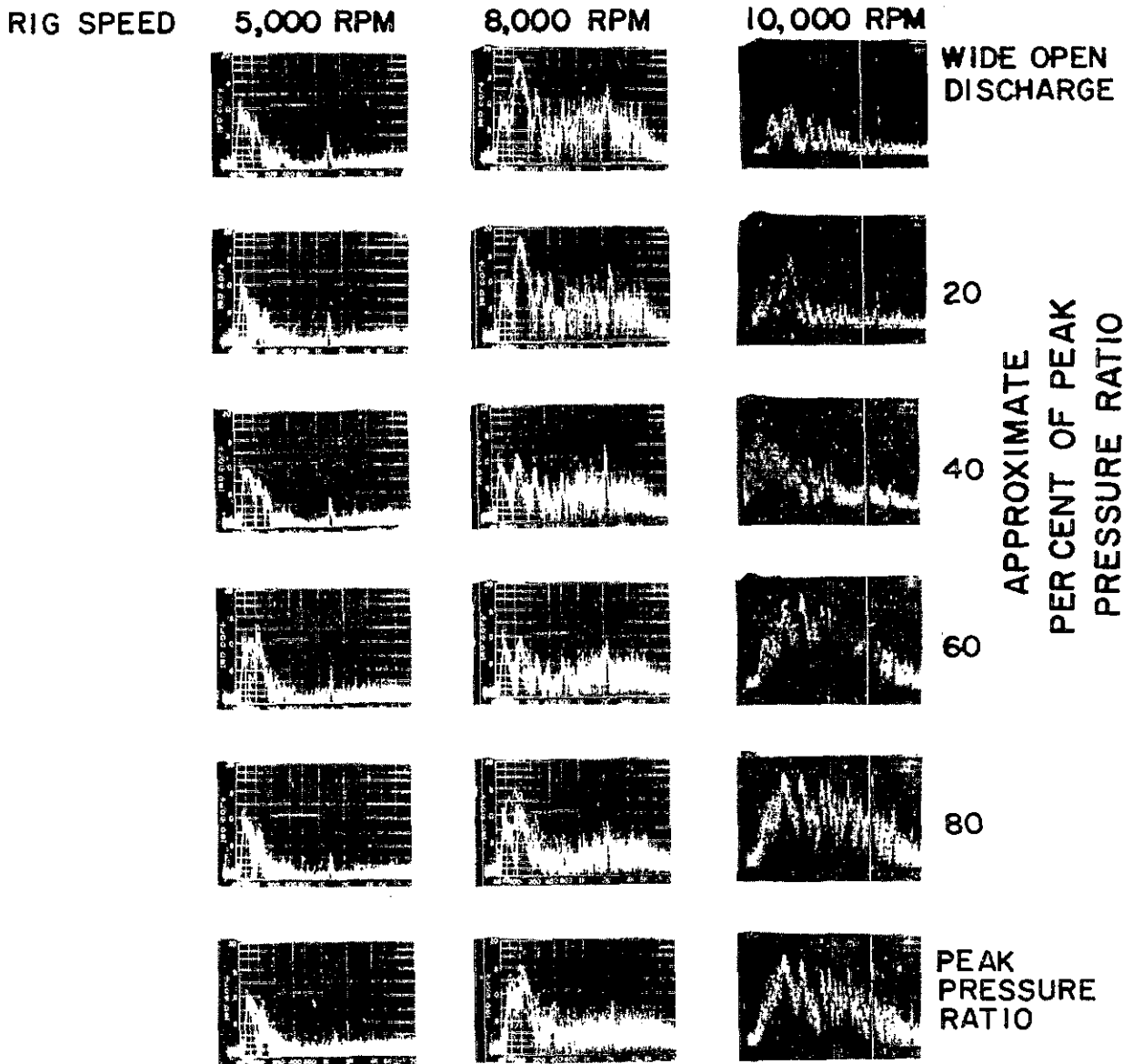


FIGURE 21

SECTION XII

TRANSDUCERS AS PRE-SAMPLING FILTERS IN
PULSE CODE MODULATION TELEMETRY SYSTEMS

by

Lawrence W. Gardenhire
Radiation, Incorporated
Melbourne, Florida

TABLE OF CONTENTS

<u>Title</u>	<u>Page</u>
Summary	2
Introduction	3
The Sampling Process	4
Pre-Sampling Filters	7
Errors Of Omission For Analog Filters	11
Study Results	16
Determining Spectra Of Transducers	26
Conclusions	33

SUMMARY

Any transducer has limited output in both frequency and phase response. These limitations, if understood, can serve as a means of selecting the proper sampling rate for a Pulse Code modulation telemetry system.

Studies have shown that the proper sampling rate is a function of the frequency characteristics of the input data and the degree of accuracy desired in the recovered data. This accuracy is determined by an interpolation process which determines what happened between samples.

The interpolation error is made up of two parts, errors of omission and errors of commission. The error of omission is purely those omitted by various filters in the instrumentation system. The transducer is one of these filters. If we could determine the frequency characteristics, in both phase and amplitude of a transducer, we could match it to the mathematical filters used in a previous study to determine errors of omission. This would show a degrading of accuracy as the cut-off frequency of the transducer was reached. Why then, choose your sampling rate at some value to yield higher accuracies than possible.

These problems, along with a method for determining the frequency and phase response of transducers, will be explored and examples of the results given. A typical example is an accelerometer with a natural frequency of fifteen cycles, which is only good only to 1.4 cycles at 1% when excited by second order data. Yet the accelerometer is relatively flat to 15 cycles. If 1% data is desired, why then use a frequency above 1.4 cycles for determining the sampling rate.

INTRODUCTION

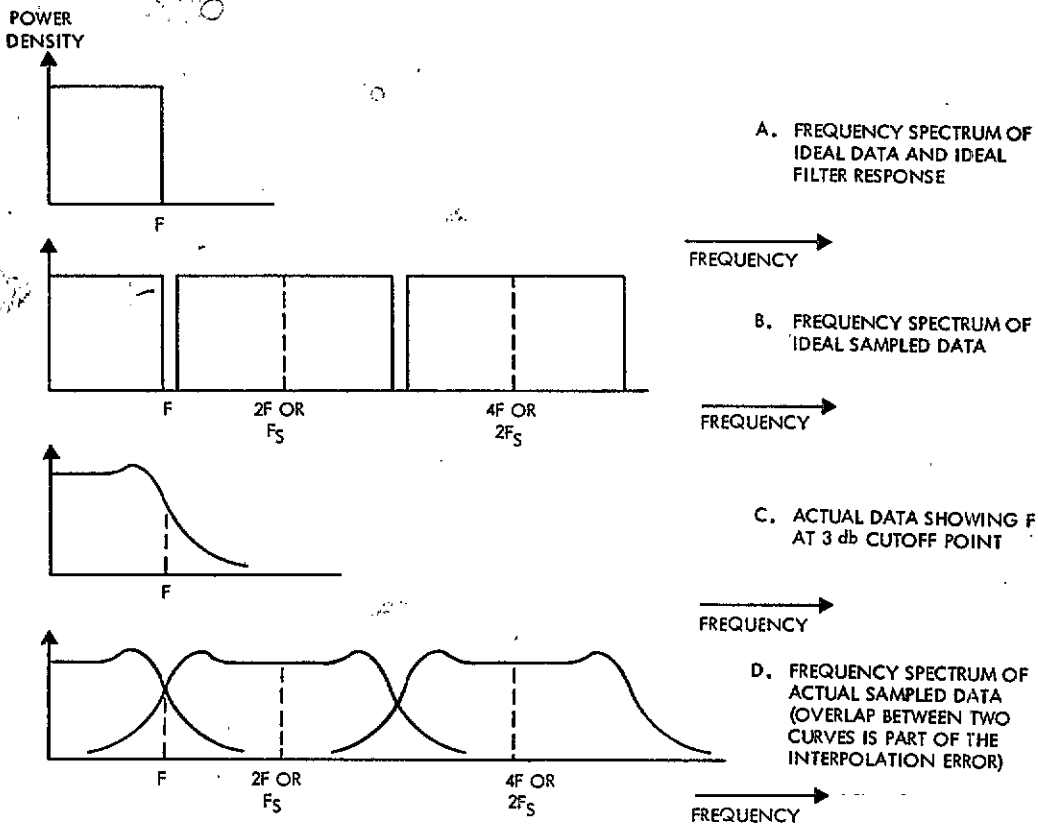
Before attempting to use a sampled data system, the errors due to the sampling process should be known and understood. These errors are a result of connecting the output samples together with some kind of a line. The resulting waveform does not match the continuous input waveform. The process of connecting these samples is known as interpolation and the difference between the input and output waveform is known as interpolation errors.

THE SAMPLING PROCESS

If data existed as described by the sampling theorem and if ideally sharp cutoff filters could be built, there would be no interpolation error. The sampling theorem states: "2F samples per second suffice to represent perfectly and permit perfect recovery of a time function, if that time function contains only frequency components below F cycles per second". Figure 1A shows the spectrum of ideal data as described by the sampling theorem which has "only frequencies below F cycles per second".

Figure 1B shows the frequency spectrum of ideal data after it has been sampled. The series of spectra following the ideal spectrum are a result of the sampling frequency plus and minus the data frequency, and its harmonics. These images are similar to the spectrum of the input data. The relative height of each of these images is a function of the sampling time compared with the time between samples. Since there is no overlap or "foldover" between the original data and its sampled image around 2F, there is no interpolation error.

In actual practice, however, data looks more like that in Figure 1C. If F is chosen to be the 3 db point on the curve, one can see that a considerable amount of spectrum exists above F. This spectrum will produce large errors if the sampling rate is only 2F, as seen in Figure 1D. The amount of overlap, as seen on these two curves, is what is known as foldover or aliasing error. A better name for this foldover is "errors of commission". This error can be reduced by increasing the sampling rate or by utilizing a low-pass or pre-sampling filter. The cutoff characteristic of this filter is arranged so the frequencies above F are reduced before the sampling process is performed. Unfortunately, however, this filter tends to remove or shift the relative phase of the desired spectral components and omits part of the original spectra producing "errors of omission". This, however, is only part of the errors of omission; since the same type of omission will be made when an interpolation filter is used in the output of the digital system. The sum of these errors make up the interpolation error and are illustrated in Figure 2.



32894

Figure 1. Ideal and Actual Data Shown in the Frequency Domain

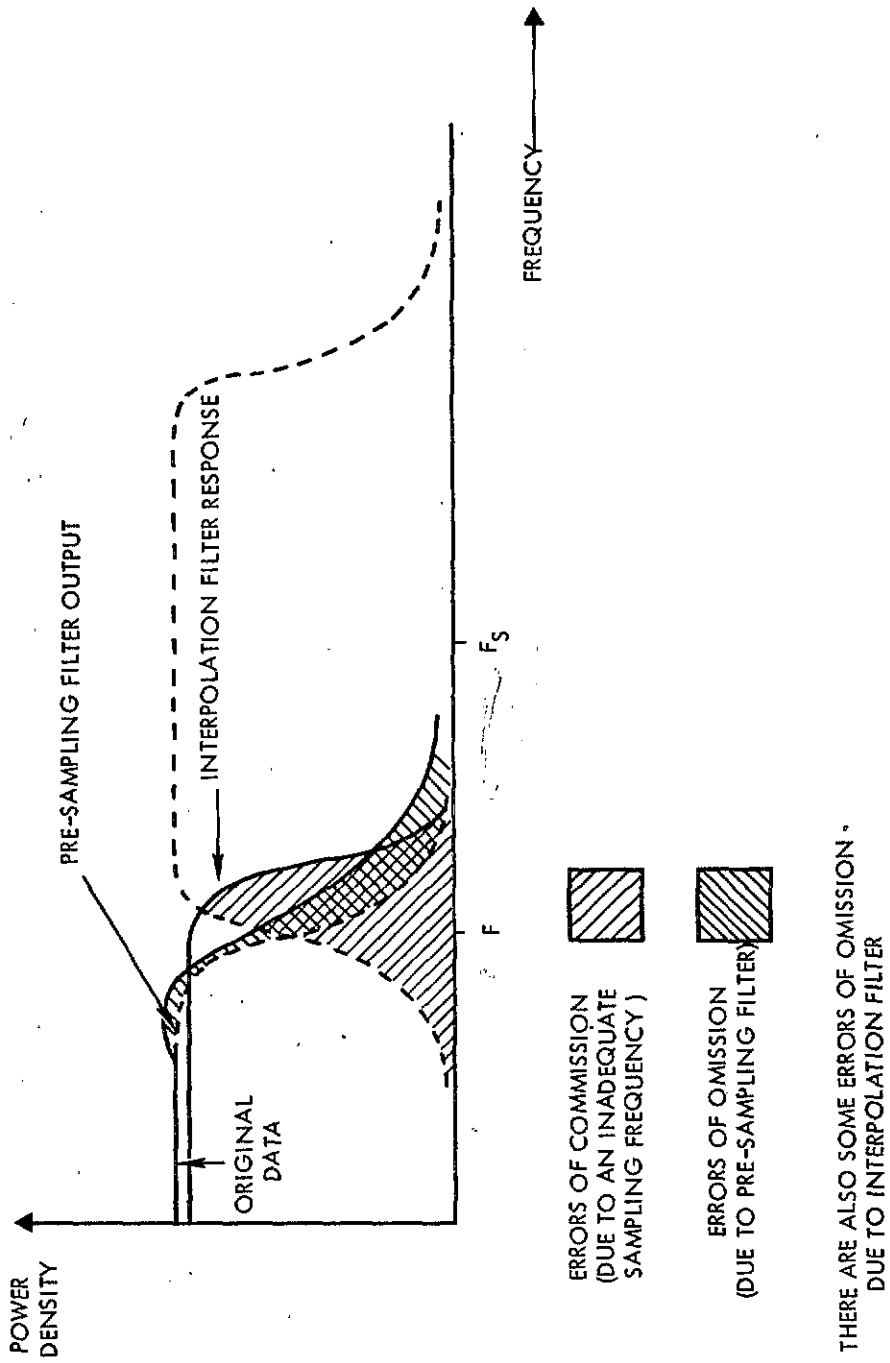


Figure 2. Errors of Commission and Omission

PRE-SAMPLING FILTERS

The errors of omission due to the pre-sampling filter is the one of interest for this report. It has been generally noted that most users of sampling systems are lead to a false sense of security when they use a pre-sampling filter. When in actuality they do themselves harm by omitting part of the input data. This damage is usually greater than the errors of commission would be if the pre-sampling filter were not used. The real answer to the problem is to increase the sampling rate to the point where the errors of commission are below the desired accuracy. In order to study this matter further we will divide the requirement for pre-sampling into two categories:

- A. when the signal into the filter is not contaminated by unwanted interference,
- B. when the signal into the filter is contaminated by unwanted interference.

PRE-SAMPLING FILTERING WHEN ALL OF THE SIGNAL INTO THE FILTER IS WANTED: In the case where all of the signal entering a pre-sampling filter is wanted, it is apparent that the filter must distort this wanted signal; i.e., introduce error, if it is to do anything at all. However, by considering the interpolation process, it can be seen that attenuation of the higher-frequency content of the data can reduce the "foldover error" or errors of commission. Thus, the question is whether this reduction in interpolation error is sufficient to counteract the errors of omission introduced by removing part of the high frequency content.

Spilker, Reference 1, has determined that when Wiener optimum pre-sampling filters are used in conjunction with Wiener optimum interpolation filters, a net gain can be realized as compared to the same process without the pre-sampling filter. The amount of gain varies as a function of data characteristics. Typically, with third order data, an optimum system using pre-sampling filtering can, with a 10% lower sampling rate, achieve approximately the same accuracy as an optimum system without the pre-sampling filter.

Ref. (1) "Optimization and Evaluation of Sampled Data Filters" by J. J. Spilker, Jr., Lockheed Aircraft Corporation Report LMSD-48335, November 18, 1958.

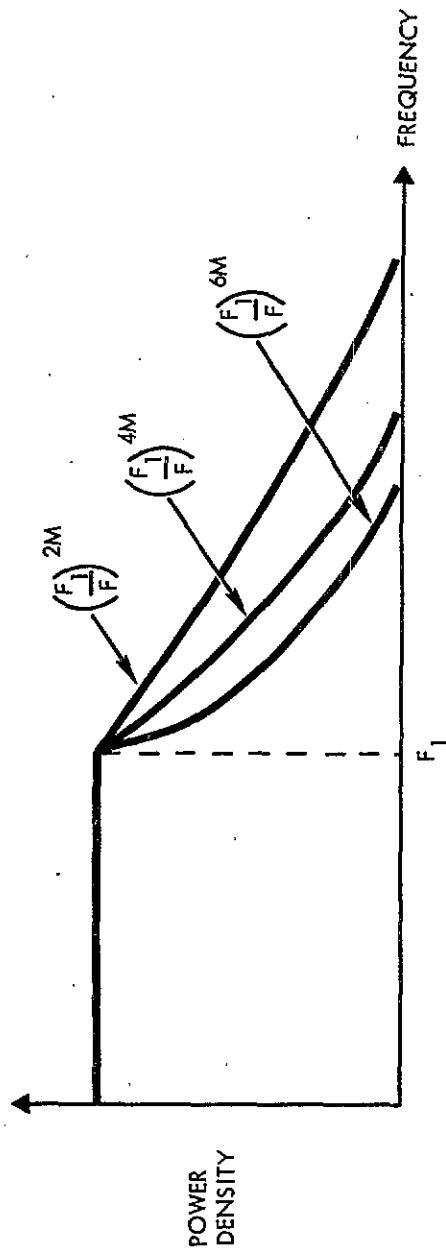
Unfortunately, most systems cannot afford the complexity imposed by a requirement of Wiener optimum pre-sampling filtering. The case in which simple lumped-parameter filters are used as pre-sampling filters is considered in Reference 2. In this case the complexity of the problem precluded a rigorous general mathematical solution; however, the results achieved indicate that use of pre-sampling filters of the simple variety considered (Butterworth, Gaussian or binomial) is not desirable since the additional errors of omission caused by these non-optimum filters will usually be greater than the reduction in errors of commission and in any case only a small gain can be realized. Because of this, and because of the small gain provided when even an optimum configuration is used, it appears reasonable to conclude that for most applications in which all of the data from the transducer is wanted, a pre-sampler filter should not be used.

PRE-SAMPLING FILTERING OF UNWANTED SIGNALS: In many cases the signal existing on the transducer lines may contain both wanted and unwanted components. The unwanted components may be due to pickup from power lines such as 60 cps or 400 cps ripple or unwanted outputs from the transducer, such as vibration when vehicle acceleration is desired. The wanted and unwanted components are often separable by virtue of their frequency spectra, the wanted spectral components being principally located in a lower-frequency region. In such cases a pre-sampler filter of even the simple variety can be of value.

Since we have shown that pre-sampling can in general produce problems, we should attempt to operate without them. When the waveform to be sampled comes from a transducer, it has already been filtered by the transducer. Why not then chose your sampling rate based on the transducer as a pre-sampling filter? This is possible if a method is used for selecting the sampling rate, as given in Reference 3. Here a method of more nearly representing data has been established. This is shown in Figure 3. The data spectrum is described

Ref. (2) "Computer Interpolation Technical Report No. 2 Part 2", by D. D. McRae & E. F. Smith, Radiation Incorporated.

Ref. (3) The Use of Digital Data Systems L. W. Gardenhire, 1963 National Telemetering Conference.



F_1 = DATA CUTOFF FREQUENCY

M = SLOPE OF DATA IN UNITS OF 6 DB/OCTAVE

NON-IDEALIZED DATA SPECTRA

Figure 3. Non-Idealized Data Spectra

as being flat, to a break frequency, f_b , beyond which the data has a rolloff of various integer multiples of 6 db/octave. These are described as "orders" of data. In other words, first order data ($m = 1$) rolls off at 6 db/octave, second order data ($m = 2$) rolls off at 12 db/octave, etc., with $m = \infty$ for ideal bandlimited data. Although actual data may not fall exactly into one of these orders, it provides a method of categorizing data. Even though it may be unlikely that the user will know ahead of time exactly what spectrum his data will have, it gives him approximate way of estimating what his data bandwidth (and shape) will be.

The resonant frequency of the transducer can be used as the break frequency, since this is the highest frequency at full amplitude that will come from the transducer regardless of the frequency of the input data, transducers roll off at some db/octave depending usually on the number of degrees of freedom. This represents the maximum case and actually if a frequency response matching the resonance of the transducer is desired one should use a transducer with higher frequency response.

By matching the spectral response of a given transducer with that of an analog filter, the errors of omission at a given frequency can be determined. It is obvious that any filter will in some way alter the data, and this error becomes greater as the break frequency is approached. When the desired accuracy is less than that at the break frequency of the transducer, one should reduce the data break frequency used for selecting the sampling rate, until the errors of omission are less than the desired accuracy. Since the transducer has altered the data, it is foolish to choose the sampling based on an error less than that at the break point of the transducer. The transducer cannot reproduce the input data to any better accuracy, therefore, no matter how many samples are used the data is only as good as the transducer error.

ERRORS OF OMISSION FOR ANALOG FILTERS

A study has previously been performed (Reference 4) which yields errors of omission for various filters with different orders of input data. The method used a numerical integration solution illustrated in Figure 4.

The input, $f_i(t)$, is passed through a filter providing an output $f_o(t)$. The difference between the actual output (which is the input with some allowable time delay) is the error omission; $e_o(t)$.

All functions involved are random waveforms, and the power spectral density of the input waveform $f_i(t)$ is known. The rms errors of omission $e_o(t)$ will be determined.

The problem can be simplified by considering the input waveform to be approximated by a large number of small sine waves spaced equally in frequencies with relative magnitudes corresponding in height of the power spectral density curve at the frequency in question.

The normalized mean squared error for one of these frequencies is given by

$$e_{nms} = 1/2 a \cos(\phi + \omega T) + a^2$$

where

$a = B/A =$ attenuation of filter at frequency ω

$\phi =$ Phase Shift

$T =$ an allowable time delay

Ref. (4) Interpolation Errors, by D. D. McRae, Radiation Incorporated, Advanced Telemetry Study, Technical Report No. 1 Part 2.

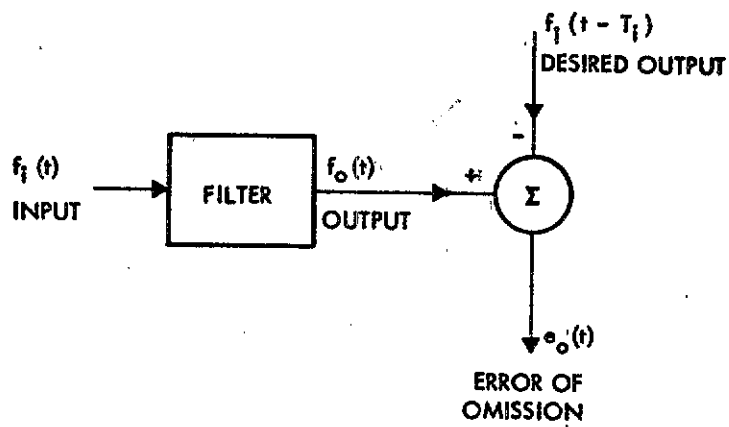


Figure 4. Model for Errors of Omission

The total rms error of omission can be obtained by intergrating the error spectrum over all frequencies. The normalized rms error is:

$$E_{\text{rms}} = \left(\frac{\int_0^{\infty} S(\omega) e_{\text{rms}}(\omega) d\omega}{\int_0^{\infty} S(\omega) d\omega} \right)^{1/2}$$

where:

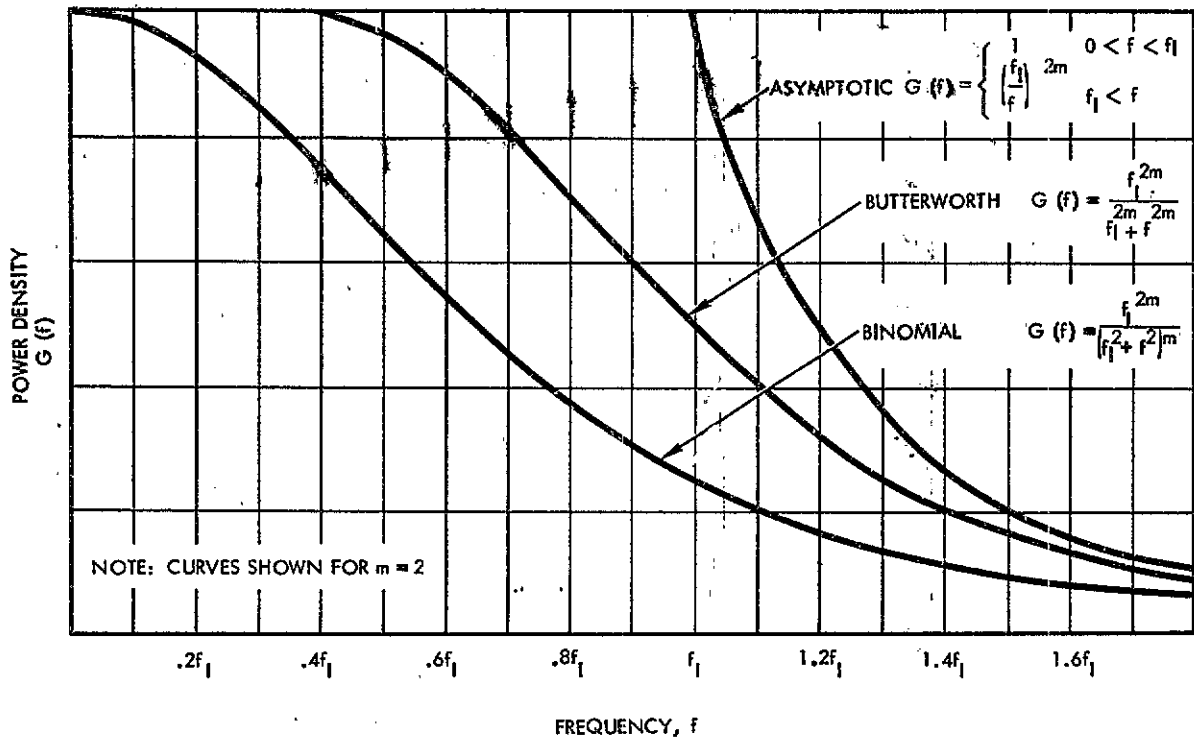
$S(\omega)$ is the original data spectrum. By operating on the above equations, the normalized rms error introduced by a given filter for a given spectrum, is obtained. The detailed operation of this process is given in Reference 4.

The above process was performed on the following filters:

- o Binominal
- o Butterworth
- o Gaussian or Linear Phase

The spectral shapes of these filters are shown in Figure 5. A given transducer may be matched to one of these shapes.

For a specific application, we shall match the transducer whose frequency response curve is shown in Figure 6. This shape matches that of a 2nd order Butterworth filter since it is relatively flat out to its natural frequency, and the slope drops off at 12 db/octave.



31120

Figure 5. Special Shapes

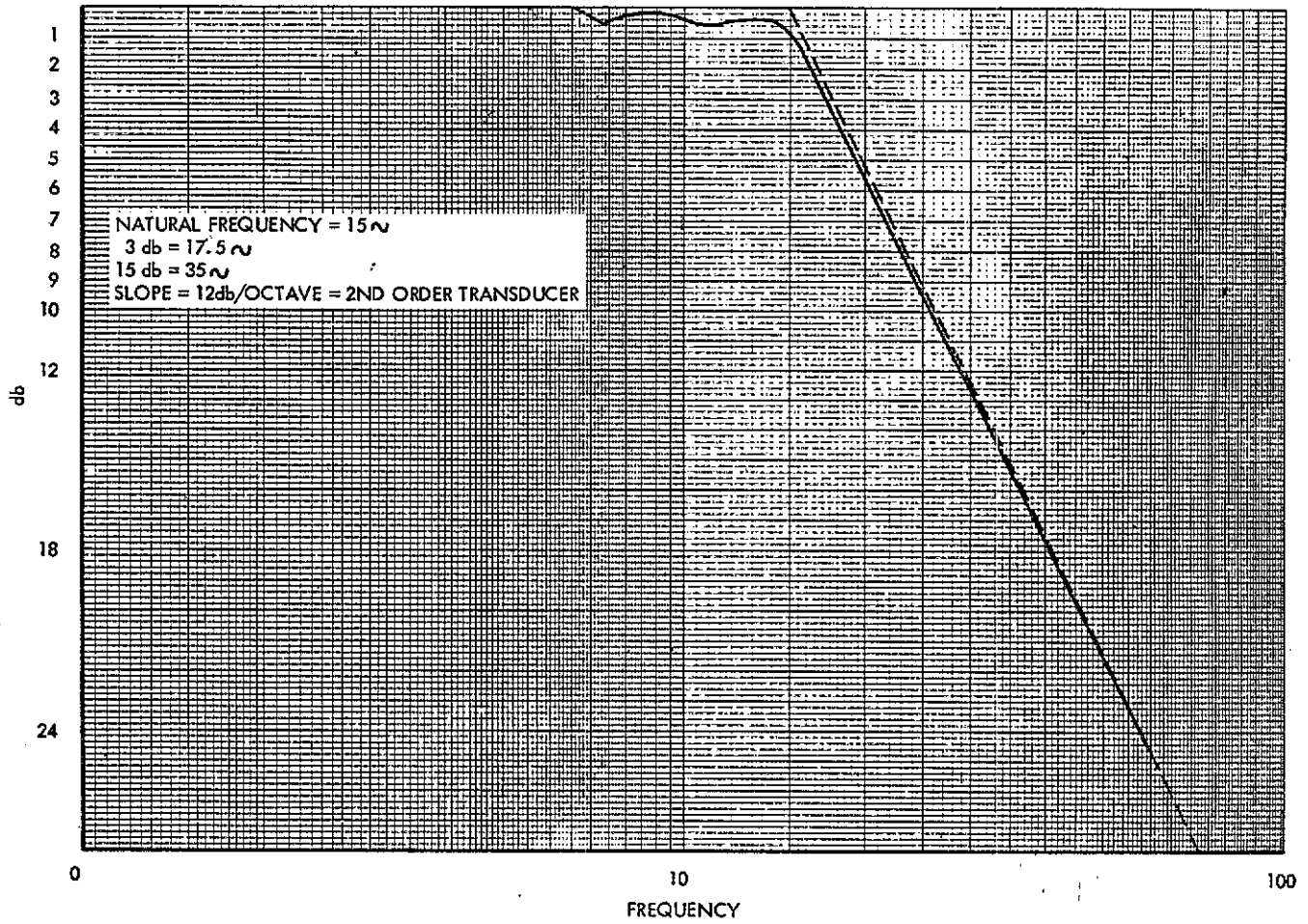


Figure 6. Bode Frequency Response of Bourns Accelerometer Model 602A Serial 1331

STUDY RESULTS

The results of the above study are presented in Figures 7, 8, 9 and 10 for Butterworth type filters.

To demonstrate the use of these results, let us assume that the input data just matches the response of the transducer, in other words, it is flat to 15 cycles per second and then drops off at 12 db/octave. Referring to Figure 8, with $n = 2$ we see that K is equal to 1; when f_c is the cutoff frequency and f_i the information frequency is the same.

Since the data into the transducer was second order, we now have fourth order output which has been altered by 35% rms error at 15 cycles. It would be undesirable to sample at extremely high rates with this existing error, therefore 10% rms error, due to interpolation, will be used which gives a total error of 36.5% rms. Using Figure 11, which comes from Reference 3, the sampling rate can be determined. Using linear interpolation at 10% rms, 5 samples per cycle or $5 \times 15 = 75$ samples per second would be required. Reducing the error to 35.008% (1% interpolation error) the rate would increase to 240.

If a 1% rms error were required, 0.707% for the transducer and 0.707% for the interpolation error, the transducer would be good up to:

$$F_i = f_c/K = 15/13.5 = 1.1 \text{ cycles}$$

Again if the input data were second order and we used linear interpolation, we can go to the second order curves in Figure 12. It should be pointed out that these curves were calculated for input data spectrum with only one break point. When second order data of a low frequency is fed into a second order transducer, the output will have two break frequencies, one at the information break frequency and one where the information spectrum cross the spectrum of the transducer. It will then become fourth order data. When however, the information frequency is low compared with the transducer break point, the second break point occurs at such a high frequency little error is introduced if the second order curves are used. In this case at 0.707% rms interpolation error, 50 samples per cycle or 55 samples per second are required to obtain a total error of 1%.

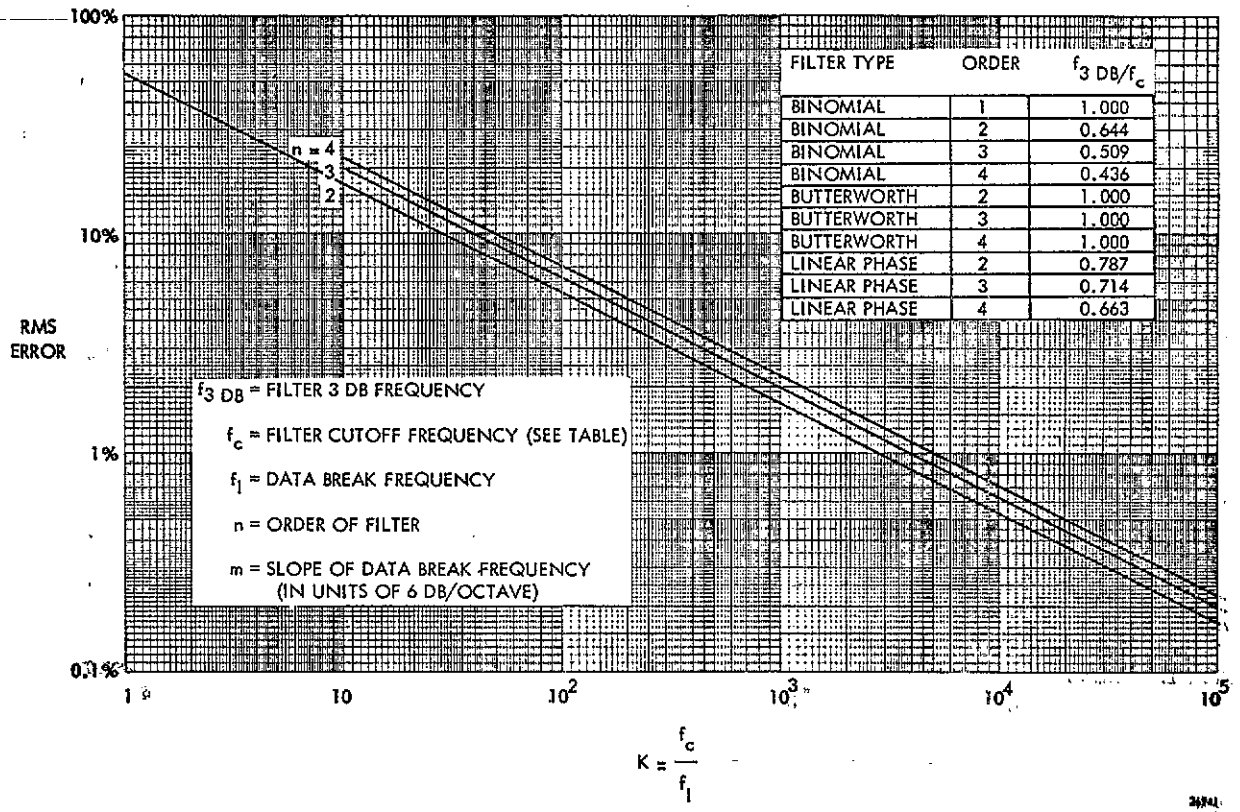


Figure 7. Errors of Omission, $m=1$, Butterworth Filter

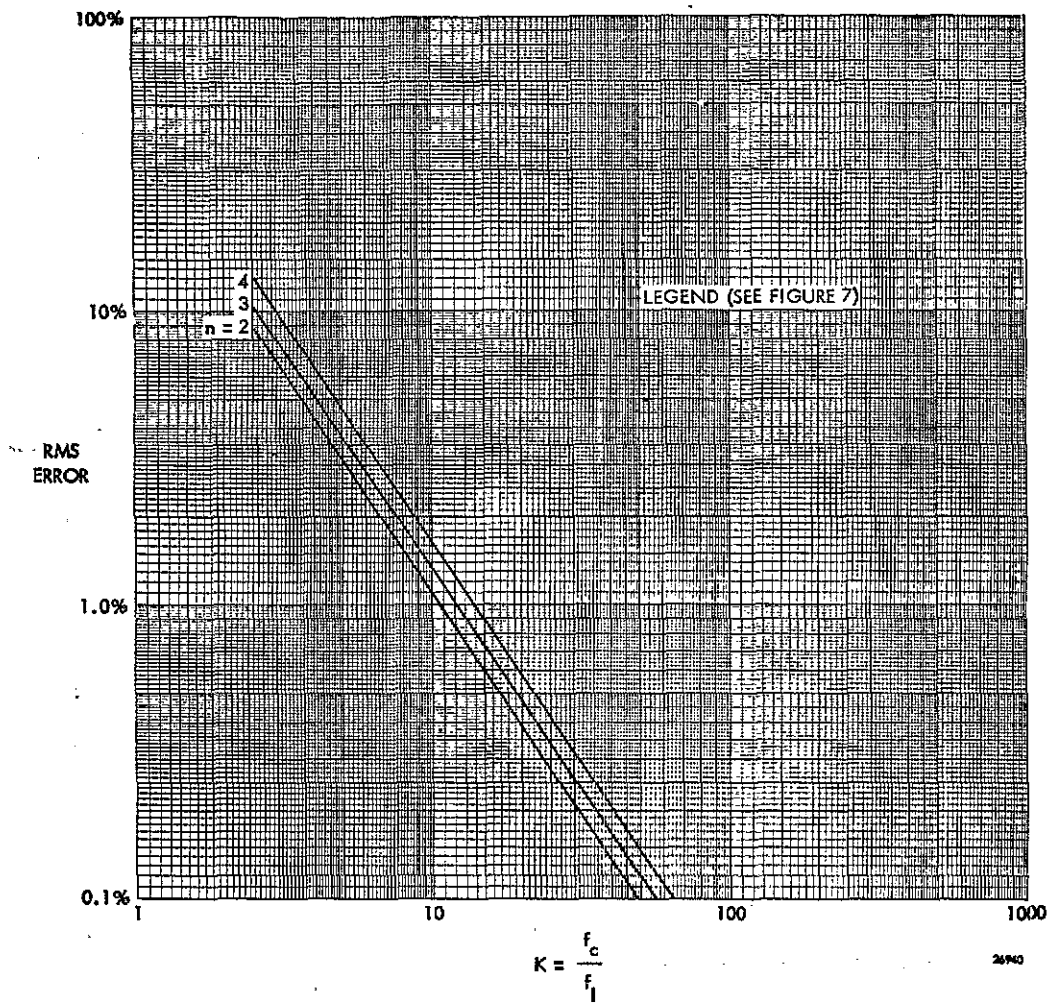


Figure 8. Errors of Omission, m=2, Butterworth Filter

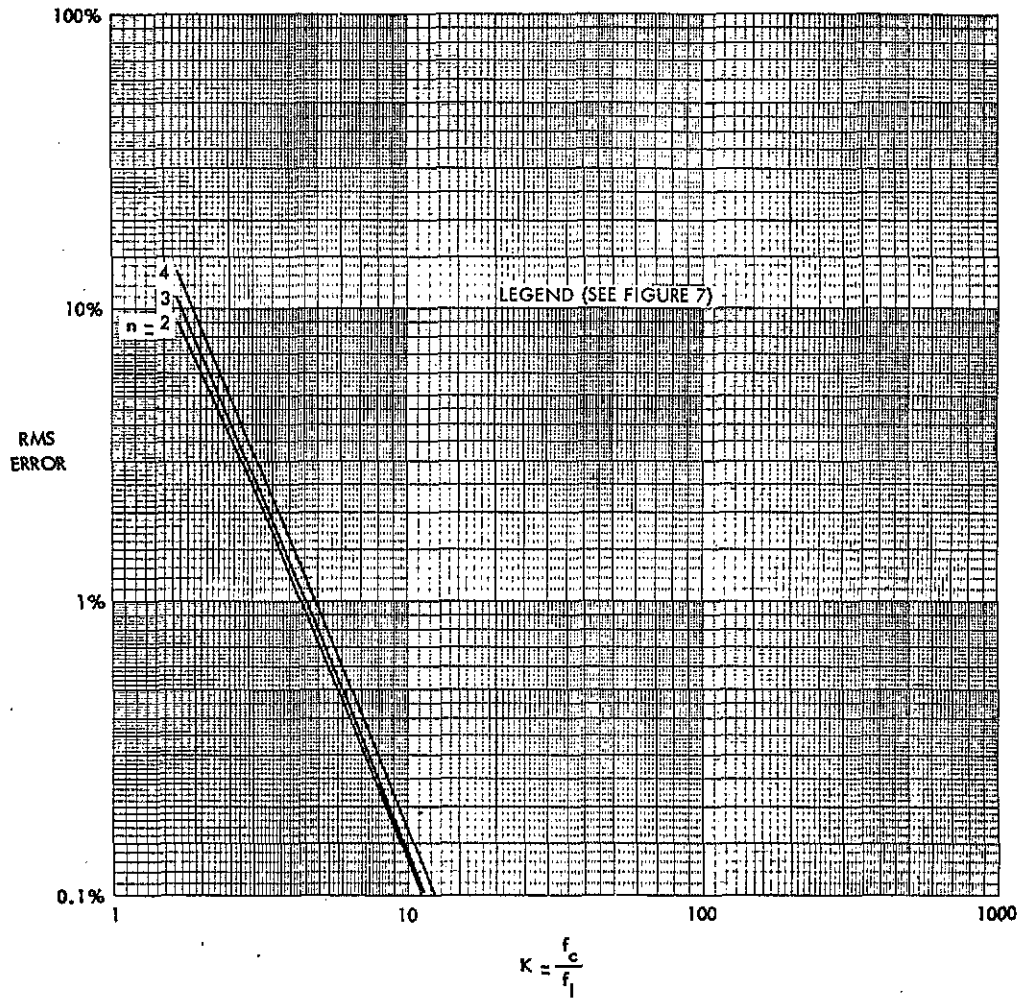
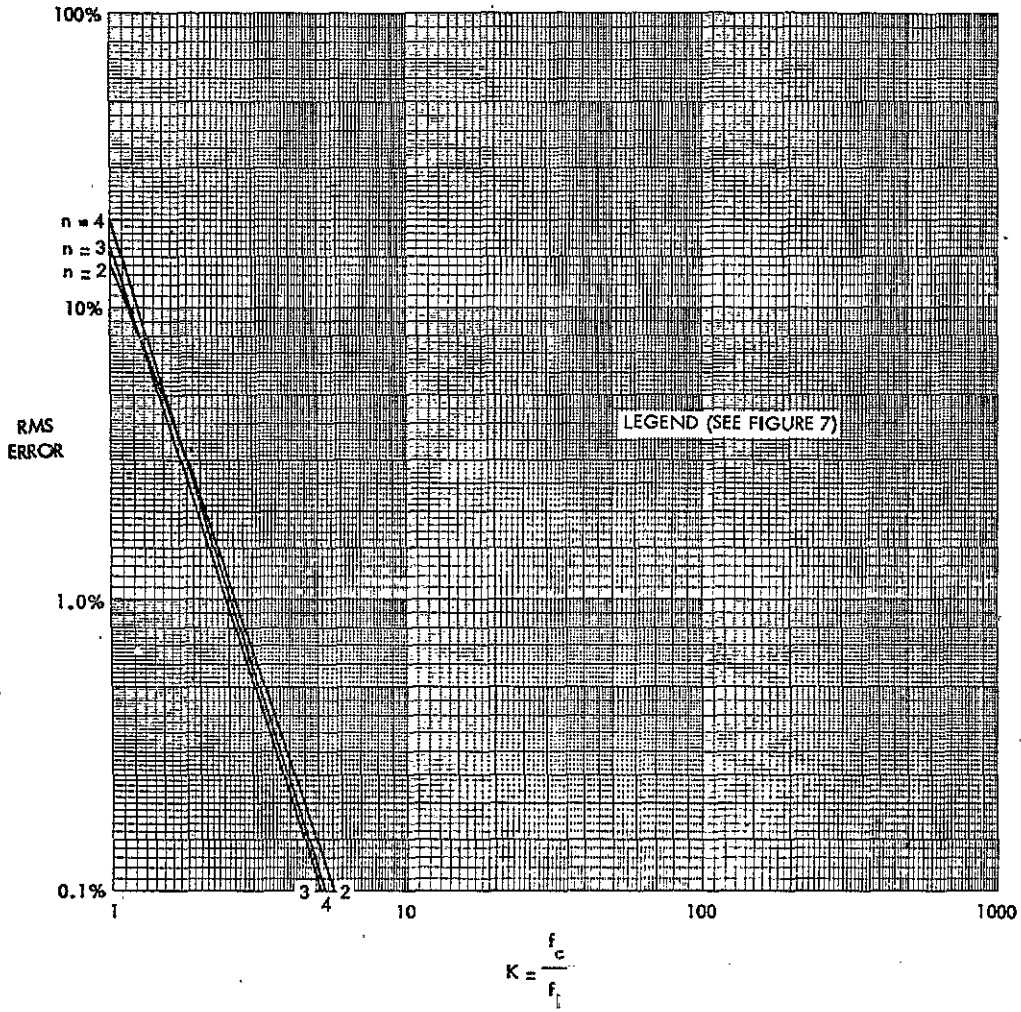


Figure 9. Errors of Omission, $m=3$, Butterworth Filter



21938

Figure 10. Errors of Omission, $m=\infty$, Butterworth Filter

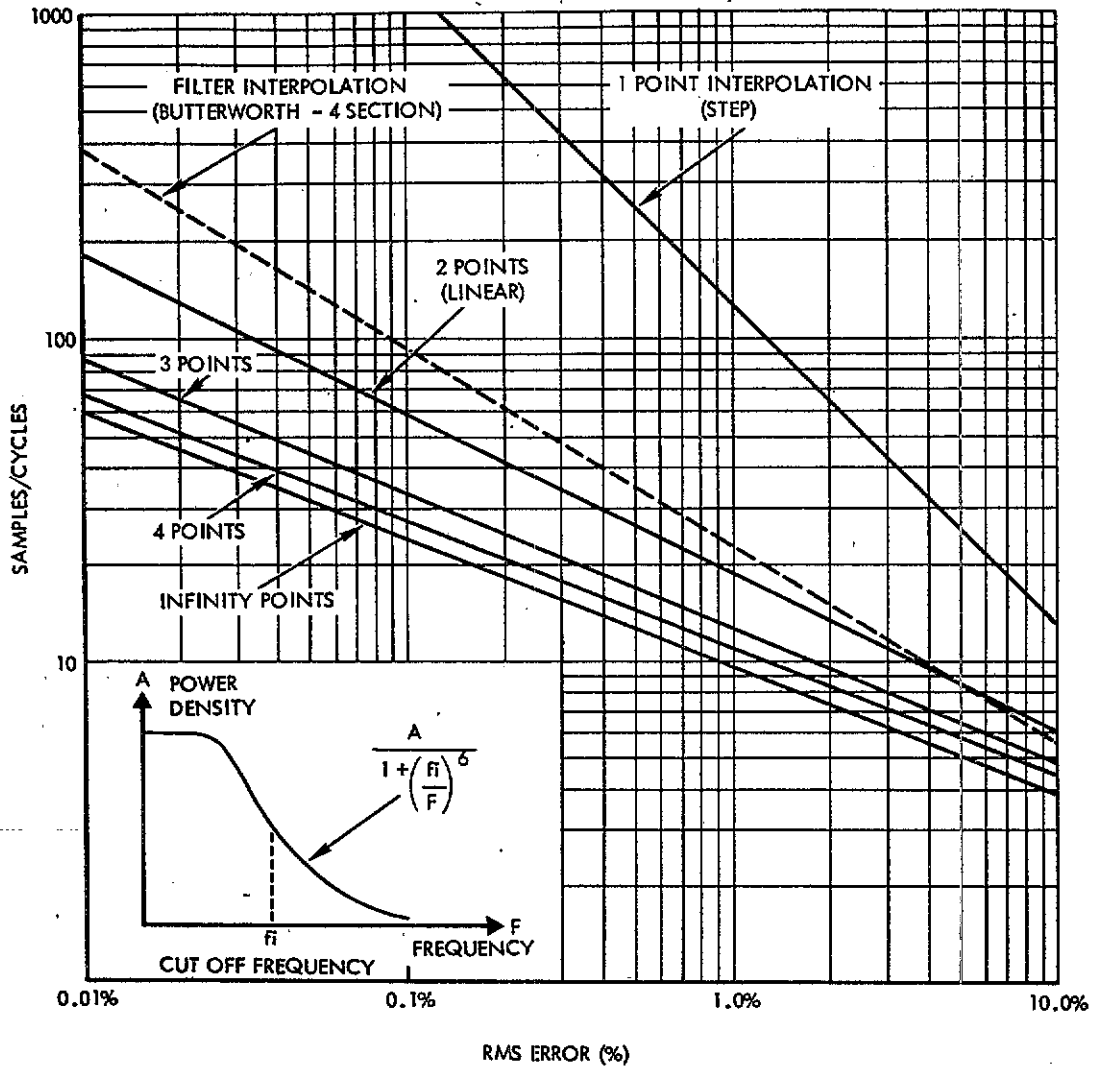


Figure 11. Error (% RMS) vs Samples/Cycle ($\frac{f_s}{f_i}$) for Third Order Data

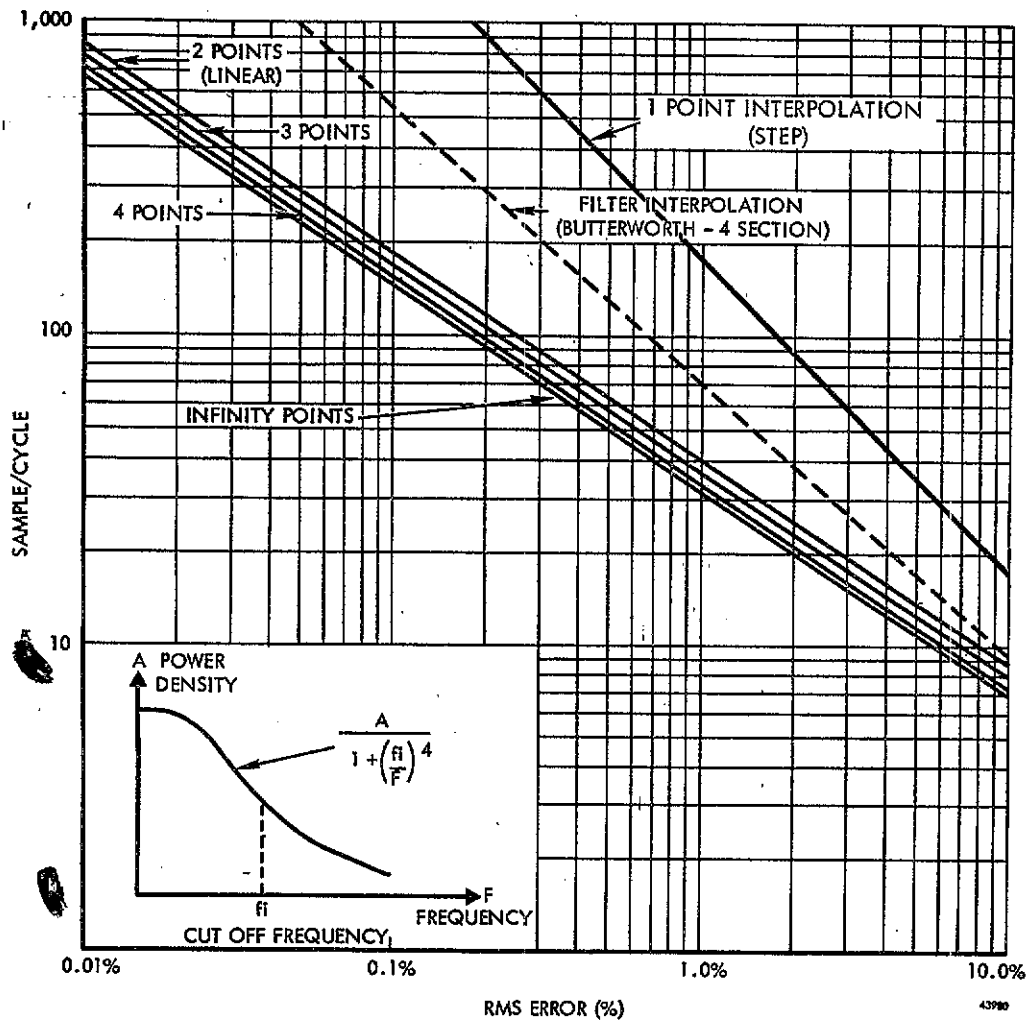


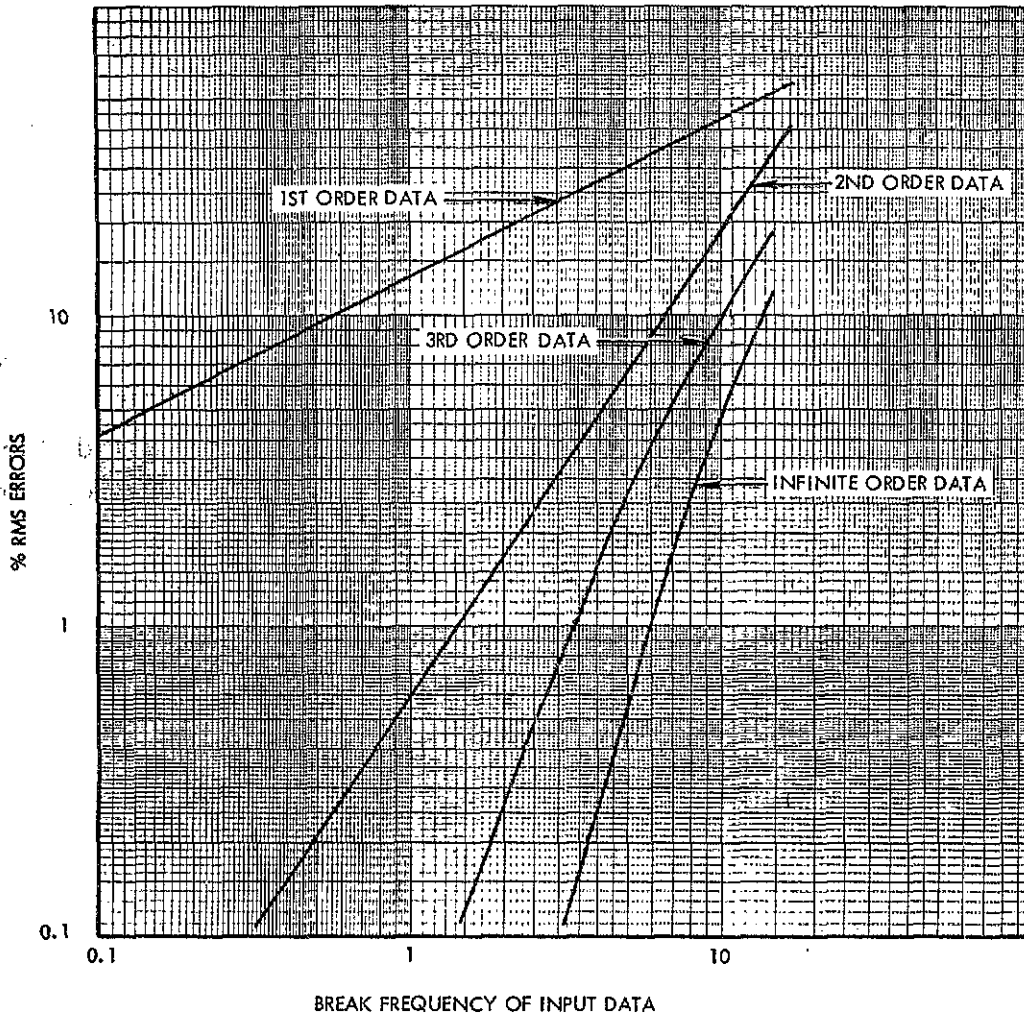
Figure 12. Error (% RMS) vs Samples/Cycle ($\frac{f_s}{f_i}$) for Second Order Data

If one were to use a method assuming the accelerometer was flat to 15 cycles cutoff frequency and an error of 1% rms., the sampling rate would be $50 \times 15 = 750$ samples per second. It is therefore clear that 695 samples per second have been wasted since the error above 1.1 cycles will always be greater than 1% no matter how many samples are used.

Using the errors of omission for the subject accelerometer as shown in Figure 7 through 11, the rms errors vs break frequency is plotted for 1st, 2nd, 3rd and infinite order data. These curves are shown in Figure 13.

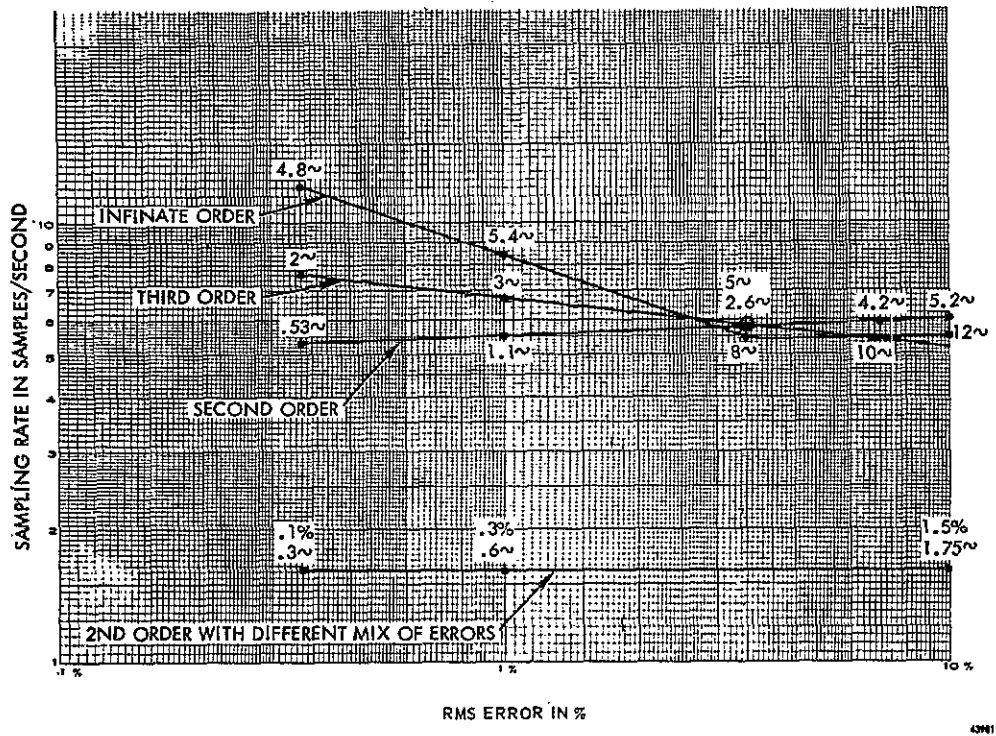
These curves show the best accuracy that can be obtained with a given frequency spectra at various orders.

This of course is a maximum sampling rate which will always be safe in that any higher sampling rate will not improve the error. Using a sampling rate of around 60 samples per second would always make the transducer the limiting factor regardless of what the input to the transducer is or what accuracy is desired. This is an operation that should never be allowed. If the input data is that close to the response of the transducer a transducer with a higher resonance frequency should be used. In actuality you should operate at some sampling rate below this if the characteristics of the data are known. If for instance, the order of the input is known, the error mix can be changed by lowering the transducer error and increasing the interpolation error, thus allowing a lower sampling rate for a given error. The lower line in Figure 14 is for 2nd order data with transducer error chosen to allow a constant sampling rate. This illustrates that the more is known about the input data the lower the sampling rate can be.



31053

Figure 13. Errors of Omission for Bourns Accelerometer, Model 602A



TOTAL RMS ERRORS EQUALLY DIVIDED BETWEEN
 TRANSDUCER ERRORS OF OMISSION AND
 INTERPOLATION ERROR AT GIVEN SAMPLING RATE

Figure 14. Required Sampling Rates with Different Orders of Input
 Using Linear Interpolation for Model 602A Accelerometer

DETERMINING SPECTRA OF TRANSDUCERS

In many cases this is a very difficult thing to do in that the transducer cannot be excited with a pure frequency. In the case of accelerometers, it can be accomplished on a vibration table. However, most calibration curves are not carried to a high enough frequency to determine the final slope or order of the spectrum. For many years the Instrumentation Engineer has attempted to overcome this problem by exciting the transducer with a known input step function (or nearly so) and in turn measuring the time response of the output. Graphical methods have been employed to determine the rise time, natural frequency, and damping ratios. Such a method is described by Tallman, Reference 5. This process is extremely time consuming. In addition, it is not possible to obtain enough information about the roll off characteristics to determine the final slope or order of the transducer, which is the most important item for determining which electrical filter to use as a comparison.

Many analog methods have been employed in an effort to determine the frequency response from a time response. The Bureau of Standards, Reference 6, has used a scheme whereby the time response to the step function of a transducer is recorded on a magnetic recorder and subsequently repetitive playback of this transient is fed into an electronic frequency analyzer. This process yields the various resonance frequencies of the time response, but the accuracy of the amplitude is very questionable, also no information is obtained on either phase response nor final slope, both of which are needed to determine the transfer function to any degree of accuracy.

Another method which has been used is a trial and error method of adjusting analog circuits constants whereby they have the same resonance frequencies and peak amplitude as the time function. This analog circuit will produce a response to a step function analogous to that of the mechanical system, the frequency response being the same as that of the mechanical system. The frequency response of this analog can then be determined by measuring the voltage response of the circuit to a constant amplitude current input and dividing that voltage response by the frequency. This method, however, is only as good as the experimental match of the original transient, and it is "practically" very difficult to obtain perfect simulation.

Ref. (5) "Transducer Frequency Response Evaluation for Rocket Instability Research" by Charles R. Tallman, Aerojet General Corporation, Azusa, California.

Ref. (6) NBS Telemetering Transducer Program by Paul S. Lederer

Several people have attempted to use a digital computer for determining frequency response from a time response by reading points on the time function response and evaluating a Fourier integral. The most valuable of these appears to be the work done by Bowersox, Reference 7, of the Jet Propulsion Labs. However, many problems still exist in his method. The main two being that he has not been able to obtain phase response and he must sample the entire time function until the oscillations damp completely out. This requires a great deal of hand read samples. Also the final slope is not obtained.

In order to solve some of these problems, Radiation Incorporated performed a study resulting in a program for the IBM 1620 computer. The results of many people were carefully studied and it became obvious that the only way to be sure of our results was to start with a theoretical system where its transfer function could be calculated very accurately. By knowing the exact frequency content of the input step, the exact amplitude at any time on the time response curve, and finally the exact frequency response, we could compare our solution to the theoretical and discover what our problems and errors were.

The data used was the time response, of a second order system, with 0.2 damping to a step function, as shown in Figure 15. The frequency response curve is shown in Figure 16. The equation shown in Figure 15 was solved by the computer at 13 samples for each cycle. The results of the frequency response curve obtained is shown in Figure 17. The comparison with the theoretical yielded many interesting facts.

First of all, it showed that we were not taking adequate samples in order to determine the final slope. The accuracy of the computer output was quite good up to 15 cycles. From this point, the accuracy degraded rapidly as the frequency increased. This degrading was found to be not only a function of inadequate sampling but largely due to the method used in determining a given integral in the Fourier series process.

Ref. (7) J. P. L. Progress Report 20-331, "Digital Computer Calculation of Transducer Frequency Response From Its Response to a Step Function", by Ralph B. Bowersox and Joseph Carlson.

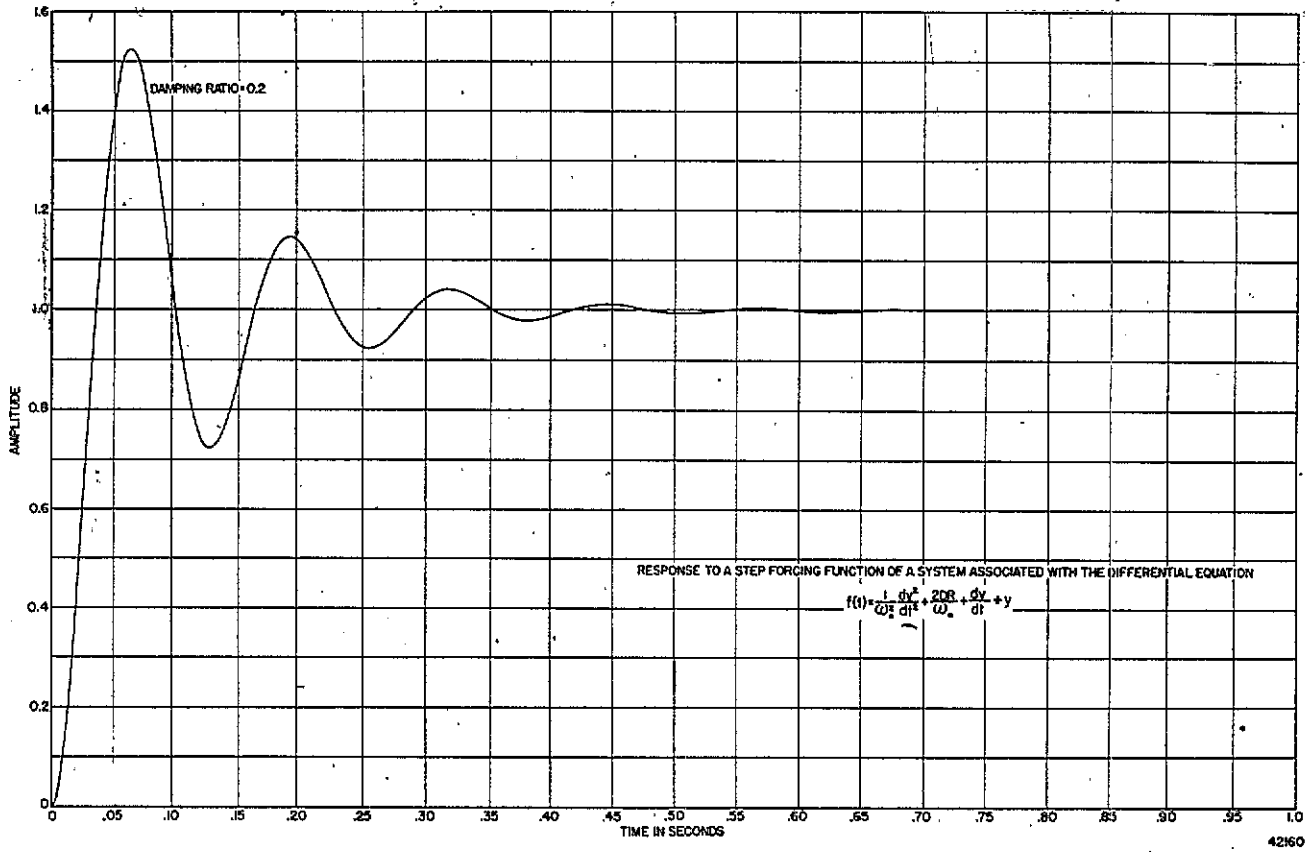
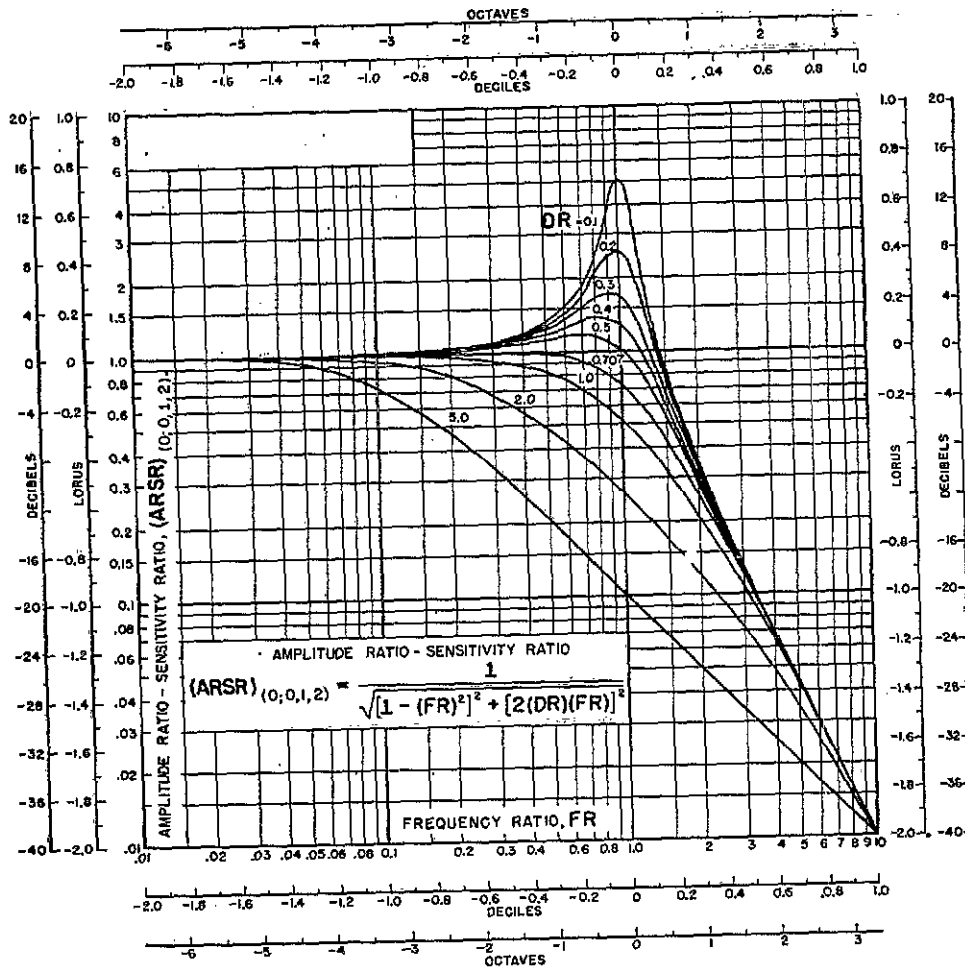


Figure 15. Time Response of Theoretical Second Order System



$$FR = \omega / \omega_n$$

LOG-LOG PLOT OF STEADY-STATE SINUSOIDAL RESPONSE CHARACTERISTICS

35049

Figure 16. Log-Log Plot of Steady-State Sinusoidal Response Characteristic

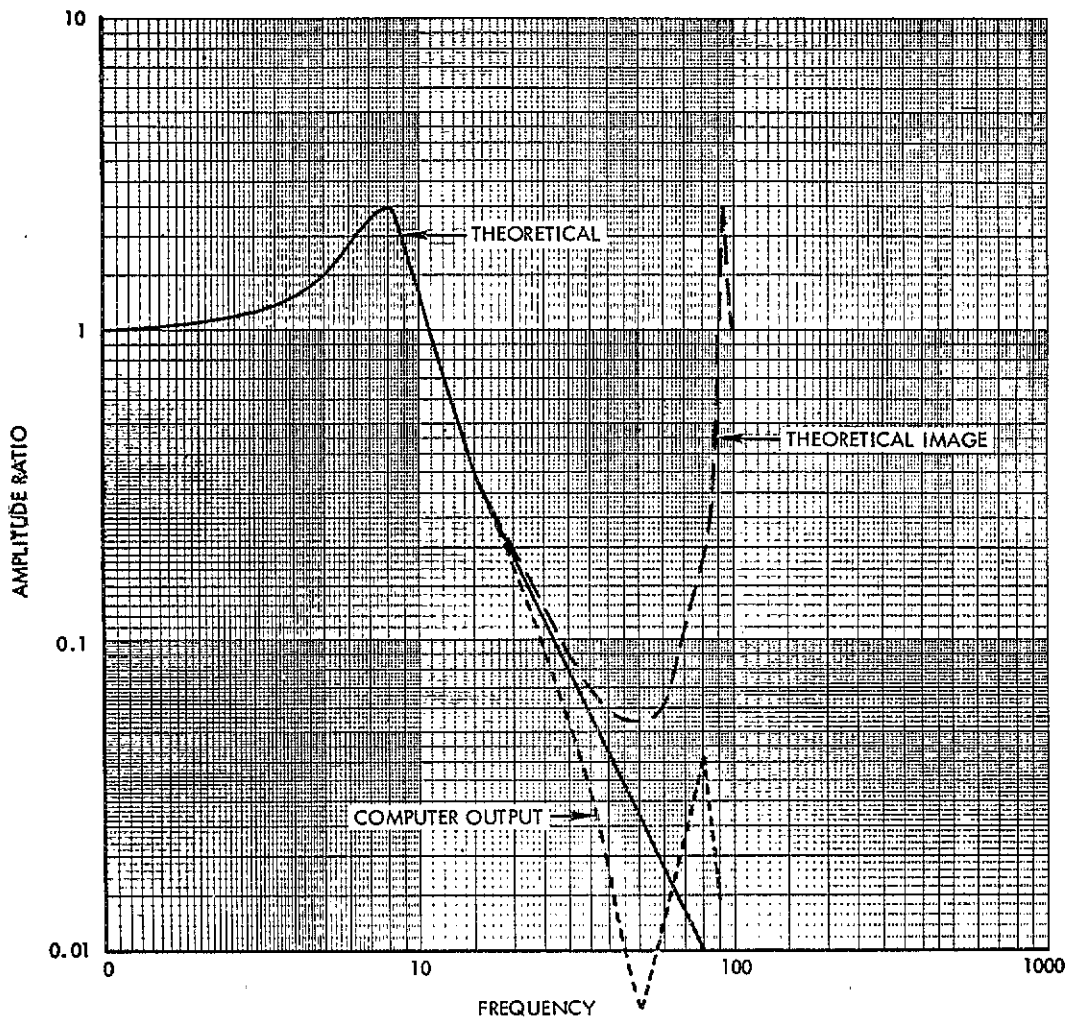


Figure 17. Frequency Response of Second Degree System

Using the results of the sampling study as covered in Reference 3, the computer program was changed whereby the accuracy was improved out to approximately 100 cycles, for both amplitude and phase as shown in Figure 18. These improvements were possible due to our understanding of the sampling theorem and by using the computer to interpolate points between the samples, whereby a large number of samples were not necessary yet the sampled image could be increased to a point where the final slope could be obtained.

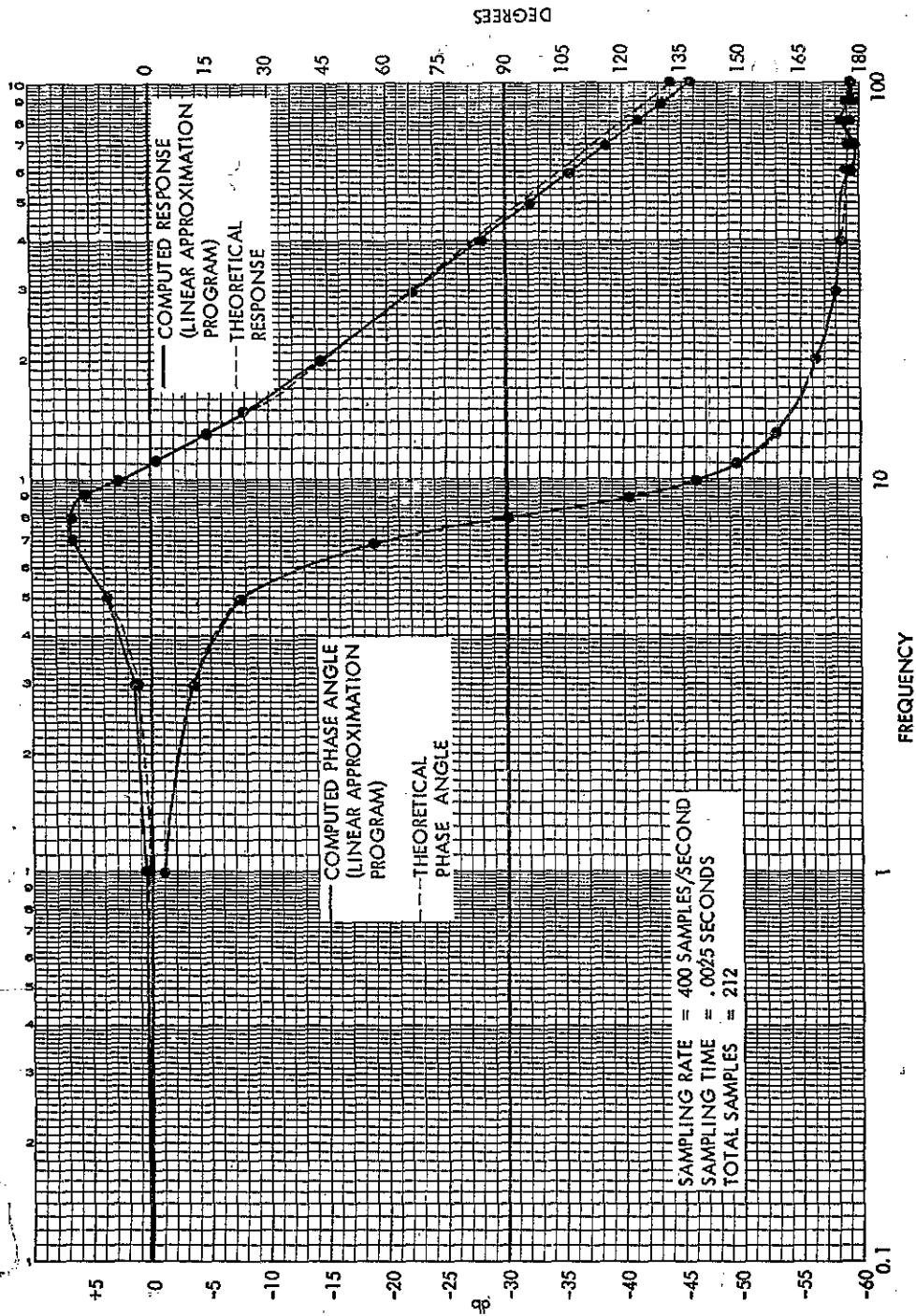


Figure 18. Frequency Response and Phase Angle for a Second Degree System

CONCLUSIONS

The results presented above show that a transducer is a presampling filter, whether used as one or not. When the spectral characteristics of the transducer is known, they can be used to determine an optimum sampling rate.

The large errors of omission shown at the natural frequency proves that a transducer should not be used for data near the natural frequency.

The method for determining phase response, frequency response including the final slope, which has been presented can be used for evaluating transducers that cannot be excited by pure frequencies.

A study should be undertaken which would evaluate all transducers that are planned for use with PCM systems.

SECTION XIII

TRANSDUCER TECHNOLOGY AT THE
AIR FORCE ROCKET PROPULSION LABORATORY
EDWARDS, CALIFORNIA

by

James B. Lake
Air Force Rocket Propulsion Laboratory
Edwards, California

INTRODUCTION

The AF Rocket Propulsion Laboratory at Edwards, California has 37 static firing positions where in-house research efforts are carried on. The research projects range from propellant and material evaluations through combustion studies. The large number of research projects and variety of test objectives naturally require a large number and variety of transducers. It is the purpose of this paper to discuss the types of transducers in use at AFRPL; the problems encountered in using them; and the new transducers being developed by AFRPL. This paper will cover three areas of transducer technology: (1) flow, (2) pressure, and (3) thrust.

FLOW MEASUREMENTS

The AF Rocket Propulsion Laboratory is involved in the use of many highly reactive propellants such as fluorine, fluorine compounds, N_2O_4 , perchlorate, etc. Accurate flow measurements of these propellants are difficult at best. Since much of the work at AFRPL is propellant and engine performance evaluations, AFRPL has a very keen interest in obtaining the most accurate flow measurements possible. The turbine type volumetric flowmeter is used almost exclusively to do the job. At this time there has not been significant evidence to indicate other flow measuring devices are capable of measuring flow rates more accurately.

Flowmeter Bearings

One of the main contributing factors that determines the performance obtained from the turbine flowmeter is the bearings. The bearings must be constructed of materials compatible with highly reactive propellants, sufficiently rugged to withstand the harsh treatment, and additionally, the bearing materials should be such that the frictional forces do not change with time or use. The last requirement becomes increasingly more important as the flowmeter size becomes smaller. Based on a study conducted at AFRPL the recommendations are made concerning the use of flowmeter bearings.

Sapphire Bearings

Sapphire bearings are not presently being recommended for use with most of the propellants. AFRPL has purchased several flowmeters equipped with sapphire bearings and received very poor results from their use. The flowmeter rotor tends to vibrate while in operation which causes a reduction in rotor angular velocity resulting in gross errors. This problem must be overcome before the flowmeters can become operational. The sapphire bearings, however, may prove suitable for use in slurries. AFRPL has a few flowmeters equipped with sapphire bearings specially designed and built by Rocketdyne for use with slurries. So far there is no indication they are not performing properly.

Graphitar 30

AFRPL purchased a number of flowmeters equipped with Graphitar 30 bearings. These flowmeters were built for use with N_2O_4 . Graphitar 30

has proven not to be compatible with N_2O_4 . After exposure to N_2O_4 , the bearing surface becomes soft and clings to the shaft.

Bearing Recommended for Use

AFRPL is switching to the use of either stainless steel ball bearings or teflon (but not necessarily limited to these materials). The stainless steel ball bearings can be used with all propellants at AFRPL. Teflon bearings can be used with all propellants in use at AFRPL except fluorine and fluorine compounds. It should be noted, however, that when teflon is used with N_2O_4 or Lox, the bearing should be enlarged by about two thousandths of an inch. Teflon will swell slightly in N_2O_4 and the added clearance is required. When teflon is used at cryogenic temperatures, the bearing will shrink thus requiring extra clearance. Since excess bearing clearance normally reduces flowmeter precision, the flowmeters with excess bearing clearance should not be used where it is not required.

Calibration and Installation

Based on experience AFRPL has found the flowmeters in use should be recalibrated at least once every six (6) months. Flowmeters smaller than one (1) inch and flowmeters in fluorine service will require more frequency calibrations. Any meter removed from a system should normally be recalibrated prior to reinstalling. The flowmeter manufacturers usually recommend that flowmeters be installed a minimum of ten pipe diameters from covating venturies. Flow straighteners will help in cases where proper installation cannot be achieved. When the recommended installations cannot be achieved, it is advisable to calibrate the pipe section with the flowmeter. When installing the flowmeters equipped with the flared tube fitting, it is easy to distort the fitting even when recommended torques are not exceeded. The inside diameter of the flared end can be decreased, necessitating machine shop work before the meter can be disassembled. This condition can be relieved by the use of a soft seal, thereby allowing smaller torque value to seal the fitting.

Special Technical Factors

Accurate flow measurements and good precision factors are easily obtained when operating under the ideal conditions of a flow calibration laboratory. However, in field operation, additional variables are encountered. The AFRPL is undertaking a study of the effect these variables have on propellant flow measurement accuracy. As a prime tool in this study, AFRPL has awarded a contract to Flow Technology, Incorporated to design and build a flow proving system. The flow proving system will provide an on-site flowmeter calibration during rocket motor firing. The operating principle of the system is simple: a piston is released during a test run which sweeps out a known volume of propellant during a measured time interval. The system is shown in Figure 1. The system will have the following operational capabilities:

1. Flow rates from 10-130 gpm.
2. Operating pressures up to 6000 pounds.
3. Operating temperature range 0-120°F.

4. The system shall be designed for operation in winds up to 50 miles per hour, dust, sand, and freezing rain.
5. The system shall operate with liquids or slurry propellants.
6. Reset capability without disassembly.
7. Remote operation.
8. Designed for convenient flushing.
9. Operation accuracies of 0.1% and repeatability of 0.1%.

Low Flow Requirement

The pulsed motor research program at AFRPL requires the accurate measurement of flow rate pulses. The flow pulse magnitude will vary from 0.01 to 0.03 lbs/sec and the duration will range from 0.001 to 1 second. AFRPL has awarded a contract to Aerojet-General to provide study, research, and development of a flowmeter to meet these requirements. Aerojet has proposed to develop an electro magnetic flowmeter shown in Figure 2. This device has most of the requirements of an ideal measuring device: no moving parts; no obstructions in the propellant; has a theoretical frequency response much higher than required; well above 10 KC. The device will use a non-varying magnetic field allowing the high frequency response.

PRESSURE AND THRUST TRANSDUCERS

The majority of pressure and thrust transducers in use at AFRPL are considered as general service transducers. The general service transducer is a bonded strain gage type used to meet the general requirements at all test locations. These transducers must not only be rugged but also constructed of materials compatible with the highly reactive propellants in use at AFRPL. Some of the technical requirements are listed below that are called for in the general specifications:

1. Excitation voltage 10 volts nominal.
2. Output: 3 mv per volt full scale.
3. Linearity: 0.2% full scale.
4. Hysteresis: 0.1% full scale - deviation from linearity curve.
5. Repeatability: 0.075% F.S.
6. Combined Effect: \pm 0.25% F.S.
7. Temperature: 0°F to +250.
8. Insulation Resistance: 1000 megohm minimum at 50 VDC.

These transducers are in general the standard product of the manufacturer with four special requirements called for. The type of pressure transducer construction generally preferred at AFRPL is the proving ring type construction. This type construction is rugged and gives dependable performance. Vacuum compensation will be included in the specifications for some of the general service thrust cells. The vacuum compensation load cells will be purchased for installation in altitude chambers. The load cell will be subjected to temperatures between -300 and +500°F. The vacuum compensation can be taken care of in at least two ways. The load cells can simply be vented or electrical compensation can be achieved. If the load cell is vented, then precautions must be taken to protect the inside structures from the corrosive environments. In general the transducers presently being manufactured meet the general service requirement. However, it is believed the following areas of improvement would be beneficial: more rugged construction; a greater overload capability; a significant increase in output. An increase in temperature compensation range and a decrease in size with no sacrifice to quality. A transducer with a dual range or equivalent is also desired for use in studying the performance of throttling engines. The type engine being studied is expected to have a 50-1 throttling range.

Pressure Calibrations

Presently over 90% of all pressure transducers at AFRPL receive in-place, end-to-end calibrations. Due to the increase in rocket propulsion system testing, this method is no longer practical. AFRPL is, therefore, converting to a resistive shunt calibration method. Consolidated Systems Corporation has been awarded a contract to study and design and construct a calibration system to fit the need at AFRPL. The following technical considerations are included in the specifications:

1. The system shall be designed primarily for the calibration of 350 ohm resistive bridge strain gage type transducers. However, provision will also be made for other types in use at AFRPL.
2. The calibration range will be from 0-2000 psig, psia and psid with capabilities of expansion up to 10,000 psig. At pressures up to 2000 psig the calibrator shall use gaseous nitrogen. At above 2000 psig distilled water shall be used.
3. The calibration system calibration standard shall be traceable to the National Bureau of Standards.
4. The system shall be capable of up to 50 calibrations per day.
5. The system will be compatible with the data acquisition systems presently in use at AFRPL.

Thrust Calibrations

The present methods used to calibrate thrust consists of on-site end-to-end calibrations. Since most of the rocket engines being tested are liquid and require plumbing connections into the stand, end-to-end

calibrations are preferred. Whenever a new test stand is installed or modified, a complete evaluation of the stand is performed. As an evaluation tool, AFRPL has designed a universal thrust adapter which will fit all test stands at AFRPL. The universal thrust adapter is a structure which is attached to the aft end of the stand and has provisions for the installation of a standard cell. In this manner the calibration load can be applied externally to the stand and compared with the built-in calibration methods. Errors as large as 7% have been detected in the built-in calibration method. Usually the error resulting from the plumbing frictional forces amount to less than fifteen pounds. Errors due to the bordon tube effect when propellant lines are pressurized can easily amount to 100 pounds or greater if propellant lines are not properly installed. In general, these errors are eliminated easily when they are detected.

Methods of Thrust Calibrations

Two (2) methods of thrust calibrations are presently being used at AFRPL, dead weight calibrations and standard cell calibrations. Although the integrity of dead weight calibrations are realized, the standard cell has proven more suitable for the general field requirements at AFRPL. The standard cell has the advantage of being smaller in size, more economical, easier to operate, and can easily be calibrated against secondary standards.

SPECIAL SERVICE TRANSDUCERS

The combustion instability studies at AFRPL require high frequency pressure measurements up to 10KC. The requirement will be expanded to 20 KC within the next twelve months. Presently the capacitive type transducers are operationally easy to handle; rugged, and have a high output. They have the disadvantage that they are large and suffer from zero shifts during operation. Also the frequency response is not as flat as desired. Piezoelectric thrust transducers are presently being used to measure the pulsed motor thrust valves. The transducer outputs are fed into charge amplifiers. The biggest problem encountered in the use of the piezoelectric transducers has been zero drift. The problem has been solved by shielding the transducer from heat and shortening the cable going into the charge amplifier.

NEW DEVELOPMENTS

AFRPL has awarded a contract to Rocketdyne to develop and construct a high frequency, low range thrust transducer. The operating range will be from 0.25 pound to 10 pounds. The transducer will respond from 10% to 90% of load in 0.0005 second. The transducer is expected to have an accuracy of 0.5% in the range from 20% to full scale. The transducer operating temperature range will vary from 0-160°F. Rocketdyne has proposed a bonded semi-conductor strain gage type transducer. The significantly larger gage factor of the semi-conductor permits the use of low compliance strain member. This fact provides the necessary increase in frequency response over the conventional bonded strain gage transducers.

ADDITIONAL TECHNICAL NOTES

1. AFRPL has in operation a very accurate thrust measuring system for determining the total impulse of solid propellants. The system is an Air Force standard to compare performance of solid propellants. The total system accuracy is 0.1% or better. The unique feature of this system is that it utilizes a Ruska dead weight hydraulic calibration system.

2. The precision measurement and evaluation laboratory at Edwards is scheduled in July to put into operation a 1,000,000 pound calibration system. The system range is from 25,000 pounds, to 1,000,000 pounds. The system will use straight dead weight up to 200,000 pounds, providing an accuracy of 0.02%. The system will use a give to one lever arm from 200,000 pounds to 1,000,000 pounds, providing an accuracy of 0.05%.

3. The precision measurement and evaluation laboratory has in operation one of the larger flowmeter calibration systems in the country. The calibration range is from 40 to 9000 gallons/min with a calibration accuracy of 1%. The system is being modified to increase the calibration range to 12,000 gallons/min.

ON LINE FLOWMETER SYSTEM

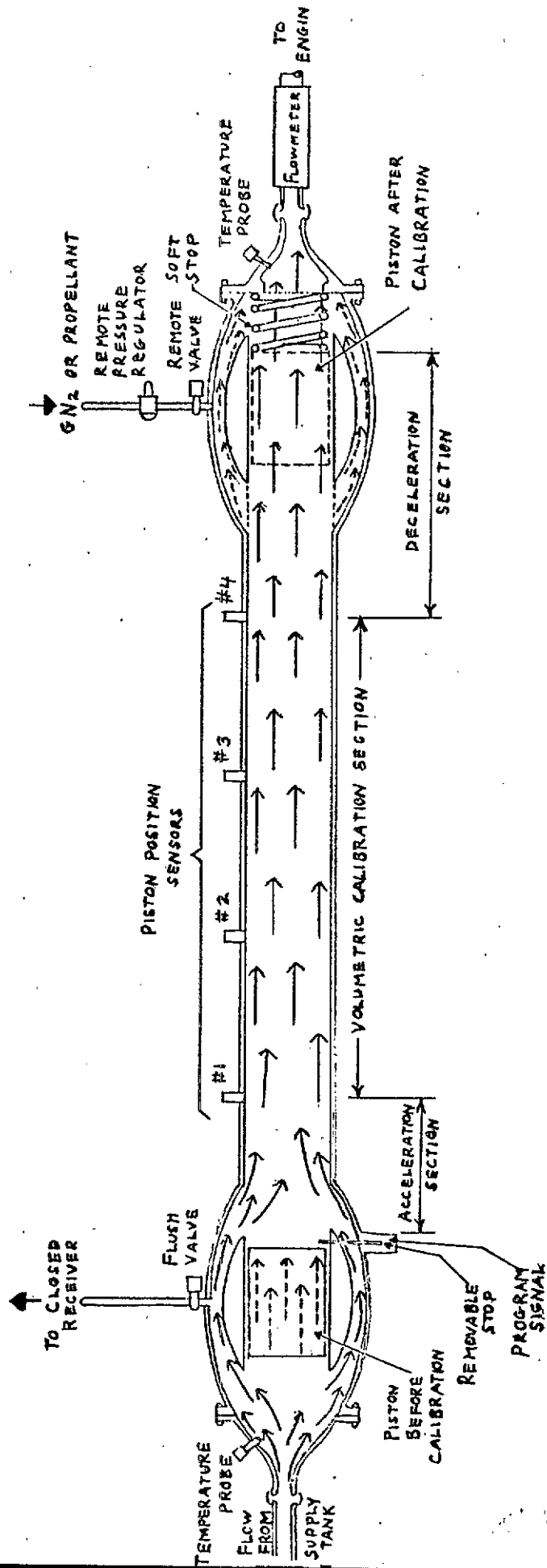


FIGURE 1

SECTION XIV

RESEARCH ON TRANSDUCERS FOR
EXTREME ENVIRONMENTAL TEMPERATURES

by

Lawrence Fleming
Bell & Howell Research Center
Pasadena, California

RESEARCH ON TRANSDUCERS FOR
EXTREME ENVIRONMENTAL TEMPERATURES

Lawrence Fleming

Bell & Howell Research Center
Pasadena, California

Abstract

The considerations underlying the choice of operating principles for extreme-temperature transduction are discussed. An experimental displacement pickup is described which uses a mutual-inductance principle and functions well at 2100°F.

Introduction

The problem of sensing mechanical variables in extreme environments is one that involves the choice of the principle of transduction as well as the technology of materials. At very high temperatures, resistance elements oxidize, adhesives fail, permanent magnets lose their magnetism and soft magnetic materials their permeability.

The immediacy of the instrumentation requirements in a major "hardware" project tends to emphasize extensions of development of sensors based on currently-used principles. This tendency is abetted by the existence of large stocks of conventional signal-conditioning equipment and by the investment of user personnel in skills at using transitional types of instrumentation. Thus, although hundreds of effects and phenomena are known which might be used in transduction, only a half-dozen or so are used in practice, and relatively little effort is spent in exploring the rest. References (1) and (2) for example refer to many programs directed to the extension of metallic strain-gage technology to higher temperatures.

In order to devise a transducer which will work in extremely hot environments, it is necessary to consider what principles of transduction make

the most lenient demands on the properties of the materials. After choosing an appropriate principle, we can then implement it with refractory materials, and have an instrument with above-the-ordinary immunity to environmental temperatures.

Strain gages, both metallic and semiconductor, are subject to the temperature limitations of the piezoresistive effect itself. Unbonded gage devices are somewhat the better in respect to temperature, and also radiation, because bonded gage instruments depend additionally on another factor - the cement or adhesive. Potentiometer instruments suffer from oxidation and friction difficulties. Transducers which employ permanent magnets are limited by the magnets to around 1,000°F. Variable-reluctance transducers, including conventional types of differential transformers, are limited by the curie points of soft ferromagnetic materials (under 1,500°F for iron, 800°F for nickel alloys). Multilayer coils pose difficulties at high temperatures, due to distortion and cracking of inorganic potting compounds. At 2,000°F, the resistivity of copper and silver is about 4 times that at room temperature, of platinum about 6 times.

Hence, a 2,000°F instrument must not depend for its performance and calibration, on any of the following phenomena remaining constant: ferromagnetism, piezoresistivity, contact resistance, friction, piezoelectricity, resistivity of conductors, conductivity of insulators. In addition, multilayer wire coils and conventional electronic components must be avoided.

These considerations limit our choice, practically, to two principles which relate the geometry of arrangements of electrical conductors to their electrical properties: capacitance and inductance. The capacitive transducer appears to be a good candidate for extreme-temperature work because its transfer characteristics depend only on the geometry of the conducting surfaces. The effects of insulation leakage can be minimized by operation at a high carrier frequency, where its capacitive reactance is relatively low. However, practical capacitive transducers have capacitance values which tend to be low compared to the capacitance of practical connecting cables, so that the cables or leads control the sensitivity. The only way to reduce the effect of the leads would be to locate a transformer or an amplifier at the transducer, which the environment will not permit.

Mutual Inductance

So we are led to consider inductance transducers. To avoid iron cores and multilayer windings, we must use some system of relatively movable single-layer coils. The configuration of a differential transformer is most appropriate, with one of the coils made movable. Reference (3) discusses this type of transducer and suggests its applicability to high-temperature work. A somewhat different air-core mutual inductance transducer has been

described (Ref. 4) for use in another sort of adverse environment: buried in soil. The advantages of a differential or "push-pull" configuration are primarily that the transfer curve is linear for small displacements, as shown by Neubert (Ref. 5).

The air-core, single-layer differential transformer must be operated at a high frequency, e.g. 1 megacycle, to get adequate sensitivity. In common with other mutual-inductance devices, the secondary (output) voltage can be made independent of the resistance of the windings. With convenient parameters, the calibration can be made quite independent of cable capacitance up to cable lengths of 20 feet or so.

Figure 1 shows a cross-sectional sketch of a typical sensing element which employs this principle. The movable primary coil P has a few turns of conductor in a single layer. The stationary secondary S_1, S_2 may have about twice as many turns, split into two sections which are connected in inverse series. Alternatively, the two halves of the secondary may be wound in opposite directions. Overall length and diameter of the outer coil, in practice, is typically of the order of 1 cm x 1 cm.

Figure 2 indicates the kind of circuit employed. The primary is fed exciting current i_p from a constant-current source. The secondary voltage e_s is then

$$e_s = M \frac{di_p}{dt},$$

where M is the mutual inductance between primary and secondary. $\frac{di_p}{dt}$ can

be held constant by designing the source A as constant-frequency, current-regulated r.f. supply, so that i_p will not change when the resistance of winding P changes with temperature. e_s will depend only on M, which is a function solely of the geometry of the coils; and e_s will not be affected by changes in the resistivity of the coil S so long as it is, electrically, lightly loaded.

Insulation resistance need only be a few orders of magnitude greater than the impedance of coil S, which is of the order of a few ohms. Thus the requirements on the resistivity of both the conducting and the insulating components are very lenient.

Shapes

A solenoid configuration of the high-frequency differential transformer (HFDT) of approximately square shape, as in Figure 1, has been found to be linear within 2% of full scale for a stroke equal to about 16% of the length

of the longer coil. Other configurations are practical. A flat spiral shape in one version measured was linear within 1 percent over about 30% of the spacing between the two stator coils.

Cables and Sensitivity

The sensitivity $\frac{\Delta e_s}{\Delta x}$ attainable in practice depends on (1) the r.f.

power level conveniently deliverable to the primary coil, and (2) the degree of independence of cable length required. If one or both the coils be operated at electrical resonance, the sensitivity will be very large, but will depend strongly both on cable length and coil resistance.

For a practical experimental system, it was found best to operate at a frequency about a decade lower than the frequency of resonance of the largest coil with the maximum cable capacitance expected (in this case, 1,000 pf), i.e. at a frequency of about 1 mc. This had been found to permit operation with any cable length up to 20 feet of 50 pf/ft. cable with no adjustment, this change in length of cable producing less than 2 percent change in calibration. The value of exciting current was dictated primarily by transistor and power consumption considerations.

Under these conditions, a 1/2" x 1/2", 10 turn transducer gave the following results:

Linear range (2%), $\pm .038''$

e_s , 4.2 millivolts per .001 inch per ampere of i_p , at 1 mc.

(± 0.125 v at $i_p = 0.8$ A)

The output signal power is relatively large. Assuming conservatively an impedance of 10 ohms, including cabling, the power at full-scale displacement ($\pm .038''$) was roughly 1.5 milliwatts. For comparison, the 40 mv. output of a typical 300-ohm wire strain-gage bridge is only about 5 microwatts.

The interrelation between inductance, frequency, and cable requirements is rather complex. While a practical system can be worked out empirically rather readily for a given set of requirements, it does not appear a simple matter to produce a set of equations and charts which would permit ready design on paper. Similarly, the calculation of coupling coefficients for coils of various shapes is not simple. At this stage, it is not thought practical to attempt it, since empirical data are easy to obtain, and the more obvious configurations are found to work quite well.

Circuitry

Figure 3 shows a simple exciter and demodulator circuit for these applications. Q_1 is an oscillator, Q_2 a tuned amplifier. The transformers are

wound on ferrite toroidal cores. The synchronous demodulator diodes D_1 , D_2 are excited from a small winding on the amplifier coil T_2 . D.C. output is typically of the order of ± 0.1 volt. While this circuit does not provide automatic current regulation, it provides convenient and reproducible data at small cost.

High-Temperature Tests

Figure 4 is a photograph of a "hot" model of the H.F.D.T. mounted in a furnace. The transducer coils were wound at the ends of two telescoping pieces of high-alumina ceramic tubing about 9 inches long, of which about a third protruded into the furnace. The outer coil diameter was $1/2$ " , the inner $3/8$ " , and the coil lengths $1/2$ " and $1/4$ " . The windings were each 5 turns of $.030$ " platinum wire, wound in grooves and held in place with Saureisen cement. The outer tube was clamped to a stationary plate, and the inner tube moved up and down by means of a micrometer screw.

Figure 5 shows overall transfer curves, from micrometer screw to amplified and demodulated output voltage, for temperatures of 70° , $1,460^\circ$, and $2,100^\circ\text{F}$. Figure 6 shows the same data plotted to show the range or span of the transducer as a function of temperature. These data were taken using a more elaborate current-regulated exciter which includes about 50X amplification before the demodulator.

The zero was quite stable, shifting imperceptibly up to $1,000^\circ\text{F}$ and only 1.8% at $2,100^\circ$. This, as well as the span data, repeats within the observational error of about $.0002$ " (0.4% of full scale) from day to day, and there has been no perceptible drift during several hours at $2,000^\circ\text{F}$.

The sensitivity increased about 9 percent at $2,000^\circ\text{F}$ over the room temperature value. This may be due to thermal expansion, or to phase shifts engendered by the increase in coil resistance (about 6:1) or to capacitive effects due to the resulting increase in exciting voltage.

Miscellaneous Properties

Transducers of this type are not particularly sensitive to lead dress or the proximity of nearby conductive objects. Generally, the only necessary electrical precautions are to avoid inductive coupling between the exciting and the output cables, and to avoid "stray" common impedances between output and input in the layout of the electronics.

The leniency of the requirements on the electrical properties of the materials argues that these transducers should be resistant to radiation. Moreover, the voltages at the coils are so low (< 1 volt) that operation in ionizable atmospheres should present no problems.

The shapes of the windings can be designed to minimize thermal expansion effects, by balancing the effect of the increase in diameter against that of the increase in length. Such procedures are described in the older literature on radio receiver coil design. At extreme temperatures, however, it is not safe to assume that the whole coil structure is at the same temperature. Analytical compensation would have to be based on experimental data for the particular case.

The problem of utilizing this kind of sensing element in a pressure or acceleration transducer is chiefly one of finding and fabricating materials for springs and diaphragms which have good elastic properties at elevated temperatures. Studies made at Culton Industries have concluded that no metal is available which has adequately low elastic hysteresis and creep above 1,000°F. Structural non-metallics such as beryllia and high-alumina ceramics show, however, considerable promise.

The present stroke range of about .05" was chosen as being reasonably large (but not too large) compared to the expected dimensional changes due to thermal expansion. It was not deemed wise to put too much faith in expansion compensation because in real life there are always temperature gradients. Since, however, the "hot model" data shows good reproducibility within .001", a pressure sensor may be practical with a stroke considerably shorter than .05", such as .01" or even less.

The barrier to testing at temperatures above 2,100°F was the oxidation rate of Pt in the furnace atmosphere. Higher temperature tests will have to be made by means of electric heating in an inert atmosphere or in vacuum.

The upper temperature limit appears at present to be dictated at least as much by the availability of suitable cable as it is by the transducer itself. Swage-lead appears to be the only appropriate kind now available.

At cryogenic temperatures, plated or coated coils would be quite satisfactory.

Acknowledgement

Credit is due Mr. R. L. Brownell for the design and fabrication of the "hot model" transducer and test furnace, and Mr. Bert H. Dann for development of the final regulated version of the electronics package.

References

1. R. J. Molella and C. R. Nelson, "Requirements for High-Temperature Strain Gages in Structural Testing," Aeronautical Structures Lab., U.S. Naval Air Materiel Center, Philadelphia. Report No. R360FR101-ASL(14), July 1962, 15 pp., 40 refs.
2. S. W. Leszynski, "The Development of Flame Sprayed Sensors," presented at ISA Summer Conference, Toronto, 8 June 1961. ASTIA AD-283958 (12 pp. and bibliography of 44 items).
3. "A Study of Force and Displacement Measuring Techniques", Part II, Armour Research Foundation. WADD Technical Report 61-180; ASTIA AD-260147, November 1960, pp. 43-59. (Available from OTS.)
4. W. B. Truesdale, "Development of a Small Coil Strain Gage," (Armour Research Foundation of IIT), Final Report, March 1963, ASTIA AD-402706.
5. F. W. Grover, "Inductance Calculations, Working Formulas, and Tables," Dover, 1962, 286 pp.
6. H. K. P. Neubert, "Instrument Transducers," Oxford University Press, 1963, p. 214.

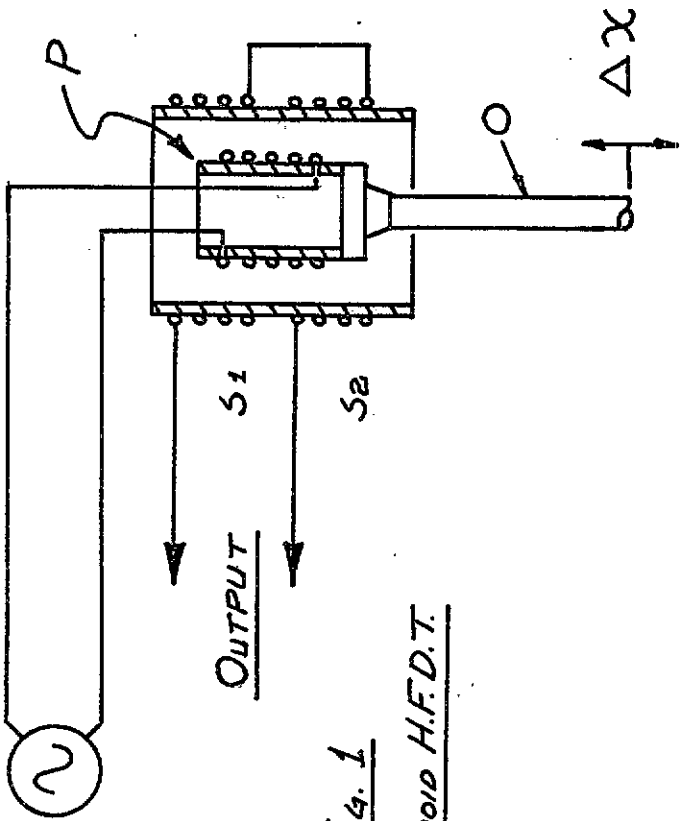


Fig. 1

SOLENOID H.F.D.T.

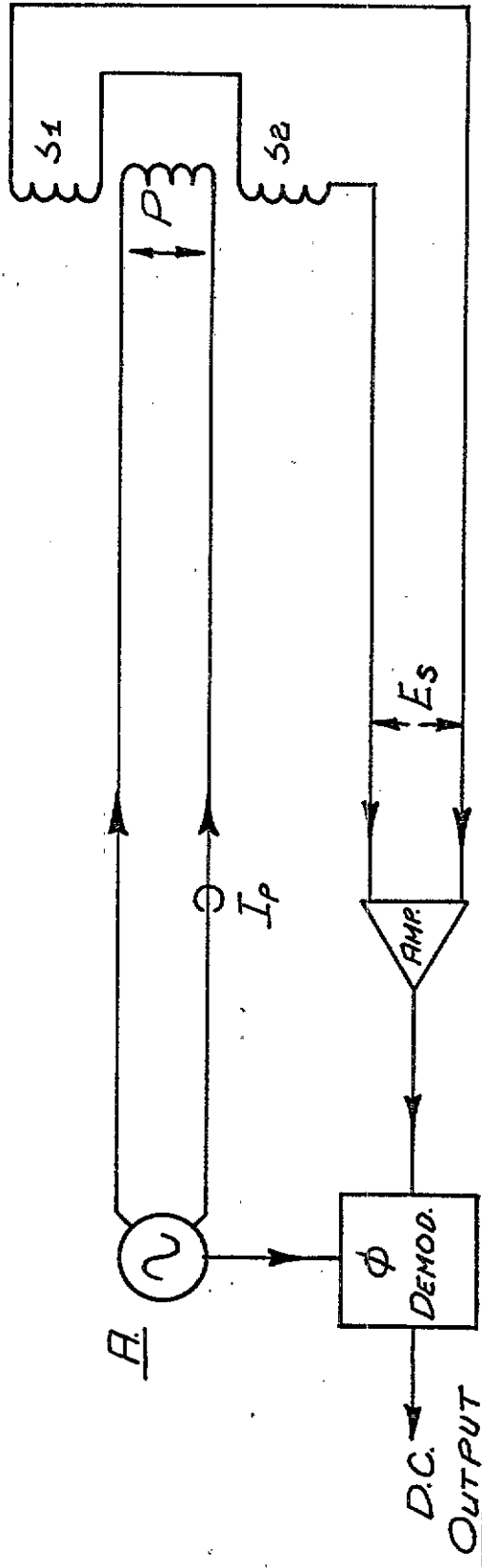
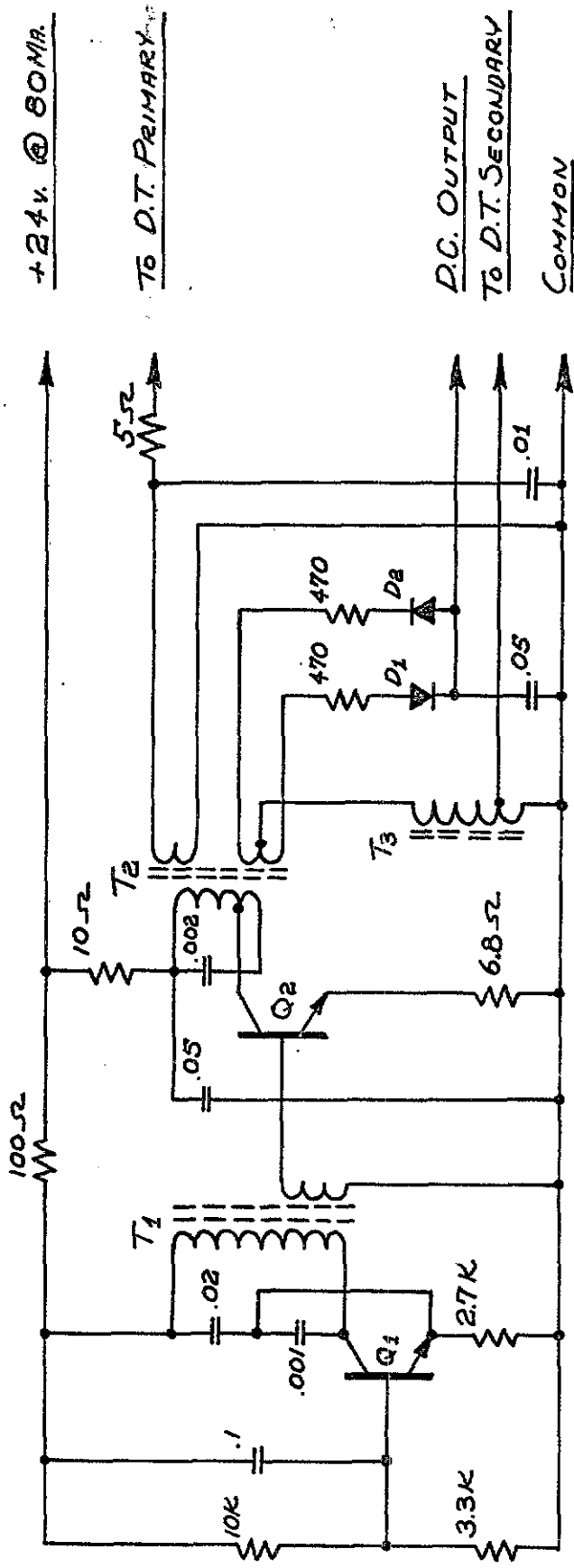


Fig. 2

CIRCUIT ARRANGEMENT

$$E_s = M \frac{dI_p}{dt}$$



+24v @ 80MA

TO D.T. PRIMARY

D.C. OUTPUT

TO D.T. SECONDARY

COMMON

FIG. 3.

A 1 Mc. Exciter & Phase Demodulator Circuit

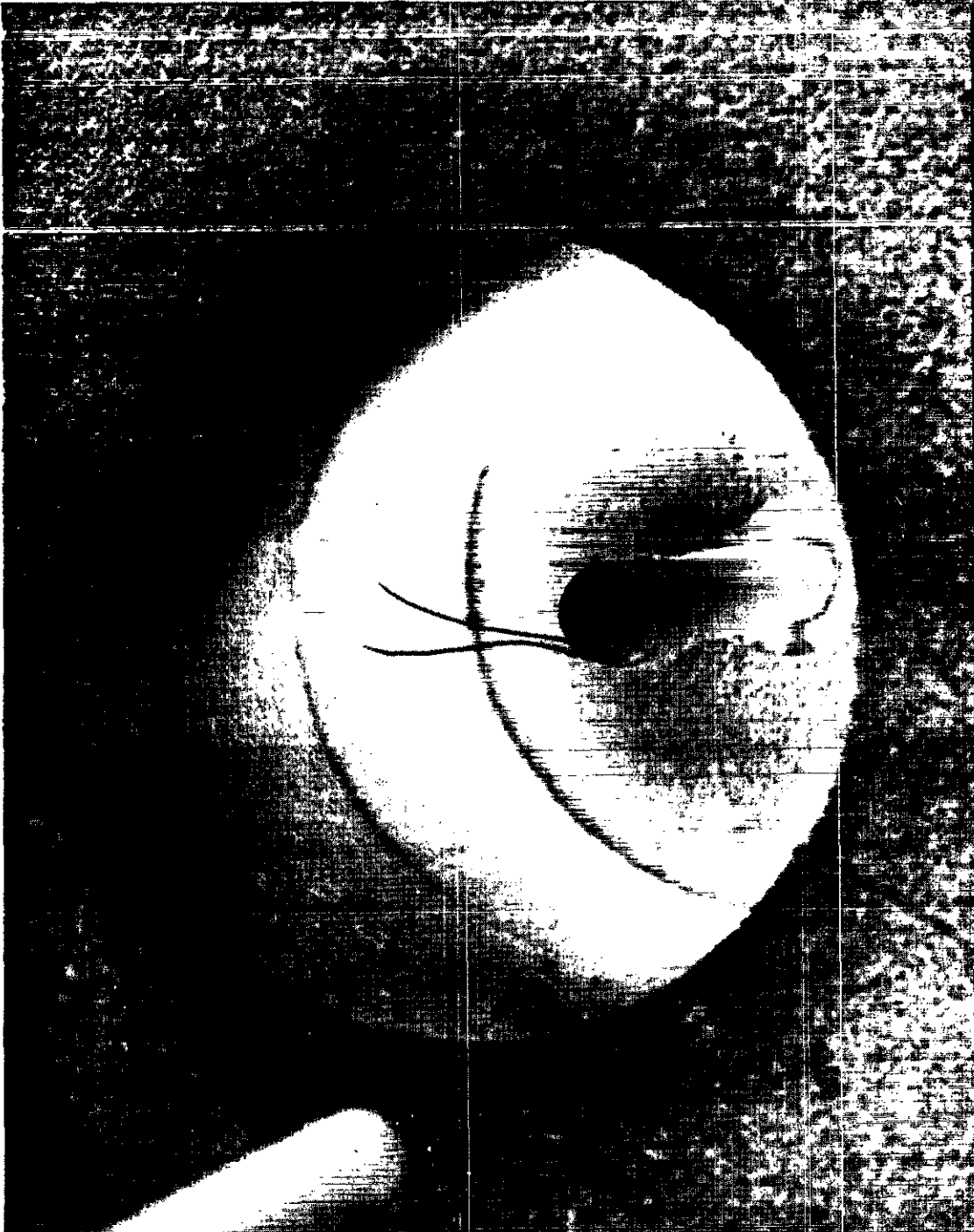
$Q_1 \& Q_2 = 2N697$

$T_1 = 20t = 25 \mu hy.$

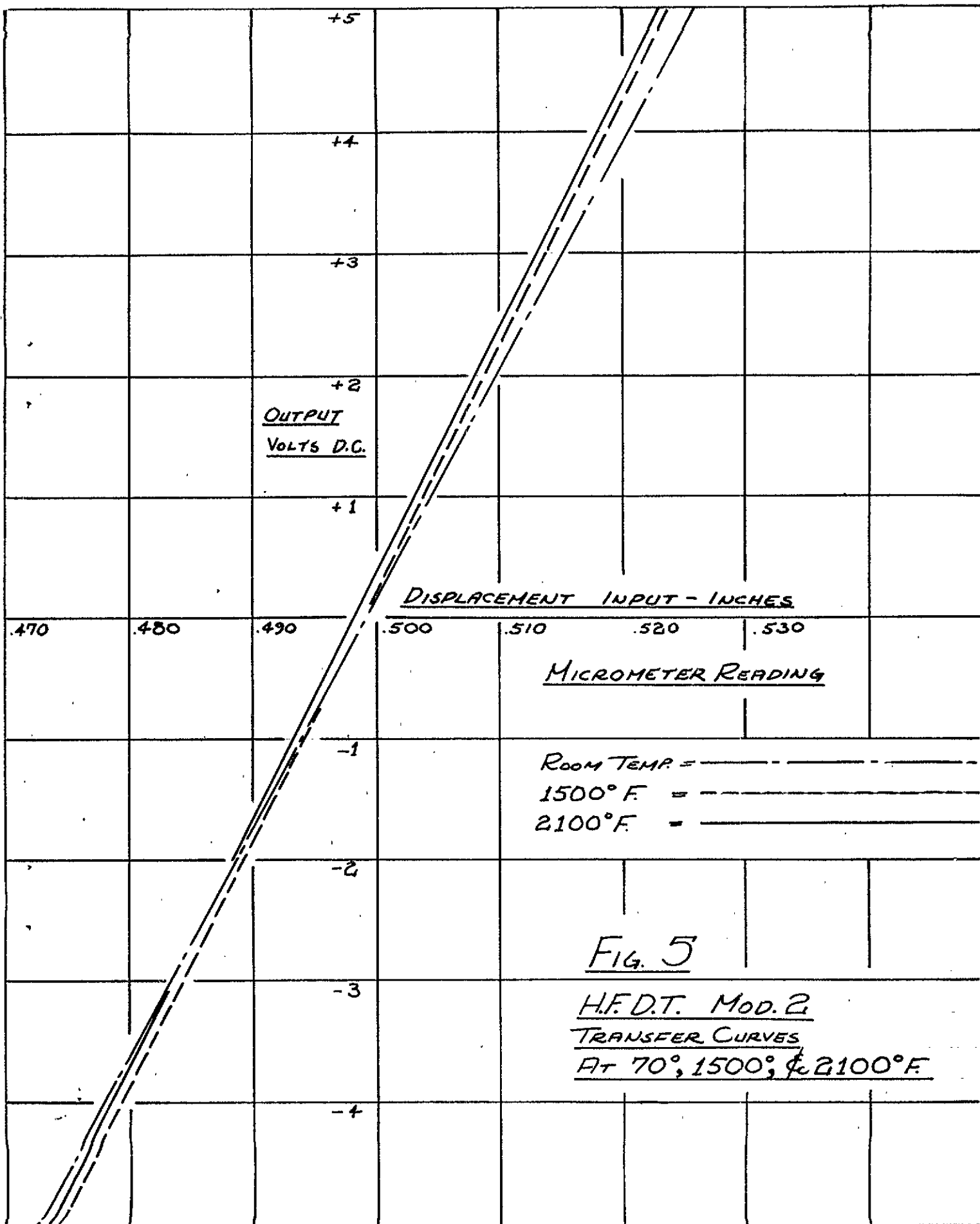
$T_2 \text{ Pri.} = 20t, \text{ Tap AT } 5t = 15 \mu hy.$

$T_2 \text{ Sec.} = 4t \& 4t.c.t.$

$T_3 = 36t, \text{ Tap AT } 4t = 800 \mu hy.$

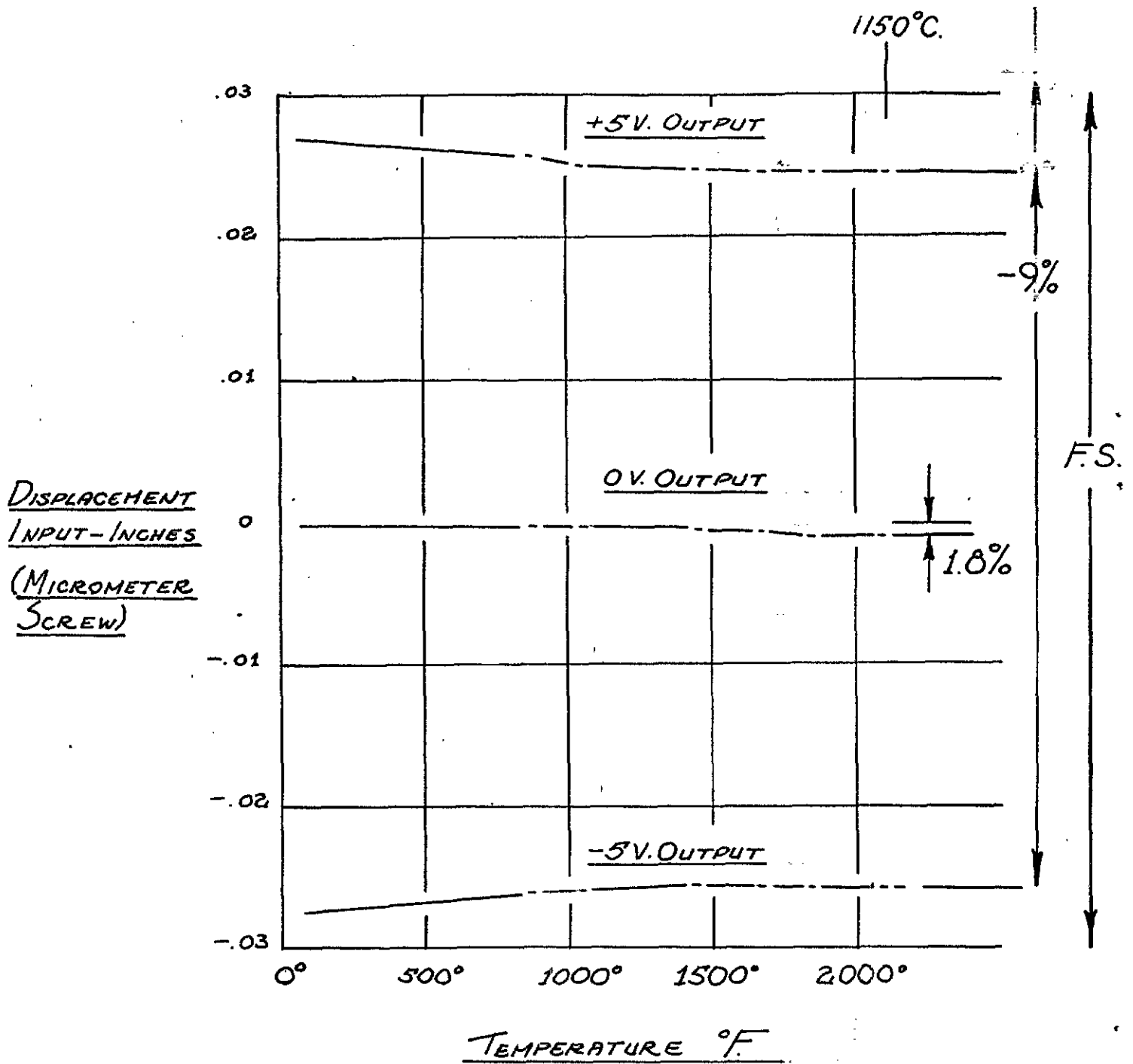


Experimental high-frequency
differential transformer
operating in a 2000^o F furnace.



ROOM TEMP = _____
 1500°F = _____
 2100°F = _____

FIG. 5
H.F.D.T. MOD. 2
TRANSFER CURVES
AT 70°, 1500°, & 2100°F.



TEMPERATURE °F

FIG. 6

H.F.D.T. MOD. 2

DISPLACEMENT INPUT VS. TEMP.

FOR CONST. ELECTRICAL OUTPUTS

OF +F.S., 0, -F.S. (5-0-5V)